From the Institute of Veterinary Pathology

Department of General Pathology and Pathological Anatomy

Chair: Prof. Dr. W. Hermanns

Ludwig-Maximilians-Universität München

Under the supervision of

Dr. N. Herbach and Prof. Dr. R. Wanke

Mechanisms of β-cell loss
in male Munich *Ins2*^{C95S} mutant mice

Inaugural-Dissertation

to achieve the doctor title of veterinary medicine

at the Faculty of Veterinary Medicine of the

Ludwig-Maximilians-Universität, Munich

by Sabine Martha Kautz

from Schwanstetten

Munich 2010

Gedruckt mit der Genehmigung der Tierärztlichen Fakultät

der Ludwig-Maximilians-Universität München

Dekan: Univ.-Prof. Dr. Braun

Berichterstatter   Univ.-Prof. Dr. Wanke

Korreferent/en: Univ.-Prof. Dr. Gabius

                    Univ.-Prof. Dr. Aigner

                    Prof. Dr. Kaltner

                    Univ.-Prof. Dr. Ammer

Tag der Promotion: 13. Februar 2010

Für meine Eltern

und meinen Freund Lothar

Table of content

1 Introduction

Diabetes mellitus has become a global concern, with over 240 million people suffering from this disease (IDF 2009h). The increasing prevalence of diabetes mellitus, severe diabetic complications, premature mortality and enormous economic costs are a serious socio-economic burden (Wild et al. 2004; Roglic et al. 2005).

In the recent years, it was demonstrated that long-term high blood glucose concentrations cause oxidative stress (Robertson 2004). Chronical hyperglycaemia and oxidative stress result in reduced insulin action, disturbed β-cell function and increased β-cell apoptosis, and are involved in the development of long-term diabetic complications (Kaiser et al. 2003; Brownlee 2005; Houstis et al. 2006). Studies in autopsies showed that the relative β-cell volume and β-cell mass in type 2 diabetic patients are significantly reduced compared to non-diabetics (Sakuraba et al. 2002; Butler et al. 2003).

Animal models are essential tools to investigate the pathogenesis of diabetes mellitus and diabetic complications. Especially mutant mice exhibiting defined point mutations in diabetes-relevant genes are valuable model systems and are a complementary approach to so far established transgenic and knockout models, since the same mutations may be found in diabetic patients. Munich $Ins2^{C95S}$ and Akita mutant mice exhibit point mutations in the $Ins2$ gene, leading to the loss of the intrachain and interchain disulfide bond of insulin 2, respectively (Wang et al. 1999; Herbach et al. 2007). Male Munich $Ins2^{C95S}$ mutant mice exhibit a progressive diabetic phenotype, characterised by severe hyperglycaemia, insulin resistance, disturbed insulin secretion and profoundly decreased β-cell mass. Female mutant mice show a milder form of diabetes compared to male mutants and preserved β-cell mass, probably due to antioxidative effects of female sexual hormones, especially estrogen (Katalinic et al. 2005; Le May et al. 2006).

Akita mice exhibit a similar diabetic phenotype as Munich $Ins2^{C95S}$ mutants. The pathogenesis of diabetes-development and β-cell loss has been extensively studied, and it could be demonstrated that misfolded (pro-)insulin accumulates in the β-cells of Akita mice, leading to ER stress and β-cell dysfunction (Izumi et al. 2003; Nozaki et al. 2004; Zuber et al. 2004). Several other studies demonstrated that misfolded and accumulated proteins can

induce ER stress and cell apoptosis (Xu et al. 2005; Scheuner and Kaufman 2008).

In the present study, the mechanisms of β-cell loss in male Munich $Ins2^{C95S}$ mutant mice were investigated. In order to examine the involvement of glucotoxicity and oxidative stress in the pathogenesis of β-cell destruction, one group of heterozygous mutant mice was treated with insulin-pellets. Placebo-treated wild-type and mutant mice served as controls.

The effects of insulin treatment, and therefore normalised blood glucose concentrations, on the endocrine pancreas were analysed using qualitative-histological and quantitative-stereological methods. Additionally, various clinical parameters were determined to examine β-cell function and insulin sensivity, and oxidative stress in the serum and ER stress in isolated islets were investigated.

2 Literature review

2.1 Diabetes mellitus

2.1.1 Prevalence

The prevalence of diabetes mellitus is increasing worldwide. About 30 million people were estimated to have suffered from this disease in 1985 (IDF 2009o; WHO 2009). In 2000, 171 million people were assumed to have diabetes (Wild et al. 2004; WHO 2009), and in 2007, 246 million people were affected by this disease, according to the IDF. Therefore, diabetes prevalence has increased by about 216 million in 22 years. This number is expected to increase further to 380 million by 2025 (IDF 2009h). Population growth, aging, urbanisation, unhealthy diet, obesity and sedentary lifestyle are main reasons for this increase in diabetes prevalence (Wild et al. 2004; IDF 2009h).

The prevalence of diabetes is supposed to be equal in rural and urban areas in developed countries, whereas in developing countries, the prevalence in urban areas is at least 2-fold higher than in rural regions. The majority of people with diabetes is older than 64 years in developed countries and 45 - 64 years of age in developing countries (Wild et al. 2004). Diabetes type 2 is the most common form of diabetes, which accounts for approximately 85 - 95% of all diabetes cases (IDF 2009o). The number of young people exhibiting type 2 diabetes, but also of subjects suffering from type 1 diabetes is growing (IDF 2009m, k).

The increase in diabetes prevalence is higher in developing than in industrialised countries (Wild et al. 2004; IDF 2009i). The countries with the highest prevalence of diabetes are India, China and the USA (Wild et al. 2004).

2.1.2 Costs

The economic burden of diabetes is enormous. The costs imply expenditures to prevent and treat diabetes, including diabetic complications, and loss of economic growth (IDF 2009d).

The IDF estimated worldwide healthcare expenses of at least USD 232 billion for diabetes mellitus in 2007. If the prognosis of diabetes prevalence comes true, in 2025 these costs will rise over USD 302 billion (IDF 2009d). Health

care costs for diabetes range up to 15% of the annual healthcare budget (WHO 2009). The treatment of diabetic complications make up the largest part of the healthcare costs (IDF 2009n).

Indirect costs of diabetes based on lost production caused by disability and mortality are estimated to be much higher than direct healthcare costs (IDF 2009d; WHO 2009).

2.1.3 Definition, description, classification and diagnosis of diabetes mellitus

An appropriate definition and description, an uniform and functional classification as well as useful diagnostic criteria are essential for epidemiological and clinical research and clinical management, in order to reduce the morbidity and mortality associated with diabetes. In May 1995, an international expert committee, working under the sponsorship of the American Diabetes Association (ADA) – The expert committee on the diagnosis and classification of diabetes mellitus – was created to revise the old terminology and classification of diabetes, which was mainly based on the type of pharmacological treatment. In their report, diabetes is classified according to its aetiology and/or pathogenesis. Recommendations for diagnosing and screening this disease are given (The expert committee on the diagnosis and classification of diabetes mellitus 2002).

2.1.3.1 Definition and description

Diabetes mellitus is a group of different aetiological and clinical metabolic disorders. It is primarily defined by hyperglycaemia resulting from insulin resistance, disturbed insulin secretion, or both (ADA 2006).

Marked hyperglycaemia causes typical symptoms like polyuria, polydipsia and weight loss. Some patients show polyphagia, blurred vision, retarded growth and increased susceptibility to distinct infections (ADA 2006). Uncontrolled hyperglycaemia can cause the two most common acute, live-threatening complications, diabetic ketoacidosis (DKA) and hyperglycaemic hyperosmolar syndrome (HHS) (Umpierrez et al. 2002; ADA 2006).

Chronically elevated blood glucose levels are associated with the development of long-term complications like cardiovascular disease (CVD), nephropathy, retinopathy and neuropathy (ADA 2006; IDF 2009e). CVD is the major cause

of death in diabetes and includes angina, myocardial infarction, stroke, congestive heart failure and peripheral artery disease (IDF 2009b). Diabetic nephropathy results in renal failure and is the most common single cause of end stage kidney disease (IDF 2009f). Moreover, macular oedema and retinopathy can cause blindness in diabetic patients (IDF 2009j). Gastrointestinal and genitourinary dysfunction due to autonomic neuropathy is another complication of chronic hyperglycaemia. Loss of feeling, numbness or pain of different characters are caused by peripheral neuropathy, which can lead to Charcot joints. Peripheral neuropathy and/or peripheral artery disease are frequent reasons for foot ulcers and amputations in diabetics (ADA 2006; IDF 2009g, a).

2.1.3.2 Classification

According to the developing knowledge of this multifactorial disease, the classification for diabetes was revised several times.

The first generally accepted systematic classification was published by the National Diabetes Data Group (NDDG) in 1979 (The expert committee on the diagnosis and classification of diabetes mellitus 2002). Based mainly on the treatment, diabetes was divided into four groups, insulin-dependent diabetes mellitus (IDDM, type 1 diabetes), non-insulin dependent diabetes mellitus (NIDDM, type 2 diabetes), gestational diabetes mellitus and diabetes associated with other conditions and syndromes (Porte et al. 2002). The classification was supported and developed further by the WHO expert committee on diabetes and later by the WHO study group on diabetes mellitus. They distinguished between five groups: IDDM, NIDDM, malnutrition-related diabetes, gestational diabetes and other types. The expert committee on the diagnosis and classification of diabetes mellitus revised the NDDG/WHO classification in 1997. The classification was constantly adapted to the current knowledge by The expert committee on the diagnosis and classification of diabetes mellitus and published by the ADA (The expert committee on the diagnosis and classification of diabetes mellitus 2002, 2003, ADA 2006). Diabetes is now divided into different groups with regard to its aetiology and/or pathogenesis (Table 2.1).

Aetiologic classification of diabetes mellitus			
I	Type 1 diabetes	A	Immune-mediated	
		B	Idiopathic	
II	Type 2 diabetes			
III	Other specific types	A	Genetic defects of β-cell function	e.g. MODY1 - 6
		B	Genetic defects of insulin action	e.g. Type A insulin resistance, Leprechaunism, Lipoatrophic diabetes
		C	Diseases of the exocrine pancreas	e.g. Pancreatitis, Trauma, Pancreatectomy, Neoplasia, Cystis fibrosis
		D	Endocrinopathies	e.g. Acromegaly, Cushing's syndrome, Pheochromo-cytoma, Hyperthyroidism
		E	Drug- or chemical-induced	Vacor, Glucocorticoids, Diazoxide, β-adrenergic agonists, Thiazides
		F	Infections	e.g. Congenital Rubella, Cytomegalovirus
		G	Uncommon forms of immune-mediated diabetes	e.g. "Stiff-man" syndrome, Anti-insulin receptor antibodies
		H	Other genetic syndromes sometimes associated with diabetes	e.g. Down's syndrome, Wolfram's syndrome, Myotonic dystrophy
IV	Gestational diabetes mellitus (GDM)			

Table 2.1 Aetiologic classification of diabetes mellitus (ADA 2006)

2.1.3.3 Diagnosis

The criteria for the diagnosis of diabetes were revised by The expert committee on the diagnosis and classification of diabetes mellitus in 1997 and 2003 (Lehmann and Spinas 2005).

Three possibilities to diagnose diabetes exist (ADA 2006):

1. Plasma glucose concentration ≥ 200 mg/dl at any time of the day, independent from the time of the last meal, plus classic symptoms (polyuria, polydipsia, unexplained weight loss)
2. Fasting plasma glucose (FPG) ≥ 126 mg/dl; i.e. no caloric intake for at least 8 hours
3. Plasma glucose 2 hours after glucose challenge during an oral glucose tolerance test ≥ 200 mg/dl; glucose load contains the equivalent of 75 g anhydrous glucose dissolved in water

Positive test results should be confirmed on a subsequent day, using one of the 3 methods (ADA 2006). This confirmation is mainly necessary for individuals without diabetic symptoms. Severe infections, trauma or stress can lead to transient hyperglycaemia in non-diabetics (Lehmann and Spinas 2005).

Some individuals present plasma glucose levels, which are abnormally elevated, but lower than in diabetic patients. The fasting plasma glucose is impaired (impaired fasting glucose (IFG)) when fasting glucose levels range from 100 - 125 mg/dl. In oral glucose tolerance tests, people suffer from an impaired glucose tolerance (IGT), when plasma glucose levels 2 hours after glucose challenge, are between 140 - 199 mg/dl (ADA 2006). The values for normal plasma glucose (NPG, after fasting for at least 8 hours) were reduced from 110 mg/dl to 100 mg/dl in 2003, mainly with regard to elevated cardiovascular risks in individuals with blood glucose levels over 100 mg/dl (The expert committee on the diagnosis and classification of diabetes mellitus 2003; Lehmann and Spinas 2005).

2.2 Types of diabetes mellitus

2.2.1 Diabetes type 1

Diabetes type 1 accounts for 5 - 10 % of all diabetes cases.

In the majority of type 1 diabetic patients, a cellular-mediated autoimmune response results in the destruction of pancreatic β-cells (immune-mediated diabetes, diabetes type 1A). Autoantibodies to islet cells (ICA), to glutamic acid decarboxylase (GAD_{65}), to tyrosine phosphatases IA-2 and IA-2β or to insulin (IAA) can be detected (The expert committee on the diagnosis and classification of diabetes mellitus 2002; Al-Mutairi et al. 2007).

Genetic and environmental factors contribute to the development of diabetes type 1. More than eighteen different chromosomal regions are associated with the susceptibility to diabetes type 1 in humans. Several genes which are located in the major histocompatibility complex region on chromosome 6p21 play a leading role in the pathogenesis of this disease (Pociot and McDermott 2002; Al-Mutairi et al. 2007). Environmental factors e.g. virus infections (Coxsackie B virus, Cytomegalovirus, Epstein-Barr virus, Rubella), proteins in bovine milk and chemicals were assumed to induce the generation of autoantibodies (Kukreja and Maclaren 1999; Spinas and Lehmann 2001; Al-Mutairi et al. 2007).

Predominantly children and adolescents suffer from diabetes type 1, but individuals at any age can be affected. The rate of β-cell destruction is normally more rapid in younger patients than in adults (ADA 2006). When hyperglycaemia is diagnosed, about 80% of the β-cells are already destroyed (Spinas and Lehmann 2001). The onset of this disease is often abrupt in children and adolescents, symptoms are severe (ketoacidosis) and the patients are insulin-dependent (Pociot and McDermott 2002). Others show modest fasting hyperglycaemia which possibly changes to severe hyperglycaemia and/or ketoacidosis due to stress or infections. In some individuals, primarily in adults, residual β-cell function prevents ketoacidosis for a long time until they finally become insulin-dependent (ADA 2006).

In approximately 10 - 20% of type 1 diabetics, no autoantibodies can be found and the aetiology remains unknown (idiopathic diabetes, diabetes type 1B). These individuals are prone to ketoacidosis and show insulin deficiency to different extents. This form of diabetes demonstrates a strong inheritance (The

expert committee on the diagnosis and classification of diabetes mellitus 2002; Al-Mutairi et al. 2007).

2.2.2 Diabetes type 2

Diabetes type 2 is a heterogeneous disease, based on genetic and environmental factors (Ahren 2005; Lehmann and Spinas 2005). The genetic predisposition is stronger than in patients with diabetes type 1 (ADA 2006). Brothers and sisters of type 2 diabetic patients present a high prevalence of this disease. Monozygous twins have a similar risk to develop diabetes type 2 (Lehmann and Spinas 2005). Lacking physical activity and high caloric diet cause obesity, which contributes to the development of diabetes (Lehmann and Spinas 2005; ADA 2006). It was shown that lifestyle interventions (healthy diet, exercise) and weight loss reduce the incidence of diabetes in persons with a high risk of getting diabetic (Resnick et al. 2000; Knowler et al. 2002).

In type 2 diabetes, hyperglycaemia results from an imbalance between increased insulin requirement due to reduced insulin action, and insufficient insulin availability (Ahren 2005). Obesity, particularly an increased amount of visceral fatty tissue, is associated with insulin resistance (Lehmann and Spinas 2005). Initially, in most of the subjects with reduced insulin action, the enhanced insulin demand is compensated by increased insulin secretion. When insulin secretion becomes inadequate in relation to the elevated demand, individuals present hyperglycaemia. Reduced β-cell mass, diminished insulin gene expression, impaired insulin processing and/or disturbed insulin secretion can be the reasons for insufficient insulin secretion (Kaiser et al. 2003; Ahren 2005). It was reported that the reduction of the relative β-cell volume in diabetes type 2 is caused mainly by increased apoptosis, not by diminished β-cell replication or islet neogenesis (Butler et al. 2003). Glucotoxicity, lipotoxicity and aggregation of islet amyloid in humans seem to contribute to disturbed β-cell function and apoptosis (Ahren 2005; Lehmann and Spinas 2005).

Type 2 diabetes often remains undiagnosed for several years due to the gradual increase of plasma glucose concentrations (ADA 2006). Associated complications and elevated glucose concentrations in blood or urine in accidentally performed tests frequently lead to the diagnosis (IDF 2009l). Chronically elevated blood glucose levels are responsible for the development

of long-term complications (ADA 2006; IDF 2009c). Diabetes type 2 is often associated with the metabolic syndrome. People showing central adiposity, elevated concentrations of triglycerides, low HDL cholesterol levels or elevated blood pressure have an increased risk to be affected by diabetes type 2 (Lorenzo et al. 2003).

2.2.3   Monogenic forms of diabetes mellitus

About 1 - 2% of all diabetes cases are monogenic. These monogenic forms can be classified into two major groups: Maturity-onset diabetes of the young (MODY) and neonatal diabetes mellitus (NDM) (Hattersley 2005; Edghill et al. 2008).

2.2.3.1   Maturity-onset diabetes of the young (MODY)

Subtypes of MODY are the most common forms of monogenic diabetes (Edghill et al. 2008). Autosomal dominant mutations in six genes causing MODY1 - 6 have been identified. These genes are encoding for the glycolytic enzyme glucokinase (MODY2) or for the β-cell transcription factors hepatic nuclear factor 4α (HNF4α, MODY1), HNF1α (MODY3), HNF1β (MODY5), insulin promoter factor 1 (IPF1, MODY4) and NeuroD1 (MODY6). MODY3 is the most common form (Hattersley 2005; ADA 2006), whereas patients rarely exhibit MODY4, 5 or 6 (Edghill et al. 2008). In France, UK, Spain and Germany, unknown MODY loci (MODYX) account for 16 - 45% of individuals showing typical MODY symptoms (Costa et al. 2000). Recently, insulin gene (INS) mutations were found in 2 MODY patients, 1 tested negative for *HNF1A* and glucokinase gene (*GCK)* mutations, the other tested negative for *HNF1A, HNF4A* and *GCK* alterations (2.2.3.3 Mutations in the insulin gene).

MODY is usually diagnosed in children and adolescents younger than 25 years (Vaxillaire and Froguel 2006; Edghill et al. 2008). Mutations in *GCK* (MODY2) cause mild fasting hyperglycaemia directly after birth. Due to stable blood glucose concentrations, pharmacological treatment is not necessary in most MODY2 cases. Patients exhibiting mutations in the genes of β-cell transcription factors (MODY1, 3, 4, 5 and 6) are normoglycaemic at birth. Their blood glucose levels rise continuously, leading to the diagnosis of diabetes as adolescents or young adults. In order to avoid long-term complications these patients normally require pharmacological treatment (Hattersley 2005).

2.2.3.2 Neonatal diabetes mellitus (NDM)

The incidence of neonatal diabetes mellitus is 1 : 215,000 (Stanik et al. 2007) to 1 : 500,000 newborns (Støy et al. 2007; Polak et al. 2008). It usually develops within the first weeks of life (< 6 months) (Støy et al. 2007; Aguilar-Bryan and Bryan 2008) and is characterised by mild to severe hyperglycaemia combined with low levels of insulin (Polak et al. 2008). NDM can be transient (TNDM) or permanent (PNDM). TNDM accounts for over the half of all neonatal diabetes cases (Polak and Cavé 2007; Aguilar-Bryan and Bryan 2008).

Due to similar clinical symptoms (intrauterine growth retardation, failure to thrive, hyperglycaemia, ketoacidosis and reduced serum insulin levels) it can not be distinguished between TNDM and PNDM in the neonate.

Most patients with TNDM recover within a few months, but possibly suffer from persistent glucose intolerance and/or may relapse to a permanent diabetic state in childhood or adulthood (Polak and Cavé 2007). The most common forms of TNDM are based on mutations in the imprinted region on chromosome 6q24, whereas aberrations in the *KCNJ11* and *ABCC8* gene are less frequent (Hattersley and Pearson 2006; Aguilar-Bryan and Bryan 2008). These genes encode for the protein subunits Kir6.2 and SUR1 of the ATP-sensitive potassium channel in pancreatic β-cells, respectively (Støy et al. 2007).

In contrast to TNDM, the deficient insulin secretion remains in patients with PNDM (Polak and Cavé 2007). The most frequent causes of PNDM are activating mutations in the *KCNJ11* and *ABCC8* gene (Edghill et al. 2008). Mutations in *INS* were recently described to cause PNDM (2.2.3.3 Mutations in the insulin gene). Inactivating homozygous mutations in the glucokinase gene *(GCK)* have been found in patients with PNDM, but are rare (Njolstad et al. 2001; Edghill et al. 2008). Mutations in several genes (*IPF1, PTF1A, FOXP3, GLIS3, GLUT2, TCF2, EIF2AK3*) can cause PNDM and show additional non-pancreatic features (Støy et al. 2007; Edghill et al. 2008).

2.2.3.3 Mutations in the insulin gene

In a recent study 16 different *INS* mutations were found in 227 probands with diabetes onset before 1 year of age (Edghill et al. 2008). Ten of these mutations were also described in an earlier study involving 83 patients with

PNDM (Støy et al. 2007). In both studies, 94% of the individuals with PNDM were younger than 6 months. The median age of diagnosing PNDM in the probands with *INS* mutations was 9 (Støy et al. 2007) and 11 weeks (Edghill et al. 2008). Patients suffered from marked hyperglycaemia including polyuria and polydipsia, or ketoacidosis. C-peptide levels were low or undetectable. Due to reduced insulin secretion in utero, the birth weights were decreased. The symptoms of PNDM patients with *INS* mutations were similar to those with alterations in *KCNJ11* and *ABCC8*, apart from individuals with *INS* mutations being older at time of diagnosis and not presenting neurological aberrations. Neither mutations in *KCNJ11* or *ABCC8* nor autoantibodies could be found in the probands with mutated *INS* (Støy et al. 2007; Edghill et al. 2008).

The 16 detected *INS* mutations in PNDM patients affected highly conserved residues within preproinsulin. Nine of the mutations created an unpaired cysteine residue either by substituting an existent cysteine residue within a disulfide bond (A7-B7 (C96Y and C96S), B19-A20 (C43G)) or by introducing a new cysteine residue (F48C, R89C, G90C, S101C, Y103C, Y108C), probably leading to incorrect processing and conformational changes of the mutated preproinsulin (Støy et al. 2007; Edghill et al. 2008). Mutations not involving cysteine residues seem to be important for correct insulin processing and conformation, too. Replacement of glycine residues (G32S, G32R, G47V) and the H29D and L35P mutations are described to disturb correct disulfide pairing and folding of proinsulin (Hua et al. 2006; Nakagawa et al. 2006; Støy et al. 2007; Edghill et al. 2008). Defective cleavage of the signal peptide could be caused by the A24D alteration, and possibly induces endoplasmic reticulum (ER) stress (Støy et al. 2007). The molecular consequences of the G84R mutation are not completely understood (Edghill et al. 2008).

In over 80% of the PNDM probands, the *INS* mutation appeared de novo, comparable to mutations in the *KCNJ11* gene (Støy et al. 2007; Edghill et al. 2008). Edghill et al. (2008) analysed the frequency of different mutations in another cohort of 279 PNDM patients diagnosed before 6 months of age. Eighty-seven individuals (31%) exhibited a *KCNJ11* mutation. The *INS* gene was altered in 33 (12%), the *ABCC8* gene in 29 patients (10.4%). Mutations in the *GCK* (4%), the *EIF2AK3* (8%) and the *FOXP3* (1.4%) gene were less common. In 108 probands (39%) no mutation was detected (Edghill et al. 2008).

Polak et al. (2008) investigated 38 PNDM patients from the French neonatal diabetes cohort and 1 child with non-autoimmune early infancy diabetes. Three already known *INS* mutations (A24D, R89C and C96Y) were found in 4 probands (3 PNDM patients, the 1 child with early infancy diabetes). In two cases (R89C mutation carriers), an autosomal dominant inheritance was observed. Clinical symptoms were similar to those observed by other groups (Stoy et al. 2007; Edghill et al. 2008). Age at diagnosis of PNDM was 4.25 years in the child compared to 0.8, 4.8 and 8.5 months in the other 3 patients (Polak et al. 2008).

In contrast to *INS* mutations in the PNDM patients, which arose mainly *de novo*, the *INS* mutations of 2 MODY patients were inherited and the affected individuals demonstrated a less severe diabetic phenotype than PNDM patients (Edghill et al. 2008; Molven et al. 2008). One MODY patient, as well as his mother and the maternal grandmother exhibited an *INS* mutation (R6C) and demonstrated a MODY-like phenotype (Edghill et al. 2008). A R46Q mutation was found in another MODY proband, his diabetic father and a paternal aunt. The three family members demonstrated a relatively mild form of diabetes (Molven et al. 2008). Age of diagnosis was 15 years and older in the described MODY patients.
Furthermore, a L68M (Edghill et al. 2008) and a C43G (Støy et al. 2007) mutation in *INS* were found in 2 patients with type 2 diabetes. Both patients were diagnosed with diabetes at 30 years of age.

In earlier studies, different *INS* mutations have already been detected. Affected individuals showed a mild diabetic phenotype and/or glucose intolerance (V92L (Nanjo et al. 1986; Nanjo et al. 1987), F48S (Haneda et al. 1983), F49L (Tager et al. 1979; Kwok et al. 1983)) In contrast to the later studies described above, insulin levels were increased in all patients. Biological activity of insulin was stated to be diminished, leading to reduced clearance by receptor-mediated endocytosis and therefore to hyperinsulinaemia. The mutations were inherited in an autosomal dominant manner (Steiner et al. 1990).
INS mutations which lead to familial hyperproinsulinaemia (R89H (Collinet et al. 1998), R89L (Yano et al. 1992) and H34D (Chan et al. 1987; Oohashi et al.

1993)) are also inherited in an autosomal dominant manner (Steiner et al. 1990; Collinet et al. 1998). Substitution of arginine on position 65 of proinsulin with histidine and leucine, respectively (R89H, R89L) impairs cleavage at the C-peptide-A-chain junction of proinsulin, resulting in the release of type II proinsulin intermediates, whereas the exchange of histidine on position 10 of proinsulin with aspartic acid (H34D) impairs conversion of proinsulin to insulin. The relative proportion of proinsulin and proinsulin intermediates, respectively in the circulation of affected individuals was approximately 4-fold increased compared to control subjects (Collinet et al. 1998). Familial hyperinsulinaemia was considered relatively asymptomatic in earlier studies (Steiner et al. 1990), but subsequent studies demonstrated that with increasing age affected subjects became glucose intolerant (Oohashi et al. 1993; Collinet et al. 1998).

The different studies indicate that *INS* mutations exhibit a spectrum of different phenotypes, ranging from mild, hyperinsulinaemic and hyperproinsulinaemic diabetes (Steiner et al. 1990; Collinet et al. 1998), to MODY (Edghill et al. 2008; Molven et al. 2008) and type 2 diabetes and finally to PNDM (Støy et al. 2007; Edghill et al. 2008).

2.3 Animal models of diabetes mellitus

Animal models are essential tools in order to investigate the genetics and pathogenesis of human diseases and to test new therapeutic strategies. Due to the high reproduction, practical aspects and lower expenses compared to larger animals like pigs and dogs, mice and rats are appropriate model systems (Clee and Attie 2007; Srinivasan and Ramarao 2007). Additionally, mice exhibit similar genome organisation, biochemical pathways and physiology as humans (HelmholtzCenter 2009).

Diabetes mellitus in animals can occur spontaneously or may be induced by treatment with chemicals (e.g. streptozotocin (STZ), alloxan (ALX)), dietary methods (e.g. high fat diet), surgical manipulations (e.g. partial pancreatectomy) or combinations. In the recent years, transgenic animals as well as general and tissue specific knockout models were generated, using reverse genetic techniques (Srinivasan and Ramarao 2007; Aigner et al. 2008). It can be distinguished between obese models like *ob/ob* mouse,

Zucker fatty rat, uncoupling protein 1 (UCP1) knockout mouse, and non-obese models (e.g. Akita mutant mouse, GK rat, STZ- or ALX-treated rodents, partial pancreatectomised animals, IRS-1, IRS-2 or GLUT-4 knockout mice) (Srinivasan and Ramarao 2007).

2.3.1 ENU mouse mutagenesis projects

ENU mouse mutagenesis projects existed worldwide, e.g. in Australia (Canberra), Canada (Toronto), USA (Texas, Maine), Japan (Yokohama), England (Harwell) and Germany (Neuherberg) (Aigner et al. 2008). The Munich ENU Mouse Mutagenesis Screen also called Munich ENU Project (MEP) was founded in 1997. It produced and analysed novel mouse models, which are important for the investigation of the genetics and pathogenesis of inherited human diseases (HelmholtzCenter 2009). Mutant mice were created large scale, using systematic, phenotype-driven methods. Random mutations were induced by the chemical *N*-ethyl-*N*-nitrosourea (ENU) and clinical relevant phenotypes were identified by distinct screening protocols. After proving the inheritance of the aberrant phenotype and establishing the corresponding mouse lines, the mutation was determined by molecular genetic analysis (Aigner et al. 2008).

2.3.1.1 ENU mutagenesis

N-ethyl-*N*-nitrosourea (ENU), an alkylating agent, mainly causes point mutations and therefore allows detailed functional analysis of genes (Stanford et al. 2001). ENU demonstrates strong mutagenic action on spermatogonial stem cells (Russell et al. 1979), leading to 1 mutation in 100,000 – 2,500,000 bp (Concepcion et al. 2004; Augustin et al. 2005; Keays et al. 2006; Aigner et al. 2008). From over 1,000 mutations per animal, only few demonstrate phenotypic consequences. The mutants produced by ENU may exhibit hypomorphic (partial loss of function), loss-of-function, dominant negative or gain-of-function alleles of the affected genes (Aigner et al. 2008).

2.3.1.2 Munich ENU Mouse Mutagenesis Project

The Munich ENU Mouse Mutagenesis Project was carried out on the inbred strain C3HeB/FeJ (C3H), which is diabetes resistant (Clee and Attie 2007). At the age of 10 weeks, male C3H mice were injected intraperitoneally with ENU

3 times in weekly intervals. After a sterility period, ENU-treated male mice were bred to wild-type C3H females. As identifying of recessive mutations needs more time and space compared to dominant mutations, only the dominant breeding scheme was performed since the end of 2004. The aberrant phenotypes in the G1 generation were identified, using the so called Munich protocol. This screening protocol was created to reveal congenital abnormalities of mutant phenotypes, including dysmorphological malformations and alterations in clinical chemistry, biochemistry, immunology, allergy and behaviour (Aigner et al. 2008; HelmholtzCenter 2009). G1 mice exhibiting an aberrant phenotype were mated to C3H wild-type mice in order to confirm the inheritance of the mutation in the G2 offspring. Phenotypic mutant mice were back-crossed with C3H wild-type mice for several generations to reduce the amount of non-causative mutations (Keays et al. 2006; Aigner et al. 2008). To obtain an identical genetic background and to avoid interactions of the ENU-induced mutations in different genotypes, it is necessary to back-cross mutagenised mice with wild-type mice of the same inbred strain (Aigner et al. 2008).

The chromosomal position of the causative mutation was determined by linkage analysis. Phenotypic mutant mice were mated with wild-type mice of a second inbred strain. After screening for the aberrant phenotype, hybrid mutant G1 offspring were back-crossed to wild-type mice of the second inbred strain. The G2 offspring were examined again for the abnormal phenotype and separated into mutant and non-mutant mice. DNA samples were analysed by genome-wide linkage analysis in order to determine the chromosomal location of the causative mutation. The accurate position of the mutation within the identified chromosomal section was examined by further linkage and candidate gene analysis, including sequencing methods (Aigner et al. 2008).

2.3.1.3 Phenotype screen for hyperglycaemic mouse lines

Between the distinct laboratories, many variables existed which could not be entirely standardised. Therefore, each ENU mouse mutagenesis project had to determine the physiological plasma glucose concentrations of the used inbred strain and the cut off level to define hyperglycaemic phenotypes. In the Munich ENU mouse mutagenesis project, the plasma glucose concentrations of overnight-fasted 3-month-old male and female C3H wild-type mice were

determined large scale (male: 128 mg/dl, female: 123 mg/dl). Mice exhibiting plasma glucose concentrations over 200 mg/dl in two measurements within a 3-week interval were defined as hyperglycaemic.

From 15,000 G1 offspring, 12 exhibited plasma glucose levels over 200 mg/dl. In 4 of these non-obese G1 variants (GLS001, GLS004, GLS006, GLS007) the inheritance was proven, and a new hyperglycaemic mouse line (GLS008) seems to bequeath the mutation, too (Aigner et al. 2008).

GLS001 and GLS006 mutants demonstrate alterations in *Gck* and therefore provide suitable animal models for MODY2 (heterozygous *Gck* mutation) and PNDM (homozygous *Gck* mutation) (van Bürck et al. personal communication). GLS004 mice exhibit a mutation in the insulin 2 gene (*Ins2*). Alterations in the insulin gene can also be found in humans (e.g. PNDM patients; 2.2.3.2 Neonatal diabetes mellitus (NDM)), and another mouse model (2.3.3 The Akita mouse).

Hyperglycaemic mouse lines, created in other ENU mouse mutagenesis projects, demonstrate dominant mutations in the *Gck*, the insulin receptor (*Insr*) and the single-minded homolog 1 (*Sim1*) gene. In other diabetic mouse strains, the causative mutation is still unknown (Aigner et al. 2008).

2.3.2 The Munich *Ins2*^{C95S} mutant mouse

The Munich *Ins2*^{C95S} mutant mouse was generated within the Munich ENU Mouse Mutagenesis project. The genetic background of this non-obese diabetic mouse model is the inbred strain C3HeB/FeJ (C3H) (Herbach et al. 2007; Aigner et al. 2008). Mutant mice exhibit a T→A transversion at nucleotide position 1903 in exon 3 of the *Ins2* gene on chromosome 7. This point mutation results in the amino acid exchange from cysteine to serine at position 95 of preproinsulin (C95S), which leads to the loss of the A6-A11 intrachain disulfide bond.

The mutation is inherited in an autosomal dominant manner and exhibits complete phenotypic penetrance corresponding to the sign test after Dixon and Mood (Herbach et al. 2007).

2.3.2.1 Heterozygous mutant mice

At the age of 3 and 6 months, male heterozygous Munich *Ins2*^{C95S} mutant mice exhibited significantly lower fasted body weights than male wild-type

mice, whereas female mutant and wild-type mice showed similar body weights.

From 1 month of age onwards, fasted and 1.5 h postprandial blood glucose levels of male and female mutants were significantly higher than those of sex- and age-matched littermate controls. Fasted blood glucose levels of male mutant mice deteriorated with age, reaching nearly 400 mg/dl. Female mutants featured a mild diabetic phenotype with fasted blood glucose levels lower than 200 mg/dl.

During oral glucose tolerance tests (OGTT) at the age of 1, 3 and 6 months, mutant mice of both genders exhibited significantly elevated blood glucose concentrations versus wild-type mice.

At the age of 1 month, male and female mutant mice demonstrated slightly, but significantly reduced serum insulin levels 10 minutes after glucose challenge compared to age and sex-matched controls, whereas the insulin concentration 10 minutes after glucose challenge was largely decreased in 3- and 6-month-old mutants compared to age- and sex-matched wild-type-mice. However, no differences concerning the fasted and 1.5 h postprandial serum insulin levels were detected between mutants of both genders and their sex-matched controls.

Male and female mutant mice demonstrated a significantly lower pancreatic insulin content than sex-matched wild-type mice at the age of 3 and 6 months, whereas the insulin content in the pancreas of female mutant mice was significantly higher than that of male mutants.

The HOMA of β-cell function index of 1-, 3-, and 6-month-old mutants of both genders was significantly reduced.

In contrast to female mutant mice, male mutants exhibited a significantly higher HOMA of insulin resistance index than wild-type mice at the age of 3 and 6 months. Four-month-old male mutant mice featured a smaller decrease in blood glucose levels 10 minutes after insulin injection compared to male wild-type mice. These findings indicate a reduced insulin sensitivity in male mutants at the age of 3 months and older versus male wild-type mice.

The exocrine pancreas of 6-month-old mutant mice exhibited no gross morphological or histopathological changes, and no evidence of insulitis was found in the endocrine pancreas. Immunostaining for insulin and glucagon showed a disturbed islet structure: The amount of glucagon producing α-cells

was increased and non-β-cells were distributed over the islet profile. Islets of wild-type mice presented a typical murine structure, with few non-β-cells bordering a core of insulin-expressing cells. In addition, the staining intensity of insulin-positive cells in mutants was very weak compared to wild-type mice (Herbach et al. 2007). However, the described alterations were more distinct in male mutant mice compared to female mutants (Herbach et al. personal communication).

The total islet volume, the total β-cell volume as well as the volume density of β-cells in the islets were significantly decreased in male, but not in female mutant mice compared to sex-matched wild-type mice. The volume density of α-cells was elevated in mutants of both genders versus wild-type animals, whereas only male mutant mice exhibited a significantly higher volume density and total volume of somatostatin expressing δ- and pancreatic polypeptide positive PP-cells than male wild-type mice.

Transmission electron microscopy of β-cells of 6-month-old mutant mice featured several ultrastructural alterations. In male mutant mice, very few small insulin secretory granules were found, in contrast to wild-type mice. The mitochondria appeared to be swollen, the rough endoplasmic reticulum to be dilated as compared to male wild-type mice. Myelin figures as well as cytoplasmic vacuolisation were detected. In female mutants, these alterations were less distinct compared to male mutant mice, in particular, female mutant mice demonstrated more secretory granules compared to male mutants, but less than female wild-type mice.

There were no signs of apoptosis such as chromatin condensation or apoptotic bodies (Herbach et al. 2007).

Additional quantitative-stereological analysis of pancreata at the age of 3 months revealed that the total β-cell volume of male mutants was only slightly, but not significantly reduced compared to age- and sex-matched wild-type mice (Herbach et al. personal communication).

In conclusion, male and female heterozygous Munich *Ins2*[C95S] mutant mice develop diabetes mellitus. Male mutants exhibit a progressive diabetic phenotype with severe hyperglycaemia, insulin resistance and profound reduction of β-cell mass, whereas female mutants demonstrate a mild and

stable diabetic phenotype, no signs of insulin resistance and unaltered β-cell mass.

2.3.2.2 Homozygous mutant mice

Homozygous Munich $Ins2^{C95S}$ mutant mice were phenotypically unsuspicious until the age of 18 days, when glucosuria was detected. At the age of 21 days, homozygous male and female mutants suffered from severely elevated blood glucose levels of approximately 400 mg/dl. The body weight was reduced versus wild-type mice at the age of 28 days, and further decreased until time of death. Male and female homozygous mutant mice died at a mean age of 46 and 52 days, respectively (Herbach et al. 2007).

2.3.3 The Akita mouse

The Akita mouse line arose from a spontaneous point mutation in a female C57BL/6 mouse (Yoshioka et al. 1997). The mutation is inherited by an autosomal dominant mode. A stable mouse line was established by breeding male heterozygous mutants with female wild-type C57BL/6J (B6) mice. The Akita mouse shows a G→A transversion at nucleotide position 1907 in exon 3 of the $Ins2$ gene on chromosome 7. Therefore, the cysteine on position 96 in the A chain of preproinsulin 2 is substituted by tyrosine (C96Y), which results in the loss of the A7-B7 interchain disulfide bond of insulin 2 (Wang et al. 1999).

In humans with PNDM, the identical mutation has been found in the INS gene (2.2.3.2 Neonatal diabetes mellitus (NDM)).

2.3.3.1 Heterozygous mutant mice

At the age of 4 weeks, male and female Akita mice presented significantly higher randomly fed blood glucose concentrations compared to sex- and age-matched B6 control mice (male: ~270 mg/dl vs. ~145 mg/dl; female: ~220 mg/dl vs. ~160 mg/d). In male mutants, blood glucose levels increased until the age of 9 weeks and remained relatively stable afterwards (approximately 550 - 600 mg/dl). In female mutants, blood glucose concentrations were lower than in male mutants (< 330 mg/dl).

The body weight of female mutant and wild-type mice was similar during the investigation period. Up to an age of 18 weeks, no differences in body weight

between male mutant and wild-type mice were detected. Afterwards male mutants demonstrated no further weight gain and lost body weight from 30 weeks of age onwards. The 50% survival rate of male mutants was less than half that of sex-matched wild-type mice, whereas the life expectancy of female mutant and wild-type mice was similar (Yoshioka et al. 1997).

The randomly fed plasma insulin levels of 7-week-old male and female mutants were significantly lower than those of sex- matched wild-type mice (male: 193 ± 51 pmol/l vs. 471 ± 73 pmol/l; female: 248 ± 82 pmol/l vs. 379 ± 78 pmol/l) (Yoshioka et al. 1997).

At 2 weeks of age, the insulin content in the pancreas of Akita mice was approximately half as high than that of wild-type mice (178 ± 2 vs. 361 ± 2 pmol/pancreas), whereas the glucagon content was similar in both genotypes (approximately 330 pmol/pancreas) (Kayo and Koizumi 1998). The insulin content in the pancreas of 8-week-old Akita mice was approximately 1/6 to 1/5 of that of wild-type mice (Oyadomari et al. 2002b).

In contrast to the reduced pancreatic insulin content, transcription of both *Ins1* and *Ins2* in isolated islets of 8- to 12-week-old Akita mice was barely altered. Total insulin mRNA levels in isolated islets of Akita mice were slightly reduced compared to wild-type mice, representing 85 - 90% of the total insulin mRNA of wild-type mice. In the islets of wild-type and mutant mice, around 25% of the transcripts accounted for *Ins1* and 75% for *Ins2*. The mutated and the wild-type *Ins2* alleles in the islets of mutant mice were transcribed in similar amounts (Wang et al. 1999). In contrast, Oyadomari et al. reported that insulin mRNA levels in the pancreas of 3-, 6- and 9- week old heterozygous mutant mice were higher than those of wild-type mice, probably in order to compensate for defective insulin secretion (Oyadomari et al. 2002b).

In pancreas sections of 4-, 10-, 20- and 30-week-old mice, immunostained for glucagon and insulin, no signs of inflammation were detected. The relative areas (%) of islets in the pancreas of male and female mutants were similar to those of age- and sex-matched wild-type mice, irrespective of age at sampling. At the age of 4 weeks, male and female mutant mice showed a significantly lower proportion of insulin-positive cells in the islets than sex-matched wild-type mice (male: 20.7 ± 4.7% vs. 71.2 ± 2.2%; female: 45.9 ± 2.7% vs. 83.1 ± 3.1%), whereas the proportion of glucagon-positive cells was similar in male mutant and wild-type mice (approximately 25%). In 30-week-old male mutants,

the proportion of insulin positive-cells was decreased to 9.1%, whereas it remained stable in female mutants and wild-type mice of both genders.

Immunofluorescence analyses using anti-insulin and anti-C-peptide antibodies, revealed a remarkably weaker staining intensity in most β-cells of 8- to 12-week-old mutants compared to age- and sex-matched wild-type mice. Since the insulin-autoantibody only detects the wild-type and not the mutated insulin, the reduced insulin-staining intensity in mutant β-cells indicates a reduction of wild-type insulin, the reduced C-peptide staining intensity a reduction of wild-type and mutant proinsulin (Wang et al. 1999).

The amount of TUNEL-positive cells in the islets of 13-week-old mutants was very low, but slightly increased compared to wild-type mice (0.47 vs. 0.15 TUNEL-positive cells per islet) (Izumi et al. 2003).

Electron microscopic analysis showed that the cytoplasm of β-cells of 4- to 18-week-old wild-type mice is loaded with dense-core secretory granules (Wang et al. 1999; Izumi et al. 2003). The average volume and the volume density of secretory granules of mutant mice were severely reduced versus wild-type mice (Zuber et al. 2004). In addition, earlier studies stated that the number of secretory granules was diminished in Akita mice versus control mice (Wang et al. 1999; Izumi et al. 2003), however, the numerical volume density of secretory granules was not altered (Zuber et al. 2004). The lumina of ER-like organelles distended progressively with age. In older mice, enlarged lysosomes were detected and mitochondria were often swollen and exhibited disrupted crests (Izumi et al. 2003). Morphometric analysis and quantitative immunogold labelling of the pancreas of 8- to 12-week-old mice showed that proinsulin accumulates mainly in the pre-Golgi intermediates of β-cells of mutant mice. In β-cells of mutants, the volume density of transitional ER was increased 2.8-fold and that of pre-Golgi intermediates 4.5- to 5.8-fold compared to control mice (Zuber et al. 2004). Immunogold labelling for C-peptide demonstrated that the distribution of proinsulin was different in wild-type and mutant mice: C-peptide immunoreactivity in the pre-Golgi intermediates of mutant mice accounted for 40% as compared to 20% in wild-type mice. In addition, mutants showed reduced C-peptide immunoreactivity in the secretory granules versus wild-type mice (43% vs. 80%). These findings indicate that proinsulin accumulates in the pre-Golgi intermediates of Akita

mice (Zuber et al. 2004). The studies of Wang et al. (1999) showed similar results: Insulin and C-peptide immunogold labeling in wild-type mice was mainly detected in the secretory granules of β-cells, whereas mutant mice exhibited weak labelling intensity in the secretory granules (Wang et al. 1999). No signs of apoptosis like nuclear chromatin condensation or fragmentation were detected in the β-cells of mutant and wild-type mice (Izumi et al. 2003).

In *in vitro* studies, using isolated islets of 4-week-old male mutant mice, a disturbed insulin secretion after incubation with 27.5 mM glucose compared to wild-type mice was shown (Yoshioka et al. 1997). An impaired insulin secretion was also detected in insulinoma cells, expressing one mutant *Ins2*[C96Y] allele (Nozaki et al. 2004).

2.3.3.2 Homozygous mutant mice

At day of birth, homozygous Akita mice demonstrated slightly elevated blood glucose levels and reduced body weight compared to heterozygous mutant and wild-type mice. Blood glucose concentrations rose rapidly, reaching approximately 450 mg/dl at the age of 14 days. The insulin content in the pancreas was severely reduced compared to wild-type mice at birth (15.6 vs. 114.6 pmol/pancreas) and further decreased to 3.9 pmol/pancreas at the age of 14 days (Kayo and Koizumi 1998).

The relative area (%) of islets in pancreas sections of 1- and 14-day-old homozygous mutants was less than half of that in heterozygous mutants and wild-type mice. The proportion of insulin-positive cells in the islets was only about 11%, whereas the proportion of glucagon-positive cells in the islets was largely increased, accounting for 51% and 41% at the age of 1 and 14 days, respectively. Electron microscopy of the pancreas of 14-day-old mice showed a decreased density of secretory granules, increased amount of ER and swollen mitochondria (Kayo and Koizumi 1998).

2.3.3.3 ER stress in the Akita mouse

It was demonstrated that the mutant proinsulin in the β-cells of Akita mice has an increased hydrophobicity compared to wild-type proinsulin. Therefore, mutant proinsulin tends to aggregate more easily than wild-type proinsulin, due to hydrophobic interactions between molecules. Furthermore, the free

cysteine residue on B7 of proinsulin can lead to incorrect disulfide bond formation, and the loss of the A7-B7 disulfide bond results in a reduced stability of mutant compared to wild-type proinsulin (Yoshinaga et al. 2005). Accumulation of misfolded (pro-)insulin was estimated to cause ER stress in the Akita mouse (Nozaki et al. 2004), which was evidenced in several studies (detailed information on ER stress is given in chapter 2.4 Endoplasmic reticulum stress (ER stress)):

It was shown that the ER stress chaperone binding Ig protein (BiP), also called glucose regulated protein 78 (GRP78), was overexpressed in the pancreatic islets of 8- to 12-week-old mutants, and probably forms complexes with proinsulin (Wang et al. 1999).

Allen et al. (2004) demonstrated that BiP and the ER-associated degradation (ERAD) components Hrd1 and SelIL were upregulated in the islets of Akita mice, and X-box binding protein 1 (XBP-1) splicing levels were elevated compared to wild-type mice. These findings led to the conclusion that the misfolded insulin is selectively ubiquitinated and degraded by a HRD1-mediated ERAD pathway (Allen et al. 2004).

In $Ins2^{WT/C96Y}$ insulinoma cells, the expression of the chaperones BiP/Grp78, Grp94 and oxygen-regulated protein 150 (ORP150) was induced in an ER stress response element (ERSE)-dependent mode. Furthermore it was shown that the levels of activating transcription factor 6 (ATF6) and spliced XBP-1 were also increased in $Ins2^{WT/C96Y}$ insulinoma cells compared to in $Ins2^{WT/WT}$ insulinoma cells (Nozaki et al. 2004).

$Chop$ knockout mice expressing the mutant $Ins2^{C96Y}$ were created to investigate the involvement of C/EBP homologous protein (CHOP)/growth arrest and DNA damage 153 (GADD153) in the ER stress response of Akita mice. In 8-week-old $Ins2^{C96Y/C96Y}$ mice, the disruption of $Chop$ had no influence on body weight, blood glucose concentration and pancreatic insulin content. In $Ins2^{WT/C96Y}$ $Chop^{-/-}$ mutants the onset of diabetes was delayed by 8 - 10 weeks compared to $Ins2^{WT/C96Y}$ $Chop^{+/+}$ and $Ins2^{WT/C96Y}$ $Chop^{-/+}$ mice. Additionally, it was demonstrated that the number of apoptotic cells in islets of 4-week-old $Ins2^{WT/C96Y}$ $Chop^{-/-}$ mice was significantly lower than in those of $Ins2^{WT/C96Y}$ $Chop^{+/+}$ mice (Oyadomari et al. 2002b).

Targeted disruption of the chaperone ORP150 aggravated the diabetic phenotype of Akita mice ($Ins2^{WT/C96Y}$ $ORP150^{-/+}$ mice), whereas

overexpressing of the chaperone ORP150 improved insulin sensitivity in Akita mice ($ORP150^{CAG}Ins2^{WT/C96Y}$ mice) (Ozawa et al. 2005).

In conclusion, these findings show that misfolded (pro-)insulin 2 aggregates and accumulates in the β-cells of Akita mice, which leads to the induction of the unfolded protein response (UPR), resulting in the activation of chaperones (e.g. BiP) and in the partial degradation of misfolded insulin via ER-associated degradation I (ERADI). The activation of CHOP in heterozygous Akita mice is involved in β-cell apoptosis and enforces the progression of diabetes mellitus in heterozygous Akita mice.

2.3.4   *Ins1* and *Ins2* null mutant mice

Insulin deficient ($Ins1^{-/-}$, $Ins2^{-/-}$) and single *Ins1* or *Ins2* knockout mice ($Ins1^{-/-}$, $Ins2^{+/+}$ and $Ins1^{+/+}$, $Ins2^{-/-}$) were created by disruption of *Ins1* and/or *Ins2* via gene targeting. For the creation of $Ins2^{-/-}$ mice, *LacZ* was inserted under the control of the *Ins2* promoter for β-cell identification. The targeting vectors were transfected into D3 embryonic stem (ES) cells and recombinant D3 ES cells were used to create different male germ-line chimeras. Stable mouse lines were established by back-crossing male germ-line chimeras with female wild-type C57BL/6J (B6) mice (Duvillie et al. 1997).
The absence of insulin 1 and insulin 2 mRNA in the islets of single and double homozygous mice was proven via reverse transcriptase-PCR, the absence of C-peptide 1 and C-peptide 2 via immunohistochemistry (Duvillie et al. 1997; Leroux et al. 2001).

2.3.4.1   Double homozygous null mutant mice

The embryonic mortality of $Ins1^{-/-}$, $Ins2^{-/-}$ mutant mice was not increased compared to wild-type and various heterozygous mutant mice. A growth-retardation of 15 -20 % was already observed at day 18 of fetal life (Duvillie et al. 1997). At embryonic day 18.5 (E18.5) $Ins1^{-/-}$, $Ins2^{-/-}$ showed similar blood glucose concentrations compared to $Ins1^{-/-}$, $Ins2^{-/+}$ mutants (56 ± 10 mg/dl vs. 58 ± 12 mg/dl) (Duvillie et al. 2002). Soon after suckling, $Ins1^{-/-}$, $Ins2^{-/-}$ mutants exhibited glucosuria and ketoacidosis. A few hours after birth, double homozygous mutants were around 20% lighter than wild-type and heterozygous mutant mice. Hepatomegaly and liver steatosis were observed.

The homozygous mutant pubs died at a mean age of 48 hours (Duvillie et al. 1997).

$Ins1^{-/-}$, $Ins2^{-/-}$ mutant mice showed a significantly increased mean islet area from day E18.5 onwards compared to $Ins1^{-/-}$, $Ins2^{-/+}$ mutants and wild-type mice (Duvillie et al. 1997; Duvillie et al. 2002). The relative increase of mean islet size detected in $Ins1^{-/-}$, $Ins2^{-/-}$ was probably due to a higher replication rate of endocrine cells within the existent islets. Additionally, the level of apoptosis was significantly lower in $Ins1^{-/-}$, $Ins2^{-/-}$ compared to $Ins1^{-/-}$, $Ins2^{-/+}$ mutants at E18.5 and at birth (Duvillie et al. 2002).

Most of the endocrine cells in the islets of all animal groups investigated were β-cells, as visualised by insulin immunohistochemistry or X-Gal staining (Duvillie et al. 1997; Duvillie et al. 2002). Morphometric analysis revealed that at E18.5 around 75% of the endocrine cells in the islets of $Ins1^{-/-}$, $Ins2^{-/-}$ and $Ins1^{-/-}$, $Ins2^{-/+}$ mutants were β-cells, and 16 - 21% represented α-cells. Due to an increase of the mean islet area in the pancreas, both, the total estimated β-cell and α-cell mass were increased in $Ins1^{-/-}$, $Ins2^{-/-}$ as compared to $Ins1^{-/-}$, $Ins2^{-/+}$ and wild-type mice. The authors conclude that insulin may be a negative regulator of islet size *in utero* (Duvillie et al. 2002).

The mRNA levels of pancreatic polypeptide and somatostatin of newborn $Ins1^{-/-}$, $Ins2^{-/-}$ were severely reduced compared to wild-type mice (Duvillie et al. 1997).

2.3.4.2   Single homozygous null mutant mice

It was demonstrated that compensatory mechanisms prevent single homozygous mutant mice from developing diabetes mellitus. Since insulin 2 is the major form of insulin in wild-type mice, the compensatory mechanisms were more pronounced in mice lacking *Ins2* than in those lacking *Ins1* (Leroux et al. 2001).

Single homozygous null mutants for *Ins1* ($Ins1^{-/-}$, $Ins2^{+/+}$) or *Ins2* ($Ins1^{+/+}$, $Ins2^{-/-}$) were viable and fertile (Duvillie et al. 1997). $Ins2^{-/-}$ mice showed transient hyperglycaemia during the first week of life. From 1 week of age onwards, blood glucose concentrations of $Ins1^{-/-}$ and $Ins2^{-/-}$ mutants were similar to those of wild-type mice. Four- to 6-month-old $Ins2^{-/-}$ mice showed intraperitoneal glucose tolerance tests comparable to wild-type mice (Leroux et al. 2001).

In 2- to 4-month-old $Ins2^{-/-}$ mutants, the absence of insulin 2, which accounts for the major proportion of total insulin transcripts in the pancreas of wild-type mice, was compensated by a large increase in $Ins1$ transcripts. $Ins2$ transcription levels of $Ins1^{-/-}$ mutants were comparable to those of wild-type mice.

According to western blot analysis, $Ins2^{-/-}$ mutants seemed to exhibit a considerable higher insulin 1 expression in the pancreas than wild-type mice. In $Ins1^{-/-}$ mutants, the expression of insulin 2 appeared to be slightly increased compared to wild-type mice.

Total insulin levels in the plasma and in the pancreas of 2- to 4-month-old wild-type mice, $Ins1^{-/-}$ and $Ins2^{-/-}$ mutants were similar, demonstrating that the increased transcription of $Ins1$ in the pancreas of $Ins2^{-/-}$ mutants results in a quantitative compensation on the protein level (Leroux et al. 2001).

At the age of 2 to 4 months, pancreatic sections immunostained for C-peptide 1, C-peptide 2, glucagon, somatostatin and pancreatic polypeptide exhibited normal islet morphology and unaltered distribution of the distinct endocrine cells in both single homozygous mutant mouse strains. In sections immunostained for insulin, the β-cell mass of $Ins2^{-/-}$ mutants was elevated almost 3-fold, in $Ins1^{-/-}$ mutants, β-cell mass was slightly but significantly increased as compared to wild-type mice (Leroux et al. 2001).

The compensatory $Ins1$ transcription of $Ins2$ deficient β-cells was confirmed in *in vitro* studies with βIns2$^{-/-lacZ}$ cells. These cells showed largely elevated $Ins1$ transcription levels and similar total insulin content compared to other murine β-cell lines, in which both Ins genes are functional. Additionally, a dose dependent elevation of insulin secretion after incubation of βIns2$^{-/-lacZ}$ cells in Krebs-Ringer secretion buffer with different glucose concentrations was observed (Leroux et al. 2003).

2.4 Endoplasmic reticulum stress (ER stress)

2.4.1 The Endoplasmic reticulum

The endoplasmic reticulum (ER) is a cell organelle which plays a crucial role in lipid and sterol synthesis, protein folding and post-translational modification. Additionally it serves as calcium store (Oyadomari et al. 2002a; Rajan et al. 2007).

Specific transport systems ensure that proteins are targeted to the endoplasmic reticulum. A signal recognition particle (SRP) binds to the signal sequence of a nascent protein as it emerges from the ribosome, which results in the formation of the SRP/ribosome-nascent-chain (RNC) complex. The SRP/RNC complex binds to the SRP-receptor of the ER membrane and the protein is translocated co- or sometimes post-translationally across the ER membrane via a channel mainly formed by the Sec61 protein (Walter and Johnson 1994; Römisch et al. 2003; Luirink and Sinning 2004). The SRP and SRP-receptor dissociate from each other and can enter the next targeting cycle. In most cases the signal sequence of the protein is cleaved by a signal peptidase on the luminal side of the ER membrane. In yeast also a SRP-independent pathway was identified (Walter and Johnson 1994).

The ER exhibits a calcium-rich and oxidative environment, essential for oxidative protein folding like disulfide bond formation and for post-translational modifications (Ma and Hendershot 2002; Xu et al. 2005). There exist several post-translational modifications such as acetylation, amidation, phosphorylation, sulfation, hydroxylation, glycosylation and disulfide bond formation. The most common form is glycosylation, which plays a crucial role for protein conformation, trafficking and function (Walsh and Jefferis 2006; Gabius (Ed.) 2009). Disulfide bond formation, catalysed by protein disulfide isomerases (PDI) and their relatives (Dsb proteins), is essential for folding, stability and function of proteins (Arolas et al. 2006). Lectins, e.g. the calnexin-calreticulin cycle, protein foldases and molecular chaperones like binding Ig protein (BiP)/glucose regulated protein 78 (GRP78) and GRP94 are important for protein folding (Rajan et al. 2007).

Properly folded proteins are transferred from the ER to the transitional ER, from there to the pre-Golgi intermediate, and finally to the Golgi apparatus.

COPII-coated vesicles derived from the transitional ER, mediate the anterograde trafficking from the ER to the Golgi apparatus, whereas COPI-coated vesicles are essential for the retrograde transfer from the Golgi back to the ER (Fan et al. 2003; Lee et al. 2004).

A so called "quality control" system in the ER ensures that only correctly folded, assembled and modified proteins are transported out of the ER, whereas most misfolded or unassembled proteins are retained and degraded (Ellgaard and Helenius 2001; Kincaid and Cooper 2007b).

2.4.2 ER stress and the unfolded protein response (UPR)

ER stress can be induced pharmacologically and by changes in the physiological environment (Ma and Hendershot 2002). Agents like thapsigargin, tunicamycin and dithiothreitol (DTT) are frequently used to activate ER stress in *in vitro* studies (Harding et al. 2000; Rutkowski et al. 2006; Scheuner and Kaufman 2008). Mutations of ER chaperones, viral infections, metabolic disorders like glucose deprivation and hypercysteinaemia, aberrant Ca^{2+} regulation, hypoxia, changes in the redox status, misfolded proteins or an increased synthesis of client proteins can cause ER stress and induce the so called unfolded protein response (UPR) (Ma and Hendershot 2002; Rutkowski and Kaufman 2004; Scheuner and Kaufman 2008). The UPR recognises the accumulation of un- and misfolded proteins and activates target genes in the nucleus. These target genes have a consensus sequence in their promoters, the ER stress response element (ERSE), ERSE II and the unfolded protein response element (UPRE) (Oyadomari et al. 2002a; Yamamoto et al. 2004).

At least 3 distinct mechanisms of the UPR exist to reduce ER stress and restore normal ER function. Transcriptional induction of ER chaperones like BiP, GRP94 and activation of enzymes like PDI facilitate protein folding. To avoid further accumulation of un- and misfolded proteins the translation of mRNA is attenuated by inactivation of eucaryotic initiation factor 2 alpha (eIF2α). Misfolded proteins are eliminated by ER-associated degradation (ERAD) (Oyadomari et al. 2002a; Shen et al. 2002; Laybutt et al. 2007). Soluble proteins are retrotranslocated to the cytosol and degraded by the ubiquitin-proteasome system (ubiquitin/proteasome ERAD; ERAD I). Another

ERAD system (autophagy/lysosome ERAD; ERAD II) was reported to degrade insoluble, aggregated proteins by autophagy (Fujita et al. 2007).

When these 3 adaptive mechanisms don't succeed in restoring normal ER function, severe and chronic ER stress causes apoptosis of the affected cell, the fourth ER stress response of the UPR (Oyadomari et al. 2002a; Liu and Kaufman 2003).

2.4.2.1   Signal transduction

The transmembrane proteins inositol requiring 1 (IRE1), double-stranded RNA-activated protein kinase (PKR) – like endoplasmic reticulum kinase (PERK) and activating transcription factor 6 (ATF6) transmit ER stress signals across the ER membrane (Rajan et al. 2007; Yamamoto et al. 2007). The chaperone BiP regulates the 3 stress transducers and therefore controls the expression of most ER stress target genes (Shen et al. 2002) (Figure 2.1).

PERK and IRE1 are type-I-transmembrane serine/threonine protein kinases and exhibit limited homology in the amino acid sequences of the ER luminal domain (Liu et al. 2000). In the inactive state, the ER chaperone BiP forms a stable complex with the luminal domain of PERK and IRE1. ER stress induces the dissociation of BiP, which results in the oligomerisation of PERK and IRE1 (Bertolotti et al. 2000). ATF6, a type II transmembrane protein, is also bound to BiP in its inactive state. Upon ER stress, BiP dissociates from ATF6, and ATF6 is translocated to the Golgi apparatus (Shen et al. 2002).

PKR-like endoplasmic reticulum kinase (PERK)

Oligomerised and autophosphorylated PERK phosphorylates eIF2α at serine 51 of the α-subunit and the transcription factor Nrf2 (Oyadomari et al. 2002a; Cullinan et al. 2003). Phosphorylated eIF2α (PeIF2α) can not longer mediate the binding of the initiator Met-tRNA to the 43S ribosomal unit. Protein synthesis and thereby protein-folding load are reduced (Harding et al. 1999; Rajan et al. 2007). Although phosphorylation of eIF2α represses the translation of most mRNAs, it increases that of activating transcription factor 4 (ATF4) (Vattem and Wek 2004; Rajan et al. 2007).

ATF4 induces the transcription of chaperone BiP and transcription factor CHOP, the latter being involved in the regulation of apoptosis (2.4.2.2 Apoptotic pathways) (Scheuner et al. 2001; Kojima et al. 2003; Scheuner and

Kaufman 2008). Furthermore, ATF4 activates genes which participate in amino acid transport, metabolism and assimilation, and those which are known to be induced by oxidative stress like heme oxygenase-1 (Hmox-1) and sequestosome-1/A170 (Sqsm1) (Harding et al. 2003).

In the cytoplasm of unstressed cells, Nrf2 forms a complex with actin-binding protein Keap1. In response to ER stress, PERK induces the phosphorylation of Nrf2 and thereby the dissociation of Keap1. Nrf2 is translocated to the nucleus where it activates the transcription of genes involved in detoxification and antioxidant defence like phase II detoxifying enzymes, catalase, superoxide dismutase 1, γ-glutamylcysteine synthase and UDP-glucuronosyl-transferase. Therefore Nrf2 plays an important role for cellular redox homeostasis and cell survival (Chan and Kan 1999; Chan et al. 2001; Cullinan et al. 2003).

Inositol requiring 1 (IRE1)

In mammalians two IRE1 proteins exist, IRE1α and IRE1β. IRE1α is broadly expressed, whereas IRE1β is gut-specific (Rajan et al. 2007; Yamamoto et al. 2007). IRE1 contains serine/threonine kinase and cytoplasmic ribonuclease domains (Pirot 2007). Oligomerisation of IRE1 enables the autophosphorylation of IRE1 and the activation of its endoribonuclease activity. Activated IRE1 splices a small intron from the X-box binding protein-1 (XBP-1) mRNA (Calfon et al. 2002; Lee et al. 2003). The cleaved XBP-1 mRNA is translocated to the nucleus and induces transcription of ER resident chaperones, ERAD and other components of the quality control system, including EDEM, Derlin 1-3, and HRD1, RAMP4, PDI-P5, p58IPK, Erdj4 (Lee et al. 2003; Rajan et al. 2007).

The involvement of XBP-1 in the activation of CHOP is controversially discussed. It was stated that cleaved XBP-1 binds to ERSE and induces CHOP transcription in a NF-Y dependent manner (Oyadomari and Mori 2003), whereas in XBP-1$^{-/-}$ mouse embryo fibroblasts (MEF) the induction of CHOP was not or only slightly impaired (Lee et al. 2003).

IRE1 causes rapid degradation of a specific subset of mRNAs, independ from XBP-1, and therefore reduces the intracellular protein load (Hollien and Weissman 2006).

Furthermore, IRE1 is involved in ER stress-mediated apoptosis by activating c-Jun NH_2 terminal kinases (JNK) and nuclear factor-κB (NF-κB) (2.4.2.2 Apoptotic pathways).

Activating transcription factor 6 (ATF6)

ATF6α and ATF6β are expressed ubiquitously in mammalian cells (Yamamoto et al. 2007). Experiments with distinct knockout mice and mouse embryo fibroblasts (MEF) demonstrated that ATF6β is less important concerning the ER stress response than ATF6α (Lee et al. 2003; Yamamoto et al. 2007). The dissociation of BiP from ATF6 results in the unveiling of Golgi localisation signals (GLS) on ATF6. ATF6 is then translocated from the ER to the Golgi, where it is cleaved by site-1 and site-2 protease (S1P, S2P). The cleaved cytosolic fragment of ATF6 dissociates to the nucleus to activate ER stress target genes, encoding chaperones such as BiP, GRP94 and PDI-like folding enzyme P5 and Erp61 (Shen et al. 2002; Yamamoto et al. 2007).

In *in vitro* studies, ATF6 was unable to bind to UPRE, in contrast to XBP-1 (Lee et al. 2003; Yamamoto et al. 2007). However, it was stated that ATF6 can heterodimerise with cleaved XBP-1 from the IRE1-XBP-1 pathway in order to bind to UPRE and activate ERAD components like EDEM and HRD1. The IRE1-XBP-1 heterodimer had an 8-fold higher affinity to the UPRE than the XBP-1 homodimer (Yamamoto et al. 2007).

ATF6 seems to be marginally, if at all, involved in the activation of CHOP (Ma et al. 2002; Okada et al. 2002; Lee et al. 2003; Yamamoto et al. 2007).
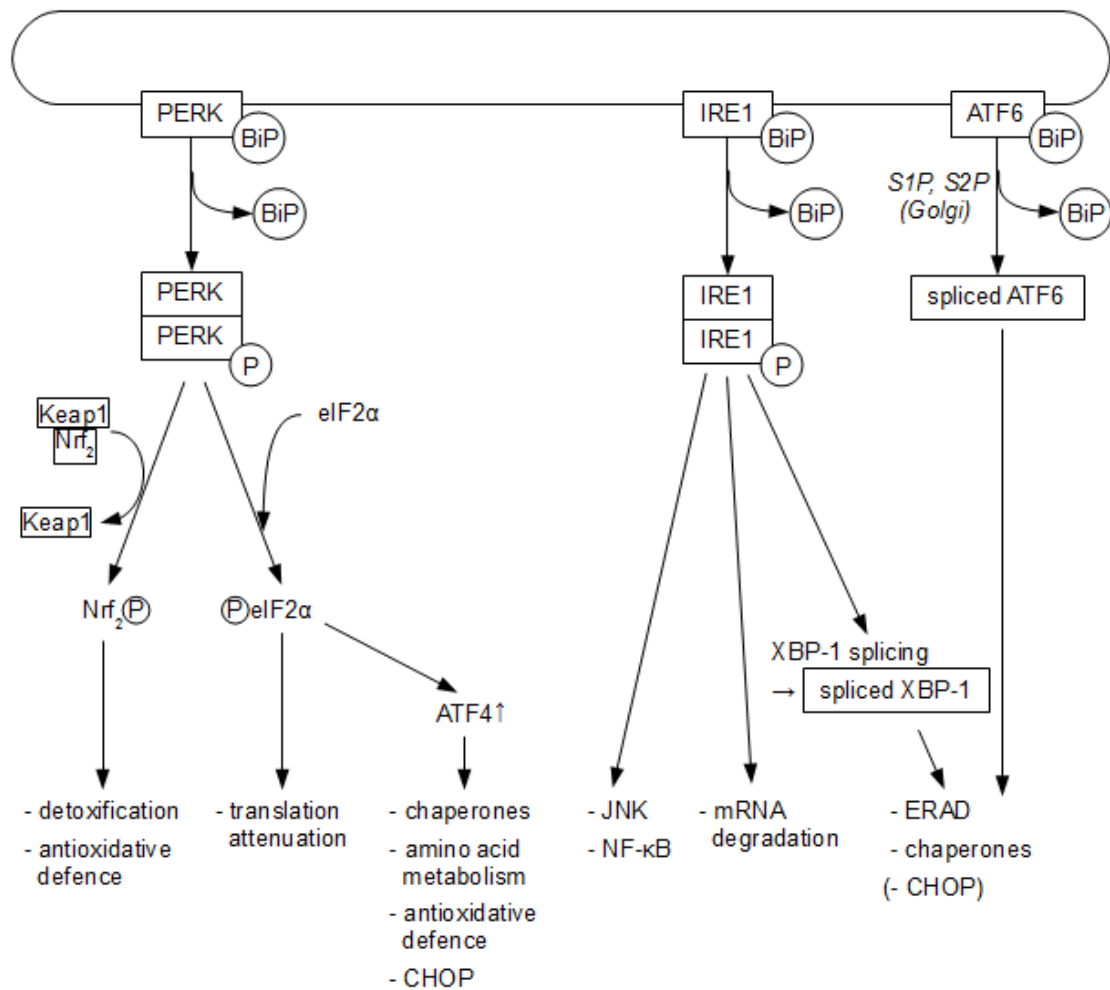
Figure 2.1 ER stress signal transduction

In the inactive state, the transmembrane proteins PERK, IRE1 and ATF6 form stable complexes with the chaperone BiP. Upon ER stress, BiP dissociates from PERK, IRE1 and ATF6, which results in the activation of PERK, IRE1 and ATF6. Homodimerised and autophosphorylated PERK phosphorylates eIF2α and Nrf2. Phosphorylated eIF2α (PeIF2α) attenuates the translation of most mRNAs and activates that of ATF4 mRNA. ATF4 regulates the expression of genes involved in amino acid metabolism, anti-oxidative defence, protein folding (chaperones) and apoptosis (CHOP). In the inactive state Nrf2 is bound to Keap1. Phosphorylation of Nrf2 leads to the dissociation of Keap1 and activated Nrf2 is translocated to the nucleus to induce the transcription of genes participating in detoxification and redox homeostasis. Oligomerised and autophosphorylated IRE1 splices XBP-1 mRNA, degrades a specific subset of mRNAs and is involved in apoptosis via activation of JNK and NF-kB. After BiP dissociation from ATF6, ATF6 is translocated to the Golgi, where it is cleaved by proteases (S1P and S2P). Spliced XBP-1 and ATF6 induce the expression of genes encoding for chaperones and ERAD-associated proteins. The involvement of XBP-1 and ATF6 in the activation of CHOP is unclear.

2.4.2.2 Apoptotic pathways

When the UPR fails to resolve ER stress, affected cells undergo apoptosis. Three different apoptotic pathways concerning ER stress have been identified, the activation of CHOP, JNK and caspases 12 and 8 (Jimbo et al. 2003; Liu and Kaufman 2003; Rajan et al. 2007).

C/EBP homologous protein (CHOP)

The transcription factor CHOP, also called growth arrest and DNA damage 153 (GADD153), is a member of the CCAAT/enhancer binding proteins (C/EBP) and is expressed at very low levels under physiological conditions. CHOP can be induced upon different adverse conditions, including ER stress (Oyadomari and Mori 2003). ATF4 activates CHOP, whereas the involvement of spliced ATF6 and XBP-1 in the induction of CHOP transcription is controversially discussed (2.4.2.1 Signal transduction).

CHOP directly activates transcription of *GADD34*, which results in the dephosphorylation of PeIF2α via an eIF2α-specific phosphatase, and therefore results in increased client protein synthesis and protein load in the ER (Kojima et al. 2003; Marciniak et al. 2004). The transcription of several genes is regulated by CHOP, including those that are involved in apoptosis. Death receptor 5DR5, tribbles 3 (TRB3) and the BH3-only member protein Bim, for example, are upregulated by CHOP (Ohoka et al. 2005; Pirot 2007; Puthalakath et al. 2007; Scheuner and Kaufman 2008), whereas the anti-apoptotic protein Bcl2 was stated to be down-regulated when CHOP is overexpressed (McCullough et al. 2001).

CHOP seems also to induce oxidative stress, since increased expression of CHOP is associated with up-regulation of ER oxidoreductase 1 (ERO1) (Marciniak et al. 2004), depletion of glutathione and elevated production of reactive oxygen species (ROS) (McCullough et al. 2001).

C-Jun NH$_2$ terminal kinase (JNK) and nuclear factor-κB (NF-κB)

JNKs are members of the mitogen-activated protein kinases (MAPK) family. JNK is triggered by several activators like proinflammatory cytokines, distinct infections and ER stress (Bogoyevitch and Kobe 2006). In response to ER stress the cytoplasmic domain of IRE1 binds to the adaptor protein TNF receptor-associated factor 2 (TRAF2) (Urano et al. 2000). IRE1 and TRAF2

form a complex together with apoptosis signal-regulating kinase 1 (ASK1), which results in the phosphorylation and activation of JNK (Nishitoh et al. 2002). Activated JNK phosphorylates target proteins on serine and threonine residues, leading either to the enhancement or inhibition of their activity. Many of these proteins are transcription factors like *c*-Jun, *c*-Myc, TRAF2, ELK1, p53, STAT1; STAT3 and Pax2, others are nuclear hormone receptors like glucocorticoid receptor, retionic receptor RARα and RXRα and further non-transcription factors. Some of the transcription factors activated by JNK, are involved in apoptosis, like *c*-Myc, p53 and mitochondrial transcription factors Bcl-xL, Bax and Bim (Bogoyevitch and Kobe 2006).

The activation of NF-κB was reported to be involved in ER stress-mediated apoptosis, too. NF-κB can be activated by various endogenous and exogenous stimuli, like hyperglycaemia, oxidative stress, elevated free fatty acids, TNFα, IL-1, growth factors (Bierhaus et al. 2001) and ER stress (Hu et al. 2006). In the inactive state, NF-κB forms a complex with inhibitor κB (IκB). Activation of IκB kinase (IKK) leads to the phosphorylation and degradation of IκB and to the translocation of NF-κB to the nucleus. It was reported that upon ER stress, IRE1α forms a complex with IKK, mediated by TRAF2, resulting in the degradation of IκB and subsequently in the activation of NF-κB. NF-κB regulates the transcription of several genes including those demonstrating proapoptotic (e.g. Fas ligand, TNFα, TRAIL) or antiapoptotic functions (e.g. TRAF1, TRAF2, c-FLIP) (Hu et al. 2006).

Caspase 12 and 8

Caspases, a family of cysteine proteases, play a crucial role in the regulation of apoptosis (Degterev et al. 2003). Calcium release from the ER due to ER stress, activates the cytosolic protease calpain, which cleaves and activates the initiator caspase 12 (Tan et al. 2006). Cleaved caspase 12 in turn can activate caspase 9 in a cytochrome *c* independent manner (Morishima et al. 2002; Tan et al. 2006).

Upon ER stress, caspase 8 is also activated and cleaves Bid, a member of the Bcl-2-family. The Bid fragment is translocated to the mitochondria and stimulates cytochrome *c* release, resulting in the activation of caspase 9 (Jimbo et al. 2003).

2.4.3 Diabetes mellitus and ER stress

2.4.3.1 Pathophysiological induction of ER stress

The main function of pancreatic β-cells is the production, storage and secretion of insulin. Increasing blood glucose levels, for example after meal intake, stimulate the biosynthesis of insulin (Andrali et al. 2008). Elouli et al. (2007) demonstrated that stimulation of rat islets with different glucose concentrations (2 - 30 mM) activates the UPR, in a protein biosynthesis dependent manner (Elouil et al. 2007). Elevated insulin demand in insulin resistant and/or hyperglycaemic diabetic individuals leads to increased proinsulin biosynthesis and proinsulin folding, which can induce ER stress (Scheuner and Kaufman 2008).

In Type 1 diabetes, cytokines are produced during the autoimmune destruction of β-cells (2.2.1 Diabetes type 1). It was demonstrated that exposure of insulin-producing insulinoma-1E ((INS)-1E) cells to cytokines like IL-1β and interferon-γ (IFNγ) results in an indirect and time-dependent activation of ER stress, via nitric oxide ($^{\bullet}$NO) production (Kharroubi et al. 2004). Il-1β alone or in combination with IFNγ, but not IFNγ alone, reduced the expression of sarcoendoplasmic reticulum pump Ca^{2+} ATPase 2b (SERCA2b), which resulted in the depletion of ER Ca^{2+} and activation of ER stress (Cardozo et al. 2005).

Type 2 diabetes is often associated with obesity and elevated triglyceride levels (2.2.2 Diabetes type 2). Incubation of insulin-secreting (INS)-1E cells, MIN6 cells and isolated islets of obese insulin-resistant *db/db* mice with the free fatty acid (FFA) palmitate induced ER stress and caused apoptosis in a time-dependent mode (Kharroubi et al. 2004; Laybutt et al. 2007). After exposure to the FFA oleate, ER stress response and β-cell apoptosis were lower (Kharroubi et al. 2004) or virtually not detectable (Laybutt et al. 2007) compared to palmitate incubation.

In type 2 diabetics, human islet amyloid polypeptide (hIAPP) can aggregate and form toxic oligomers, whereas rodent IAPP (rIAPP) doesn't show this characteristic. In experiments with homozygous transgenic mice overexpressing either rIAPP or hIAPP, hIAPP, but not rIAPP induced ER stress and β-cell apoptosis, leading to the developement of diabetes mellitus. These findings indicate that the toxic effects of hIAPP on β-cells are mainly

due the propensity of hIAPP to aggregate and less due to protein overexpression (Huang et al. 2007).

2.4.3.2 Gene alterations in animal models and men

Several human diseases and animal models serve to investigate the relationship between ER stress and diabetes mellitus.

PERK

PKR-like endoplasmic reticulum kinase (PERK) is essential for reducing the protein folding load, for activating the expression of BiP and CHOP, for reducing oxidative stress and for amino acid metabolism (2.4.2.1 Signal transduction).

Mutations in the *EIF2AK3* gene, which encodes for PERK, were detected in patients suffering from the Wolcott-Rallison syndrome (WRS). This autosomal recessive disease shows different clinic manifestations including early-infancy diabetes mellitus. A slight residual enzyme activity was associated with a delayed onset of WRS compared to patients with complete PERK inactivation (Senee et al. 2004).

PERK$^{-/-}$ mice were born with a normally developed endo- and exocrine pancreas and physiological blood glucose concentrations. Within less than 4 weeks they showed growth retardation, severe hyperglycaemia, reduced insulin secretion and increased β-cell loss. In addition to the progressive diabetic phenotype, PERK$^{-/-}$ mice developed exocrine pancreas insufficiency. IRE1α levels were increased, indicating ER stress (Harding et al. 2001).

ATF6

Activating transcription factor 6 (ATF6) participates in protein folding and degradation under ER stress conditions (2.4.2.1 Signal transduction).

Double knockout (ATF6$\alpha^{-/-}$ and ATF6$\beta^{-/-}$) resulted in embryonic death, whereas mice carrying single null mutations (ATF6$\alpha^{-/-}$ or ATF6$\beta^{-/-}$) developed normally (Yamamoto et al. 2007). Upon ER stress, ATF6$\alpha^{-/-}$ mouse embryonic fibroblasts demonstrated a reduced activation of ER stress-associated chaperones like BiP, Grp94 as well as folding enzymes (ERp72 and P5) and a decreased induction of various ERAD components, resulting in diminished

viability of ATF6$\alpha^{-/-}$ MEFs compared to ATF6$\alpha^{+/+}$ MEFs under ER stress conditions.

Amino acid variants in the *ATF6* gene were associated with type 2 diabetes in Pima Indians (Thameem et al. 2006).

CHOP

The transcription factor C/EBP homologous protein (CHOP) is involved in ER stress-mediated apoptosis (2.4.2.2 Apoptotic pathways).

The targeted disruption of *Chop* reduced β-cell apoptosis in 4-week-old heterozygous Akita mice and delayed the onset of diabetes (2.3.3.3 ER stress in the Akita mouse). Song et al. (2008) reviewed distinct mouse models for diabetes (e.g. Lepr$^{-/-}$, eIF2$\alpha^{S/A}$ and STZ-treated mice) in which *Chop* deletion improved glycaemic control, β-cell function and β-cell survival upon ER stress (Song et al. 2008).

Insulin gene

Different mutations in the insulin gene were described in men and mice. Mutations which disturb disulfide bond formation result in a severe diabetic phenotype, with early onset and profound β-cell loss, as it is described in human patients with PNDM (2.2.3.2 Neonatal diabetes mellitus (NDM)), in the Munich *Ins2*^{C95S} mutant mouse (2.3.2 The Munich *Ins2*^{C95S} mutant mouse), and in the Akita mouse (2.3.3 The Akita mouse). It was demonstrated that misfolded (pro-)insulin 2 induces ER stress in the Akita mouse (2.3.3.3 ER stress in the Akita mouse).

Wolfram syndrome

Wolfram syndrome is a rare autosomal rezessive disorder causing juvenile onset diabetes mellitus, optic atrophy and often sensorineural hearing loss or diabetes insipidus (Fonseca et al. 2005; Ueda et al. 2005). *WFS1* encodes for a protein located in the ER membrane and plays an important role in maintaining homeostasis in the ER of pancreatic β-cells. WFS1 might be involved in the UPR, and ER stress activates WFS1 expression. Inactivation of *WFS1* in β-cells resulted in chronic ER stress (Fonseca et al. 2005; Ueda et al. 2005).

2.4.3.3 Therapeutic strategies for reducing ER stress

Chemical chaperones were demonstrated to stabilise protein conformation and increase ER folding capacity. Oral treatment of *ob/ob* mice with 4-phenyl butyric acid (PBA) or tauroursodeoxycholic acid (TUDCA) improved blood glucose concentrations, glucose tolerance and insulin sensitivity and reduced ER stress in liver and fatty tissue (Özcan et al. 2006).

Oxidative stress can induce ER stress and vice versa, and antioxidative treatment reduced ER stress *in vitro* (2.6 Linkage between oxidative and ER stress). Therefore, treatment with antioxidants possibly contributes to the reduction of ER stress (Malhotra et al. 2008).

CHOP is involved in apoptosis upon ER stress, and deletion of *Chop* delayed the onset of diabetes in heterozygous Akita mice. *Chop*^{-/-} mice were phenotypically inconspicuous and presented a normal lifespan. Therefore specific CHOP inhibitors would be another promising therapeutic approach to preserve β-cells mass upon ER stress (Scheuner and Kaufman 2008).

2.5 Glucotoxicity and oxidative stress

Chronically elevated blood glucose concentrations over months and years have adverse effects on pancreatic β-cell function and viability, can disturb insulin signalling and lead to the development of long-term diabetic complications like retinopathy, nephropathy, neuropathy and cardiovascular disease (Evans et al. 2002; Kaiser et al. 2003; Robertson 2004; Robertson and Harmon 2006; Tsuboi et al. 2006; Shah et al. 2007).

Several pathways have been identified, demonstrating how long-term hyperglycaemia results in these adverse effects: glucose autoxidation (Robertson 2004; Ahmed 2005), polyol pathway (Chung et al. 2003), hexosamine pathway (Du et al. 2000; Brownlee 2005), protein kinase C (PKC) activation (Koya and King 1998; Ohshiro et al. 2006), production of advanced glycation endproducts (AGEs) (Schmidt and Stern 2000; Ahmed 2005), and increased oxidative phosphorylation (Korshunov et al. 1997; Nishikawa et al. 2000; Brownlee 2005). All these pathways lead to the generation of free radicals, which cause chronic oxidative stress (Robertson 2004).

Additionally, in type 1 diabetes, the autoimmune response results in inflammation and increased oxidative stress, e.g. due to superoxide ($^{\bullet}O_2^{-}$)

release from monocytes and production of reactive oxygen species (ROS) by cytokines (Devaraj et al. 2006; Robertson and Harmon 2006).

2.5.1 Free radicals and oxidative stress

Free radicals have both, beneficial and deleterious effects.

In physiological concentrations, free radicals like nitric oxide ($^{\bullet}NO$) and $^{\bullet}O_2^-$ support reactions like vasodilation (Beckman et al. 2003), immune response and other physiological pathways. Several ROS-mediated reactions even maintain redox homeostasis (Valko et al. 2007).

A disturbed equilibrium between generation of free radicals and antioxidant capacity, due to increased production of free radicals, reduced antioxidant defence mechanism or both, results in oxidative stress (Betteridge 2000; Maritim et al. 2003). Oxidative stress is involved in aging and is associated with several diseases like cancer, cardiovascular disease, Alzheimer's disease, Parkinson's disease, rheumathoid arthritis and diabetes mellitus (Valko et al. 2007). Due to low levels of antioxidant enzymes, pancreatic β-cells are very susceptible to oxidative stress (Lenzen et al. 1996; Tiedge et al. 1997; Shah et al. 2007).

Oxygen free radicals are produced at low levels during several physiological reactions via reduction of oxygen (Betteridge 2000; Chong et al. 2005). It can be distinguished between reactive oxgen species (ROS) like $^{\bullet}O_2^-$, hydroxyl ($^{\bullet}HO$), peroxyl ($^{\bullet}RO_2$), and hydroxyperoxyl ($^{\bullet}HO_2^-$) radicals, hydrogen peroxide (H_2O_2) and hydrochlorus acid (HOCl), and reactive nitrogen species (RNS) like $^{\bullet}NO$, nitrogen dioxide ($^{\bullet}NO_2^-$), peroxynitrite ($OONO^-$), and nitrous oxide (HNO_2) (Evans et al. 2002).

The most common free radical is $^{\bullet}O_2^-$ (Chong et al. 2005). $^{\bullet}O_2^-$ is produced in the mitochondria during oxidative phosohorylation. Under physiological conditions, 0.4 - 4% of the consumed oxygen is converted into $^{\bullet}O_2^-$. The mitochondrial manganese superoxide dismutase (MnSOD) transforms $^{\bullet}O_2^-$ into H_2O_2, which in turn is converted into H_2O and O_2, either by glutathione peroxidase (GSH-Px) in the mitochondria or by catalase (CAT) in cytosolic peroxisomes. $^{\bullet}O_2^-$ can also be generated by xanthine oxidase, NADPH oxidase, cycloxygenase and lipoxygenase. In the presence of transition metals like copper (Cu) or iron (Fe), H_2O_2 can be transformed to highly reactive $^{\bullet}HO$ and OH^- by the so called Fenton reaction (Evans et al. 2002; Valko et al.

2007). Furthermore, $^{\bullet}O_2^-$ can react with $^{\bullet}NO$ to $OONO^-$ (Pfeiffer et al. 2001) (Figure 2.2).

Several studies demonstrated that in diabetic animals and humans, oxidative stress is increased, as evidenced by various oxidative stress markers (2.5.4.2 Measurement of oxidative stress).
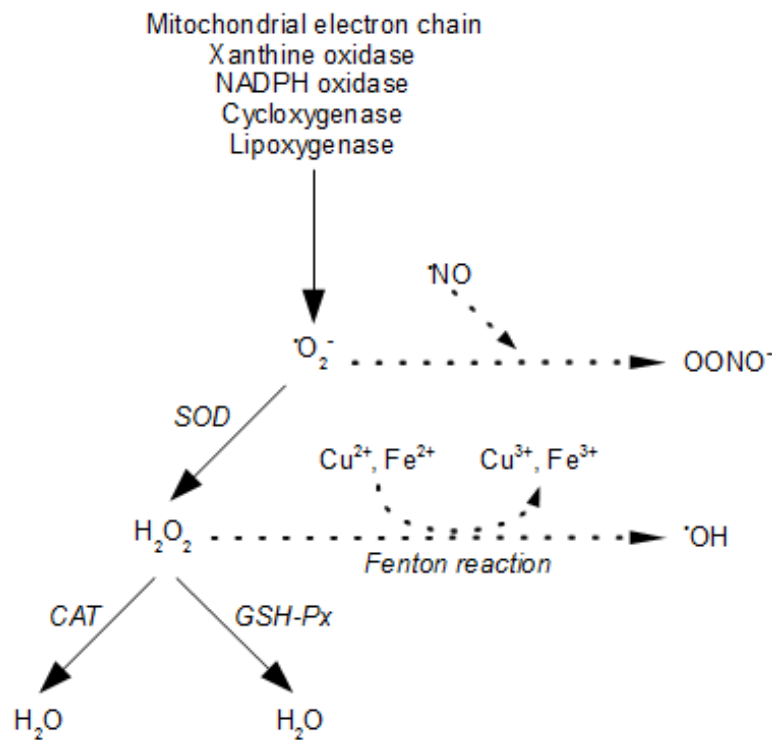
Figure 2.2 Radical generation and detoxification

Superoxide ($^{\bullet}O_2^-$) is generated during the oxidative phosphorylation in mitochondria and during several other reactions. $^{\bullet}O_2^-$ is converted to H_2O and O_2 via the endogenous antioxidant enzymes superoxide dismutase (SOD), glutathione peroxidase (GSH-Px) and/or catalase (CAT). Exaggerated $^{\bullet}O_2^-$ production, for example due to chronic hyperglycaemia, results in the generation of reactive oxygen (and nitrogen) species. $^{\bullet}O_2^-$ can react with nitric oxide ($^{\bullet}NO$) to peroxynitrite ($OONO^-$). In the presence of transition metals like copper (Cu^{2+}) and iron (Fe^{2+}), hydrogen peroxide (H_2O_2) is transformed to highly reactive hydrogen peroxide ($^{\bullet}OH$) (Fenton reaction).

2.5.2   Adverse effects of hyperglycaemia-induced oxidative stress

Free radicals are highly reactive and can cause tissue damage by directly reacting with lipids, proteins and DNA, leading to lipid peroxidation (Kalaivanam et al. 2006; Ramakrishna and Jailkhani 2007; Song et al. 2007), DNA damage (Song et al. 2007) and protein alteration (Palmeira et al. 2007; Ramakrishna and Jailkhani 2007; Bonnard et al. 2008). Furthermore, reaction

of $\cdot O_2^-$ with $\cdot NO$ to $OONO^-$ reduces $\cdot NO$ concentrations, which results in impaired vasodilation (Cai and Harrison 2000).

Adverse effects of hyperglycaemia-induced oxidative stress can also be indirect by induction of several pathways like JNK, p38 MAPK, and NF-κB (Evans et al. 2002).

C-Jun NH$_2$ terminal kinase (JNK) and p38 mitogen-activated protein kinase (p38 MAPK)

JNK and p38 MAPK, also called stress activated protein kinases 1 and 2 (SAPK 1 and 2), are members of the MAPK family, and are activated by similar stimuli like oxidative stress, hypoxia, and various cytokines (e.g. TNFα, IL-1) (Roux and Blenis 2004). Additionally, JNK can be activated by ER stress (2.4.2.2 Apoptotic pathways).

Several studies showed that JNK, is activated by hyperglycaemia-induced oxidative stress (Evans et al. 2002; Kaneto et al. 2004).
JNK activation is associated with reduced insulin sensitivity, disturbed β-cell function and increased β-cell apoptosis (2.5.3 Insulin resistance, β-cell dysfunction and β-cell apoptosis).
p38 MAPK plays an essential role in inflammation, immunity, cell growth and apoptosis (Evans et al. 2002; Roux and Blenis 2004). Exposure to high glucose concentrations activated p38 MAPK in vascular smooth muscle cells (Begum and Ragolia 2000), and treatment with H$_2$O$_2$ caused p38 MAPK induction in rat glomeruli (Dunlop and Muggli 2000).
H$_2$O$_2$ incubation of isolated rat islets induced JNK and p38 MAPK, leading to decreased *Ins* expression, which could be preserved by inhibition of JNK but not by inhibition of p38 MAPK (Kaneto et al. 2002).

Nuclear factor-κB (NF-κB)

NF-κB is activated by various stimuli including oxidative stress and regulates the transcription of several genes involved in inflammation (e.g. TNFα, IL-1, IFNγ), immune response, cell adhesion (e.g. vascular cell adhesion molecule 1 (VCAM1)), cell growth control (e.g. vascular endothelial growth factor (VEGF))

and apoptosis (2.4.2.2 Apoptotic pathways) (Baldwin 2001; Evans et al. 2002; Hu et al. 2006).

Different studies demonstrated that hyperglycaemia and oxidative stress activate NF-κB in several cells, like bovine vascular endothelial cells (Nishikawa 2000) and mononuclear blood cells of peripheral blood (Hofmann 1999). Reduction of oxidative stress via blocking the mitochondrial electron transport chain (Nishikawa 2000) or antioxidant treatment, for example with α-lipoic acid (LA) (Hofmann 1999) reduced NF-κB activation in these endothelial and blood cells, respectively. However, incubation of isolated rat islets for 1 - 7 days in 30 mM glucose or treatment with H_2O_2 over night did not affect NF-κB activity (Elouil et al. 2005).

These findings show that, different pathways can be activated by hyperglycaemia-induced oxidative stress in several tissues. However, the JNK pathway seems to be the most important concerning β-cell function and β-cell apoptosis.

2.5.3   Insulin resistance, β-cell dysfunction and β-cell apoptosis

Chronic hyperglycaemia and oxidative stress lead to reduced insulin sensitivity, disturbed β-cell function and β-cell apoptosis, which in turn results in further elevation of blood glucose concentration and therefore in further deterioration of insulin action, β-cell function and β-cell viability (Kaiser et al. 2003; Robertson 2006).

2.5.3.1   Insulin resistance

Physiologically, insulin binds to the insulin receptor (IR), which is expressed on the surface of several cell types, like myocytes, adipocytes, hepatocytes and β-cells, resulting in the autophosphorylation of IR. Phosphorylation of IR enables the binding of the insulin receptor substrates (IRS) IRS1 and 2 as well as Gab1 and Shc to the IR. The tyrosine kinase activity of the IR then activates IRS by phosphorylation of several tyrosine residues of IRS. Tyrosine-phosphorylation promotes the binding of IRS to the src homology 2 (SH2) domain of several downstream proteins like phosphatidylinositol 3-kinase (PI3-kinase), Grb2 and others. IRS1 and 2 activate PI3-kinase, which in turn activates the serine/threonine kinase Akt (also called protein kinase B (PKB))

and atypical forms of PKC (PKCγ and ζ), resulting in increased glycogen synthesis, inhibition of gluconeogenesis, elevated lipid synthesis and increased glucose uptake in adipocytes and myocytes by GLUT4 translocation to the plasma membrane. Phosphorylation of the IRS Gab1 and Shc leads to the binding of Grb2, which recruits SOS, resulting in the induction of the MAPK pathway, mediating proliferative effects of insulin (Biddinger and Kahn 2006) (Figure 2.3).
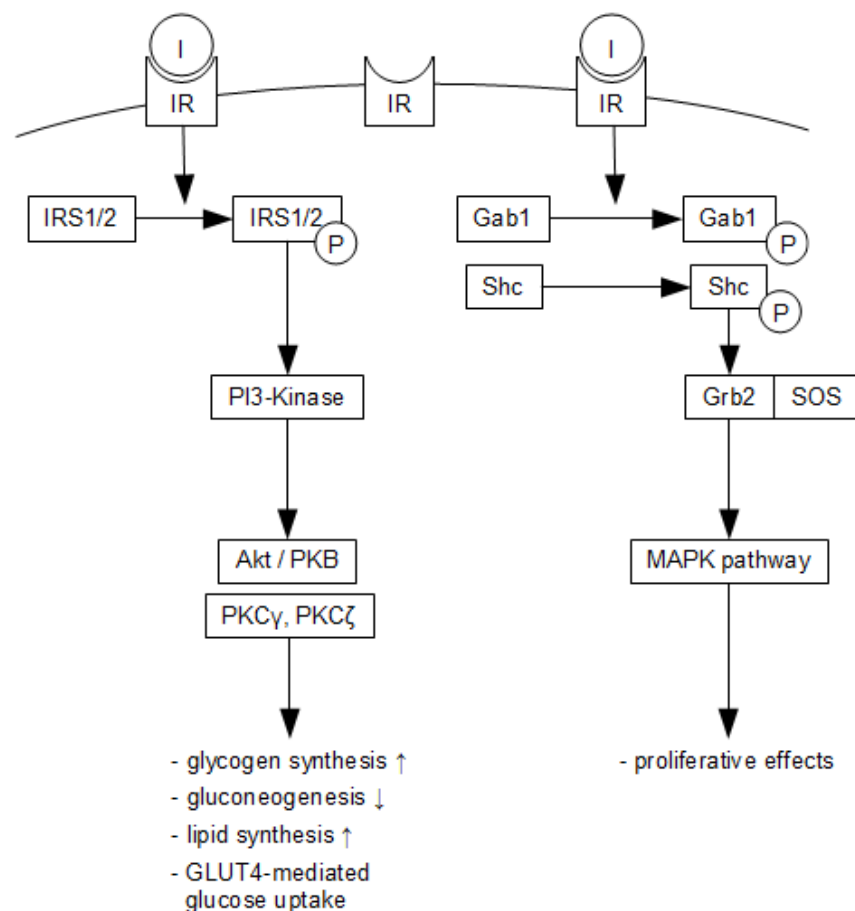
Figure 2.3 Insulin signalling
Binding of insulin (I) to the insulin receptor (IR) results in the autophosphorylation of IR and subsequently to the activation of insulin receptor substrates (IRS1, IRS2, Gab1, Shc). IRS1 and 2 activate phosphatidylinositol 3-kinase (PI3-kinase) which in turn activates Akt/PKB, PKCγ and ζ, resulting in synthesis of glycogen and lipids, in inhibition of gluconeogenesis and in glucose uptake in myocytes and adipocytes. Phosphorylation of Gab1 and Shc activates Grb2 which finally induces the MAPK pathway, realising the proliferative effects of insulin.

Oxidative stress leads to impaired insulin signalling, probably due to serine (Ser) and threonine (Thr) phosphorylation of IRS1 and 2, which disturbs binding of IRS to the IR and therefore impairs the phosphorylation of IRS on tyrosine (Tyr) residues. IRS, phosphorylated on Thr or Ser instead of Tyr,

shows impaired interaction with downstream target molecules, resulting in disturbed insulin action (Paz et al. 1997; Evans et al. 2002). JNK might be involved in reduced insulin action, since phosphorylation of IRS1 on serine 307 in Chinese hamster ovarian (CHO) cells was probably mediated by JNK (Aguirre et al. 2000).

The negative effect of oxidative stress on insulin sensitivity of adipocytes and muscle cells was demonstrated in different studies.

Treatment of 3T3-L1 adipocytes, either with TNFα or dexamethasone for several days, led to upregulation of ROS-related genes, increased ROS production and reduced insulin sensitivity compared to non-treated 3T3-L1 adipocytes, and insulin sensitivity was ameliorated by antioxidant treatment or overexpression of antioxidant enzymes (Houstis et al. 2006).

H_2O_2, generated by incubation with the enzyme glucose oxygenase and its substrate glucose, only slightly reduced basal glucose uptake in rat L6 muscle cells, overexpressing GLUT4 (L6 GLUT4 cells), whereas insulin-stimulated glucose transport was almost abolished. Pre-treatment with the antioxidant LA for 18 hours prevented insulin-stimulated glucose uptake. It was assumed that serine and/or threonine phosphorylation of IRS induced by H_2O_2 resulted in the impaired insulin action (Maddux et al. 2001).

2.5.3.2 β-cell dysfunction

Several *in vitro* and *in vivo* studies showed that chronically high glucose levels and oxidative stress reduce DNA binding activity of the transcription factors PDX-1 and MafA in β-cells, alter the expression of several β-cell genes like *GLUT2*, *GCK* and *INS* and lead to disturbed glucose-stimulated insulin secretion (GSIS) (Kaiser et al. 2003; Robertson and Harmon 2006).

PDX-1, which binds to the A3 element of the insulin promoter in β-cells, is essential for pancreas development, β-cell differentiation, regeneration and function by regulating the expression of several genes encoding for, for example, somatostatin, glucokinase, GLUT2 and insulin (McKinnon and Docherty 2001; Holland et al. 2002; Miyazaki et al. 2004; Andrali et al. 2008).

MafA binds to the RIPE3b/C1 element on the insulin promoter and is involved in the regulation of pancreatic β-cell function and GSIS (Zhang et al. 2005; Kondo et al. 2009).

Chronic incubation of HIT-T15 cells in 11.1 mM glucose resulted in diminished MafA and PDX-1 binding activity to the insulin promoter, reduced insulin mRNA content, decreased insulin concentrations and reduced GSIS. Treatment with the antioxidants *N*-acetyl cysteine (NAC) or aminoguanidine (AG) at least partially prevented these adverse effects of high glucose levels (Tanaka 1999). A more recent study, in which HIT-T15 cells were also incubated in 11.1 mM glucose for long-term, demonstrated that reduced MafA binding activity to the insulin promoter is caused by largely diminished MafA protein concentrations, whereas mRNA levels were unaltered (Harmon 2005). Incubation of isolated rat islets in H_2O_2 for 48 hours caused activation of JNK, reduced binding activity of PDX-1 to the insulin promoter and diminished insulin mRNA levels. Adenovirus-mediated expression of dominant-negative JNK or treatment with NAC preserved insulin gene expression in islets incubated in H_2O_2. Furthermore, overexpression of JNK in isolated islets resulted in reduced PDX-1 DNA binding activity and decreased insulin gene expression. These findings led to the assumption that activation of JNK reduces *Ins* expression by decreasing binding activity of PDX-1 to the insulin promoter (Kaneto et al. 2002).

One week after 85-95% pancreatectomy (Px), Sprague-Dawley rats developed mild to severe hyperglycaemia. Four weeks after pancreatectomy, islets of Px rats with blood glucose concentrations of 150 mg/dl and higher demonstrated reduced expression of several genes involved in β-cell development, differentiation and glucose metabolism (e.g. *Pdx-1, Ins, Glut2, Gck, Kir6.2, Pc* (pyruvate carboxylase)) compared to islets of shamPx rats. A relation between different degrees of hyperglycaemia and altered gene expression was detected. Treatment of severely hyperglycaemic rats for 4 weeks with phlorizin, which rapidly normalised blood glucose concentrations, reversed the alterations of gene expression (Jonas et al. 1999). Incubation of isolated rat islets in 30 mM glucose for 48 hours reduced mRNA expression of *Glut2* and *Gck* and resulted in disturbed GSIS compared to islets incubated in 10 mM glucose (Tsuboi et al. 2006). The reduced expression of *Glut2* and *Gck* was also analysed on the protein level via immuno blot analysis. Incubation of MIN6N8 cells, a mouse pancreatic β-cell line, in 33.3 mM glucose for 4 days

reduced GLUT2 and glucokinase content and impaired ATP production after glucose stimulation (Kim et al. 2005).

The findings of the different studies demonstrate that chronic hyperglycaemia and oxidative stress result in disturbed β-cell function by altering the expression of various genes. Reduced DNA binding activity of PDX-1 seem to play a major role in this context, since PDX-1 regulates the expression of several genes involved in glucose metabolism and β-cell function and the expression of these genes was reduced in various studies.

2.5.3.3 β-cell apoptosis

Chronic hyperglycaemia and oxidative stress reduce functional β-cell mass and lead to β-cell apoptosis. Several pathways were described demonstrating the molecular mechanisms underlying β-cell apoptosis via glucotoxicity (Kaiser et al. 2003).

JNK

JNK can be activated by high glucose levels and chronic oxidative stress (2.5.2 Adverse effects of hyperglycaemia-induced oxidative stress).
Human islets, incubated for 4 days with 33.3 mM glucose exhibited increased JNK activation, elevated mRNA levels of *c*-Fos, *c*-Myc and caspase 1, largely decreased insulin content and increased β-cell apoptosis compared to islets incubated in 5.5 mM glucose. Co-incubation with dominant inhibitor JNK-binding domain of IB1/JIP-1 (JNKi) reduced JNK activity and partially prevented the described alterations (Maedler et al. 2008).

Fas

Human pancreatic islets physiologically express Fas-ligand (FasL), but not Fas receptor (Fas) (Maedler et al. 2001). FasL binding to Fas results in the recruitment of adaptor proteins like Fas-associated via death domain (FADD), which in turn recruits caspase 8 (or 10), forming the death-inducing signal complex (DISC). Subsequently, caspase 8 (or 10) are activated by autoproteolysis and dissociate from Fas and FADD. Activation of caspase 8 (or 10) results in the cleavage and activation of caspase 3 and 7, which in turn cleave cellular substrates, leading to structural changes within the cell and finally to apoptosis (Movassagh and Foo 2008).

It was stated that caspase 3 and 7 also increase Bax translocation to the mitochondria, resulting in cytochrome *c* release, and connecting extrinsic and intrinsic apoptotic pathways (Lakhani et al. 2006).

Exposure of islets of dead, but heart-beating non-diabetic donors to high glucose concentrations (11.1 and 33.3 mM) for 5 days resulted in a dose-dependent increase in apoptosis compared to islets incubated in 5.5 mM glucose. The islets treated with 33.3 mM glucose demonstrated increased expression of Fas receptor and activation of caspase 8 and 3 (Maedler et al. 2001).

Mitochondrial pathway

Bcl-2 family members act pro-apoptotic (e.g. "multidomain" proteins Bax and Bak, as well as "BH3-only" proteins Bid, Bad and Bim) or anti-apoptotic (e.g Bcl-2, Bcl-xL, MCL-1). It is assumed that "BH3 only" proteins activate "multidomain" proteins Bax and Bak, leading to the permeabilisation of the outer mitochondrial membrane and to the release of cytochrome *c* into the cytosol, which in turn results in mitochondrial remodelling and dysfunction. In the "post-mitochondrial pathway" cytochrome *c* forms a complex with Apaf-1 and caspase-9, the so called "apoptosome", resulting in the activation of initiator caspase 9, which in turn activates caspase 3 and 7 (Scorrano and Korsmeyer 2003).

Incubation of human islets in 16.7 mM glucose for 5 days altered the balance of pro- and anti-apoptotic proteins and increased β-cell apoptosis compared to islets cultured in 5.5 mM glucose. Expression of Bad and Bid was increased, that of Bcl-xL decreased, as evidenced by RT-PCR and western blot analysis (Federici et al. 2001).

The treatment of MIN6N8 cells with high glucose concentrations resulted in the activation of the mitochondrial and the Fas-associated apoptosis pathway. Exposure of MIN6N8 cells to high glucose concentrations (33.3 mM) increased β-cell apoptosis and caspase 3-cleavage in a time-dependent mode. The expression of Bcl-2 and Bcl-xL was decreased, that of Bax, Fas and p53 increased compared to cells incubated in 5.5 mM glucose. Cytochrome *c* release from the mitochondria was increased, mediated by the translocation of Bax to the mitochondrial outer membrane (Kim et al. 2005).

In conclusion, long-term high blood glucose levels and oxidative stress result in decreased insulin action in insulin-sensitive tissues like muscle and fatty tissue, and in disturbed β-cell function and insulin secretion, especially in response to glucose. Apoptosis of β-cells, mediated by extrinsic and intrinsic apoptotic pathways, lead to reduced functional β-cell mass. All these adverse alterations aggravate the diabetic phenotype.

2.5.4 Antioxidants

2.5.4.1 Antioxidative defence

Organisms possess an endogenous antioxidant defence system in order to reduce oxidative stress (Chong et al. 2005; Rahimi et al. 2005). This system includes antioxidative enzymes like mitochondrial manganese superoxide dismutase (MnSOD/SOD2), cytosolic copper/zinc superoxide dismutase (Cu/ZnSOD/SOD1), glutathione peroxidase (GSH-Px), glutathione reductase (GR) and catalase (CAT), and nonenzymatic antioxidants like glutathione, vitamins E, A and C, α-lipoic acid (LA), antioxidant minerals (copper, zinc, manganese and selenium), several bioflavonids, coenzyme Q_{10} (CoQ_{10}), and cofactors (folic acid, B vitamins) (Maritim et al. 2003; Chong et al. 2005; Ramakrishna and Jailkhani 2007).

SOD, GSH-Px and/or CAT convert $^{\bullet}O_2^-$ to H_2O and O_2 (2.5.1 Free radicals and oxidative stress). GSH-Px oxidises reduced glutathione (GSH) to oxidised glutathione (GSSG), which in turn is reduced to GSH by GR, leading to the oxidation of NADPH to NADP+ (Shah et al. 2007; Lu 2009) (Figure 2.4 (B)).

Vitamins A and E are lipophilic radical scavengers. Vitamin E, whose most active form in humans is α-tocopherol, directly reacts with $^{\bullet}O_2^-$, $^{\bullet}RO_2$ and singlet oxygen, and protects membranes from lipid peroxidation. Vitamin C is hydrophilic and scavens radicals, like H_2O_2 (Berg et al. 2003; Maritim et al. 2003; Johansen et al. 2005).

Vitamins interact in recycling processes to regenerate the reduced form of vitamins, which can act as antioxidant. Vitamin C reduces the oxidised α-tocopherol radical to α-tocopherol, and is thereby converted to dehydroascorbic acid (DHA). GSH in turn reduces DHA to vitamin C (Maritim et al. 2003; Rahimi et al. 2005) (Figure 2.4 (A)). GSH can also reduce α-tocopherol radical to α-tocopherol. GSSG can be transformed to GSH via

GR or dihydrolipoic acid (DHLA) (Figure 2.4 (B), (C)). DHLA and LA are powerful antioxidants that scaven free radicals, regenerate vitamin C and GSH (Figure 2.4 (C)) and chelate metals. Furthermore LA is a coenzyme in the pyruvate dehydrogenase and α-ketoglutarate dehydrogenase mitochondrial enzyme complex and therefore plays an important role in generating energy from glucose (Evans and Goldfine 2000; Rahimi et al. 2005). CoQ_{10} is a lipophilic antioxidant and acts as an electron carrier in the mitochondrial electron transport chain (Johansen et al. 2005).

(A)

R — α-tocopherol — DHA — GSH
red | ox   red | ox   red | ox   red
RH — ˙α-tocopherol radical — Vitamin C — GSSG

(B)

H_2O H_2O_2
GSH-Px
ox
GSSG   GSH
GR
red
ox
NADPH $NADP^+$

(C)

DHLA — GSSG
red   ox
GSH
red   ox
DHA
red   ox
LA — Vit C
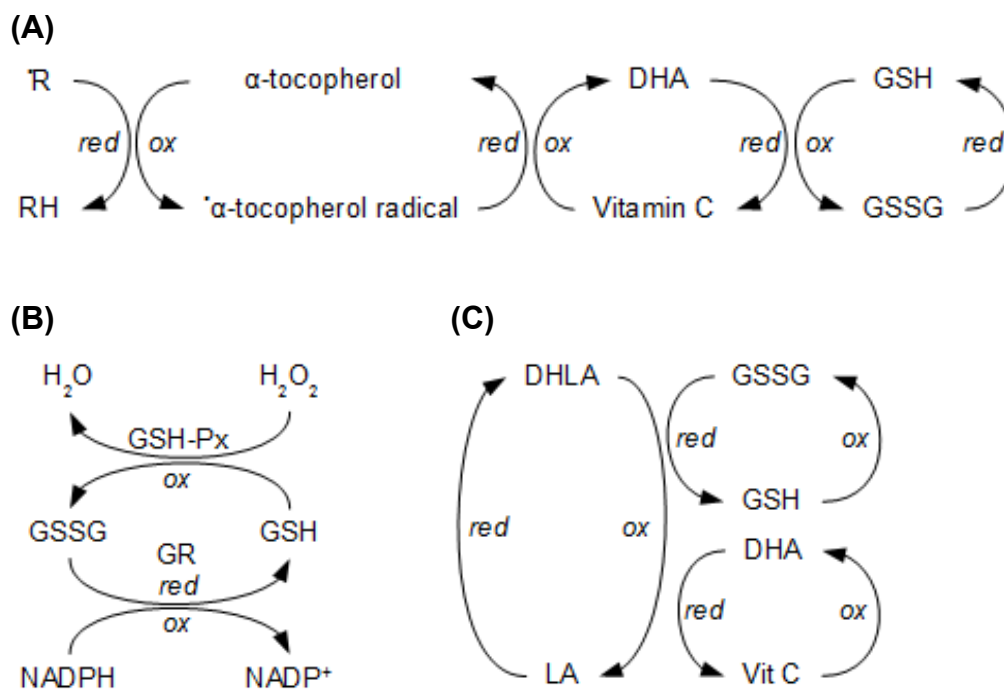
Figure 2.4 Recycling processes of endogenous antioxidants

Vitamins and other antioxidants like α-lipoic acid (LA) or glutathione (GSH) interact in recycling processes to regenerate the reduced and active form of the antioxidant.
(A) α-tocopherol, the most active form of vitamin E, directly reacts with radicals (˙R) and thereby is converted to α-tocopherol radical. Vitamin C reduces the α-tocopherol radical to α-tocopherol, being transformed to dehydroascorbic acid (DHA). Reduced glutathione (GSH) can regenerate vitamin C and is thereby oxidised to GSSG. **(B)** During the conversion of H_2O_2 to H_2O by glutathione peroxidase (GSH-Px), GSH is oxidised to GSSG. Regeneration of GSH by glutathione reductase (GR) leads to the oxidation of NADPH to $NADP^+$. **(C)** Dihydrolipoic acid (DHLA) can reduce DHA to vitamin C and GSSG to GSH.
ox: oxidation, red: reduction

2.5.4.2 Measurement of oxidative stress

The measurement of oxidative stress is necessary to examine the involvement of oxidative stress in the pathogenesis of diabetes mellitus and to investigate the effect of antioxidant treatment *in vitro* and *in vivo*.

Oxidative stress can be analysed be determining concentrations of MnSOD, Cu/ZnSOD, CAT, GR, GSH-Px, xanthine oxidase and NADPH oxidase (Maritim et al. 2003; Shah et al. 2007). Other biomarkers result from the oxidative damage on lipids, proteins and DNA. Lipid peroxidation can be determined by analysing malondialdehyde (MDA) and thiobarbituric active reactive substances (TBARS) levels (Kalaivanam et al. 2006; Ramakrishna and Jailkhani 2007; Song et al. 2007). DNA damage may be determined by measuring oxidised base 8-OHdG (8-hydroxy-2-deoxy-guanosine) levels or by comet assay (Sigfrid et al. 2004; Song et al. 2007), and protein alteration by investigating protein carbonylation (Palmeira et al. 2007; Ramakrishna and Jailkhani 2007; Bonnard et al. 2008). Further methods exist to examine oxidative stress like determination of F2-isoprostane levels, glutathione concentrations or analysing the antioxidant capacity (Rahimi et al. 2005; Shah et al. 2007).

However, different statements exist concerning the alteration of these parameters upon oxidative stress, especially the activity of SOD, CAT and GSH-Px (Maritim et al. 2003). STZ-induced diabetic Wistar rats showed decreased SOD, CAT and GSH-Px activities in the kidneys (Kedziora-Kornatowska et al. 2003) and reduced SOD and CAT activity in the liver compared to control rats (Elmalí et al. 2004). In another study using STZ-induced diabetic rats, elevated MnSOD levels were determined in liver, kidneys and pancreas compared to control rats. The GSH-Px concentrations in liver mitochondria were decreased, whereas mitochondria in pancreas and kidneys of diabetic rats showed elevated GSH-Px levels (Jang et al. 2000). In the liver of diabetic mice increased CAT concentrations were found after STZ treatment (Caballero et al. 2000).

In contrast to conflicting data on enzyme activities, the findings concerning other oxidative stress parameters are more consistent. Several studies showed that diabetic animals and humans regularly exhibit elevated TBARS levels and decreased glutathione concentrations (Kedziora-Kornatowska et al. 2003; Maritim et al. 2003). DNA damage (Ramakrishna and Jailkhani 2007) and glycated proteins (Jang et al. 2000) were also increased in diabetics.

2.5.4.3 Antioxidative treatment

Many studies demonstrated that oxidative stress plays a major role in the development of diabetes mellitus including long-term complications. Therefore treatment with antioxidants could play an important role for improvement and management of diabetes and diabetes-associated complications (Rahimi et al. 2005).

Several antioxidants were used in *in vivo* and *in vitro* studies to investigate their beneficial effects on diabetes and long-term complications. The antioxidative potential of vitamins A, E and C, LA, phytochemicals (Chanwitheesuk et al. 2005), zinc, selenium, melatonin, CoQ_{10} (Hodgson et al. 2002), taurine, nicotinamide and drugs like NAC (Kaneto et al. 1999; Fiordaliso et al. 2004), aspirin (Caballero et al. 2000), allopurinol (Desco et al. 2002), angiotensine convertase inhibitors (Kedziora-Kornatowska et al. 2000) and angiotensin receptor blockers were examined (Maritim et al. 2003; Rahimi et al. 2005). Some drugs used in diabetic therapy like metformin (Ouslimani et al. 2005), repaglinide (Gumieniczek et al. 2005) and sulphonylureas (glipizide, glibenclamide (Elmalí et al. 2004)) seem to have antioxidative effects, too (reviewed in Rahimi et al. 2005).

Examples of the use of antioxidants in *in vitro* studies are described above (e.g. 2.5.3 Insulin resistance, β-cell dysfunction and β-cell apoptosis). The beneficial effects of antioxidants detected in *in vitro* experiments were partly confirmed *in vivo*.

Treatment of diabetic C57BL/KsJ-*db/db* mice with NAC, Vitamins C and E, or with all 3 antioxidants demonstrated that NAC improved blood glucose concentrations, glucose tolerance, pancreatic insulin mRNA and insulin content compared to non-treated diabetic mice, whereas treatment with vitamins E and C didn't improve β-cell function (Kaneto et al. 1999). Oral application of vitamin E or C reduced renal lipid peroxidation, kidney weight, glomerular basement membrane thickness and urinary albumin excretion in STZ-induced diabetic Wistar rats, but didn't improve blood glucose levels compared to non-treated diabetic rats (Kedziora-Kornatowska et al. 2003).

LA treatment showed beneficial effects in several studies and therefore attracted considerable attention as an antioxidant (Johansen et al. 2005). For example, treatment of STZ-induced diabetic rats with LA improved blood

glucose concentrations, plasma insulin levels and lipid peroxidation compared to non-treated diabetic rats, and reversed hypertension (Kocak et al. 2000).

Clinical trials with humans were mainly carried out using vitamin C and E and LA (Johansen et al. 2005).
Oral treatment with vitamin E and C reduced the urinary albumin excretion rate in type 2 diabetic patients with persistent albuminuria (Gæde et al. 2001) and improved endothelium-dependent vaso-relaxation in type 1 diabetics, but not in type 2 diabetics (Beckman et al. 2003). Intravenous infusion of LA for 3 weeks, reduced symptoms of peripheral neuropathy in the ALADIN I (Ziegler et al. 1995) and SYDNEY trial (Ametov et al. 2003), whereas i.v. treatment for 3 weeks and subsequent oral LA administration showed no significant effect in the ALADIN III trial (Ziegler et al. 1999).

In conclusion, experimental studies with animal models and clinical trials showed that antioxidant treatment may have beneficial effects on diabetes and its long-term complications. However, the results of different studies were variable, which could be due to different type and duration of treatment protocols. Furthermore, treatment design in clinical trials is limited compared to investigations using animal models, since experiments with animals can be standardised and tissue samples of several organs can be analysed.

2.6 Linkage between oxidative and ER stress

Oxidative stress, protein misfolding and ER stress are interrelated. ER stress can result in oxidative stress and vice versa (Scheuner and Kaufman 2008).

2.6.1 Oxidative protein folding

The ER exhibits an environment optimised for oxidative protein folding. Many secretory proteins exhibit disulfide bonds, which are necessary for protein maturation, stability and function (Tu and Weissman 2004). Insulin, for example, contains 3 disulfide bonds (A7-B7, A20-B19, A6-A11).
Thiol-disulfide oxidoreductases like protein disulfide isomerase (PDI), catalyse disulfide bond formation, isomerisation and reduction of several substrates. PDI is reduced by oxidising disulfide bonds in proteins. Reduced PDI is regenerated by oxidation through the thiol-reductase ER oxidoreductase 1

(ERO1), which results in the production of low amounts of H_2O_2 (Tu and Weissman 2002; Tu and Weissman 2004; Scheuner and Kaufman 2008).

The oxidoreductases thioredoxin (Trx) and glutaredoxins (Grx) are members of the thioredoxin family and are involved in protein folding. Trx and Grx reduce protein disulfides to thiols, promote disulfide bond formation and interact with PDI and chaperones. Regeneration of reduced Grx is dependent on GSH (Berndt et al. 2008).

GSH reduces improperly paired disulfide bonds, and NADPH is necessary for the regeneration of GSH (Scheuner and Kaufman 2008).

Additionally, chaperones are also involved in protein folding, thereby consuming energy in form of ATP (Scheuner and Kaufman 2008).

2.6.2 ER stress induces oxidative stress and vice versa

As described above, oxidative protein folding produces little amounts of H_2O_2 and consumes GSH, which is a potential antioxidant. Therefore, high protein load and remodelling of disulfide bonds within misfolded proteins leads to oxidative stress by production of ROS and reduction of GSH levels (Kincaid and Cooper 2007a; Scheuner and Kaufman 2008).

On the other hand, oxidative stress depletes GSH, which is essential for disulfide bond formation. Furthermore, the reduction of glucose to sorbitol in the sorbitol pathways converts NADPH to NADP+, which results in decreased regeneration of GSH (Chung et al. 2003). ROS are highly reactive and can interact directly with proteins and inactivate chaperones, leading to impaired protein folding (Scheuner and Kaufman 2008).

The close link between oxidative and ER stress was demonstrated by Malhotra et al. (2008). Coagulation factor VIII (FVIII) is expressed at very low levels *in vivo* and forms high molecular weight aggregates, which results in the activation of the UPR. Chinese hamster ovarian (CHO) cells expressing wild-type human FVIII in response to sodium butyrate (NaB) were generated. NaB incubation of these CHO-FVIII cells resulted in increased wtFVIII mRNA and wtFVIII protein levels, and led to apoptosis in approximately 16% of the wtFVIII expressing cells. Most of wtFVIII was not secreted, but aggregated within the ER lumen, resulting in UPR activation. ROS concentrations were increased more than 100-fold in wtFVIII expressing CHO cells, compared to control CHO

cells. Co-incubation of CHO-FVIII cells with NaB and the antioxidant butylated hydroxyanisole (BHA) significantly reduced ROS production and apoptosis, increased wtFVIII secretion and thereby reduced intracellular wtFVIII accumulation (Malhotra et al. 2008).

These findings indicate that reducing oxidative stress, which was produced by accumulation of misfolded protein, via antioxidant treatment, could decrease ER stress and improve cell survival in diseases of protein misfolding (Malhotra et al. 2008).

3 Research design and methods

3.1 Treated male Munich *Ins2*^{C95S} mutant and wild-type mice

3.1.1 Animals

Munich *Ins2*^{C95S} mutant mice were generated within the Munich *N*-ethyl-*N*-nitrosurea (ENU) mouse mutagenesis project. Male heterozygous mutants were bred onto a C3HeB/FeJ genetic background (Herbach et al. 2007).

Animals received standard rodent diet (Altromin C1324, Germany) and tap water ad libitum. They were housed in a temperature- and light-controlled room (21 - 23°C, 55 ± 3% relative humidity, 12 hours light : 12 hours dark cycle). At the age of 21 days, mice were weaned, separated depending on sex, and marked by ear perforation. Tail tip biopsies for genotyping were taken, and blood glucose concentrations were measured. Twenty-two male heterozygous mutant mice were treated with subcutaneous sustained release insulin-pellets (Linshin, Canada; mt, ins), 21 male heterozygous mutant and 22 male wild-type mice were provided with hypodermic placebo-pellets, also called blank-pellets (Linshin, Canada; mt, pl and wt, pl, respectively). Treatment with insulin- or placebo-pellets started at 32 days of age. Body weight and randomly fed blood glucose concentrations were determined weekly in order to control therapy.

Regular clinical examinations were carried out starting with 12 wild-type, 12 insulin-treated and 12 placebo-treated mutant mice. Intraperitoneal insulin tolerance tests (ipITTs) were performed at the age of 50, 100 and 150 days. A placebo-intraperitoneal insulin tolerance test (placebo-ipITT) was accomplished with 150-day-old mice. At the age of 45, 85, 110 and 150 days, oral glucose tolerance tests (OGTTs) were carried out, and serum C-peptide levels were determined before and 10 minutes after glucose challenge. The serum of 140-day-old mice was examined concerning thiobarbituric acid reactive substances (TBARS). During the investigation period (21 - 160 days of age), 1 insulin-treated and 3 placebo-treated mutants died. The 32 remaining animals were sacrificed at the age of 160 days for examination of organ weights. Twelve mice (4 per investigation group) were used for qualitative-histological and quantitative-stereological analyses of the pancreas.

Additional 29 mice (10 wt, pl; 10 mt, ins; 9 mt, pl) were killed at the age of 100 days. The islets of 12 of these animals (4 per group) were isolated and assayed in respect of ER stress via western blot analyses. The remaining 17 mice (6 wt, pl; 6 mt, ins; 5 mt, pl) were killed by exsanguination under general anesthesia in order to examine pancreatic C-peptide levels as well as serum TBARS and serum glucagon concentrations.

All tests were performed with randomly fed mice, in order to avoid hypoglycaemia of the mutant mice treated with insulin-pellets. The number of animals used in the distinct examinations is stated in table 3.1.

All experiments were performed under the approval and in accordance with the guidelines of the responsible animal welfare authority (AZ 55.2-1-54-2531-94-07).

Number of animals investigated in distinct tests						
	Group 1			Group 2		
	wt, pl	mt, ins	mt, pl	wt, pl	mt, ins	mt, pl
genotyping	12	12	12	10	10	9
body weight	12	11-12*	9-12*	10	10	9
blood glucose	12	11-12*	9-12*	10	10	9
OGTT						
45 d	7	7	7			
85 d	8	7	7			
110 d	12	11*	11*			
150 d	12	11*	9*			
ipITT						
50 d	12	12	12			
100 d	12	9*	11*			
150 d	12	11*	9*			
placebo-ipITT 150 d	6	6	6			
C-peptide, serum						
45 d	7	7	7			
85 d	8	7	7			
110 d	12	9*	8*			
150 d	12	11*	9*			
C-peptide, pancreas 100 d				6	6	5

glucagon, serum 100 d				6	6	5
TBARS, serum 100 d 140 d	6	6	6	6	6	5
ER stress, islets 100 d				4	4	$3^{\#}$
organ weights 160 d	6	6	5			
pancreas, LM, morphometry 160 d	4	4	4			
pancreas, TEM 160 d	5	5	5			

Table 3.1: Number of animals investigated in distinct tests

Group 1: sacrifice at 160 days of age; Group 2: sacrifice at 100 days of age;
wt, pl: wild-type mice; mt, ins: insulin-treated mutant mice; mt, pl: placebo-treated mutant mice;
*: 1 mt, ins and 3 mt, pl died during the investigation period;
#: in 1 of 4 mt, pl not enough islets for western blot analysis could be obtained
d, days of age; OGTT: oral glucose tolerance test; ipITT: intraperitoneal insulin tolerance test; TBARS: thiobarbituric acid reactive substances; ER: endoplasmic reticulum; LM: light microscopy; TEM: transmission electron microscopy

3.1.2 Genotyping

The genotype of mice was determined by a restriction fragment length polymorphism (RFLP) based method as previously described (Herbach et al. 2007). The missense mutation in *Ins2* creates a new *Hpy* 188I restriction site which is used for the allelic differentiation of *Ins2*. After DNA amplification with the primers Ins2_5for and Ins2_6rev, which are specific for *Ins2*, and digestion of the 529 bp PCR amplificates, wild-type mice show a 521 bp fragment, heterozygous Munich *Ins2*[C95S] mutant mice show both the 473 bp and the 521 bp fragment, and homozygous mutants demonstrate the 473 bp fragment (Fig. 3.1).

Tail tip biopsies of approximately 0.4 cm length were taken at weaning and stored at -80°C until assayed. For DNA extraction, the tail tip was incubated in 400 µl master mix over night in a heating block at 55°C. Thereafter, undigested components were separated by centrifugation for two minutes at 15,000 rpm. The supernatant was poured into another Eppendorf cup, and 400 µl isopropanol (neoLab, Germany) were added to precipitate DNA. The DNA pellet was washed twice with 900 µl 70% EtOH (Merck, Germany), the

liquid phase was discarded and the DNA pellet was dried at room temperature. DNA was suspended in 100 - 200 µl TE buffer, according to the size of the pellet when dried. To make sure that the DNA was dissolved completely, it was stored at 4°C for at least 24h before proceeding with the PCR.

Nineteen µl of the PCR master mix and 1 µl of the suspended DNA were mixed carefully in PCR analysis cups (Eppendorf, Germany), which were then placed into a Mastergradient thermocycler (Eppendorf, Germany) and the program was run. PCR-H_2O served as quality control. If needed, PCR samples were stored at -20°C until further use. Enzymatic digestion took place in a thermocycler (Eppendorf; 37°C, 30 minutes), using 9 µl of the amplified DNA sample, and 11 µl of restriction enzyme master mix. After enzymatic digestion, 4 µl of loading dye were added to each sample. Then the samples were transferred into the sample wells of a 2% agarose gel, which was positioned in an Easy Cast™ gel chamber (PeqLab, Germany) filled with TAE (1x) running buffer. At the beginning of the row 12 µl pUC Mix Marker 8 (MBI Fermentas, Germany) were placed in a well in order to allow estimation of amplified fragment size. Electrophoresis was run at 65 volt for the first 15 minutes, afterwards at 110 volt for about 80 minutes (PowerPac 300, Bio-Rad, USA). The gel was stained in ethidium bromide solution (Roth, Germany) for 20 minutes. The amplified products were visualised (Universal Hood, Bio-Rad, USA) under UV light (306 nm), and a digital picture was taken to document the result.

Materials:

Reagents were stored at room temperature if not stated differently.

Master mix for DNA isolation:
Cutting Buffer:	375 µl
20% SDS (Roth, Germany):	20 µl
Proteinase K (20 mg/ml):	5 µl

Cutting buffer:
     Tris/HCl 1 M, pH 7.5 (Roth, Germany):   2.5 ml
     EDTA 0.5 M, pH 8.0 (Sigma, Germany):   5.0 ml
     NaCl 5 M (AppliChem, Germany):   1.0 ml
     Dithiothreitol (DTT) 1 M (Roth, Germany):   250 µl
     Spermidine (500 mg/ml; Sigma, Germany):   127 µl
     ad 50 ml distilled water
     stored at 4°C

Proteinase K (Roche, Germany):
     20 mg/ml diluted in distilled water, stored at -20°C

TE buffer:
     Tris/HCl 10 mM, pH 8.0 (Roth, Germany)
     EDTA 1 mM (Sigma, Germany)

PCR master mix:
     Taq PCR Master Mix Kit (Quiagen, Germany)
     10x Buffer: 2 µl
     $MgCl_2$:   1.25 µl
     Q-solution: 4 µl
     Taq polymerase: 0.1 µl

     Redistilled water: 8.65 µl

     dNTP 1 mM (Eppendorf, Germany):   1 µl

     Primer sense (Ins2_5for):   1 µl
     Primer antisense (Ins2_6rev):   1 µl
     Primer concentration 2 µM each
     (Genzentrum/DNSynthese, Germany; primer sequences:
     Ins2_5for: 5'-TGA CCT TCA GAC CTT GGC AC-3'
     Ins2_6rev: 5'-TAG CTG CCA TCA CCC ATG CC-3')
     all reagents stored at -20°C

Restriction enzyme master mix:
     Restriction enzyme *Hpy* 188I
     (New England BioLabs, UK):   0.8 µl
     NEBuffer 4 (New England BioLabs, UK):   2.0 µl
     Redistilled water: 8.2 µl
     stored at -20°C

Loading dye 6x:
     Glycerine (Merck, Germany):   3 ml
     Bromphenol blue (Merck, Germany):   spatula tip
     Redistilled water: 7 ml
     stored at 4°C

Agarose gel, 2%:
        Agarose (Roth, Germany):   4 g
        dissolved in boiling TAE (1x) buffer: 200 ml

Marker:
        100 bp DNA Ladder (New England BioLabs, UK):   25 µl
        Loadind dye 6x: 25 µl
        Redistilled water: 100 µl
        stored at 4°C

Ethidium bromide solution:
        Ethidium bromide 1% (Roth, Germany):   100 µl
        TAE (1x):   1,000 ml

EDTA 0.5 M pH 8.0, stock solution:
        EDTA (Roth, Germany):   14.89 g
        Distilled water: 80 ml
        adjust to pH 8.0 with NaOH 5 M (Merck, Germany)

TRIS 1 M:
        Tris base (Roth, Germany):   6.057 g
        ad 50 ml distilled water
        adjust to pH 8.0 with 37% HCl (Merck, Germany)

TAE 50x:
        Tris base (Roth, Germany):   242 g
        Glacial acetic acid (Merck, Germany):   57.1 ml
        EDTA 0.5 M, pH 8.0:   100 ml
        ad 1,000 ml distilled water

Program for DNA amplification:

1. 94°C, 5 minutes (denaturation, initiation)
2. 94°C, 45 seconds (denaturation)
3. 62°C, 45 seconds (primer annealing) | 34 cycles
4. 72°C, 90 seconds (elongation)
5. 72°C, 10 minutes (final extension)
hold on 4°C
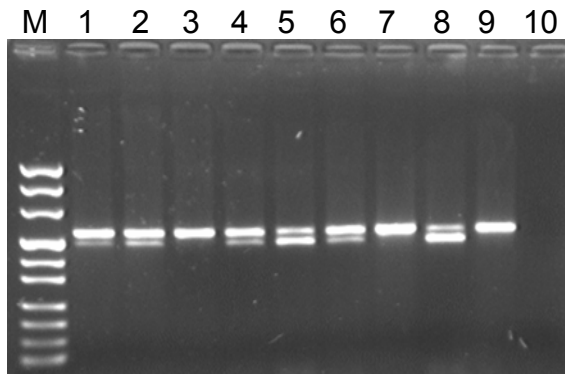
Figure 3.1: Genotyping via polymerase chain reaction (PCR) and restriction fragment length polymorphism (RFLP)

After PCR and RFLP analysis, wild-type mice (3, 7, 9) present DNA fragments of 521 base pairs (bp), heterozygous mutant mice (1, 2, 4, 6) exhibit fragments of 473 bp and 521 bp, homozygous mutants (5, 8) possess fragments of 473 bp. Due to incomplete digestion of the amplified DNA fragment, homozygous mutants show a weak band at 521 bp.
10: PCR-H_2O; M: marker; visible marker bands represent fragment sizes of 1118, 881, 692, 501, 489, 404, 331, 242, 190 and 147 base pairs (from top to bottom)

3.1.3 Treatment with insulin- and placebo-pellets

Sustained release insulin- and placebo-pellets (Linbits®, Linshin, Canada) weigh 13 mg and measure 2 mm in diameter and 3 mm in length. Insulin-pellets contain insulin and micro-recrystallised palmitic acid, and deliver 0.1 units insulin per day for about 30 days, according to the manufacturer. The placebo-pellets only contain micro-recrystallised palmitic acid.

Treatment was started with one subcutaneous pellet, as soon as male heterozygous mutant mice showed randomly fed blood glucose levels over 200 mg/dl, which occurred at a mean age of 32 days. Heterozygous mutant mice were treated with insulin-pellets (mt, ins), placebo-treated heterozygous mutant mice (mt, pl), and wild-type mice (wt, pl) served as controls. Body weight and blood glucose concentrations were controlled weekly. As soon as blood glucose levels of insulin-treated heterozygous mutants reached more than 180 mg/dl, another insulin- or placebo-pellet was applied, according to the treatment group.

Pellet application:

For analgesia after pellet application, each mouse received 10 µl of Metacam® solution (15 mg/ml Meloxicam, Boehringer, Germany) per os, using a pipette. An anaesthetic mixture of Medetomidine (0.5 mg/kg body weight, Domitor®,

Pfizer, Germany), Midazolam (5 mg/kg body weight, Midazolam-ratiopharm®, Ratiopharm, Germany) and Fentanyl (0.05 mg/kg body weight, Fentanyl DeltaSelect®, Delta Select, Germany) was injected intraperitoneally with a 30-gauge needle. A dexpanthenol containing ointment (Bepanthen®, Bayer, Germany) was applied into both eyes. Approximately 15 minutes after the injection, an area of 1 cm^2 in the mid dorsal region of the mouse was shaved using an electric shaver. The skin was cleaned and disinfected with a 10% povidone-iodine solution (Braunol® 10%, B.Braun, USA). A 16-gauge needle, a 12-gauge trocar, and a stylet were placed into a container filled with a 2% povidone-iodine solution (Braunol® 10%, diluted 1:5 in distilled water) for disinfection. The pellets were submerged in the 2% povidone-iodine solution for about 5 seconds and inserted into the cone end of the 12-gauge trocar. The shaved and disinfected skin was penetrated with the 16-gauge needle to create a small hole, and the trocar containing the pellet was pushed through the skin orifice. Using the stylet, the pellet was placed under the skin approximately 1 cm away from the orifice. The injection site was covered with a Chlorhexidine healing powder (Riemser, Germany). Finally, an antagonist mixture of Atipamezole (2.5 mg/kg body weight, Antisedan®, Pfizer, Germany), Flumazenil (0.5 mg/kg body weight, Anexate®, Roche, Germany) and Naloxone (1.2 mg/kg body weight, Naloxon DeltaSelect®, DeltaSelect, Germany) was injected subcutaneously to end anaesthesia.

In order to avoid hypothermia, an infrared lamp was used during anaesthesia until the mice recovered.

3.1.4 Body weight

Body weights of randomly fed mice were determined weekly during the investigation period to the nearest 0.1 g, using a precision balance (KERN, Germany).

3.1.5 Blood glucose concentration

From 21 days of age onwards, blood glucose levels were measured weekly at 11 am. Blood samples were taken from the nicked tail tip with a 10 µl open-end capillary (HITADO, Germany) by softly massaging the tail. The capillary was placed into a tube filled with 500 µl hemolysis solution (glucapil®,

HITADO, Germany), and blood glucose concentration was determined, using the blood glucose analyser SUPER GL® (HITADO, Germany).

Blood glucose levels during oral glucose tolerance tests and intraperitoneal insulin tolerance tests were evaluated in an analogue way.

Additionally, the glucose concentration in blood collected from the retroorbital plexus of 100-day-old mice was determined, as described above.

3.1.6 Oral glucose tolerance test (OGTT)

At the age of 45, 85, 110 and 150 days, oral glucose tolerance tests were performed. To avoid hypoglycaemia of insulin-treated mutants, mice were not fasted over night.

At 10 am, each mouse was placed into an individual cage with tap water access ad libitum. The tail tip was nicked, and blood samples were collected to analyse basal blood glucose and serum C-peptide concentrations. The mice received 11.1 µl of a 1 M glucose solution per gram body weight (α-D-Glucose, Sigma, Germany; diluted in tap water) into the stomach via gavage tube. Ten minutes after glucose administration, further blood samples for determination of blood glucose and serum C-peptide levels were taken. At 20, 30, 60, 90 and 120 minutes, samples for analysing the blood glucose concentrations were collected. Blood glucose levels were measured immediately as described above (3.1.5 Blood glucose concentration). The area under the glucose curve was calculated using the program GraphPad Prism 3.0 (GraphPad Software, USA).

To assay the serum C-peptide concentrations, about 100 - 120 µl blood were collected from the tail tip using a 75 µl capillary tube (Hirschmann, Germany). After centrifugation (1K15 centrifuge, Sigma, Germany; 10 minutes, 10,000 rpm), the serum was removed and stored at -80°C until assayed.

3.1.7 Insulin tolerance test and placebo-insulin tolerance test

3.1.7.1 Intraperitoneal insulin tolerance test (ipITT)

Intraperitoneal insulin tolerance tests (ipITTs) were carried out at the age of 50, 100 and 150 days.

Each mouse was placed into a separate cage with tap water access ad libitum. At 2 pm, blood samples were collected from the nicked tail tip to determine basal blood glucose levels. Subsequently, 0.75 I.U. insulin per

kilogramme body weight (40 U/ml, Insuman® Rapid, Aventis, Germany; diluted 1:247 in 0.9 % NaCl; 120 µl injection volume) were administered intraperitoneally, using a 30G x ½" cannula. Further blood samples were taken 10, 20, 30, 60 and 90 minutes after insulin application. Blood glucose concentrations were measured immediately as described above (3.1.5 Blood glucose concentration).

3.1.7.2   Placebo-intraperitoneal insulin tolerance test (placebo-ipITT)

At the age of 150 days, a placebo-insulin tolerance test was accomplished to investigate the influence of the pellet-insulin in insulin-treated mutant mice on the ipITT. Instead of insulin, the mice were injected 120 µl 0.9% NaCl intraperitoneally. The test procedure was otherwise identical to the ipITT. In the placebo-ipITT 6 mice per investigation group were analysed and compared to the ipITT of the identical animals at the age of 150 days.

3.1.8   C-peptide concentration in serum and pancreas

3.1.8.1   Serum C-peptide concentration

During the oral glucose tolerance tests at the age of 45, 85, 110 and 150 days (3.1.6 Oral glucose tolerance test (OGTT)), the serum C-peptide concentrations were determined from randomly fed mice (0 minutes), and 10 minutes after oral glucose challenge, using a Rat C-Peptide RIA Kit (Linco Research, USA). This radioimmunoassay fully cross-reacts with murine C-peptide.

Due to small sample volumes (55 - 70 µl serum), the assay was performed using the half amount of sample and assay reagents as denoted in the instruction sheet. The exact procedure of the RIA Kit is described in the Appendix (10.2.1.1 C-peptide).

Additionally, the difference between the C-peptide levels 10 minutes after glucose application and basal values (0 minutes) were calculated.

3.1.8.2   Pancreatic C-peptide content

At the age of 100 days, 17 randomly fed mice (6 wild-type, 6 insulin- and 5 placebo-treated mutant mice) were anaesthetised by intraperitoneal injection of 200 µl of a ketamine/xylazine mixture, and euthanised by exsanguination. The serum was separated from cellular components via centrifugation (1K15

centrifuge, Sigma, Germany; 10 minutes, 10,000 rpm) and stored at -80°C until assayed. The pancreas was separated carefully from the adjacent tissues, and homogenised for 1 minute in 4 ml acetic acid (2 M), using a Polytron PT 1200 E tissue homogeniser (Kinematic AG, Switzerland). After boiling the homogenate for 5 minutes in water bath (GFL, Germany), it was centrifuged for 15 minutes at 15,000 x g (4K15C centrifuge, Sigma, 4°C). Samples were aliquoted and stored at -80°C until assayed.

Pancreatic C-peptide levels were analysed by the same radioimmunoassay used to determine serum C-peptide concentrations (3.1.8.1 Serum C-peptide concentration). Pancreas homogenate was diluted 1:1,000 (wild-type mice), 1:400 (insulin-treated mutant mice) and 1:100 (placebo-treated mutant mice) in PBS.

The protein content in the pancreas homogenate was measured, using a spectrophotometer (NanoDrop ND-1000, peqlab, Germany). C-peptide levels were expressed as C-peptide-to-protein-ratio.

Materials:

Anaesthetic:
Ketamine 10% (Selectavet, Germany):	1 ml
Xylazine 2% (Rompun 2%, Bayer, Germany):	0.25 ml
NaCl 0.9%:	5 ml

Acetic acid 2 M:
Glacial acetic acid (Merck, Germany):	11.9 ml
Distilled water:	88.1 ml

Phosphate buffered saline (PBS):
NaCl (AppliChem, Germany):	7.95 g
Na_2HPO_4 (Roth, Germany):	1.15 g
KCl (Merck, Germany):	0.20 g
KH_2PO_4 (AppliChem, Germany):	0.20 g
ad 1,000 ml distilled water	
adjust to pH 7.4	

3.1.9 Serum glucagon concentration

The serum glucagon levels of 100-day-old mice (see 3.1.8.2) were determined, using a Glucagon RIA KIT (Linco Research, USA) which fully cross-reacts with murine glucagon.

The assay was performed according to the manufacturer's protocol, using half the reaction batch volumes (10.2.1.2 Glucagon).

3.1.10 Serum lipid peroxidation

Lipid peroxidation in the serum of 100- and 140-day-old mice was examined, using a TBARS Assay Kit® (Cayman, USA), according to the manufacturer's protocol (10.2.3 Thiobarbituric Acid Reactive Substances (TBARS)). Serum was diluted 1:1 in HPLC grade water (Applichem, Germany).

Serum samples were obtained from the nicked tail tip (140 days; see 3.1.6) or the retroorbital plexus (100 days; see 3.1.8.2). Additionally, the corresponding blood glucose concentrations were determined (3.1.5 Blood glucose concentration).

3.1.11 Western blot analysis of isolated islets

Isolated islets of 100-day-old mice (4 wild-type, 4 insulin- and 4 placebo-treated mutant mice) were examined with regard to the endoplasmic reticulum stress markers BiP/Grp78 (Binding Ig protein/Glucose regulated protein 78), PeIF2α (phosphorylated eukaryotic initiation factor 2α), and GADD153/CHOP (Growth arrest and DNA damage 153/C/EBP homologous protein). Actin was used as loading control. The optical density of BiP, PeIF2α and CHOP was determined, using ImageJ 1.41o (NIH 2004) and divided by the optical density of actin.

3.1.11.1 Islet isolation

The 12 mice were anaesthetised by intraperitoneal injection of 200 µl of ketamine/ xylazine mixture, and killed by cervical dislocation. The bowel was placed to the right side of the mouse in order to expose the pancreas and the bile duct. The bile duct was ligated near the liver with a thin string. The small intestine was clamped with a compressor on each side of the bile duct orifice. Using a winged infusion set (Venofix®, B.Braun, Germany), the bile duct was cannulated via the small intestine, and 2 ml collagenase solution (Sigma,

Germany) were injected into the pancreas. The bloated pancreas was cautiously removed from the adjacent tissue and placed into a screw-cap tube, filled with 3.75 ml perfusion solution and 1.5 ml collagenase solution. Pancreatic tissue was digested for at least 20 minutes in a water bath (GFL, Germany; 37°C). The tube was gently shaken occasionally. The digested pancreas was transferred into a petri dish filled with ice cold HANK's with 0.3% BSA to stop digestion. Islets were hand picked on ice with a pipette under a stereomicroscope (Stemi DV4, Zeiss, Germany; magnification x 32), and transferred into a 1.5 ml Eppendorf tube. After all visible islets were collected, tubes were centrifuged (1 minute, 1,000 rpm), the supernatant was discarded, and 30-50 µl of protein extraction buffer were added to the islets. Cell membranes were destroyed by freezing at -80°C, thawing on ice for 30 minutes, followed by sonication (B15, Branson, USA), and lysing on ice for another 30 minutes. After centrifugation (1K15 centrifuge, Sigma, Germany; 5 minutes, 5,000 rpm), the supernatant was separated, and stored at -20°C until assayed.

Materials

Anaesthetic:
      described above (3.1.8.2)

Collagenase solution:

Perfusion solution:		20 ml
Collagenase type 1 (C0130, Sigma, Germany):		40 mg
on ice		

Perfusion solution:

HANK's 1x:		40 ml
CaCl$_2$ 1 M (Merck, Germany):		94 µl
Hepes 1 M (Sigma, Germany):		1 ml
on ice		

HANK's 1x:

HANK's 4x:		250 ml
α-D-Glucose (Sigma, Germany):		0.40 g
Distilled water:		750 ml
adjust to pH 7.25		
on ice		

HANK's 4x:

NaCl (Applichem, Germany):	8.0 g
Hepes (Sigma, Germany):	2.38 g
KCl (Roth, Germany):	400 mg
$NaHCO_3$ (Merck, Germany):	350 mg
KH_2PO_4 (Roth, Germany):	60 mg
Na_2HPO_4 (Roth, Germany):	60 mg
$MgSO_4$ (Merck, Germany):	200 mg
$CaCl_2$ (Merck, Germany):	185 mg
Distilled water:	250 ml
stored at 4°C	

HANK's 1x with 0.3% BSA:

HANK's 1x:	960 ml
Bovine serum albumin (BSA; Sigma, Germany):	2.88 g

Protein extraction buffer:

20 mmol/l Tris/HCl pH 7.6 (Roth, Germany)
0.5% Ipegal CA 630 (MP Biomedicals, USA)
250 mmol/l NaCl (AppliChem, Germany)
3 mmol/l EDTA
3 mmol/l EGTA
1 mmol/l phenylmethylsulfonyl fluoride (PMSF)
2 mmol/l sodium-orthovanadate
1 mmol/l DTT (dithiothreitol, Roth, Gerrmany)
Complete (Roche, Germany)

Sodium-orthovanadate stock solution (200 mmol/l):

1. dissolve 0.92 g sodium-orthovanadate (MP Biomedicals, USA) in 20 ml distilled water on a magnetic stirrer
2. adjust to pH 10 with 1 N NaOH or 1 N HCl until solution turns yellow
3. boil for approximately 10 minutes until solution clears
4. cool down, using an ice bath
5. repeat step 2 - 4 until solution stays clear and pH 10 stabilises
6. fill up to 22.5 ml with distilled water
7. store aliquots of 1 ml at -20°C
Thaw before use by heating to 90 - 100°C in order to dissolve crystals.

PMSF 100x:

PMSF (Sigma, Germany):	17.4 mg
ad 1 ml isopropanol	
store at -20°C	

EDTA 0.3 M, 100x:

EDTA (Sigma, Germany):	1.116 g
ad 10 ml distilled water	

EGTA 0.3 M, 100x:
        EGTA (Sigma, Germany):   1.141 g
        ad 10 ml distilled water

Complete, 25x (Roche, Germany):

Dissolve 1 pellet in 2 ml distilled water, aliquot and store at 4°C (stable for 1 -
2 weeks) or freeze at -20°C (stable for 12 weeks)

3.1.11.2 Islet protein content

The protein content in isolated islets was analysed via Bradford method. A
protein standard was produced by dissolving 10 mg of bovine serum albumin
(BSA, Sigma, Germany) in 1 ml phosphate buffered saline (PBS). The
standard concentrations 250, 125, 62.5, 31.3, 15.6, 7.8, 3.9, 2.0 µg/ml were
produced by serial dilution in a 96-well plate. One µl of the sample was added
to 199 µl PBS in one well of the 96-well plate, and diluted 1:2 in PBS in the
adjacent well. Subsequently, 100 µl of a 40% Bradford reagent (Bio-Rad,
Germany) was added to all wells. After incubation for 5 minutes, the protein
content was determined photometrically at 595 nm, using a plate reader
(SUNRISE, Tecan, Germany) and the program Magellan 2 (Tecan, Germany).

Materials:

PBS:
        described above (3.1.8.2)

Bradford reagent:
        Bio-Rad Protein Assay 100% (Bio-Rad, Germany):   2 ml
        Distilled water: 5 ml
        protected from light and stored at 4°C

3.1.11.3 Sodium dodecyl sulfate polyacrylamide gel electrophoresis (SDS-PAGE)

A 10%-SDS gel was poured in a gel casting chamber (Mini-Protean III®, Bio-
Rad, Germany) and covered with isopropanol. After polymerisation for about
45 minutes, the isopropanol was drained, and the stacking gel was casted
onto the 10% separation gel. A comb was immediately placed into the still fluid
stacking gel in order to create sample wells. After polymerisation of the
stacking gel (approximately after 40 minutes), the comb was removed

carefully, and the gel was set into an electrophoresis cell (Protean III®, Bio-Rad, Germany). The inner cell of the electrophoresis chamber was filled to the top, the outer cell was filled about 3 cm with running buffer.

The islet samples were diluted to a protein content of 12 µg/20 µl, but at least 1:2 in sample buffer. Denaturation of proteins took place in a thermoblock (TB1, Biometra, Germany; 10 minutes, 100°C).

A molecular weight standard (Precision Plus Protein™, Bio-Rad, Germany) was pipetted into the first well of the gel, samples were loaded into the other wells. Gel electrophoresis was run at 200 volt for 50 minutes (Power PAC 300, Bio-Rad, Germany).

Materials:

Reducing sample buffer:
Sample buffer, stock solution:	475 µl
β-mercaptoethanol (Sigma, Germany):	25 µl

Sample buffer, stock solution:
Tris/HCl 0.5 M, pH 6.8:	1.2 ml
SDS 10% (Sigma, Germany):	2 ml
Glycerol (Merck, Germany):	1 ml
Bromphenol blue 0.05% (Merck, Germany):	0.6 ml
Distilled water:	4.8 ml

10%-SDS polyacrylamide gel:
Distilled water:	2.085 ml
Tris/HCl 1.5 M, pH 8.8:	1.25 ml
SDS 10% (Sigma, Germany):	50 µl
Acrylamide 30% (Roti Phenol®, Roth, Germany):	1.665 ml
Ammonium persulfate (APS) 10% (Bio-Rad, Germany):	25 µl
Tetraethylethylenediamine (TEMED) (Roth, Germany):	5 µl

Stacking gel:
Distilled water:	1.525 ml
Tris/HCl 0.5 M, pH 6.8:	0.625 ml
SDS 10% (Sigma, Germany):	25 µl
Acrylamide 30% (Roti Phenol®, Roth, Germany):	0.325 ml
Ammonium Persulfate (APS) 10% (Bio-Rad, Germany):	25 µl
Tetraethylethylenediamine (TEMED) (Roth, Germany):	5 µl

Tris/HCl 0.5 M, pH 6.8:
      Tris base (Roth, Germany):   6.057 g
      ad 100 ml distilled water
      adjust to pH 6.8 with HCl 37% (Merck, Germany)

Tris/HCl 1.5 M, pH 8.8:
      Tris base (Roth, Germany):   18.5 g
      ad 100 ml distilled water
      adjust to pH 8.8 with HCl 37% (Merck, Germany)

Running buffer, ready to use:
      Stock solution: 40 ml
      SDS 10% (Sigma, Germany):   4 ml
      ad 400 ml distilled water

Running buffer, stock solution:
      Tris base (Roth, Germany):   30.3 g
      Glycine (Merck, Germany):   144 g
      ad 1,000 ml distilled water

3.1.11.4 Western blot analysis

Two fibre pads, 6 absorbent papers and 1 nitrocellulose membrane (Schleicher & Schuell, Germany) were cut approximately to the gel size and moistened in Towbin buffer. After electrophoresis, gels were placed on the pre-wetted nitrocellulose membrane (Schleicher & Schuell, Germany) between three layers of absorbent paper, and fibre pads each side, and the sandwich was set in the gel holder cassette. Two cassettes were placed into the electrode module, which was then inserted in the buffer tank along with a frozen cooling unit (Mini Trans-Blot Cell, Biorad, Germany), and a magnetic stir bar. The tank was set into a styrofoam box which was filled with crushed ice for cooling. After filling the tank with cold (4°C) Towbin buffer, the transfer was run for 90 minutes at 100 volt on a magnetic stirrer (IKA, Germany). The nitrocellulose membrane was marked at one edge and washed in Tris buffered saline-Tween (TBS-T).

Silver staining of the gel was performed to demonstrate blotting success (3.1.11.5 Silver staining and drying).

For immunostaining, a tumbling shaker (Heidolph, Germany) was used while washing and incubating the nitrocellulose membrane. Washing was carried out

3 times for 5 minutes with TBS-Tween (TBS-T) if not stated differently. All antibodies were diluted in 10 ml of 1% BSA in TBS-T.

To avoid non-specific binding of the used antibodies, the membrane was blocked in 1% bovine serum albumin (BSA) in TBS (1 hour, room temperature). After washing, the membrane was simultaneously incubated in polyclonal rabbit anti-Grp78 (Stressgen, Canada; 1:10,000), monoclonal rabbit anti-PeIF2α (Cell Signaling, USA; 1:1,000), and polyclonal rabbit anti-GADD153 (Santa Cruz Biotechnology, USA; 1:500) antibodies over night at 4°C.

The next day, the membrane was washed and incubated with a horseradish peroxidase conjugated anti-rabbit antibody (Cell signalling, 1:10,000) for 1 hour at room temperature. After another washing step, the membrane was covered with Luminol Reagent (Santa Cruz Biotechnology, USA) for 1 minute. Afterwards, the membrane was placed into a film cassette (Ortho Fine, AGFA, Germany), and covered with a plastic transparency to avoid dehydration. In a darkroom, an Amersham Hyperfilm ECL (GE Healthcare, Germany) was laid upon the covered membrane and exposed for about 2 minutes. The film was developed (Kodak professional developer, Kodak, USA), shortly rinsed in a 12% acetic acid solution, fixed (Kodak professional fixer, Kodak, USA), rinsed thoroughly with tap water, and dried. The membrane was removed from the film cassette, washed for 5 minutes in TBS-T, incubated for 10 minutes in stripping buffer, washed for 2 x 10 minutes in PBS and for 2 x 5 minutes in TBS-T (mild stripping protocol according to Abcam, UK). After blocking in 1% BSA in TBS (1 hour, room temperature) and washing, the membrane was incubated with a monoclonal mouse anti-actin antibody (Chemicon international, Germany; 1:10,000, over night, 4°C). The membrane was washed, and a horseradish peroxidase rabbit anti-mouse antibody was added (DAKO, Germany; 1:10,000). Detection of immunoreactivity was performed as described.

Materials:

Towbin buffer:

Tris base (Roth, Germany):	3.03 g
Glycine (Merck, Germany):	14.4 g
Methanol (neoLab, Germany):	200 ml
Distilled water:	800 ml
stored at 4°C	

Tris buffered saline (TBS), ready to use:

TBS, stock solution:	500 ml
Distilled water:	4,500 ml

Tris buffered saline (TBS), stock solution x10:

Tris base (Roth, Germany):	60.6 g
NaCl (AppliChem, Germany):	87.6 g
ad 1,000 ml distilled water	
adjust to pH 7.4 with HCl 37% (Merck, Germany)	

TBS-T:

TBS, stock solution x10:	50 ml
Distilled water:	450 ml
Tween 20 (Merck, Germany):	250 µl

Luminol Reagent (Santa Cruz Biotechnology, USA):

Solution A:	5 ml
Solution B:	5 ml

Developer:

Kodak professional developer (Kodak, USA):	7.8 g
Distilled water:	50 ml

Fixer:

Kodak professional fixer (Kodak, USA):	9.2 g
Distilled water:	50 ml

Stripping buffer:

Glycine (neoLab, Germany):	15 g
SDS 10% (Sigma, Germany):	1 g
Tween 20 (Merck, Germany):	10 ml
ad 1,000 ml distilled water	
adjust to pH 2.2 with 37% HCl (Merck, Germany)	

3.1.11.5 Silver staining and drying

The 10%-SDS gel was incubated for 30 minutes in fixation solution. Subsequently, it was washed 3 times for 20 minutes with 50% ethanol (Merck,

Germany). After pre-treating the gel for 1 minute in sodium thiosulfate solution, it was rinsed with distilled water (3 x 20 seconds). The gel was impregnated for 20 minutes and washed (2 x 20 seconds) with distilled water. Development was performed under visual control until bands could be seen. After rinsing the gel in distilled water (20 seconds), the procedure was stopped with EDTA solution. The gel was washed 3 times for 2 minutes with distilled water and incubated in drying solution on a tumbling shaker (over night, 4°C). The next day, two sheets of cellophane (DryEase Mini Cellophane, Novex, Germany) were moistened in drying solution for 30 seconds. One part of the DryEase gel drying frame (Novex, Germany) was placed on a dryer base (DryEaseMini-Gel Drying Base, Novex) and covered with one of the cellophane films. The gel was laid in the centre of the film and the other cellophane sheet was placed onto the gel. Air blisters and wrinkles were carefully removed. The gel/cellophane sandwich was closed with the other part of the frame, using 5 plastic clamps. The gel was set in an upright position and let dry for 36 hours in a draft-protected place. Finally, the dried gel was taken out of the frame and placed under a heavy book for straightening.

Materials

Fixation solution:

Ethanol 100% (Merck, Germany):	500 ml
Glacial acetic acid (Merck, Germany):	120 ml
Formaldehyde 37% (SAV-LP, Germany):	0.5 ml
ad 1,000 ml distilled water	

Pre-treating solution:

$(Na_2S_2O_3)$ x 5 H_2O (Merck, Germany):	50 mg
Distilled water:	50 ml

Impregnation solution:

$AgNO_3$ (AppliChem, Germany):	50 mg
Distilled water:	50 ml
Formaldehyde 37% (SAV-LP, Germany):	35 µl

Development solution:

Na_2CO_3 (Merck, Germany):	1.5 g
$(Na_2S_2O_3)$ x 5 H_2O (Merck, Germany):	0.1 mg
Distilled water:	100 ml
Formaldehyde 37% (SAV-LP, Germany):	50 µl

Stop solution:
   EDTA 0.1 M, pH 8.0 (Sigma, Germany):   14.8 g
   Distilled water: 400 ml

Drying solution:
   Methanol 15%
   Glycerol 3%
   diluted in distilled water

3.1.12 Organ preparation and weighing

3.1.12.1 Perfusion

At the age of 160 days, 17 animals (6 wild-type, 6 insulin- and 5 placebo-treated mutant mice) were sacrificed for determining organ weights and for qualitative-histological and quantitative-stereological analyses of the pancreas. About 90 minutes before perfusion, 300 µl of a 10 mM 5-Bromo-2'-deoxy-uridine (BrdU) solution (Roche, Germany) were injected intraperitoneally, for later determination of islet-cell replication. Each mouse was anaesthetised by ketamine/xylazine application (see 3.1.8.2), and killed by cervical dislocation. Tissue was fixed for histology via orthograde vascular perfusion. A 15-gauge needle connected with perfusion tubes was inserted into the left heart ventricle. The vena cava inferior was transsected directly after the beginning of the perfusion to enable the fluids to drain off. First, the vasculature was pre-flushed with 2 ml Lidocaine (Lidocainehydrochloride 2%, bela-pharm, Germany) in order to dilate the blood vessels, followed by perfusion with about 40 - 50 ml PBS (pH 7.4, 37°C) to wash the blood out of circulation. Then, perfusion with warm (37°C) 4% paraformaldehyde in 0.05 M cacodylate buffer was performed for 5 minutes.

The PBS buffer and the fixative were filled in open bottles which hang about 1.7 metres above the bottom in order to create a constant pressure (60 mmHg) for perfusion.

Materials:

5-Bromo-2'-deoxy-uridine (BrdU)-solution (10 mM):
   5-Bromo2'-deoxy-uridine crystals (Roche, Germany): 10 mg
   Distilled water: 3.256 ml

PBS:
　　　　described above (3.1.8.2)

Paraformaldehyde 4% in 0.05 M cacodylate buffer

Cacodylate buffer 0.05 M:
Sodium Cacodylate Trihydrate (Fluka, Germany):	10.7 g
Paraformaldehyde (Merck, Germany):	40 g
Calciumchloride-dihydrate (Merck, Germany):	0.735 g

　　　　ad 1,000 ml distilled water
　　　　clear solution with NaOH 1 N (Roth, Germany)
　　　　adjust to pH 7.2 with HCl 37% (Merck, Germany)

Dilute sodium cacodylate trihydrate in 500 ml distilled water (room temperature), adjust to pH 7.2 with HCl 37% and heat up to 80°C. Subsequently, add paraformaldehyde and calciumchloride-dihydrate. Clear the solution with 1 N NaOH. Add 500 ml distilled water, let cool down and adjust to pH 7.2 with HCl 37%.

3.1.12.2 Organ weight

After perfusion and removal of the pancreas, the animals were post-fixed in 4% paraformaldehyde in cacodylate buffer for one week at room temperature. Organs (lung, heart, thymus, liver, spleen, stomach, intestine, kidneys, mesenterial lymph node, testes, epididymes) and abdominal fat were carefully removed from the adjacent tissues, blotted dry on cellulose paper, and weighed to the nearest mg, using a BP 61S scale (Satorius, Germany).

The gastrointestinal tract was weighed filled with ingesta, and after emptying. Abdominal fatty tissue consisted of mesentery (without lymph node), and residual fatty tissue from the abdominal and pelvic cave.

3.1.12.3 Pancreas preparation

The pancreas was separated from the adjacent tissue immediately after perfusion. It was blotted dry and weighed to the nearest mg. The specific weight of the pancreas (1.10 mg/mm^3) was determined by the submersion method (Scherle 1970).

A piece of approximately 6 mm^3 was cut off the splenic end of the pancreas, in order to prepare samples for transmission electron microscopy (TEM). The remaining pancreas was placed into a plastic tissue capsule (Engelbrecht,

Germany) on a biopsy pad (Bio-optica, Italy) to avoid distorsion, and was post-fixed in 4% paraformaldehyde in cacodylate buffer.

The next day, the pancreas was embedded in agar (Bacto™ Agar, Becton&Dickinson, USA) to alleviate its later slicing, put into a tissue capsule, dehydrated and embedded in paraffin (Histomaster, Bavimed, Germany).

The following day, the pancreas was cut perpendicular to its longitudinal axis into parallel slices of 1 mm thickness, with the first cut positioned randomly within an interval of 1 mm length at the splenic end of the pancreas. The slices were positioned with the right cut surface facing downwards, and paraffin embedding (SAV-LP, Germany) was finished.

Approximately 4 µm thick sections were cut, using a HM 315 microtome (Microm GmbH, Germany) and mounted on 3-aminopropyltriethoxy-silane-treated glass slides (Starfrost® microscope slides, Light Labs, USA). Subsequently, the sections were dried and stored in a heating cabinet (37°C).

3.1.13 Immunohistochemistry of the pancreas

Immunohistochemical staining for insulin, glucagon, somatostatin, and pancreatic polypeptide producing cells was performed, using the indirect immunoperoxidase method.

For the determination of replicating and apoptotic β-cells, co-staining for insulin and BrdU or insulin and TUNEL was performed, using the indirect immunoperoxidase and alkaline phosphatase method.

All incubations were carried out at room temperature in a humidity chamber. Normal serum and antibodies were diluted in Tris buffered saline (TBS, pH 7.4). TBS was used for washing if not stated differently.

3.1.13.1 Glucagon, somatostatin and pancreatic polypeptide

The antibodies used were purchased from DAKO® (Germany).

Pancreas sections were deparaffinised in xylene (20 minutes), rehydrated in a descending alcohol series (2 x 100%, 2 x 96%, 1 x 70% ethanol), and rinsed in distilled water. Endogenous peroxidase activity of tissue sections was blocked by incubation in 1% hydrogen peroxide solution for 15 minutes. After washing for 10 minutes, sections were pre-treated with normal swine serum (MP Biomedicals, USA; dilution 1:10, 30 minutes) to reduce non-specific binding. Subsequently, an antibody cocktail containing polyclonal rabbit anti-human

glucagon (dilution 1:50), polyclonal rabbit anti-human somatostatin (dilution 1:100), and polyclonal rabbit anti-human pancreatic polypeptide (dilution: 1:500) was applied for 2 hours. The tissue sections were rinsed for 10 minutes, and incubated with a horseradish peroxidase conjugated porcine anti-rabbit IgG (1:50, containing 5% mouse serum) for 1 hour. After washing (10 minutes), immunoreactivity was visualised using 3,3'-diaminobenzidine tetrahydrochloride dihydrate (DAB, KEM-EN-TEC, Denmark) as chromogen. Slides were washed in tap water for 5 minutes, counterstained with Mayer's Hemalaun (Applichem, Germany) and washed with running tap water (5 minutes). Subsequently, the sections were dehydrated via an ascending alcohol series, cleared in xylene, and mounted under glass coverslips, using Roti$^®$ Histokitt II (Roth, Germany).

Materials:

TBS:
   described above (3.1.11.4)

Hydrogen peroxide 1%:
H_2O_2 30% (neoLab, Germany):	6 ml
Distilled water:	194 ml

3,3'-diaminobenzidine tetrahydrochloride dihydrate (DAB):
DAB pellets (KEM-EN-TEC, Denmark):	1 piece
Distilled water:	10 ml

Let the pellet dissolve for about 1 hour protected from light, filter the solution and add 1 µl H_2O_2 30% (neoLab, Germany) per 1 ml DAB solution directly before use.

3.1.13.2 Insulin

For qualitative-histological investigations and for the determination of the total volume of isolated β-cells in the pancreas, an immunohistochemistry for insulin was performed. The staining procedure was similar to that demonstrating α-, δ- and PP-cells (3.1.13.1 Glucagon, somatostatin and pancreatic polypeptide). To reduce non-specific binding, normal rabbit serum (MP Biomedicals, USA; dilution 1:10) was used. Sections were incubated with polyclonal guinea pig anti-porcine insulin (dilution 1:500, 2 hours). Horseradish peroxidase

conjugated rabbit anti-guinea pig IgG (dilution 1:50, 5% mouse serum, 1 hour) served as second antibody.

3.1.13.3 Replicating cells (BrdU)

Ninety minutes before sacrifice 300 µl of a 5-Bromo-2'-deoxy-uridine solution were injected intraperitoneally (see 3.1.12.1). A double immunohistochemistry revealing insulin- and BrdU-positive cells was accomplished in order to survey the rate of replicating β-cells.

Tissue sections were deparaffinised, rehydrated and washed as described. Antigen retrieval was performed by pre-treatment with Target Retrieval Solution (DAKO, Germany) for 20 minutes at 95°C. After cooling to room temperature (approximately 20 minutes), sections were washed (2 x 2 minutes), and endogenous peroxidase activity was blocked by incubation in 1% hydrogen peroxide solution for 10 minutes. Slices were washed (10 minutes) and normal goat serum (MP Biomedicals, USA; dilution 1:10) was applied for 30 minutes. Subsequently, a polyclonal guinea pig anti-porcine insulin antibody was added (DAKO, Germany; dilution 1:1,000) for 1 hour. The tissue sections were washed (10 minutes) and incubated with an alkaline phosphatase conjugated goat anti-guinea pig IgG for 1 hour (Southern Biotech, USA; dilution 1:100). After washing for 10 minutes, immunoreactivity was visualised, using fuchsin substrate-chromogen (DAKO, Germany). The slides were shortly rinsed with distilled water, washed 2 x 2 minutes and incubated with normal rabbit serum (MP Biomedicals, USA; dilution 1:10, 30 minutes). Subsequently, the sections were washed (2 x 2 minutes) and a rat anti-human BrdU antibody was added (Anti-Bromodeoxyuridine-Peroxidase, Roche, Germany; dilution 1: 50) for 1 hour. After washing (3 x 2 minutes), the sections were incubated with a horseradish peroxidase conjugated rabbit anti-rat antibody (DAKO, dilution 1:50) for 30 minutes. Slides were rinsed 3 x 2 minutes, and immunoreactivity was visualised, using DAB (KEM-EN-TEC, Denmark). After rinsing with distilled water, slides were counterstained with Mayer's Hemalaun (Applichem, Germany), and washed with running tap water for approximately 5 minutes. The sections were air-dried, and mounted under glass coverslips, using Aquatex® (Merck, Germany).

Materials:

5-Bromo-2'-deoxy-uridine (BrdU)-solution (10 mM):
      described above (3.1.12.1)

Target Retrieval Solution, ready to use:
      Target Retrieval Solution (DAKO, Germany):   20 ml
      Distilled water: 180 ml

Hydrogen peroxide 1%:
      described above (3.1.13.1)

Fuchsin substrate-chromogen solution:
      DAKO® Fuchsin Substrate-Chromogen System:
      Fuchsin chromogen: 120 µl
      Activating reagent: 120 µl
      Substrate: 1.76 ml

Mix 120 µl of fuchsin chromogen with 120 µl of activating reagent. Incubate for 1 minute and add 1.76 ml substrate.

DAB:
      described above (3.1.13.1)

3.1.13.4 Apoptotic cells (TUNEL)

Apoptotic β-cells were demonstrated via combined insulin and TUNEL staining, the latter using the Apop Tag® Plus Peroxidase In Situ Apoptosis Detection Kit (Chemicon, USA).

Pancreas sections were deparaffinised, rehydrated and washed as described. After being rinsed for 5 minutes, antigen retrieval was performed, using proteinase K solution (DAKO, Germany; 10 minutes, 37°C). The slides were rinsed 2 times for 2 minutes in distilled water, and endogenous peroxidase activity was blocked by applying 3% hydrogen peroxide for 5 minutes. Afterwards, the tissue sections were stained for insulin as described above (see 3.1.13.3). The washed slides were covered with equilibration buffer for 2 minutes. After carefully removing excess liquid, slides were incubated with working strength TdT enzyme for 1 hour at 37°C. Attaching of nucleotides to DNA fragments was stopped by applying stop/wash buffer for 10 minutes. The slides were washed (3 x 2 minutes), and anti-digoxigenin conjugate was applied for 30 minutes.

Sections were rinsed (3 x 3 minutes) and DAB was added for 5 minutes to demonstrate immunoreactivity. After washing with distilled water (5 minutes), sections were counterstained with Mayer's Hemalaun (Applichem, Germany), rinsed with running tap water (5 minutes), air-dried, and mounted under glass coverslips, using Aquatex$^®$ (Merck, Germany).

Materials:

Hydrogen peroxide 3%:
        H_2O_2 30% (neoLab, Germany):   18 ml
        Distilled water: 180 ml

DAB:
        described above (3.1.13.1)

Following materials were components of the assay kit:

Equilibration buffer:
        ready to use

Working strength TdT enzyme:
        TdT enzyme: 22.5 µl
        Reaction buffer solution: 52.5 µl

Stop/wash buffer:
        Stop/wash Buffer: 1 ml
        Distilled water: 34 ml

Anti-digoxigenin conjugate:
        ready to use

Kit was stored at -20°C. After the first use, TdT enzyme was stored at -20°C, the other reagents at 4°C.
Reagents were warmed up to room temperature before use. Plastic coverslips were used for incubations.

3.1.14 Quantitative-stereological analyses

The pancreas of 160-day-old mice was investigated, using state-of-the-art quantitative-stereological methods as previously described (Wanke et al. 1994; Herbach et al. 2007).

3.1.14.1 Pancreas volume

To determine the pancreas volume (V_{pan}), the complete cut surface of pancreas sections was photographed at a final magnification of x16 (M 400 photomacroscope, Wild, Switzerland). An object micrometer (Zeiss-Kontron, Germany) was photographed at the same magnification for calibration. All photographs were printed under equal conditions.

Point-counting was performed, using a point-counting grid, photocopied onto a plastic transparency. The sum of points ($\sum P$) hitting pancreatic tissue (endocrine and exocrine pancreas including connective tissue of the pancreas; $\sum P_{pan}$), and the sum of points hitting the whole section (including extra pancreatic fatty tissue, lymphatic tissue, nerves, intestinal tissue and vessels; $\sum P_{section}$) were determined separately. To calculate the volume fraction of pancreatic tissue in the section ($Vv_{(pan/section)}$), $\sum P_{pan}$ was divided by $\sum P_{section}$. The total volume of the pancreas (V_{pan}) before embedding was calculated by dividing the pancreas weight by the specific weight of the pancreas (see 3.1.12.3) and by multiplying by $Vv_{(pan/section)}$.

The area corresponding to one point was determined using the Videoplan® image analysis system (Zeiss-Kontron, Germany) after calibration with the printed object micrometer. One point equalled 0.1474 mm^2 on the point counting grid. The sum of cross-sectional areas of the pancreas ($\sum A_{pan}$) was obtained by multiplying $\sum P_{pan}$ by 0.1474 mm^2.

3.1.14.2 Volume density and total volume of islets, β-cells, non-β-cells and capillaries

Evaluations were performed on sections simultaneously immunostained for glucagon, somatostatin and pancreatic polypeptide. All islets within the pancreas sections were photographed with a Leica DFC 320 camera, connected to a microscope (Leica Microsystems, Germany), using a x25 objective. An object micrometer (Zeiss-Kontron, Germany) was photographed at the same magnification for calibration. All photographs were printed under the same conditions on a colour laser printer (HP, Germany). Using point counting morphometry, the sum of points hitting islets ($\sum P_{islets}$), non-β-cells ($\sum P_{non-β-cells}$), and capillaries ($\sum P_{capillaries}$) were analysed separately (Figure 3.2). The sum of points hitting β-cells ($\sum P_{β-cells}$) was calculated by subtracting

the sum of points hitting non-β-cells and capillaries from $\sum P_{islets}$. The area corresponding to 1 point was determined as described above (3.1.14.1) and equalled 181.8 µm^2.

The sum of cross-sectional areas of islets, β-cells, non-β-cells, and capillaries ($\sum A_{islets}$, $\sum A_{β-cells}$, $\sum A_{non-β-cells}$, and $\sum A_{capillaries}$, respectively) was attained by multiplying the sum of points hitting the respective compartment by 181.8 µm^2.
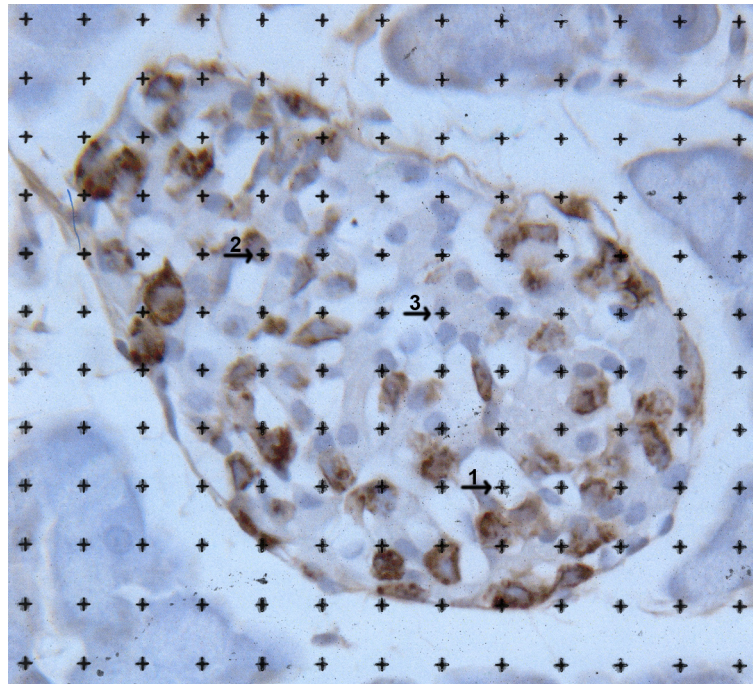
Figure 3.2 Point counting grid placed on an islet immunostained for glucagon, somatostatin and pancreatic polypeptide

A point counting grid was used in order to count the sum of points hitting islet tissue, capillaries and non-β-cells.
1: capillary, 2: non-β-cell, 3: β-cell

The volume density of islets in the pancreas ($Vv_{(islets/pan)}$) was calculated by dividing $\sum A_{islets}$ by $\sum A_{pan}$, the volume density of the endocrine compartment in the pancreas ($Vv_{(endo/pan)}$) by dividing $\sum A_{β-cells}$ plus $\sum A_{non-β-cells}$ by $\sum A_{pan}$ (($\sum A_{β-cells}$ + $\sum A_{non-β-cells}$) / $\sum A_{pan}$). The total volume of islets in the pancreas $V_{(islets,pan)}$ was attained by multiplying $Vv_{(islets/pan)}$ by V_{pan}.

Due to perfusion fixation, around one fourth of the islet profile consisted of capillary volumina. Therefore, the volume density of β- and non-β-cells in the endocrine compartment of the islets ($Vv_{(β-cells/endo)}$ and $Vv_{(non-β-cells/endo)}$) was determined by dividing $\sum P_{β-cells}$, and $\sum P_{non-β-cells}$ by the $\sum P$ hitting the endocrine compartment ($\sum P_{islets}$ - $\sum P_{capillaries}$), respectively.

The volume density of β-cells, non-β-cells, and capillaries in the islets ($Vv_{(\text{β-cells/islets})}$, $Vv_{(\text{non-β-cells/islets})}$, $Vv_{(\text{capillaries/islets})}$) was calculated by dividing $\sum P_{\text{β-cells}}$, $\sum P_{\text{non-β-cells}}$ or $\sum P_{\text{capillaries}}$ by the $\sum P_{\text{islets}}$.

The total volume of β-cells ($V_{(\text{β-cells,islets})}$) and the total volume of non-β-cells ($V_{(\text{non-β-cells,islets})}$) in the islets were obtained by multiplying $Vv_{(\text{β-cells/islets})}$ and $Vv_{(\text{non-β-cells/islets})}$ by $V_{(\text{islets,pan})}$, which is identical with multiplying $Vv_{(\text{β-cells/endo})}$ and $Vv_{(\text{non-β-cells/endo})}$ by $V_{(\text{endo,pan})}$. The total volume of capillaries in the islets ($V_{(\text{capillaries,islets})}$) was calculated by multiplying $Vv_{(\text{capillaries,islets})}$ by $V_{(\text{islets,pan})}$.

3.1.14.3 Volume density and total volume of isolated β-cells

Isolated β-cells, an indicator for neogenesis of pancreatic islets (Bonner-Weir et al. 2008; Inada et al. 2008), were defined as single β-cells and small clusters of β-cells of up to 4 nuclear profiles that were not contained within established islets. The area of isolated β-cell profiles was determined planimetrically, using the Videoplan® image analysing system (Zeiss-Kontron, Germany). Images from sections immunostained for insulin were displayed on a colour monitor at an 850x final magnification. The sum of cross-sectional areas of isolated β-cell profiles ($\sum A_{\text{isolated β-cells}}$) was quantified by circling their contours with a cursor on the digitising tablet of the image analysis system. The volume density of isolated β-cells in the pancreas ($Vv_{(\text{isolated-β-cells/pan})}$) was calculated by dividing $\sum A_{\text{isolated β-cells}}$ by $\sum A_{\text{pan}}$. The total volume of isolated β-cells ($V_{(\text{isolated-β-cells,pan})}$) was obtained multiplying $Vv_{(\text{isolated-β-cells,pan})}$ by V_{pan}.

3.1.14.4 β-cell replication

β-cell replication was determined on pancreas sections double-stained for insulin and BrdU.

The number of nuclear endocrine-cell profiles of 30 islets (10 islets per investigated group) were counted and the area that corresponds to one endocrine cell (A_{endo}) was calculated by dividing the corresponding cross-sectional areas of the endocrine compartment of those islets by the number of nuclear profiles. The area corresponding to 1 endocrine-cell profile equalled 102.6 µm^2.

The number of all nuclear β-cell profiles in the pancreas sections was calculated dividing $\sum A_{\text{β-cells}}$ (3.1.14.2 Volume density and total volume of islets, β-cells, non-β-cells3.1.16.2) by 102.6 µm^2. BrdU positive nuclear β-cell profiles

in the islets were counted and divided by the number of nuclear β-cell profiles. Data are expressed as BrdU positive β-cells per 100,000 β-cells.

3.1.14.5 β-cell apoptosis

Apoptotic β-cells were determined on pancreas sections double-stained for insulin and TUNEL. Calculations were performed analogous to replicating β-cells and data are expressed as TUNEL positive β-cells per 100,000 β-cells.

3.1.15 Transmisson Electron Microscopy (TEM)

Pancreatic islets of 160-day-old mice were investigated electron microscopically.

A piece of 6 mm^3 from the splenic end of the pancreas (3.1.12.3 Pancreas preparation) was placed into a 0.5 ml Eppendorf cup, containing 4% paraformaldehyde in 0.05 M cacodylate buffer as fixative. After one hour, the pancreas piece for TEM was cut into 5 - 6 equal cubes and post-fixed for at least 24 hours at 4°C on a tumbling shaker. Samples were washed in cacodylate buffer (3 hours, room temperature) and post-fixed in a solution consisting to 1 part of 2% osmium tetroxide and to 1 part of 0.05 M cacodylate buffer (2 hours, 4°C). Subsequently, the pancreas samples were washed in cacodylate buffer (3 x 2 minutes) and dehydrated by an ascending acetone series (Roth, Germany). Pancreatic tissue was incubated in a solution containing equal amounts of 100% acetone and Glycid ether 100 (Serva, Germany) for 1 hour at room temperature, followed by incubation in Glycid ether 100 (2 x 30 minutes, room temperature). Samples were embedded in glycidether embedding mixture in dried gelatine capsules (Plano, Germany). Polymerisation was carried out at 60°C for 48 hours.

Epon blocks were trimmed, using a Reichert-Jung TM60 milling machine (Leica, Germany). Semi-thin sections (0.5 μm) were produced with a Reichert-Jung Ultracut E microtome (Leica, Germany), and stained with Toluidine blue O and Safranin O. After identifying the islets within the semi-thin sections via light microscopy, and marking their positions in a drawing, the areas of the Epon blocks containing islets were trimmed further, and ultra-thin sections (70 - 80 nm) were prepared (Reichert-Jung Ultracut E, Leica, Germany). The sections were mounted on coated copper rings, contrasted with uranyl acetate

and lead citrate (Reynolds 1963), and examined using an EM 10 electron microscope (Zeiss, Germany).

Materials:

Cacodylate buffer 0.05 M, paraformaldehyde 4% in 0.05 M cacodylate buffer:
        described above (3.1.12.1)

Ascending acetone series (Roth, Germany):
        Acetone 50%: 3 x 2 minutes, 4°C
        Acetone 70%: 2 x 10 minutes, 4°C
        Acetone 90%: 2 x 10 minutes, 4°C
        Acetone 100%: 2 x 20 min, 4°C
        Acetone 100%: 1 x 20 min, room temperature

Osmium tetroxide 2%:
Osmium tetroxide (O_sO_4, Merck, Germany):	1 g
Distilled water:	50 ml

Glycidether embedding mixture:
Solution A:	70 ml
Solution B:	130 ml
2,4,6-tris-(dimethylaminomethyl) phenol (Serva, Germany):	3 ml

Solution A:
Glycid ether 100 (Serva, Germany):	62 ml
2-dodecenyl succinicacid anhydride (Serva, Germany):	100 ml

Solution B:
Glycid ether 100 (Serva, Germany):	100 ml
Methylnadic anhydride (Serva, Germany):	89 ml

Staining protocol: semi-thin sections: Toluidine blue O and Safranin O

Toluidine blue O:
Di-sodiumtetraborate (Borax, Merck, Germany):	1 g
Toluidine blue O (Roth, Germany):	1 g
Distilled water:	100 ml

Dissolve Borax in distilled water, add Toluidine blue 0 and stir for approximately 2 hours. Filter before use. Stain sections for 45 - 60 seconds on a heating plate (Meditel, Germany; 55°C), rinse with distilled water and let dry.

Safranin O:
Di-sodiumtetraborate (Borax, Merck, Germany):	1 g
Safranin O (Chroma, Germany):	1 g
Saccharose (Merck, Germany):	40 g

| Formaldehyde 37% (Roth, Germany): | 2-3 drops |
| Distilled water: | 100 ml |

Dissolve Borax in distilled water, add Safranin O and saccharose and stir for approximately 2 hours. The next day, add formaldehyde. Filter before use. Stain sections for 15 seconds on a heating plate (Meditel, Germany, 55°C), rinse with distilled water and let dry. Cover the sections with coverslips (Menzel GmbH & Co KG, Germany) using Histofluid (Superior®, Germany).

Contrasting ultra-thin sections with uranyl acetate and lead citrate (Reynolds 1963)

Uranyl acetate (Reynolds):
| Uranyl acetate (Merck, Germany): | 1 g |
| Redistilled water: | 50 ml |

Swing carefully, don't stir. Filter before use.
Stain sections for 30 minutes at room temperature.

Lead acetate (Reynolds):
Sodium citrate 1 M (Merck, Germany):	6 ml
Lead nitrate solution 1 M (Merck, Germany):	4 ml
Sodium hydrate solution 1 M (Merck, Germany):	8 ml
Redistilled water:	32 ml

Mix sodium citrate with redistilled water while gently stirring. Add lead nitrate drop by drop, the solution gets milky (precipitation). Use sodium hydrate to clear the solution. Filter before use. Stain sections for 10 minutes at room temperature.

3.2 C-peptide II concentration in serum and pancreas of untreated male and female Munich *Ins2*^C95S^ mutant and wild-type mice

In order to determine the expression and secretion of the mutant insulin 2, C-peptide II concentrations were analysed in the pancreas and serum of 31 untreated mice (4 male and 5 female wild-type mice, 6 heterozygous mutant and 5 homozygous mutant mice of both genders).

Due to the short lifespan of homozygous mutants (31 - 76 days; Herbach et al. 2007), mice were sacrificed at the age of 21 days. The animals were anaesthetised by intraperitoneal ketamine/xylazine injection (80 µl per mouse), and blood was collected from the retroorbital plexus (see 3.1.8.2). Afterwards

the mice were killed by cervical dislocation. The pancreas was removed and homogenised in 0.5 ml of 2 M acetic acid (see 3.1.8.2). Blood glucose concentrations were determined immediately, and serum was prepared as described (3.1.8.2).

Pancreas samples were diluted 1:20 (wild-type mice) and 1:10 (heterozygous and homozygous mutants) in distilled water. C-peptide II concentrations in the serum and the pancreas were analysed using a Mouse C-Peptide II ELISA (KAMIYA, USA) according to the manufacturer's protocol. The exact procedure of the Mouse C-Peptide II ELISA is described in the Appendix (10.2.2 C-peptide II ELISA). Protein contents in the pancreas homogenates were determined using a spectrophotometer (NanoDrop ND-1000, peqlab, Germany), and C-peptide II concentrations were expressed as C-peptide II-to-protein-ratio.

3.3 Additional investigations of untreated male and female Munich $Ins2^{C95S}$ mutant and wild-type mice

3.3.1 Animals

Additional tests were performed with 9 male and 8 female heterozygous Munich $Ins2^{C95S}$ mutant mice as well as 10 male and 10 female wild-type mice. One male mutant died during the investigation period. Housing conditions, weaning age, earmarking and genotyping was carried out as described above (3.1.1 Animals). These animals were not treated with insulin- or placebo-pellets. At the age of 230 days, the mice were killed by exsanguination under general anaesthesia (see 3.1.8.2).

3.3.2 Randomly fed body weight and blood glucose concentration

Body weight and blood glucose concentrations of randomly fed animals were measured at the age of weaning (21 days) and in 30, 90 and 180-day-old mice (3.1.4 Body weight, 3.1.5 Blood glucose concentration).

In addition, blood glucose levels were analysed at 200 and 230 days of age.

3.3.3 Intraperitoneal insulin tolerance test (ipITT)

The insulin sensitivity of Munich $Ins2^{C95S}$ mutant mice of different age-groups was previously examined via homeostasis model assessment of insulin

resistance index (HOMA IR (%)). Intraperitoneal insulin tolerance tests (ipITTs) were accomplished in male heterozygous mutant and male wild-type mice at the age of 4 months (Herbach et al. 2007).

Since the HOMA IR is not designed for mice, insulin sensitivity was to be further assessed in different age-groups (21, 30, 90 and 180 days) and both genders of Munich $Ins2^{C95S}$ mutants and wild-type mice (n≥8 per age, sex and genetic group), via intraperitoneal insulin tolerance test (3.1.7.1 Intraperitoneal insulin tolerance test (ipITT)).

3.3.4 Serum glucagon concentration

The serum glucagon levels of 20 mice (5 mice per sex and genetic group) were determined (3.1.9 Serum glucagon concentration) randomly fed (T0) and 10 minutes after intraperitoneal insulin injection (T10) at the age of 200 days. Insulin was applied as described above (3.1.7.1 Intraperitoneal insulin tolerance test (ipITT)). At 230 days of age, the glucagon concentrations of the same animals were analysed after a 15-hour fasting period (T0) and 10 minutes after oral glucose challenge (T10) (3.1.6 Oral glucose tolerance test (OGTT)).

Additionally, the differences of glucagon concentrations between T10 and T0 were calculated.

3.4 Statistical analysis and data presentation

Data were analysed using a two-tailed Student's t-test (MS Excel, Microsoft®, USA). P values < 0.05 were considered significant. Data are presented as means and either standard deviations (SD) or standard error of means (SEM), as indicated.

4 Results

4.1 Treated male Munich *Ins2*^C95S mutant and wild-type mice

4.1.1 Body weight

From the age of 21 days onwards, the body weights of randomly fed animals were measured weekly. No significant differences between insulin-treated mutants, wild-type mice and placebo-treated mutants existed until 100 days of age. Placebo-treated mutant mice were significantly lighter than wild-type mice at the age of 160 days (27.5 ± 1.4 g vs. 29.6 ± 2.1 g) (Figure 4.1).
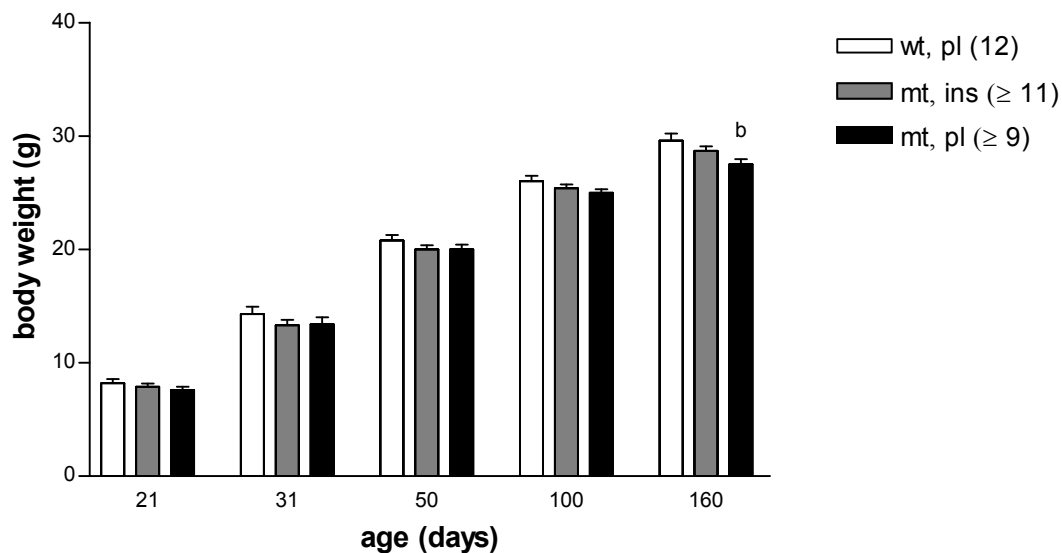
Figure 4.1: Randomly fed body weights
Body weights of insulin-treated mutants (mt, ins) are similar to those of wild-type (wt, pl) and placebo-treated mutant mice (mt, pl). At the age of 160 days, placebo-treated mutant mice are lower in body weight than wild-type mice.
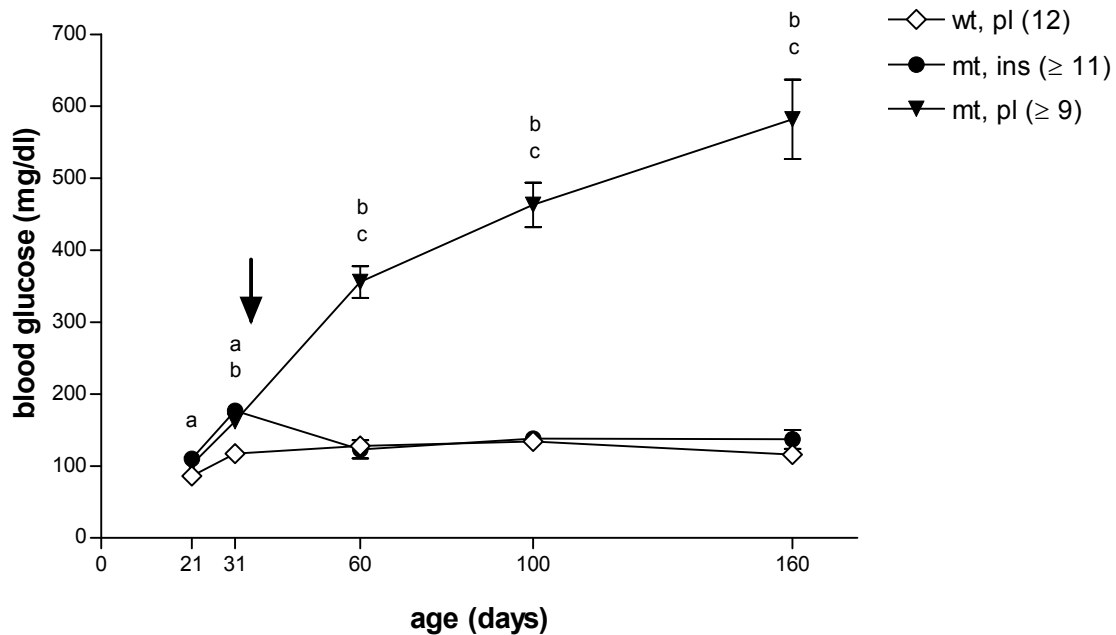Data are means ± SEM; b): wt, pl vs. mt, pl; $p < 0.05$; (n): number of animals investigated

4.1.2 Blood glucose concentration

In order to control and manage insulin therapy, randomly fed blood glucose concentrations were controlled weekly, starting with weaning at the age of 21 days until time of sacrifice at 160 days of age.

In general, insulin-treated mutant mice aged 60 days and older showed blood glucose concentrations similar to wild-type mice, ranging from approximately 100 to 140 mg/dl. Only shortly before the next pellet injection, blood glucose levels of insulin-treated mutants were higher than those of wild-type mice, but

were never over 200 mg/dl (not shown). Blood glucose levels of wild-type mice remained stable during the investigation period ($\leq 134 \pm 10$ mg/dl). From 31 days of age onwards, placebo-treated mutant mice exhibited a progressive diabetic phenotype with increasing blood glucose levels, reaching 582 ± 165 mg/dl at 160 days of age (Figure 4.2).

Figure 4.2: Randomly fed blood glucose levels between 21 and 160 days of age

Blood glucose concentrations of insulin-treated mutant mice (mt, ins) from 60 days of age onwards don't differ from those of wild-type mice (wt, pl). Placebo-treated mutant mice (mt, pl) demonstrate a progressive diabetic phenotype.

Data are means ± SEM; a,b,c: a) wt, pl vs. mt, ins; b) wt, pl vs. mt, pl; c) mt, ins vs. mt, pl; $p<0.05$; ↓: beginning of therapy (32 days of age); (n): number of animals investigated

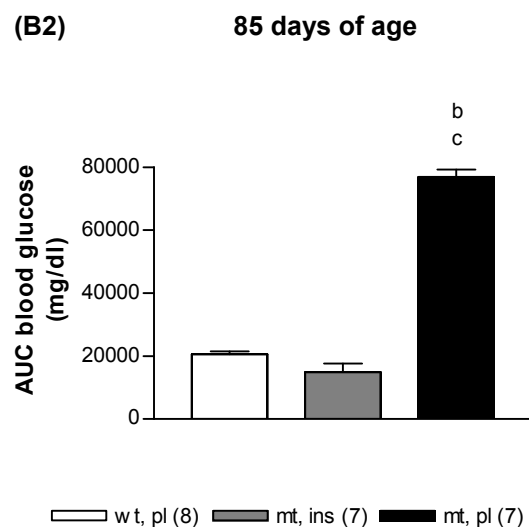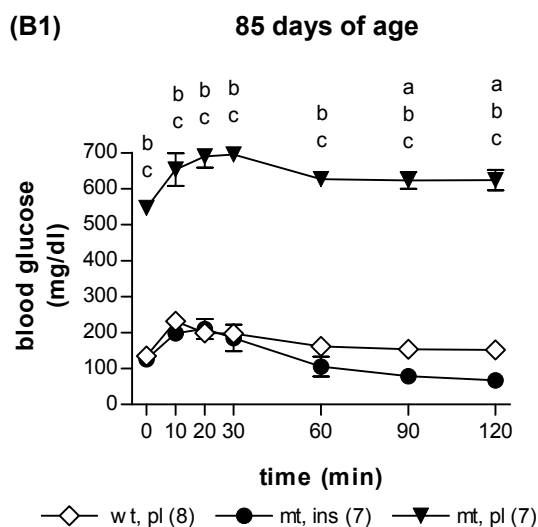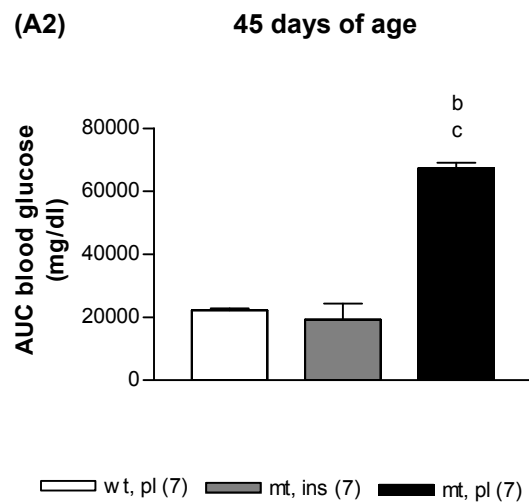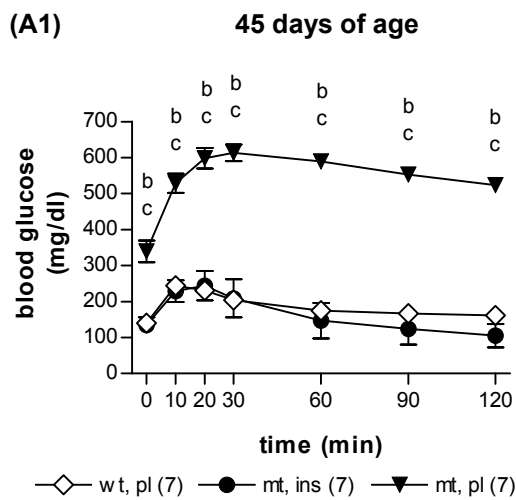### 4.1.3 Oral glucose tolerance test (OGTT)

At the age of 45, 85, 110 and 150 days, oral glucose tolerance tests were performed.
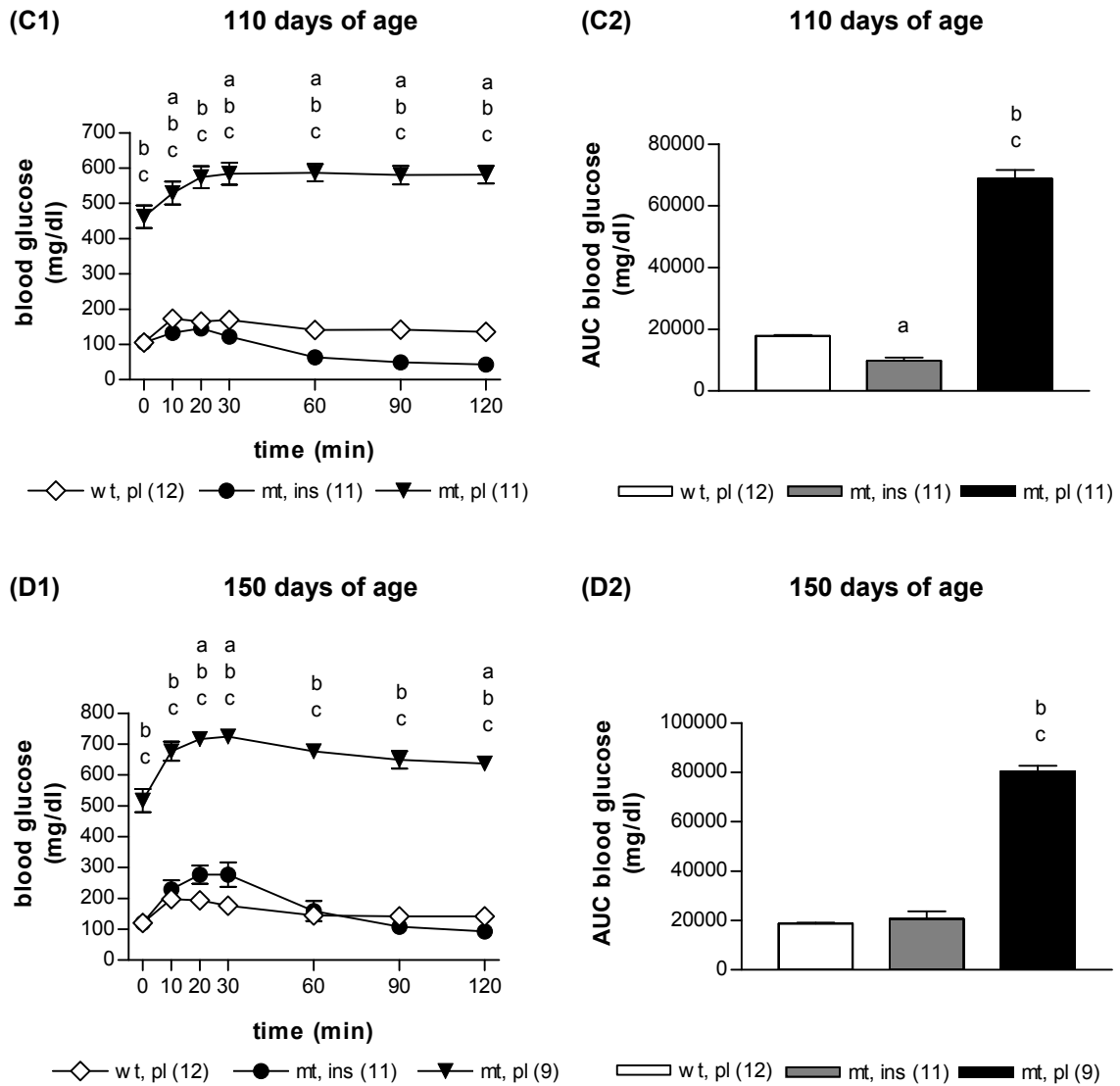
During all OGTTs, placebo-treated mutant mice featured significantly elevated blood glucose concentrations compared to wild-type mice and insulin-treated mutants. Therefore, the corresponding areas under blood glucose curve (AUC$_{blood\ glucose}$) were also increased (3.0- to 4.3-fold vs. wt, pl; 3.5- to 7.0-fold vs. mt, ins). The AUC$_{blood\ glucose}$ of insulin-treated mutants was similar to that of wild-type mice at 45, 85 and 150 days of age (Figure 4.3 (A2)-(D2)).

Blood glucose levels of insulin-treated mutant mice started to decline between 20 and 30 minutes after oral glucose application, those of placebo-treated

mutants between 30 and 60 minutes. In wild-type mice blood glucose values already declined between 10 and 20 minutes after glucose challenge. One hundred and twenty minutes after glucose challenge, the blood glucose levels of mutant mice treated with placebo-pellets were 29% (range 14% - 54%) higher, and those of wild-type mice were 19% (range 13% - 30%) higher than basal blood glucose concentrations. Due to the exogenous insulin delivered by the pellets, insulin-treated mutant mice presented 38% (range 22% - 59%) lower blood glucose concentrations at the end of the test than before glucose application (Figure 4.3 (A1)-(D1)).

These results demonstrate that placebo-treated Munich $Ins2^{C95S}$ mutant mice exhibit a diminished glucose tolerance, whereas insulin treatment partially normalises glucose tolerance in male mutants.

(A1) **45 days of age** **(A2)** **45 days of age**

(B1) **85 days of age** **(B2)** **85 days of age**

(C1) 110 days of age

(C2) 110 days of age

wt, pl (12) — mt, ins (11) — mt, pl (11)

(D1) 150 days of age

(D2) 150 days of age

wt, pl (12) — mt, ins (11) — mt, pl (9)

Figure 4.3 (A)-(D): OGTT at the age of 45 (A), 85 (B), 110 (C) and 150 (D) days

(A1)-(D1): Course of blood glucose concentrations

Placebo-treated mutant mice (mt, pl) present elevated blood glucose levels at all time points of the OGTT, irrespective of age at sampling. Blood glucose concentrations of insulin-treated mutants (mt, ins) decline later than those of wild-type mice (wt, pl), but earlier than those of placebo-treated mutants. One hundred and twenty minutes after glucose challenge, blood glucose levels are 29% and 19% higher than basal values (T0) in mutants with placebo-pellets and wild-type mice, respectively. Due to the insulin therapy, insulin-treated mutants show 38% lower blood glucose concentrations at the end of the OGTT compared to T0.

(A2)-(D2): Area under blood glucose curve (AUC_{blood glucose})

The AUC_{blood glucose} is significantly increased in placebo-treated mutant mice (mt, pl) during the OGTTs, irrespective of age at sampling. At the age of 45, 85 and 150 days, insulin-treated mutant (mt, ins) and wild-type mice (wt, pl) feature similar AUC_{blood glucose}.

Data are means ± SEM; a,b,c: a) wt, pl vs. mt, ins; b) wt, pl vs. mt, pl; c) mt, ins vs. mt, pl; $p < 0.05$; (n): number of animals investigated

4.1.4 Insulin tolerance test and placebo-insulin tolerance test

4.1.4.1 Intraperitoneal insulin tolerance test (ipITT)

The insulin sensitivity was investigated at the age of 50, 100 and 150 days via intraperitoneal insulin tolerance test (ipITT).

The percentaged decrease of the blood glucose concentration from basal value (T0=100%) after insulin injection was determined at different time points (T10, T20, T30, T60 and T90; data not shown). The corresponding area under the blood glucose curve ($AUC_{blood\ glucose}$) was calculated. At the age of 50 days, no significant differences between placebo-treated mutant and wild-type mice, regarding the $AUC_{blood\ glucose}$ were detected. One hundred- and 150-day-old placebo-treated mutants exhibited a significantly higher $AUC_{blood\ glucose}$ than wild-type mice and insulin-treated mutants. Due to the additional exogenous insulin released by the pellets, insulin-treated mutant mice showed lower $AUC_{blood\ glucose}$ compared to wild-type mice, irrespective of age at testing (Figure 4.4 (A)-(C)).

These data indicate that placebo-treated mutants become insulin resistant, whereas insulin treatment normalises insulin sensitivity.

(A) 50 days of age

(B) 100 days of age

(C) 150 days of age
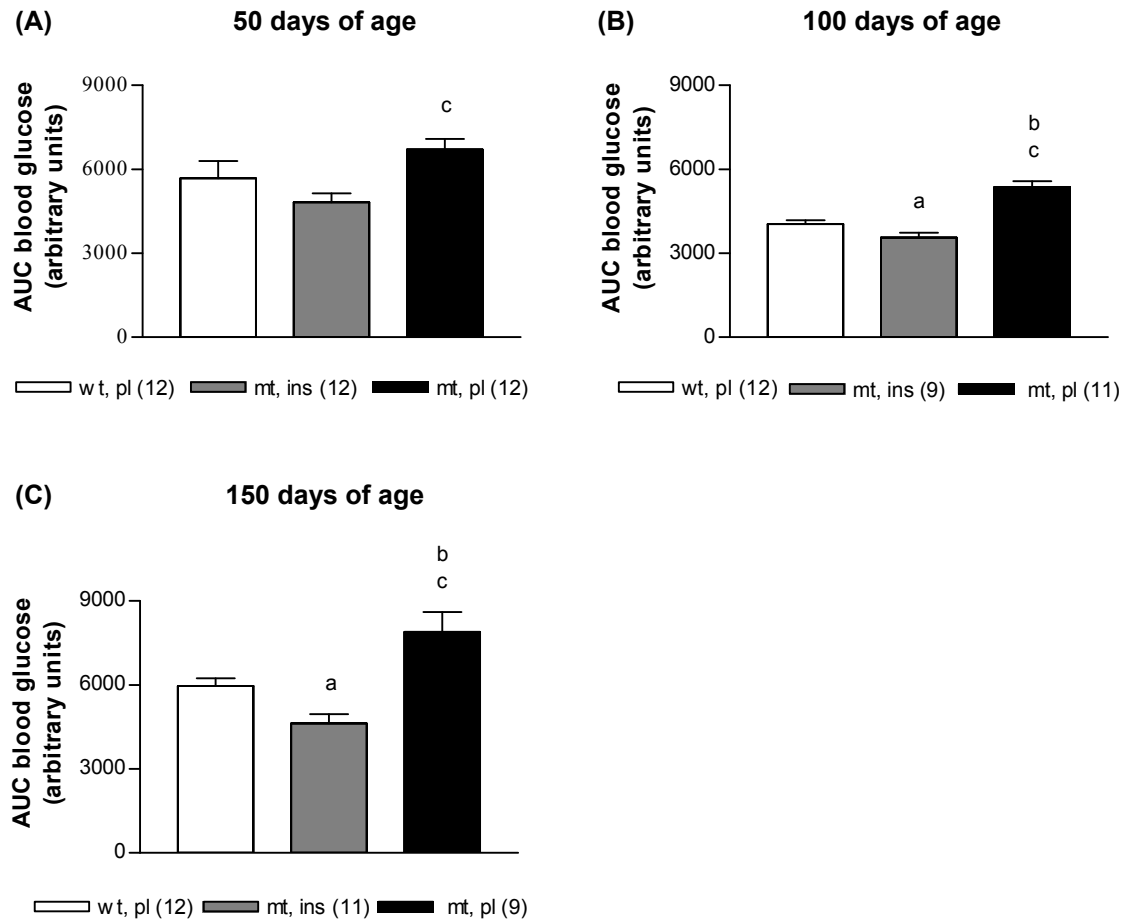
Figure 4.4 (A)-(C): Area under the curve of the percentaged blood glucose decrease from basal value (AUC$_{blood\ glucose}$) of the ipITT at the age of 50 (A), 100 (B) and 150 (C) days

The AUC$_{blood\ glucose}$ of mutant mice treated with insulin-pellets (mt, ins) are lower than those of wild-type mice (wt, pl). Placebo-treated mutant mice (mt, pl) feature a significantly elevated AUC$_{blood\ glucose}$ at the age of 100 and 150 days, compared to wild-type and insulin-treated mutant mice.

Data are means ± SEM; a,b,c: a) wt, pl vs. mt, ins; b) wt, pl vs. mt, pl; c) mt, ins vs. mt, pl $p<0.05$; (n): number of animals investigated

4.1.4.2 Comparison between intraperitoneal insulin tolerance test (ipITT) and placebo-intraperitoneal insulin tolerance test (placebo-ipITT)

To investigate the influence of the insulin released by the pellets of insulin-treated mutant mice during the ipITT, a placebo-ipITT with 0.9% NaCl was carried out at the age of 150 days. The results of the placebo-ipITT were compared to the corresponding values of the ipITT.
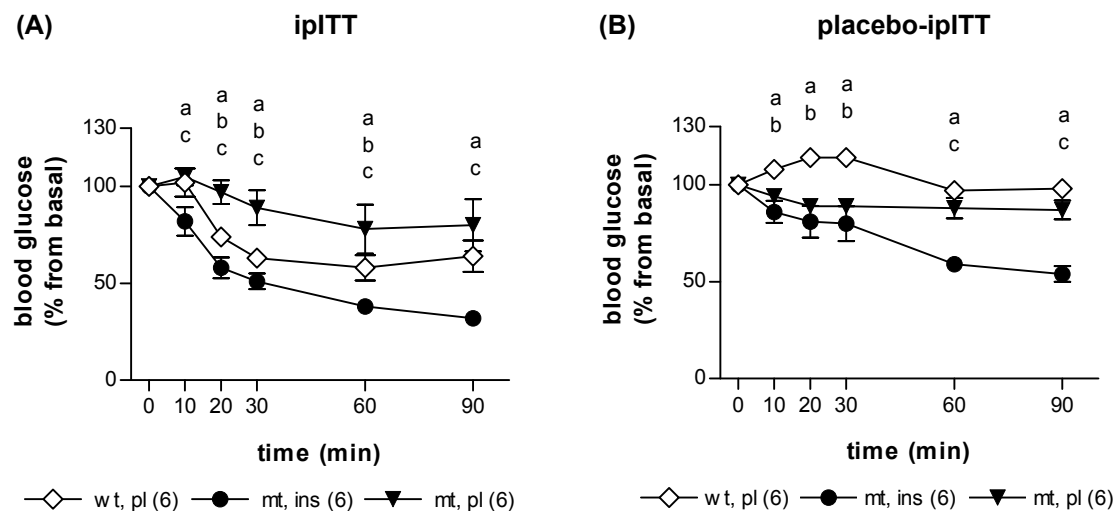
During the ipITT (Figure 4.5 (A)), the percentaged blood glucose concentrations of placebo-treated mutants only slightly decreased, despite of insulin application (T90: 80% ± 33% compared to T0: 100%). Due to the

therapy, insulin-treated mutants demonstrated a stronger decline of the percentaged blood glucose levels than wild-type mice (T90: mt, ins: 32% ± 8% vs. wt, pl: 64% ± 20%).

In the placebo-ipITT (Figure 4.5 (B)), the percentaged blood glucose concentrations of placebo-treated mutant and wild-type mice decreased little after 0.9% NaCl injection (T90: mt, pl: 87% ± 12%; wt, pl: 98% ± 3%). Although insulin-treated mutant mice featured a considerable blood glucose decrease from basal during the placebo-ipITT (T90: 54% ± 10%), the decrease was significantly weaker than that in the ipITT.
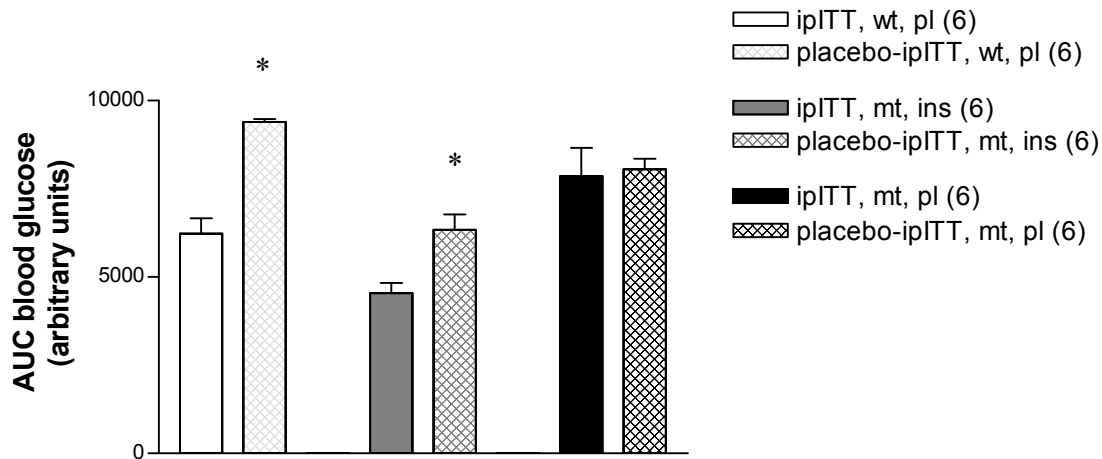
The $AUC_{blood\ glucose}$ of the ipITT and the placebo-ipITT were similar in placebo-treated mutants. Insulin-treated mutant and wild-type mice exhibited a significantly lower $AUC_{blood\ glucose}$ in the ipITT than in the placebo-ipITT (Figure 4.6).

These results demonstrate that insulin-treated mutants don't become insulin resistant in contrast to placebo-treated mutants.

Figure 4.5 (A)/(B): Percentaged blood glucose decrease from basal value during the ipITT (A) and the placebo-ipITT (B) at 150 days of age

The percentaged blood glucose concentrations of placebo-treated mutant mice (mt, pl) only decrease little after insulin injection, compared to wild-type (wt, pl) and insulin-treated mutant mice (mt, ins) (A). During the placebo-ipITT (B) placebo-treated mutant and wild-type mice demonstrate almost no decline of the percentaged blood glucose values. Due to the insulin released by the pellets, the percentaged blood glucose concentrations of insulin-treated mutants decrease during the placebo-ipITT, but not as marked as during the ipITT.
Data are means ± SEM; a,b,c: a) wt, pl vs. mt, ins; b) wt, pl vs. mt, pl; c) mt, ins vs. mt, pl
p<0.05; (n): number of animals investigated

Figure 4.6: Comparison of the AUC$_{blood\ glucose}$ between the ipITT and the placebo-ipITT at the age of 150 days

Insulin-treated mutants (mt, ins) and wild-type mice (wt, pl) exhibit a significantly lower AUC$_{blood\ glucose}$ after insulin injection (ipITT) than after administration of 0.9% NaCl (placebo-ipITT). Placebo-treated mutant mice (mt, pl) show a similar AUC$_{blood\ glucose}$ in the ipITT and the placebo-ipITT.

Data are means ± SEM; *: ipITT vs. placebo-ipITT; $p < 0.05$;
(n): number of animals investigated

4.1.5 Serum C-peptide concentration

To examine the endogenous insulin secretion, without the influence of the insulin delivered by the pellets, serum C-peptide concentrations were determined at 45, 85, 110 and 150 days of age during the OGTT. C-peptide is known to be secreted with insulin in equimolar concentrations.

Randomly fed (T0) C-peptide levels of insulin-treated mutant mice were 69 - 87% and 35 - 76% lower compared to wild-type mice and placebo-treated mutants, respectively. Placebo-treated mutants exhibited a 43 - 53% lower C-peptide concentration than wild-type mice.

Ten minutes after oral glucose challenge (T10), C-peptide concentrations of insulin-treated mutants were 91 - 96% and 43 - 75% lower versus wild-type mice and placebo-treated mutants, respectively. Compared to wild-type mice, placebo-treated mutants exhibited a 76 - 86% lower C-peptide concentration (Table 4.1).

Ten minutes after oral glucose application, serum C-peptide levels of insulin-treated mutants declined 0.7- to 0.9-fold. C-peptide concentrations of wild-type mice increased 1.5- to 3.6-fold. In placebo-treated mutant mice, the C-peptide concentrations decreased 0.6- to 0.9-fold after glucose application at the age

of 45, 85 and 110 days and slightly increased at the age of 150 days (Figure 4.7).

The analysed C-peptide levels show that insulin-treated and placebo-treated Munich $Ins2^{C95S}$ mutant mice suffer from a disturbed insulin secretion.

time	group (n ≥7)	age (days)			
		45	85	110	150
T0	wt, pl	827 ± 140	639 ± 301	636 ± 290	525 ± 237
	mt, ins	156 ± 105 [a]	126 ± 49 [a]	82 ± 66 [a]	161 ± 107 [a]
	mt, pl	473 ± 145 [b,c]	328 ± 61 [b,c]	347 ± 100 [b,c]	247 ± 93 [b]
T10	wt, pl	1225 ± 458	1576 ± 340	1480 ± 482	1870 ± 307
	mt, ins	113 ± 62 [a]	93 ± 50 [a]	61 ± 46 [a]	147 ± 79 [a]
	mt, pl	295 ± 61 [b,c]	291 ± 96 [b,c]	245 ± 91 [b,c]	257 ± 87 [b,c]

Table 4.1: C-peptide concentrations (pM) in the serum of randomly fed (T0) mice and 10 minutes after oral glucose challenge (T10)

Randomly fed and 10 minutes after oral glucose application, insulin-treated mutants (mt, ins) show lower C-peptide levels compared to wild-type mice (wt, pl) and placebo-treated mutant mice (mt, pl). The C-peptide concentrations of placebo-treated mutants are significantly lower than those of wild-type mice.
Data are means ± SD; a,b,c: a) wt, pl vs. mt, ins; b) wt, pl vs. mt, pl; c) mt, ins vs. mt, pl
$p < 0.05$; (n): number of animals investigated
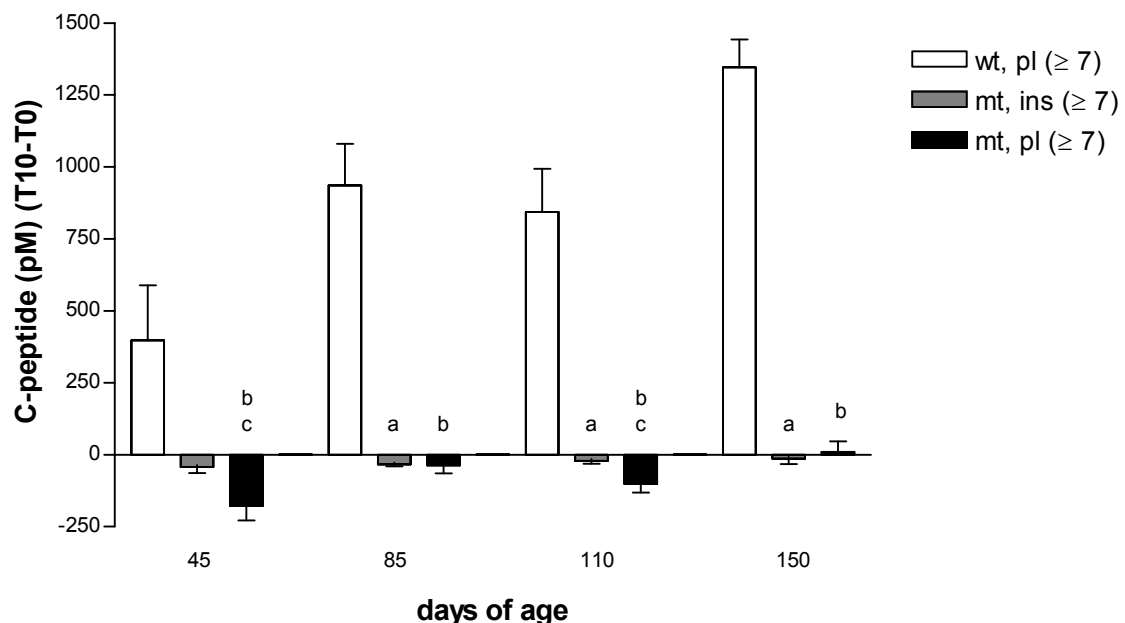
Figure 4.7: Changes in C-peptide concentrations 10 minutes after oral glucose challenge

In insulin-treated mutant mice the C-peptide levels decline 10 minutes after glucose administration. Placebo-treated mutants feature a decline of C-peptide concentrations at 45,

85 and 110 days of age, and a slight incline at the age of 150 days. In wild-type mice (wt, pl) the C-peptide levels increase 10 minutes after glucose administration.
Data are means ± SEM; a,b,c: a) wt, pl vs. mt, ins; b) wt, pl vs. mt, pl; c) mt, ins vs. mt, pl; $p < 0.05$; (n): number of animals investigated

4.1.6   Pancreatic C-peptide content

C-peptide levels in the pancreas of 100-day-old mice were determined, and were related to the pancreatic protein content.

Insulin-treated mutant mice exhibited a 59% lower C-peptide/protein level in the pancreas compared to wild-type mice. The C-peptide/protein content in the pancreas of placebo-treated mutants was 91% and 78% lower than that of wild-type and insulin-treated mutant mice, respectively (2.9 ± 0.8 nM/mg vs. 31.6 ± 17.6 nM/mg vs. 13.1 ± 4.2 nM/mg; Figure 4.8).
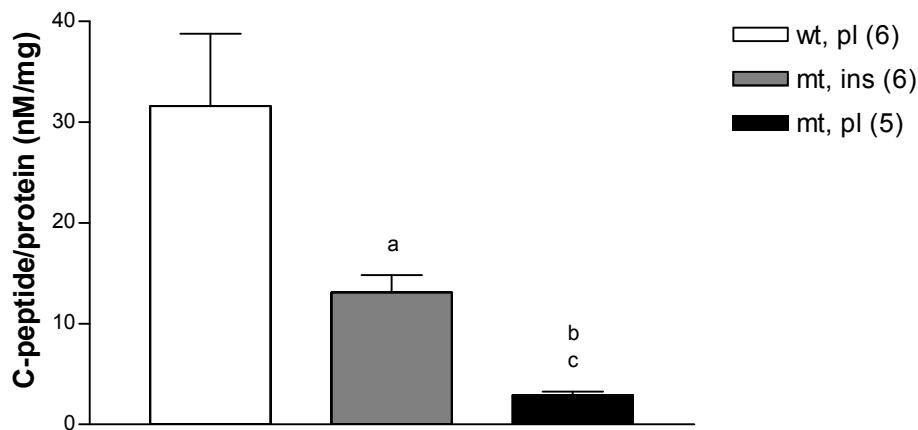
Figure 4.8: C-peptide/protein concentrations in the pancreas of 100-day-old mice
Insulin-treated mutant mice (mt, ins) present a significantly higher C-peptide/protein content in the pancreas than placebo-treated mutants (mt, pl). The C-peptide/protein concentration of wild-type mice (wt, pl) is significantly higher than that of mutant mice.
Data are means ± SEM; a,b,c: a) wt, pl vs. mt, ins; b) wt, pl vs. mt, pl; c) mt, ins vs. mt, pl; $p < 0.05$; (n): number of animals investigated

4.1.7   Serum glucagon concentration

Randomly fed serum glucagon concentrations of 100-day-old insulin-treated mutants and wild-type mice were equal. Despite of severe hyperglycaemia, placebo-treated mutant mice demonstrated 1.5-fold ($p < 0.05$) higher glucagon levels in the serum compared to wild-type and insulin-treated mutant mice (Table 4.2).

group (n)	glucagon (pg/ml)	blood glucose (mg/dl)
wt, pl (6)	87 ± 17	145 ± 13
mt, ins (6)	87 ± 27	158 ± 61
mt, pl (5)	127 ± 21 [b,c]	571 ± 39 [b,c]

Table 4.2: Serum glucagon levels and corresponding blood glucose concentrations at the age of 100 days

Placebo-treated mutant mice (mt, pl) show significantly higher serum glucagon concentrations compared to wild-type (wt, pl) and insulin-treated mutant mice (mt, ins), despite of elevated blood glucose levels.
Data are means ± SD; b,c: b) wt, pl vs. mt, pl; c) mt, ins vs. mt, pl; p<0.05;
(n): number of animals investigated

4.1.8 Serum lipid peroxidation

The amount of thiobarbituric acid reactive substances (TBARS) in the serum of 100- and 140-day-old animals was determined. TBARS, a product of lipid peroxidation due to oxygen stress, are presented in malondialdehyde (MDA) equivalents.

Insulin-treated mutant and wild-type mice showed a similar extent of lipid peroxidation in the serum (17 - 20 μM MDA), irrespective of age at sampling. Placebo-treated mutant mice exhibited 3.6- and 3.3-fold elevated MDA values versus wild-type and insulin-treated mutant mice, respectively at the age of 100 days, as well as 4.4- and 4.0-fold higher MDA concentrations versus wild-type and insulin-treated mutant mice, respectively at the age of 140 days.

One hundred-day-old placebo-treated mutant mice presented significantly elevated blood glucose values compared to wild-type (3.9-fold) and insulin-treated mutant mice (3.6-fold). At the age of 140 days, placebo-treated mutants featured 4.5-fold (vs. wt, pl) and 3.6-fold (vs. mt, ins) higher blood glucose concentrations (Table 4.3).

Blood glucose levels correlated with lipid peroxidation in the serum (Figure 4.9).

	age (days)			
	100		140	
group (n)	MDA (µM)	blood glucose (mg/dl)	MDA (µM)	blood glucose (mg/dl)
wt, pl (6)	17.6 ± 2.9	145 ± 13	16.7 ± 1.7	126 ± 12
mt, ins (6)	19.5 ± 5.3	158 ± 61	18.4 ± 3.4	157 ± 33
mt, pl (5/6)*	63.6 ± 10.2 [b,c]	571 ± 39 [b, c]	74.0 ± 12.3 [b,c]	568 ± 63 [b,c]

Table 4.3: Serum lipid peroxidation expressed in malondialdehyde (MDA) equivalents and corresponding blood glucose concentrations

Insulin-treated mutant mice (mt, ins) exhibit similar serum MDA and blood glucose levels as wild-type mice (wt, pl), irrespective of age at sampling. The serum MDA and blood glucose concentrations of placebo-treated mutant mice (mt, pl) are at least 3.3-fold higher compared to wild-type mice and insulin-treated mutants.

Data are means ± SD; b,c: b) wt, pl vs. mt, pl; c) mt, ins vs. mt, pl $p < 0.05$;
(n): number of animals investigated; *100 days: n=5, 140 days: n=6

(A) **100 days of age**   **(B)** **140 days of age**
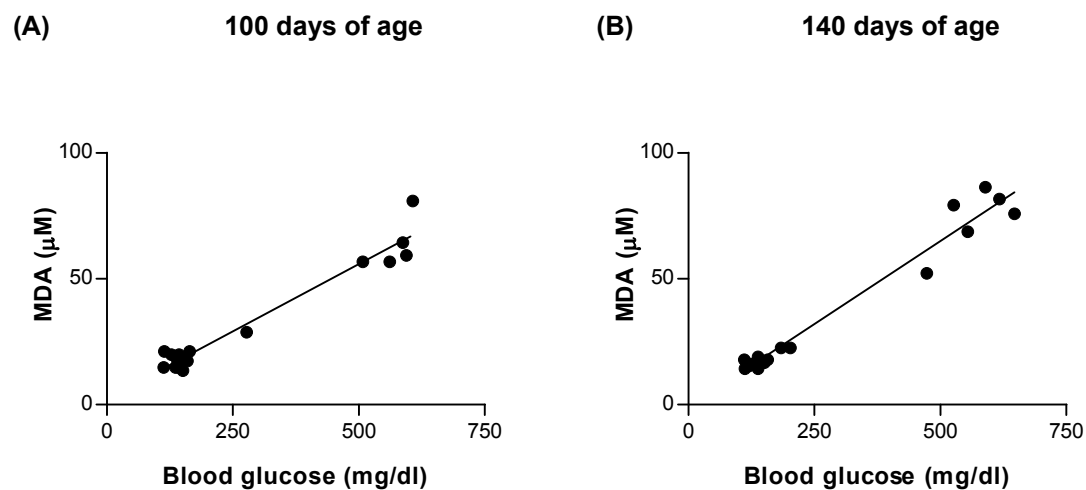
Figure 4.9 (A)/(B): Correlation of blood glucose concentrations and serum lipid peroxidation expressed in MDA equivalents at the age of 100 (A) and 140 (B) days

The blood glucose concentrations and serum MDA equivalents in the examined groups correlate by $r = 0.98$, irrespective of age at testing ($p < 0.01$).

4.1.9 Western blot analysis of isolated islets

Islets of 100-day-old mice were isolated for examination of the ER stress markers BiP, PeIF2α and CHOP/GADD153 via western blot analysis. Islets of wild-type mice were easily detected under the stereomicroscope, appearing round to oval shaped with a smooth surface, and endocrine cells within the islets being smaller than the cells of the exocrine pancreas. Using reflected light microscopy and a black background, wild-type islets appeared brighter

than exocrine tissue clusters. In transmitted light, the islets appeared brownish versus whitish exocrine pancreas. Islets of placebo-treated mutant mice were sparse, and most of them appeared as irregularly shaped clusters of endocrine cells, suggesting fragmentation of islets. With reflected light microscopy, islets of placebo-treated mutants appeared more transparent than islets of wild-type mice or exocrine tissue clusters, using transmitted light, islets of placebo-treated mutants could not be identified. Islets of insulin-treated mutants, could not be identified as easily as wild-type islets, but easier than islets of placebo-treated mutants. In transmitted light, only few of the islets could be detected, exhibiting a slightly brown colour. Using reflected light microscopy, more islets were detectable, the islets were not as bright compared to those of wild-type mice, but less transparent versus islets of placebo-treated mutants. Some islets exhibited an irregular shape, others were shaped similar to those of wild-type mice. About 100 - 150, 40 - 60, and 30 - 40 islets per animal could be harvested within 1.5 hours from pancreata of wild-type mice, insulin-treated and placebo-treated mutants, respectively. Isolated islets of wild-type mice were at least 90% pure, whereas isolates of insulin-treated mutants were contaminated with approximately 15 - 25%, those of placebo-treated mutant mice with approximately 30 - 40% exocrine pancreas tissue fragments.

In 1 placebo-treated mutant, the actin band was missing despite sufficient total protein content in the sample, as evidenced by Bradford method. This suggests degradation of proteins in the sample.

The molecular weights of the different ER stress markers were 78 kDa for BiP, 40 kDa for PeIF2α, and 25 kDa for CHOP. The optical density of bands of the ER stress markers was determined, and referred to that of actin (45 kDa).

4.1.9.1 BiP/actin

Insulin-treated mutants showed a similar optical density of BiP/actin in the islets compared to wild-type mice and a slightly higher optical density of BiP/actin than placebo-treated mutants (1.33 ± 0.54 vs. 1.21 ± 0.22 vs. 0.98 ± 0.30; n.s.; Figure 4.10).
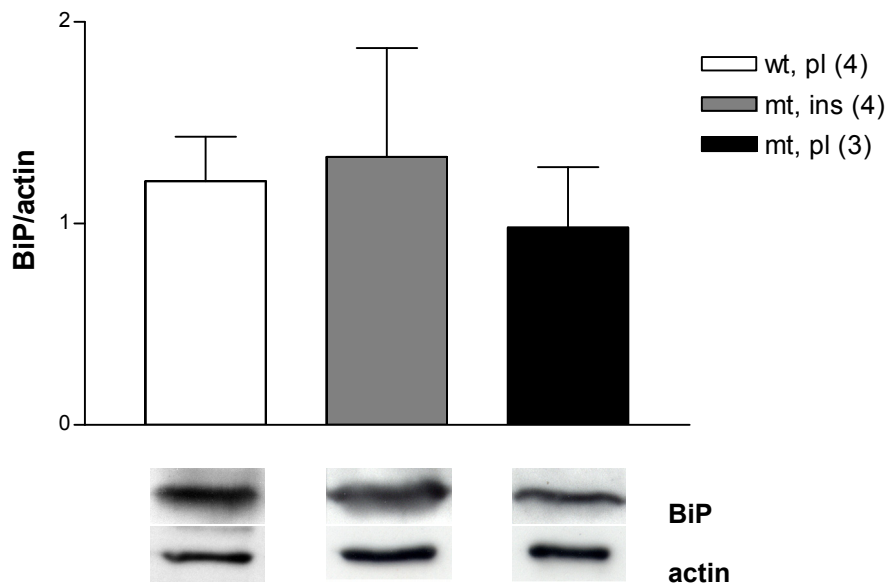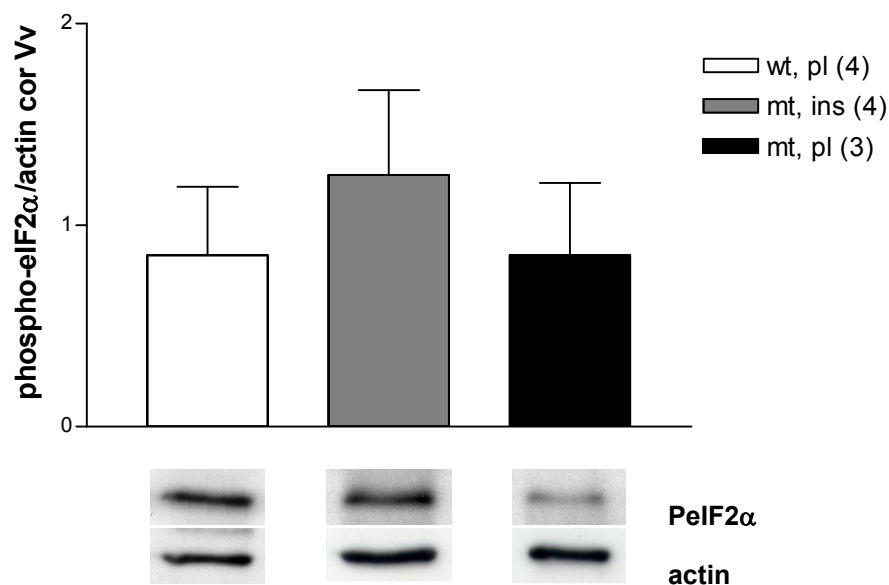
Figure 4.10: Optical density of BiP/actin in isolated islets at the age of 100 days

In insulin-treated mutants (mt, ins) the optical density of BiP/actin is similar compared to wild-type mice (wt, pl), and marginally higher than in placebo-treated mutant mice (mt, pl).
Data are means ± SEM; (n): number of animals investigated

4.1.9.2 PeIF2α/actin

The optical density of PeIF2α/actin was higher in the islets of insulin-treated mutants as compared to wild-type and placebo-treated mutant mice (1.25 ± 0.42 vs. 0.85 ± 0.34 vs. 0.85 ± 0.36; n.s.; Figure 4.11).
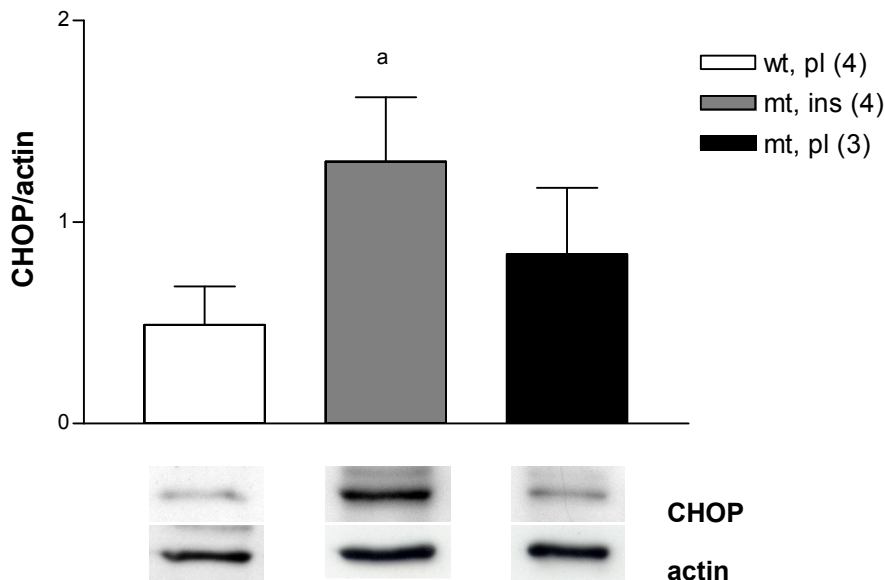

Figure 4.11: Optical density of PeIF2α/actin in isolated islets at the age of 100 days

Insulin-treated mutants (mt, ins) demonstrate a higher optical density of PeIF2α/actin in the islets than wild-type mice (wt, pl), and placebo-treated mutants (mt, pl).
Data are means ± SEM; (n): number of animals investigated

4.1.9.3 CHOP/actin

Insulin-treated mutants featured a significantly higher optical density of CHOP/actin than wild-type mice ($p < 0.01$) and a higher optical density of CHOP/actin versus placebo-treated mutant mice (1.30 ± 0.32 vs. 0.49 ± 0.19 vs. 0.84 ± 0.33; Figure 4.12).

Figure 4.12: Optical density of CHOP/actin in isolated islets at the age of 100 days

The optical density of CHOP/actin in the islets of insulin-treated mutants (mt, ins) is significantly higher than that of wild-type mice (wt, pl). Placebo-treated mutants (mt, pl) exhibit an over 1.5-fold higher optical density of CHOP/actin in the islets than wild-type mice.
Data are means ± SEM; a): wt, pl vs. mt, ins; $p < 0.05$; (n): number of animals investigated

4.1.10 Organ weight

Five to six mice per group were selected randomly for the determination of the organ weights at 160 days of age. In these selected mice, no significant differences concerning the body weight existed (compare to 4.1.1 Body weight). Placebo-treated mutants exhibited more contents in the gastrointestinal tract (GIT) than wild-type mice ($p = 0.052$) and insulin-treated mutants ($p < 0.05$). When the GIT contents were subtracted from the entire body weight, placebo-treated mutants were lighter than wild-type mice ($p = 0.06$) and insulin-treated mutants ($p < 0.05$). The emptied GIT of placebo-treated mutants was significantly heavier than that of wild-type and insulin-treated mutant mice. Mutant mice treated with insulin-pellets possessed less abdominal fatty tissue (mesenterial and residual fatty tissue from the abdominal and pelvic cave) than wild-type mice, but more than placebo-

treated mutants. The kidney and liver weights of insulin-treated mutants and wild-type mice were similar, whereas placebo-treated mutant mice featured elevated kidney and liver weights (Figure 4.13, Table 4.4). Placebo-treated mutants showed significantly lighter testes than wild-type mice. With regard to the weight of pancreas, heart and spleen, no significant differences between the examined groups were found (Table 4.4).
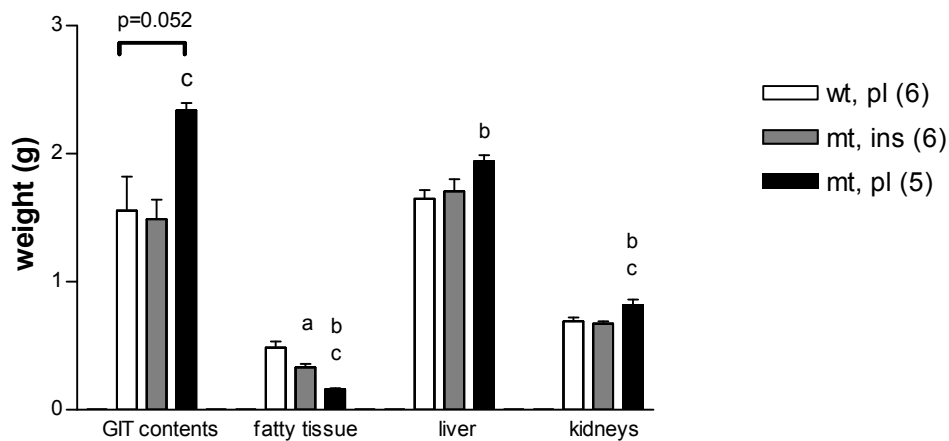
Figure 4.13: Organ weights of 160-day-old mice

Insulin-treated mutant (mt, ins) and wild-type mice (wt, pl) exhibit lower gastrointestinal tract (GIT) contents, liver and kidney weights than placebo-treated mutants (mt, pl). The abdominal fatty tissue of insulin-treated mutant mice is lighter than that of wild-type mice but heavier compared to placebo-treated mutants.

Data are means ± SEM; a,b,c: a) wt, pl vs. mt, ins; b) wt, pl vs. mt, pl; c) mt, ins vs. mt, pl; $p < 0.05$; (n): number of animals investigated

group (n)	body	body - GIT contents	GIT empty	pancreas	heart	spleen	testes
	g	g	g	mg	mg	mg	mg
wt, pl (6)	29.1 ± 2.5	27.1 ± 1.8	2.95 ± 0.50	379 ± 69	160 ± 14	164 ± 48	157 ± 6
mt, ins (6)	28.1 ± 0.8	26.6 ± 0.9	2.99 ± 0.37	362 ± 64	152 ± 13	129 ± 42	154 ± 17
mt, pl (5)	27.2 ± 1.4	24.9 ± 1.3 [c]	4.21 ± 0.37 [b, c]	375 ± 44	145 ± 15	121 ± 20	142 ± 8 [b]

Table 4.4: Organ weights at the age of 160 days

No significant differences concerning body, pancreas, heart and spleen weights are detected among the investigation groups. Placebo-treated mutant mice (mt, pl) feature higher contents in the gastrointestinal tract (GIT), and lower body weight minus GIT contents compared to insulin-treated mutant (mt, ins) and wild-type mice (wt, pl). The emptied GIT is significantly heavier and the testes are lighter in placebo-treated mutants than in wild-type and insulin-treated mutant mice.

Data are means ± SD; b,c: b) wt, pl vs. mt, pl; c) mt, ins vs. mt, pl;

(n): number of animals investigated

4.1.11 Qualitative-histological findings of the pancreas

4.1.11.1 Exocrine pancreas and pancreatic islets

Qualitative findings of the exocrine pancreas of 160-day-old mice did not reveal any pathological changes, and there were no signs of insulitis.

The amount of large islet profiles in the pancreas of insulin- and placebo-treated mutants appeared to be slightly lower compared to wild-type mice. In insulin-treated mutant mice, the average size of islet profiles seemed larger than those of placebo-treated mutants.

In sections immunostained for insulin, insulin-treated mutant mice presented less insulin-positive islet-cells than wild-type mice, but more than placebo-treated mutants.

In placebo-treated mutant mice, many of the β-cells demonstrated only weak staining intensity, indicating low insulin content. Some of the insulin-positive cells of insulin-treated mutants were stained almost as strong as those of wild-type mice, whereas other β-cells exhibited a reduced staining intensity compared to wild-type mice (Figure 4.14).

Immunohistochemistry for glucagon, somatostatin and pancreatic polypeptide demonstrated that placebo-treated mutants possessed a higher proportion of α-, δ- and PP-cells than wild-type mice. The islet structure was altered in placebo-treated mutants with non-β-cells being dispersed all over the islet profile. In insulin-treated mutant mice these alterations were not as distinct. Wild-type mice exhibited a typical murine islet composition with basically insulin-positive β-cells in the centre, surrounded by a ring of non-β-cells (Figure 4.15).
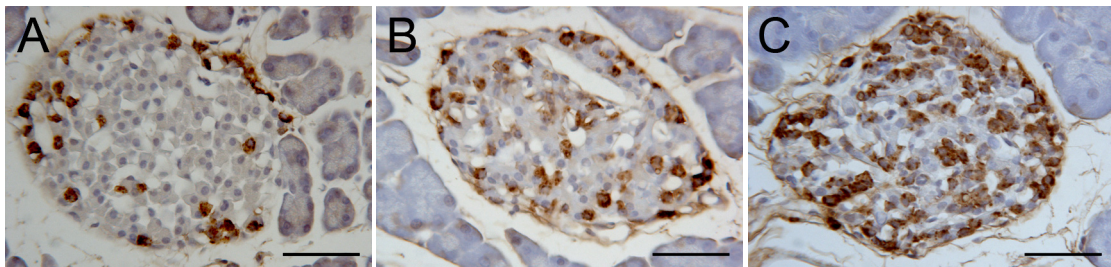
In a few islets of placebo-treated mutant mice, the endocrine cells were displaced by exocrine pancreas, and the islet structure was destroyed. This phenomenon was not observed in wild-type or insulin-treated mutant mice (Figure 4.16).
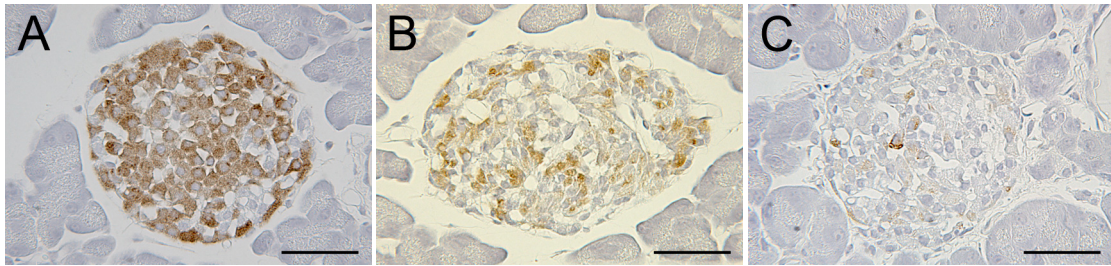
Figure 4.14 (A)-(C): Pancreas sections immunostained for insulin. Representative islet profiles of 160-day-old mice

Islet profiles of insulin-treated mutant mice (B) show a higher proportion of insulin-positive cells with stronger staining intensity than placebo-treated mutants (C). Most of the cells in the islet profiles of wild-type mice (A) are β-cells, which are stained intensively for insulin.
Bar: 50 µm

Figure 4.15 (A)-(C): Pancreas sections simultaneously immunostained for glucagon, somatostatin and pancreatic polypeptide. Representative islet profiles of 160-day-old mice

Islet structure and composition in placebo-treated mutant mice (C) are altered, with the proportion of non-β-cells being increased and non-β-cells being distributed all over the islet profile. These changes are less obvious in insulin-treated mutants (B). Wild-type mice (A) show a typical islet structure, characterised by few non-β-cells, surrounding a core of β-cells.
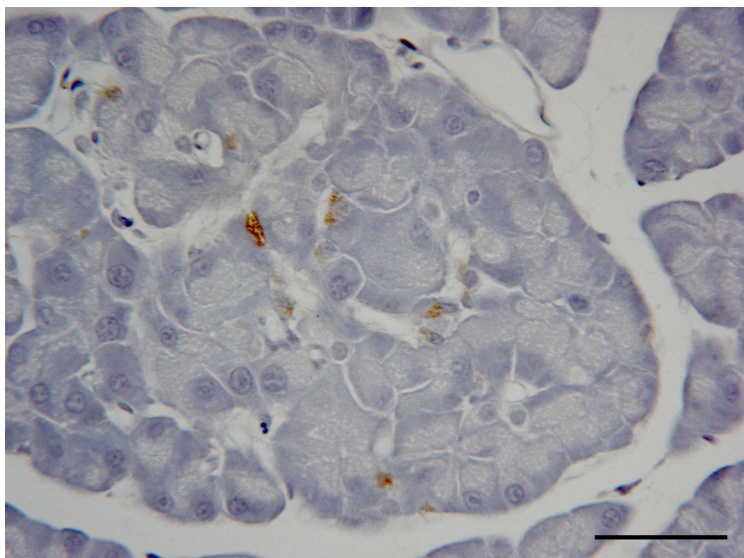Bar: 50 µm

Figure 4.16: Pancreas section simultaneously immunostained for glucagon, somatostatin and pancreatic polypeptide. Islet profile of a 160-day-old placebo-treated mutant mouse

In placebo-treated mutant mice, a few islets feature a destroyed structure with endocrine cells being displaced by exocrine pancreas; Bar: 50 µm

4.1.11.2 Isolated β-cells

Single insulin-positive cells and β-cell clusters of up to 4 nuclear profiles were identified as isolated β-cells, which are interpreted as sign of islet neogenesis (Bonner-Weir et al. 2008; Inada et al. 2008). These cells were found in all animals, either within the exocrine pancreas or associated to pancreatic ducts (Figure 4.17).
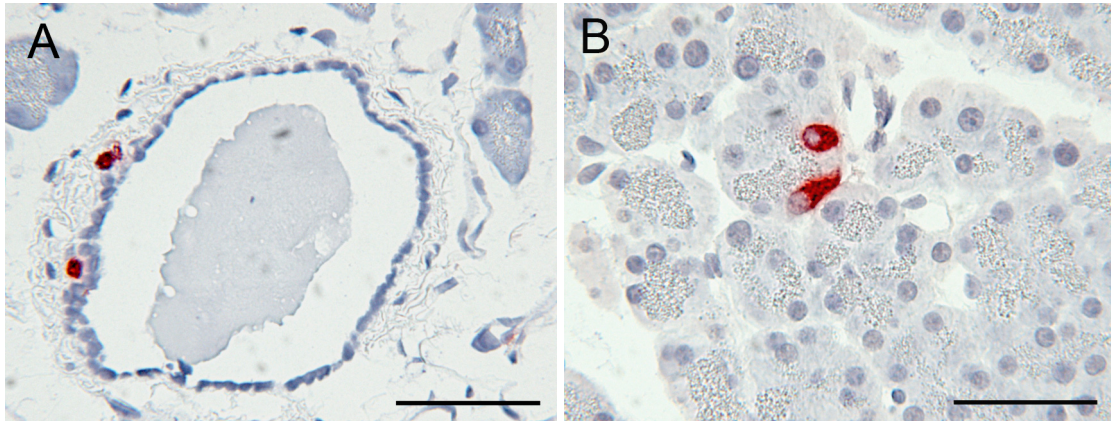
Figure 4.17: Immunohistochemistry of pancreas sections for insulin. Isolated β-cells in the pancreas of 160-day-old mice

Single isolated β-cells associated to a pancreatic duct (A) or within the exocrine pancreas (B) are found in all investigation groups.
Bar: 50 µm

4.1.12 Quantitative-stereological findings of the pancreas

4.1.12.1 Total pancreas volume

At the age of 160 days, insulin-treated mutants, wild-type and placebo-treated mutant mice showed a similar total volume of the pancreas (V_{pan}) (308 mm^3 ± 34 mm^3 vs. 328 ± 62 mm^3 vs. 326 ± 37 mm^3; Figure 4.18).
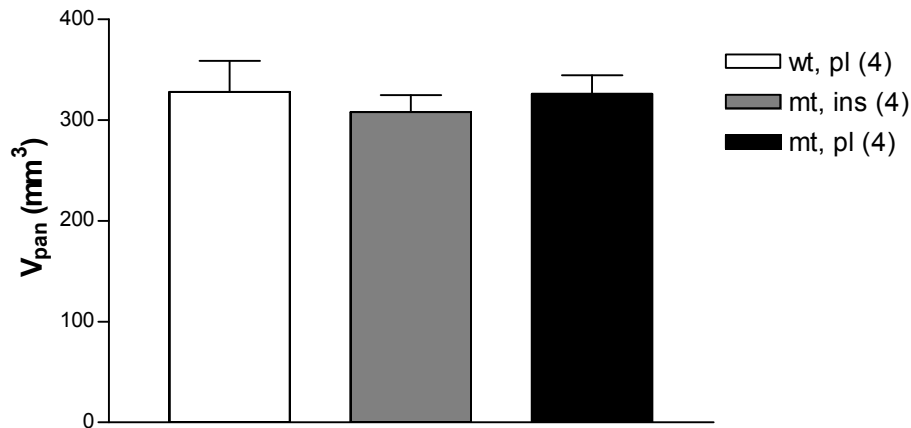
Figure 4.18: Total pancreas volume (V_{pan}) at the age of 160 days
The V_{pan} in insulin-treated mutants (mt, ins), wild-type (wt, pl) and placebo-treated mutant mice (mt, pl) is equal.
Data are means ± SEM; (n): number of animals investigated

4.1.12.2 Volume density of islets in the pancreas

The $Vv_{(islets/pan)}$ of insulin-treated mutant mice was lower than that of wild-type mice (p=0.051), but higher compared to placebo-treated mutants (0.23 ± 0.03% vs. 0.34 ± 0.07% vs. 0.18 ± 0.02%; Figure 4.19).
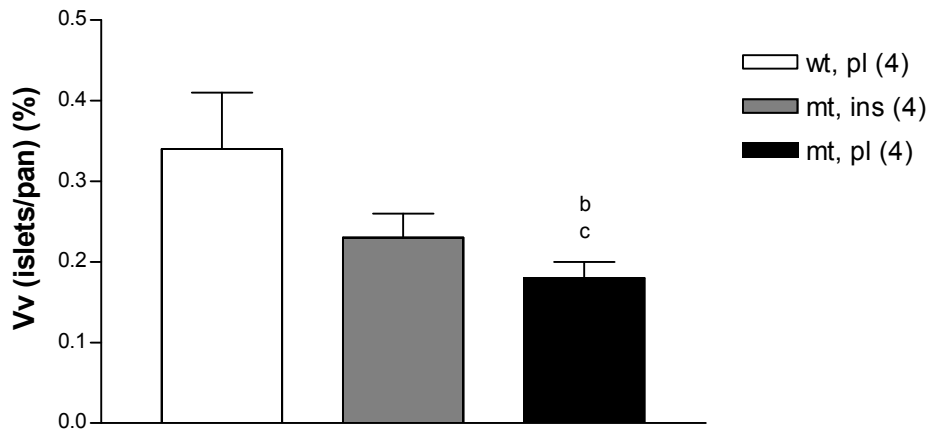
Figure 4.19: Volume density of islets in the pancreas (Vv$_{(islets/pan)}$) at the age of 160 days

The Vv$_{(islets/pan)}$ is 32% lower in insulin-treated mutant (mt, ins) versus wild-type mice (wt, pl), and 28% higher compared to placebo-treated mutants (mt, pl). Placebo-treated mutant mice demonstrate a 47% lower Vv$_{(islets/pan)}$ than wild-type mice.
Data are means ± SEM; b) wt, pl vs. mt, pl; c) mt, ins vs. mt, pl; $p < 0.05$;
(n): number of animals investigated

4.1.12.3 Total islet volume

Insulin-treated mutant mice presented a significantly lower total volume of islets in the pancreas (V$_{(islets,pan)}$) than wild-type mice, and a significantly higher V$_{(islets,pan)}$ compared to placebo-treated mutants (0.71 ± 0.06 mm^3 vs. 1.09 ± 0.19 mm^3 vs. 0.58 ± 0.03 mm^3; Figure 4.20).
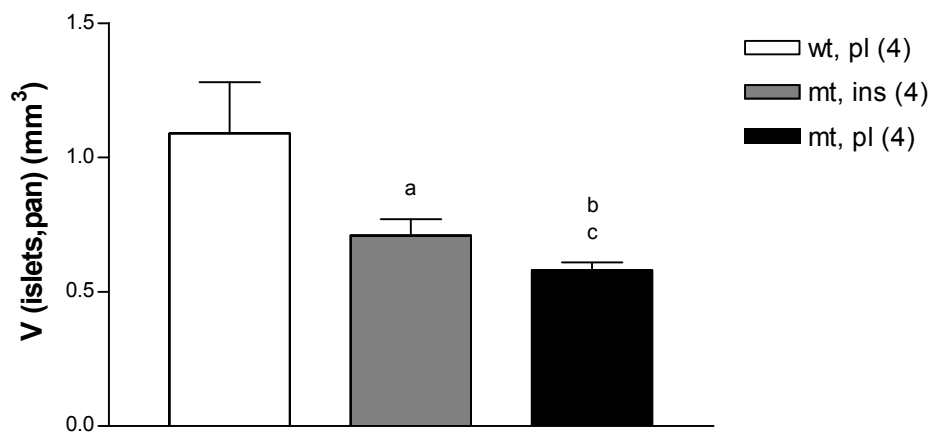
Figure 4.20: Total islet volume (V$_{(islets,pan)}$) of 160-day-old mice

In insulin-treated mutant mice (mt, ins) the V$_{(islets,pan)}$ is 35% lower compared to wild-type (wt, pl), and 22% higher compared to placebo-treated mutant mice (mt, pl). The V$_{(islets,pan)}$ of placebo-treated mutants is 47% lower than that of wild-type mice.
Data are means ± SEM; a,b,c: a) wt, pl vs. mt, ins; b) wt, pl vs. mt, pl; c) mt, ins vs. mt, pl; $p < 0.05$; (n): number of animals investigated

4.1.12.4 Volume density of β-cells in the endocrine compartment of the islets

The proportion of insulin-producing β-cells in the endocrine compartment of the islets was slightly lower in insulin-treated mutant than in wild-type mice, but higher compared to placebo-treated mutants (72 ± 4% vs. 81 ± 3% vs. 46 ± 6%; Figure 4.21).
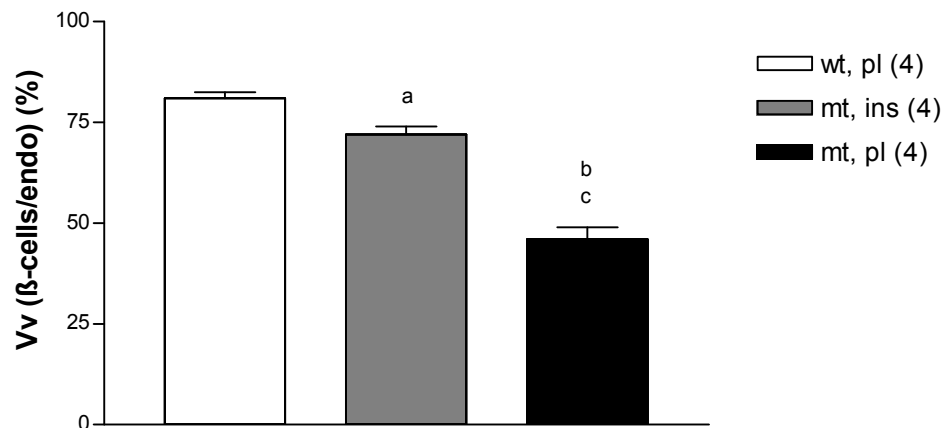
Figure 4.21: Volume density of β-cells in the endocrine compartment of the islets (Vv$_{(β\text{-cells/endo})}$) at the age of 160 days

Insulin-treated mutant mice (mt, ins) exhibit a 11% lower Vv$_{(β\text{-cells/endo})}$ versus wild-type mice (wt, pl), and a 57% higher Vv$_{(β\text{-cells/endo})}$ compared to placebo-treated mutants (mt, pl). In placebo-treated mutants the Vv$_{(β\text{-cells/endo})}$ is 43% lower than in wild-type mice.
Data are means ± SEM; a,b,c: a) wt, pl vs. mt, ins; b) wt, pl vs. mt, pl; c) mt, ins vs. mt, pl; $p < 0.05$; (n): number of animals investigated

4.1.12.5 Total volume of β-cells in the islets

The total volume of β-cells in the islets (V$_{(β\text{-cells,islets})}$) of mutants treated with insulin was significantly lower than that of wild-type mice, but significantly higher than that of placebo-treated mutants (0.37 ± 0.04 mm^3 vs. 0.65 ± 0.14 mm^3 vs. 0.21 ± 0.03 mm^3; Figure 4.22).

Figure 4.22: Total volume of β-cells in the islets (V $_{(\beta\text{-cells,islets})}$) at 160 days of age

Insulin-treated mutant mice (mt, ins) feature a 43% lower V$_{(\beta\text{-cells,islets})}$ than wild-type mice (wt, pl) and a 76% higher V$_{(\beta\text{-cells,islets})}$ compared to placebo-treated mutants (mt, pl). The V$_{(\beta\text{-cells,islets})}$ of placebo-treated mutants is 68% lower than that of wild-type mice.
Data are means ± SEM; a,b,c: a) wt, pl vs. mt, ins; b) wt, pl vs. mt, pl; c) mt, ins vs. mt, pl; p<0.05; (n): number of animals investigated

4.1.12.6 Volume density of non-β-cells in the endocrine compartment of the islets

The volume density of glucagon producing α-, somatostatin secreting δ-, and pancreatic polypeptide expressing PP-cells in the endocrine compartment of the islets (Vv$_{(non-\beta\text{-cells/endo})}$) was significantly higher in insulin-treated mutant compared to wild-type mice, but significantly lower compared to placebo-treated mutants (28 ± 4% vs. 19 ± 3% vs. 54 ± 6%; Figure 4.23).
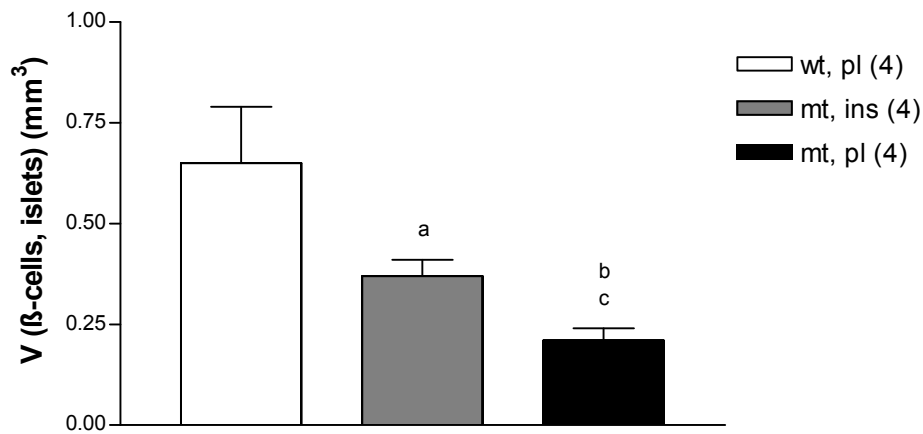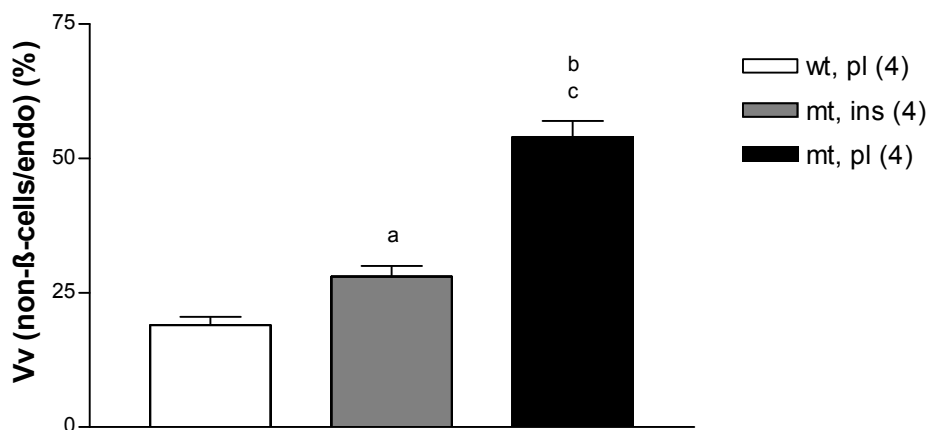

Figure 4.23: Volume density of non-β-cells in the endocrine compartment of the islets (Vv$_{(non-\beta\text{-cells/endo})}$) at the age of 160 days

Insulin-treated mutant mice (mt, ins) feature a 47% higher Vv$_{(non-\beta\text{-cells/endo})}$ than wild-type mice (wt, pl), and a 48% lower Vv$_{(non-\beta\text{-cells/endo})}$ than placebo-treated mutants (mt, pl). Compared to wild-type mice the Vv $_{(non-\beta\text{-cells/endo})}$ of placebo-treated mutants is 184% higher.
Data are means ± SEM; a,b,c: a) wt, pl vs. mt, ins; b) wt, pl vs. mt, pl; c) mt, ins vs. mt, pl; p<0.05; (n): number of animals investigated

4.1.12.7 Total volume of non-β-cells in the islets

The total volume of α-, δ-, and PP-cells in the islets ($V_{(non-β-cells,islets)}$) was equal in insulin-treated mutants and wild-type mice (0.15 ± 0.02 mm^3 vs. 0.15 ± 0.02 mm^3). Placebo-treated mutant mice showed a significantly higher $V_{(non-β-cells,islets)}$ compared to wild-type mice (0.25 ± 0.03 mm^3 vs. 0.15 ± 0.02 mm^3) and insulin-treated mutants (Figure 4.24).
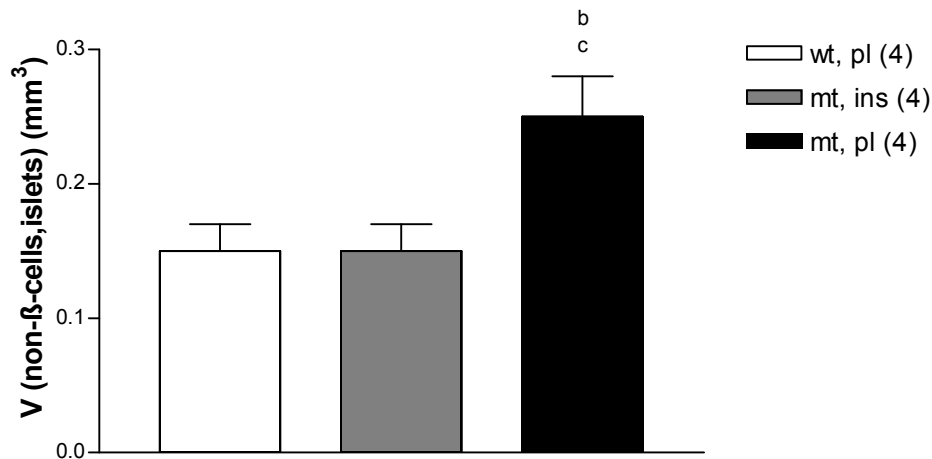
Figure 4.24: Total volume of non-β-cells in the islets ($V_{(non-β-cells,islets)}$) at 160 days of age
Placebo-treated mutant mice (mt, pl) exhibit a 67% higher $V_{(non-β-cells,islets)}$ compared to wild-type (wt, pl) and insulin-treated mutant mice (mt, ins).
Data are means ± SEM; b,c: b) wt, pl vs. mt, pl; c) mt, ins vs. mt, pl; p<0.05;
(n): number of animals investigated

4.1.12.8 Volume density of capillaries in the islets

The volume density of capillaries in the islets ($Vv_{(capillaries/islets)}$) of insulin-treated mutant mice was equal compared to wild-type mice, and higher compared to placebo-treated mutants (27 ± 4% vs. 27 ± 3% vs. 21 ± 4%; n.s.; Figure 4.25).
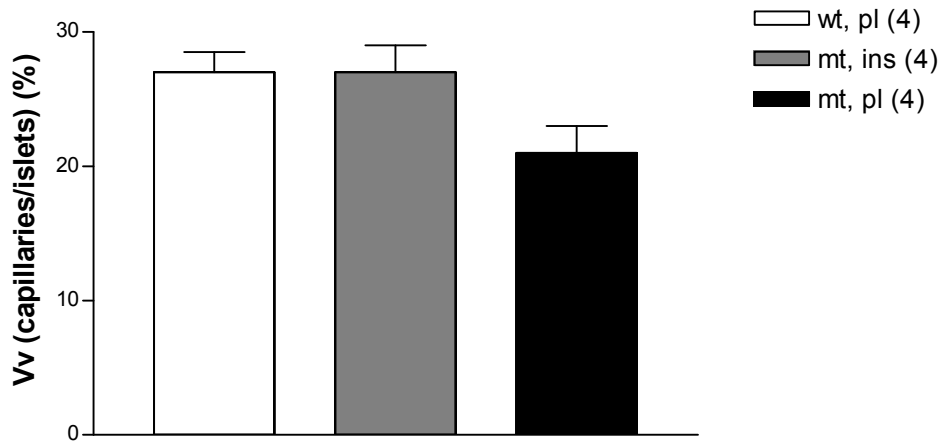
Figure 4.25: Volume density of capillaries in the islets ($Vv_{(capillaries/islets)}$) at the age of 160 days

Insulin-treated mutant (mt, ins) and wild-type mice (wt, pl) present a 29% higher $Vv_{(capillaries/islets)}$ than placebo-treated mutants (mt, pl).

Data are means ± SEM; (n): number of animals investigated

4.1.12.9 Total volume of capillaries in the islets

Insulin-treated mutant mice featured a significantly lower total capillary volume in the islets ($V_{(capillaries,islets)}$) than wild-type mice, but a significantly higher $V_{(capillaries,islets)}$ than placebo-treated mutants (0.19 ± 0.04 mm^3 vs. 0.29 ± 0.05 mm^3 vs. 0.12 ± 0.03 mm^3; Figure 4.26).
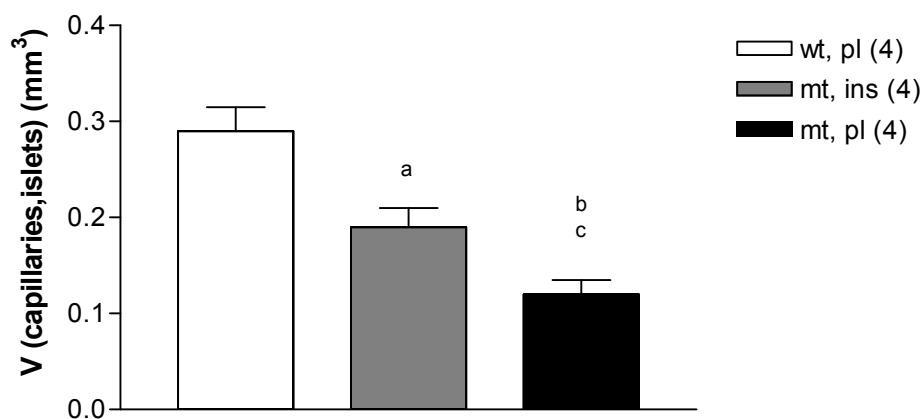
Figure 4.26: Total volume of capillaries in the islets ($V_{(capillaries,islets)}$) at 160 days of age

The $V_{(capillaries,islets)}$ of insulin-treated mutants (mt, ins) is 34% lower versus wild-type mice (wt, pl), and 58% higher versus placebo-treated mutant mice (mt, pl). Placebo-treated mutants present a 59% lower $V_{(capillaries,islets)}$ than wild-type mice.

Data are means ± SEM; a,b,c: a) wt, pl vs. mt, ins; b) wt, pl vs. mt, pl; c) mt, ins vs. mt, pl; $p<0.05$; (n): number of animals investigated

4.1.12.10 Volume density of isolated β-cells in the pancreas

The volume density of isolated β-cells in the pancreas ($Vv_{\text{(isolated β-cells/pan)}}$) of insulin-treated mice was significantly lower than that of wild-type mice, but significantly higher than that of placebo-treated mutants (0.0009 ± 0.0001% vs. 0.0013 ± 0.0002% vs. 0.0004 ± 0.0001%; Figure 4.27).
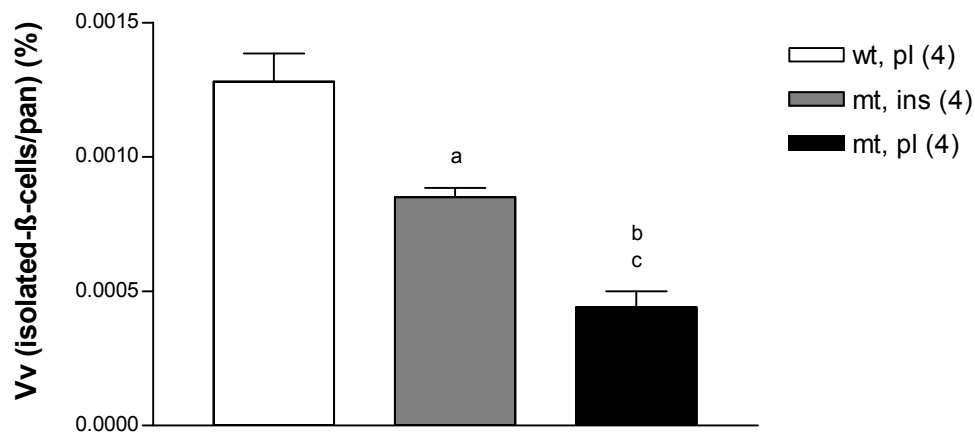
Figure 4.27: Volume density of isolated β-cells in the pancreas ($Vv_{\text{(isolated β-cells/pan)}}$) at the age of 160 days

Insulin-treated mutants (mt, ins) present a 31% lower $Vv_{\text{(isolated β-cells/pan)}}$ versus wild-type mice (wt, pl). Placebo-treated mutants (mt, pl) exhibit a 69% and 56% lower $Vv_{\text{(isolated β-cells/pan)}}$ than wild-type and insulin-treated mutant mice, respectively.
Data are means ± SEM; a,b,c: a) wt, pl vs. mt, ins; b) wt, pl vs. mt, pl; c) mt, ins vs. mt, pl; p<0.05; (n): number of animals investigated

4.1.12.11 Total volume of isolated β-cells in the pancreas

The total volume of isolated β-cells in the pancreas ($V_{\text{(isolated β-cells,pan)}}$) of insulin-treated mutants was lower (p=0.053) than that of wild-type mice, but significantly higher than that of placebo-treated mutant mice (0.0026 ± 0.0005 mm^3 vs. 0.0042 ± 0.0011 mm^3 vs. 0.0014 ± 0.0004 mm^3; Figure 4.28).
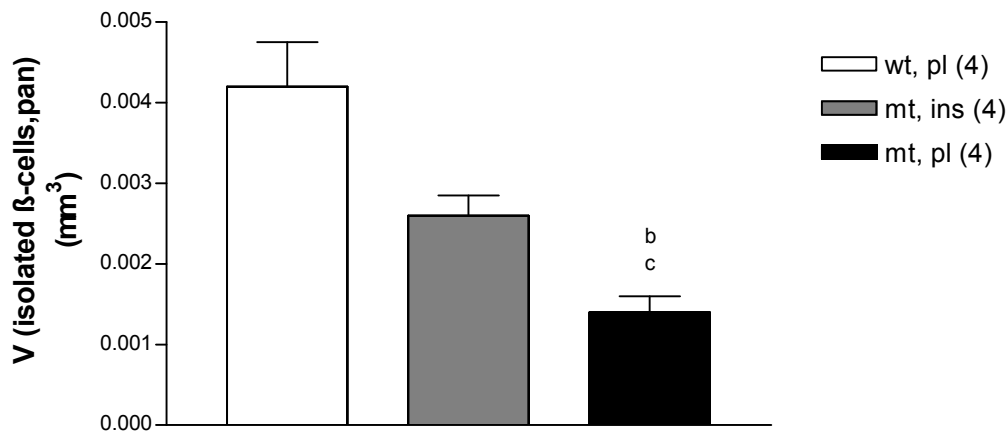
Figure 4.28: Total volume of isolated β-cells in the pancreas (V$_{(isolated\ β-cells,pan)}$) at the age of 160 days

The V$_{(isolated\ β-cells,pan)}$ of insulin-treated mutant mice (mt, ins) is 37% lower than that of wild-type mice (wt, pl), and 83% higher than that of placebo-treated mutants (mt, pl). Placebo-treated mutant mice feature a 66% lower V$_{(isolated\ β-cells,pan)}$ compared to wild-type mice.
Data are means ± SEM; b,c: b) wt, pl vs. mt, pl; c) mt, ins vs. mt, pl; $p<0.05$;
(n): number of animals investigated

4.1.12.12   β-cell replication

In order to examine the rate of replicating β-cells in the islets of 160-day-old mice, BrdU positive β-cells per 100,000 β-cells were analysed. Insulin-treated mutant mice presented a similar amount of BrdU positive β-cells per 100,000 β-cells as wild-type mice (80 ± 23 vs. 83 ± 34). In placebo-treated mutants the number of BrdU positive β-cells per 100,000 β-cells was higher compared to wild-type mice (122 ± 25 vs. 83 ± 34; Figure 4.29).
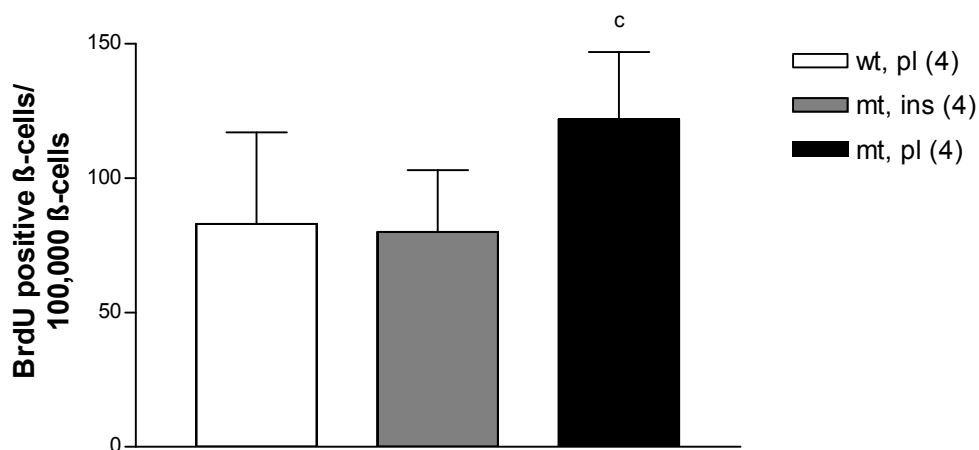
Figure 4.29: β-cell replication at the age of 160 days
Insulin-treated mutants (mt, ins) demonstrate a similar amount of BrdU positive β-cells per 100,000 β-cells compared to wild-type mice (wt, pl) and a 34% lower number of BrdU positive

β-cells compared to placebo-treated mutant mice (mt, pl). In placebo-treated mutants, the amount of BrdU positive β-cells is 47% higher than in wild-type mice.

Data are means ± SEM; c: mt, ins vs. mt, pl; $p < 0.05$; (n): number of animals investigated

4.1.12.13 β-cell apoptosis

The numerical fraction of apoptotic β-cells in the islets of 160-day-old mice was determined via TUNEL immunohistochemistry. No significant differences among the investigated groups concerning the number of TUNEL positive β-cells per 100,000 β-cells were detected. The amount of apoptotic β-cells varied substantially among the individual animals (Figure 4.30).
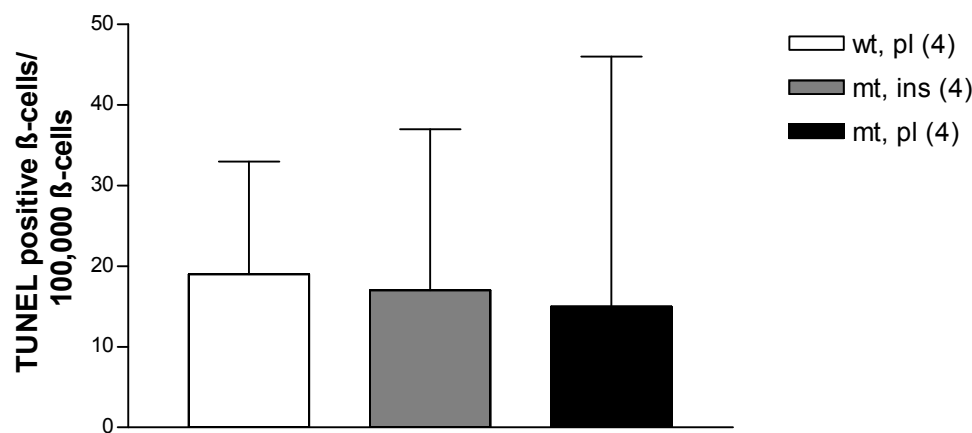
Figure 4.30: β-cell apoptosis at 160 days of age

Insulin-treated mutant (mt, ins), placebo-treated mutant (mt, pl) and wild-type mice (wt, pl) exhibit similar amounts of TUNEL positive β-cells per 100,000 β-cells.

Data are means ± SEM; (n): number of animals investigated

4.1.13 Transmisson electron microscopy (TEM)

Ultra-thin pancreas sections of 160-day-old mice were produced and examined using electron microscopy.

Concerning the amount and distribution of the distinct endocrine cells within the islets, electron-microscopical observations were identical to qualitative-histological and immunohistochemical findings (4.1.11 Qualitative-histological findings of the pancreas; Figure 4.31).

The cytoplasm of β-cells of wild-type mice was densely packed with typical insulin secretory granules, characterised by an electron-dense core, surrounded by an electron lucent halo (Figures 4.31 (A); 4.32 (A)).

In placebo-treated mutant mice, most β-cells exhibited very few and small secretory granules. Many of the granules presented a tiny core and a broadened halo compared to wild-type mice. Other granules exhibited a narrowed and obscured halo (Figures 4.31 (B); 4.32 (C), (D); 4.33).

The structure of granules in insulin-treated mutants was similar to that of wild-type mice. The size of granule profiles seemed to be slightly smaller than that of wild-type mice, but definitely bigger than that of placebo-treated mutants. The amount of secretory granules in β-cells varied substantially within an islet. In general, there were fewer insulin granules in β-cells of insulin-treated mutants than in those of wild-type mice and more than in β-cells of placebo-treated mutants (Figures 4.31 (C), (D); 4.32 (B)).

These differences in the amount and size of secretory granules are mirrored by the various immunohistochemical staining intensities of β-cells described above (4.1.11 Qualitative-histological findings of the pancreas).

In placebo- and insulin-treated mutant mice the rough endoplasmic reticulum (rER) appeared dilated as compared to wild-type mice (Figure 4.32). Due to perfusion artefacts, the width of Golgi lamellae could not be compared.

A few β-cells of placebo-treated mutant mice featured enlarged mitochondria (Figures 4.32 (D); 4.33). In the β-cells of all examination groups, the crests of some mitochondria were disrupted, probably an artefact due to the perfusion (hypoxia) or, despite perfusion fixation, beginning autolysis.

In contrast to wild-type and insulin-treated mutant mice, placebo-treated mutant mice regularly exhibited glycogen deposits in β-cells (Figure 4.32 (D)).

Residual bodies could be found in all groups. Placebo-and insulin-treated mutant mice appeared to demonstrate a few more residual bodies than wild-type mice (Figures 4.31 (B),(D); 4.33).

No apoptotic bodies were found in β-cells of the mice examined.

In all investigation groups, widened intercellular spaces could be found in some islets, which are interpreted as an artefact due to the perfusion.
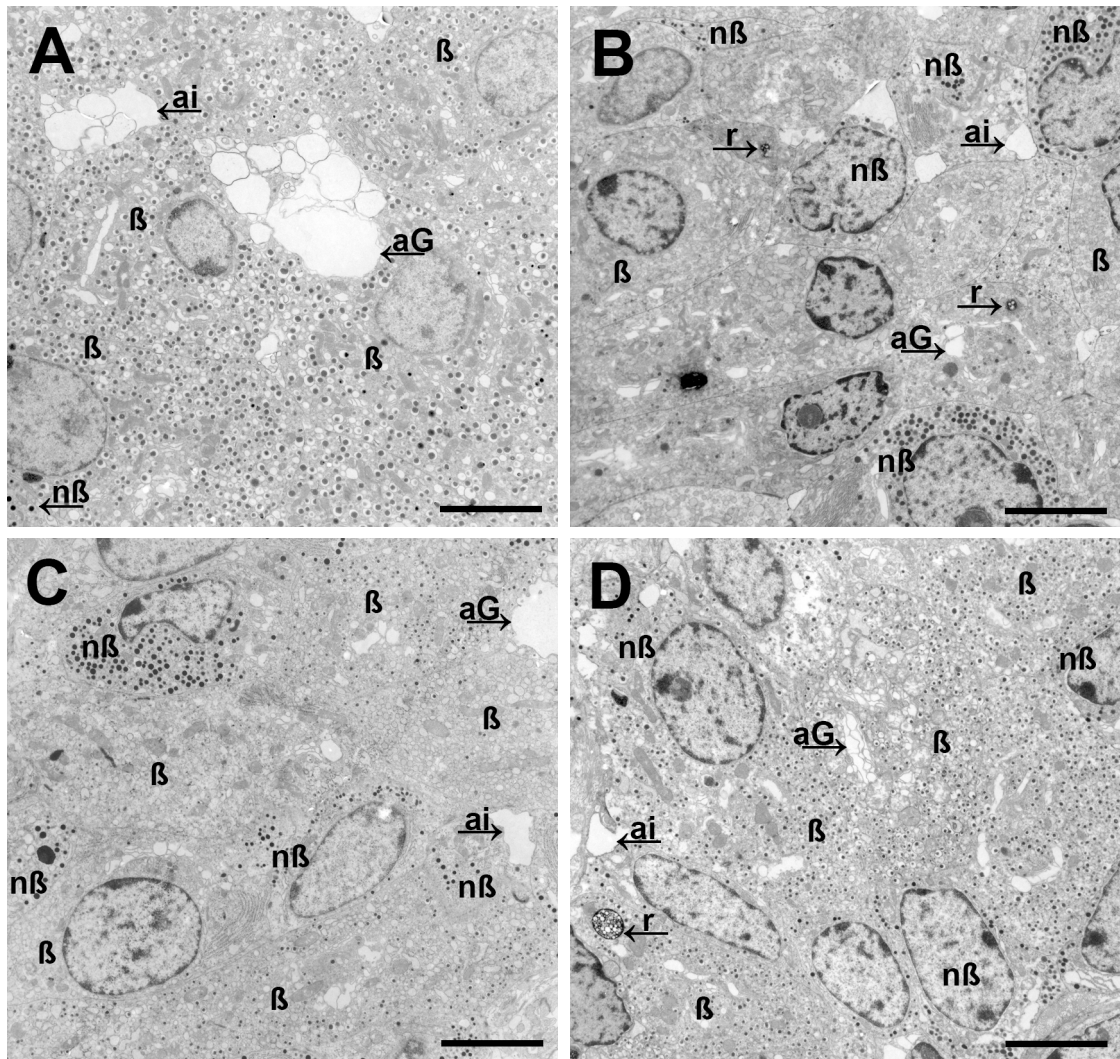
Figure 4.31 Transmisson electron microscopy (TEM) of islet-cell profiles of 160-day-old mice

Wild-type mice (A) demonstrate a typical murine islet structure with basically β-cells (β) in the centre. Non-β-cells (nβ) are located mainly at the border of the islets. The β-cells exhibit numerous secretory granules. In placebo-treated mutants (B) the amount of non-β-cells, particulary α-cells, is increased, and non-β-cells are distributed all over the islet profile. In the β-cells, there are very few and small secretory granules. Insulin-treated mutant mice (C, D) exhibit β-cells of varying amount of secretory granules within an islet. The number of residual bodies (→ r) seems to be increased in insulin- and placebo-treated mutants, compared to wild-type mice. In all examined groups, artefacts (e.g. dilated intercellular spaces (→ ai) and Golgi lamellae (→ aG)) are found, created by the perfusion

Bar: 5 µm
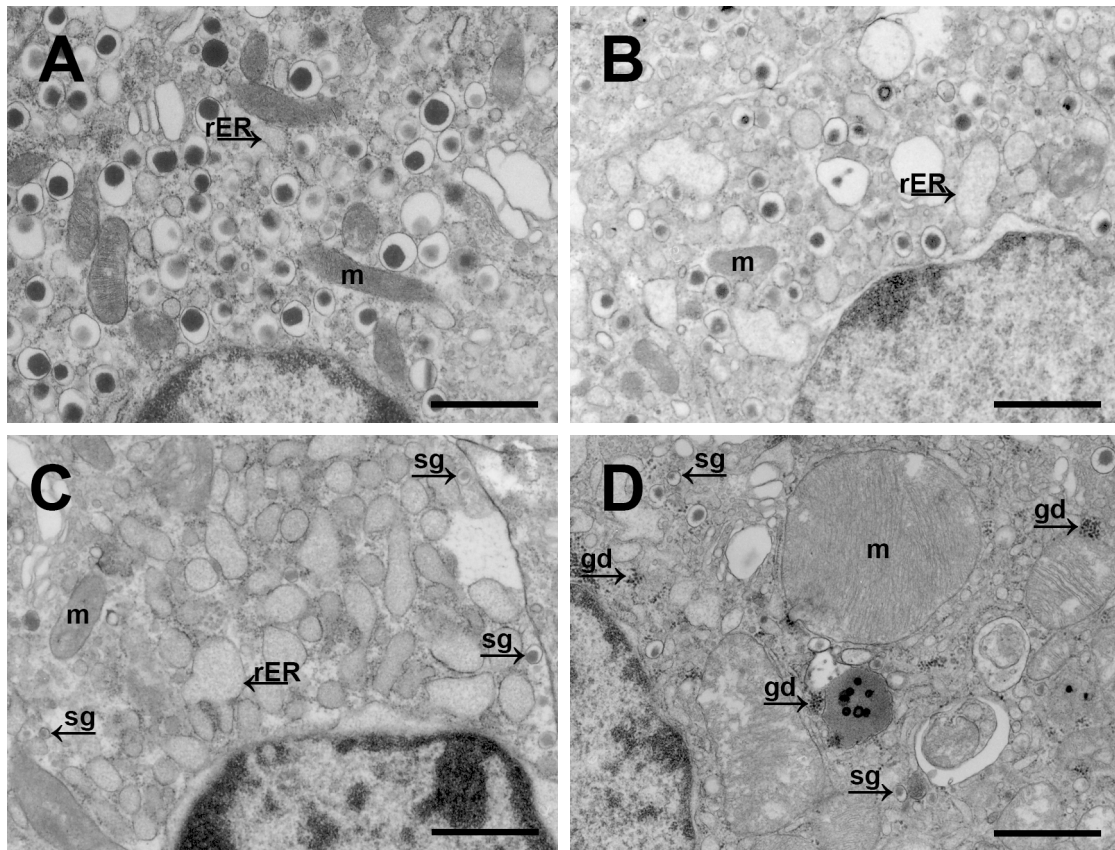
Figure 4.32 TEM of β-cell profiles at the age of 160 days

In some β-cells of placebo- (C, D) and insulin-treated mutant mice (B), the rough endoplasmic reticulum (→ rER) appears dilated, compared to wild-type mice (A), and is filled with electron-dense material. Secretory granules of insulin-treated mutants show a similar structure as wild-type mice. They are marginally smaller than those of wild-type mice, but clearly bigger than those of placebo-treated mutants. Placebo-treated mutants exhibit only few and small secretory granules (→ sg). In some granules, the halo is narrowed and obscured. Glycogen deposits (→ gd) can be found in some β-cells of placebo-treated mutants.

The size of mitochondria (m) in insulin-treated mutants is similar to that of wild-type mice (B vs. A). In placebo-treated mutants some mitochondria profiles are unchanged vs. wild-type mice (C vs. A), some are swollen (D).

Bar: 1 µm
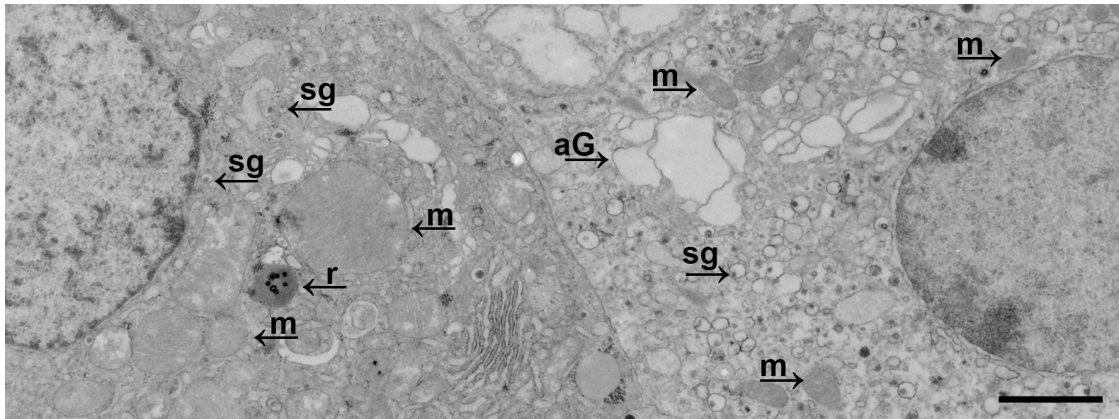
Figure 4.33 Details of β-cells of a placebo-treated mutant at the age of 160 days. TEM

In some β-cells of placebo-treated mutants several mitochondria (m) are swollen (left β-cell), in others, mitochondria appear unchanged (right β-cell). Placebo-treated mutant mice show secretory granules (→ sg) of different appearance. Some exhibit a tiny core and a broadened, clear halo compared to wild-type mice. Others present a narrowed and obscured halo
r: residual body; aG: dilated Golgi lamellae, probably an artefact;
Bar: 2 µm

4.2 C-peptide II concentration in serum and pancreas of untreated male and female Munich *Ins2*^C95S mutant and wild-type mice

4.2.1 Blood glucose concentration

At the age of 21 days, heterozygous mutant mice of both genders demonstrated slightly higher randomly fed blood glucose concentrations compared to sex-matched wild-type mice. Blood glucose concentrations of male and female homozygous mutants were severely higher versus sex-matched wild-type mice and heterozygous mutants (Table 4.5).

group (n)	blood glucose (mg/dl)	
	male	female
wt (4/5)*	112 ± 7	115 ± 4
het (6)	138 ± 15 [a]	127 ± 11 [d]
hom (5)	294 ± 42 [b,c]	271 ± 66 [e,f]

Table 4.5 Randomly fed blood glucose concentrations at the age of 21 days

Randomly fed blood glucose levels of male (m) and female (f) heterozygous mutants (het) are slightly higher compared to sex-matched wild-type (wt) mice, but lower versus homozygous mutants (hom).
Data are means ± SD; a, b, c, d, e, f: a) m, wt vs. m, het; b) m, wt vs. m, hom; c) m, het vs. m, hom; d) f, wt vs. f, het; e) f, wt vs. f, hom; f) f, het vs. f, hom; p<0.05;
(n): number of animals investigated; * n=4 (m), n=5 (f)

4.2.2 Serum C-peptide II concentration

Twenty-one-day-old homozygous mutant mice featured 0.53 ng/ml (male) and 0.43 ng/ml (female) C-peptide II concentrations in the serum. Thus, the mutant insulin 2 may be expressed and secreted.

Heterozygous mutant mice of both genders showed lower C-peptide II levels than sex-matched wild-type mice (male: 0.97 ± 0.64 ng/ml vs. 1.22 ± 0.77 ng/ml, n.s.; female: 0.86 ± 0.29 ng/ml vs. 1.41 ± 0.14 ng/ml; Figure 4.34).
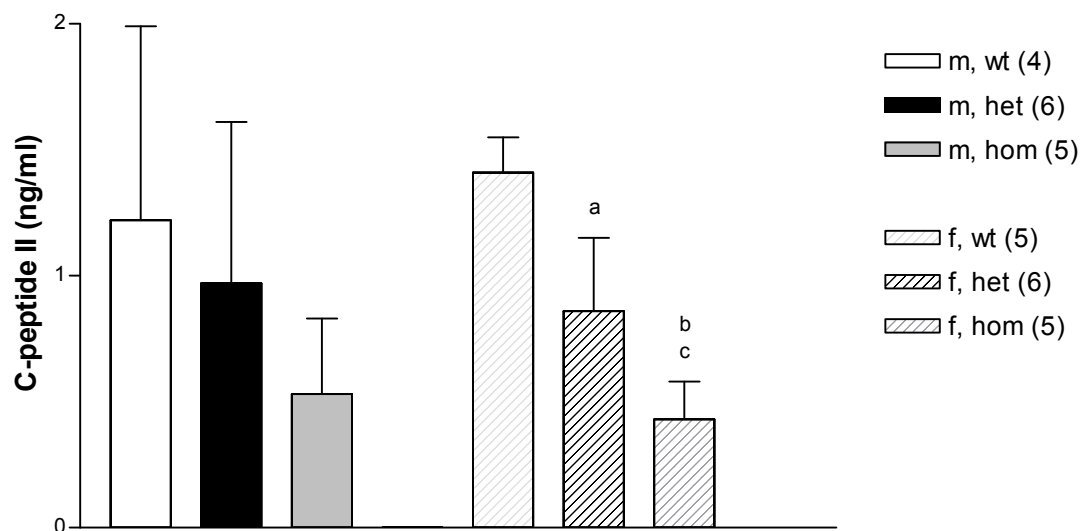
Figure 4.34 C-peptide II concentrations of 21-day-old mice

The serum C-peptide II levels of female (f) heterozygous mutants (het) are significantly lower versus female wild-type (wt) mice, but significantly higher than those of homozygous mutants (hom). In male (m) mice these differences are similar, but not significant.

Data are means ± SEM; d, e, f: d) f, wt vs. f, het; e) f, wt vs. f, hom; f) f, het vs. f, hom; p<0.05; (n): number of animals investigated

4.2.3 C-peptide II content in the pancreas

The C-peptide II/protein content in the pancreas of male heterozygous mutants was about 1/3 that of sex-matched wild-type mice (5.0 ± 1.1 ng/mg vs. 16.0 ± 2.5 ng/mg), and 4.5-fold higher versus homozygous mutants (5.0 ± 1.1 ng/mg vs. 1.1 ± 0.3 ng/mg). Female heterozgous mutant mice exhibited a 4.4-fold higher pancreatic C-peptide II/protein content than female homozygous mutants (6.1 ± 1.7 ng/mg vs. 1.4 ± 0.5 ng/mg). The C-peptide II/protein content of female heterozygous mutants was less than ½ that of female wild-type mice (6.1 ± 1.7 ng/mg vs. 13.4 ± 2.9 ng/mg; Figure 4.35).
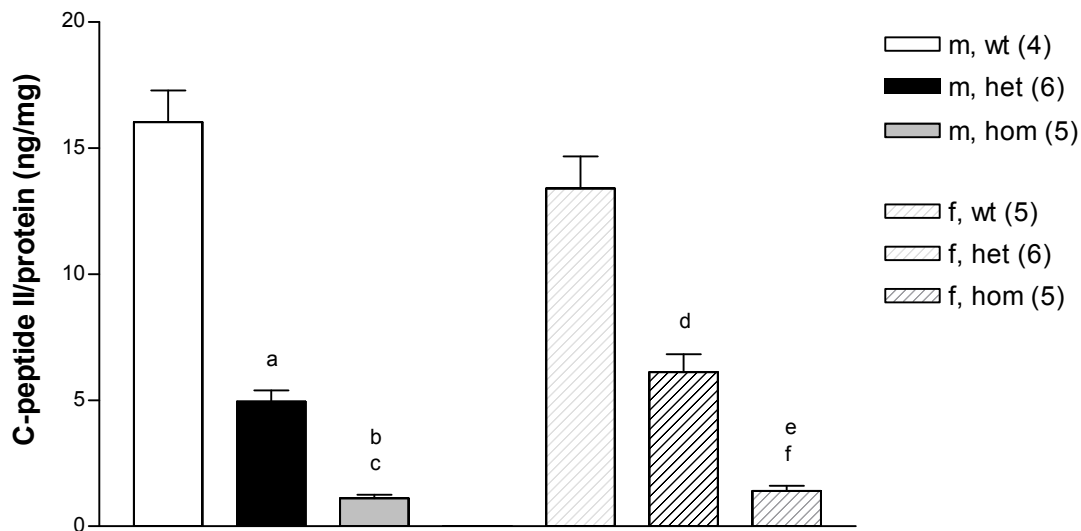
Figure 4.35: C-peptide II/protein concentrations in the pancreas of 21-day-old mice

The C-peptide II/protein content in male (m) and female (f) heterozygous mutants (het) is significantly lower compared to sex-matched wild-type (wt) mice, but significantly higher versus homozygous mutants (hom).

Data are means ± SEM; a, b, c, d, e, f: a) m, wt vs. m, het; b) m, wt vs. m, hom; c) m, het vs. m, hom; d) f, wt vs. f, het; e) f, wt vs. f, hom; f) f, het vs. f, hom; p<0.05;

(n): number of animals investigated

4.3 Additional investigations of untreated male and female Munich *Ins2*^C95S mutant and wild-type mice

4.3.1 Body weight

Male Munich *Ins2*^C95S mutant mice exhibited significantly lower randomly fed body weights at the age of 30, 90 and 180 days versus age- and sex-matched wild-type mice. Female mutant and wild-type mice showed a similar body weight, irrespective of age at sampling (Table 4.6).

	age (days)			
group (n)	21	30	90	180
m, wt (10)	8.8 ± 0.7	16.1 ± 0.8	26.1 ± 1.3	29.9 ± 1.5
m, mt (≥8)	8.4 ± 0.6	15.2 ± 1.0 [a]	24.9 ± 0.9 [a]	27.8 ± 0.8 [a]
f, wt (10)	9.1 ± 1.1	14.0 ± 1.1	23.8 ± 1.6	26.8 ± 1.4
f, mt (8)	8.7 ± 0.8	13.9 ± 0.7	23.4 ± 0.9	26.4 ± 0.8

Table 4.6: Randomly fed body weights (g)

Female (f) mutant (mt) mice demonstrate similar body weights as female wild-type (wt) mice during the investigation period. From 30 days of age onwards, body weights of male (m) mutants are significantly lower than those of sex-matched wild-type mice.

Data are means ± SD; a: m, wt vs. m, mt; p<0.05; (n): number of animals investigated

4.3.2 Blood glucose concentration

From 30 days of age onwards, male and female Munich $Ins2^{C95S}$ mutant mice featured significantly elevated randomly fed blood glucose concentrations compared to sex- and age-matched wild-type mice. The blood glucose levels of male mutant mice rose continuously, reaching 587 ± 88 mg/dl at the age of 180 days. Blood glucose concentrations of female mutants were below 185 mg/dl (182 ± 24 mg/dl). In male and female wild-type mice, the blood glucose levels remained stable (range 105 - 125 mg/dl (m, wt); 101 - 117 mg/dl (f, wt); Figure 4.36).
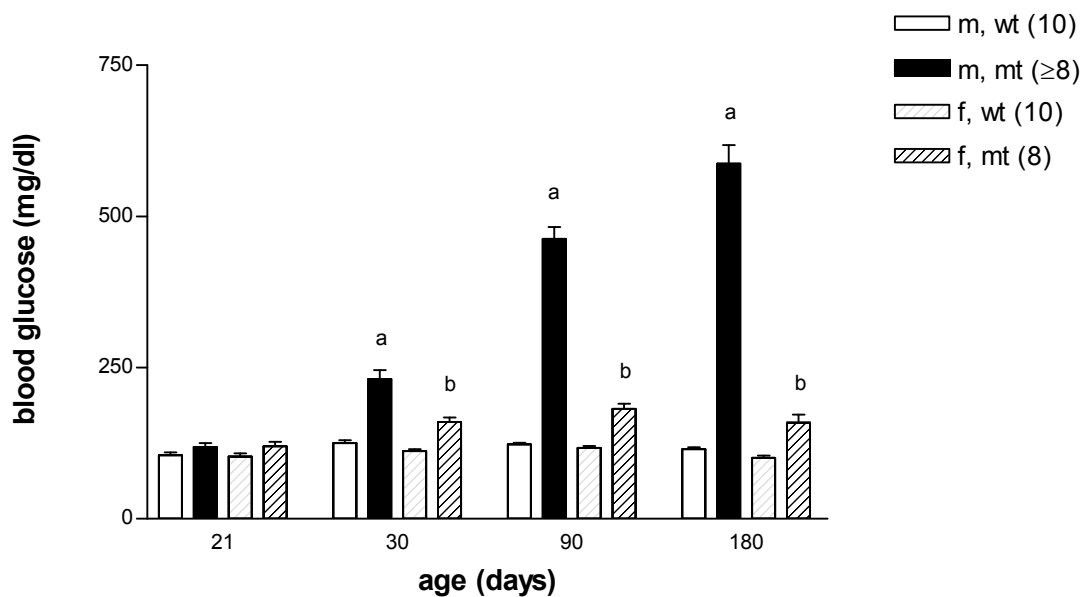
Figure 4.36: Randomly fed blood glucose concentrations
Male (m) and female (f) mutant (mt) mice exhibit significantly higher blood glucose levels than sex-matched wild-type (wt) mice from 30 days of age onwards. Blood glucose concentrations of wild-type mice of both genders remain stable. In contrast to female mutant mice, male mutants show a progressive diabetic phenotype.
Data are means ± SEM; a, b: a) m, wt vs. m, mt; b) f, wt vs. f, mt; p<0.05;
(n): number of animals investigated

4.3.3 Intraperitoneal insulin tolerance test (ipITT)

Intraperitoneal insulin tolerance tests (ipITT) were carried out with 21-, 30-, 90- and 180-day-old mice.

After insulin injection, 21- and 180-day-old female mutant and female wild-type mice exhibited a similar percentaged decrease of blood glucose levels from basal value (T0=100%) at all time points of the test. At the age of 30 and 90 days, blood glucose decrease was slightly delayed in female mutants vs. wild-

type mice (Figure 4.37) but there were no differences in the corresponding area under the curve ($AUC_{blood\ glucose}$) comparing female mutants and female wild-type mice (Figure 4.38).

Male mutants exhibited a similar course of percentaged blood glucose decrease as male wild-type mice at the age of 21 days, and at 30 days, blood glucose decrease was slightly delayed vs. wild-type males. The percentaged blood glucose decrease was lower in 90- and 180-day-old male mutants as compared to age and sex-matched wild-type mice at all time points of the ipITT (Figure 4.37). The $AUC_{blood\ glucose}$ of male mutants was similar to male wild-type mice at the age of 21 and 30 days. Ninety- and 180-day-old male mutants featured an elevated $AUC_{blood\ glucose}$ compared to male wild-type mice (Figure 4.38). These results reveal that male Munich $Ins2^{C95S}$ became insulin resistant.
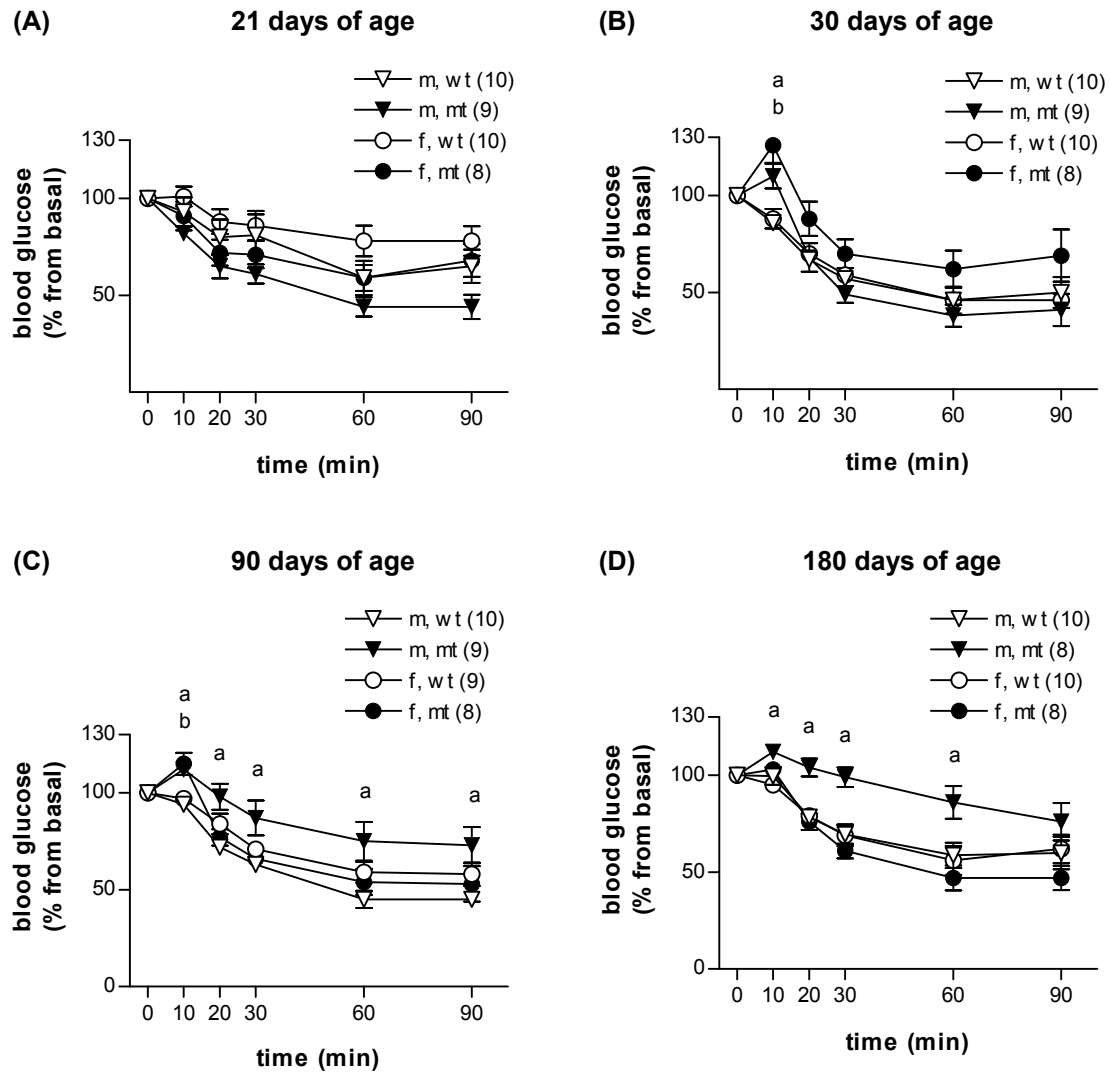
Figure 4.37 (A)-(D): Intraperitoneal insulin tolerance tests (ipITT) at the age of 21 (A), 30 (B), 90 (C) and 180 (D) days

During the entire test, the percentaged decrease of blood glucose levels from the basal value (T0=100%) after insulin application was equal in female (f) wild-type (wt) versus female mutant (mt) mice at the age of 21 and 180 days, as well as in male (m) wild-type versus male mutant mice at the age of 21 days. In 30- and 90-day-old female mutant as well as in 30-day-old male mutant mice, blood glucose decrease was delayed. At the age of 90 and 180 days, male mutants present lower percentaged blood glucose decrease compared to male wild-type mice during the entire ipITT.

Data are means ± SEM; a, b: a) m, wt vs. m, mt; b) f, wt vs. f, mt; $p<0.05$;

(n): number of animals investigated
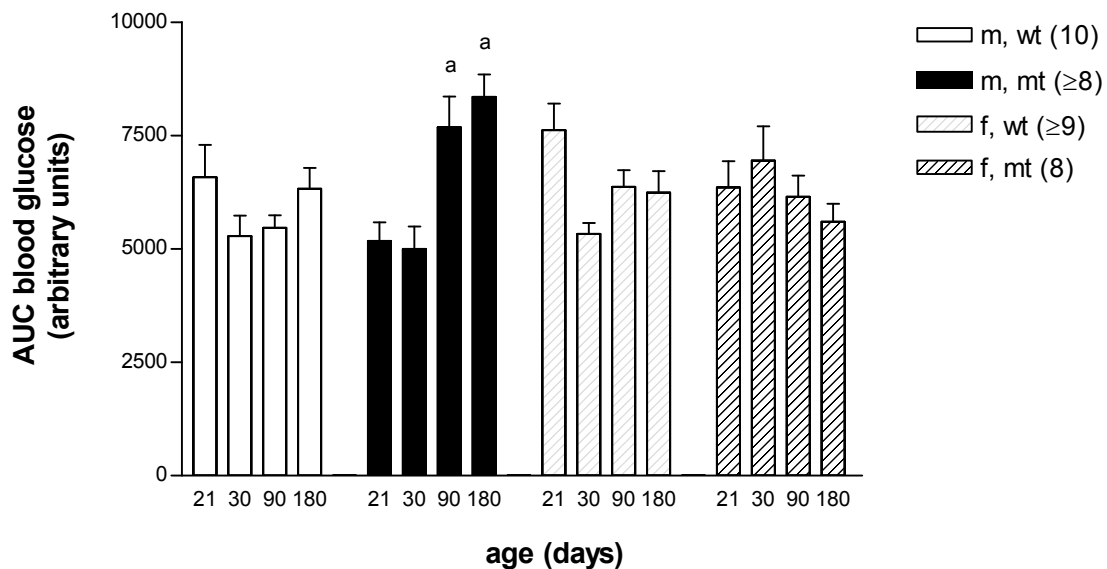
Figure 4.38: Area under the curve of the percentaged blood glucose decrease from basal values (AUC$_{blood\ glucose}$) of the ipITT

The AUC$_{blood\ glucose}$ of female (f) wild-type (wt) and female mutant (mt) mice are equal, irrespective of age at testing. Male (m) mutants show similar AUC$_{blood\ glucose}$ as male wild-type mice at 21 and 30 days of age but feature elevated AUC$_{blood\ glucose}$ compared to male wild-type mice at the age of 90 and 180 days.

Data are means ± SEM; a: m, wt vs. m, mt; $p < 0.05$; (n): number of animals investigated

4.3.4 Serum glucagon and corresponding blood glucose concentration

4.3.4.1 Randomly fed serum glucagon and glucagon concentration 10 minutes after insulin injection

At the age of 200 days, male mutant mice presented 2.3-fold (basal, randomly fed) and 1.5-fold (10 minutes after insulin application) elevated glucagon concentrations compared to sex- and age-matched wild-type mice, in spite of increased blood glucose values. Female mutant and female wild-type mice exhibited similar glucagon levels, randomly fed and after insulin injection (Figure 4.39, Table 4.7).

Glucagon concentrations of male mutant mice slightly decreased (-11 ± 30 pg/dl) after insulin injection, whereas those of wild-type mice of both genders and those of female mutant mice increased (m, wt: 35 ± 34 pg/ml; f, wt: 10 ± 53 pg/ml, f, mt: 35 ± 69 pg/ml; Figure 4.40).

(A)   randomly fed (T0)   **(B)   10 minutes after insulin injection (T10)**
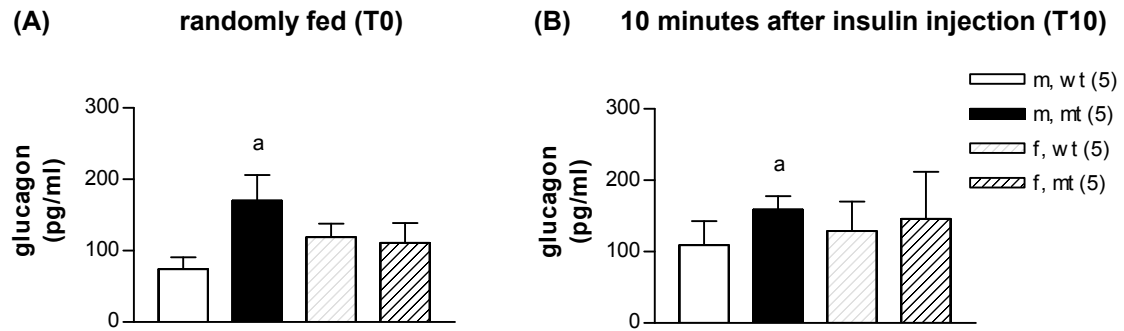
Figure 4.39 (A)/(B): Serum glucagon concentrations, randomly fed (T0; (A)) and 10 minutes after insulin injection (T10; (B)) at the age of 200 days

Male (m) mutants (mt) feature significantly higher serum glucagon levels than male wild-type (wt) mice at T0 and T10. The glucagon concentrations of female (f) mutants are equal to those of female wild-type mice.

Data are means ± SEM; a: m, wt vs. m, mt; p<0.05; (n): number of animals investigated

group (n)	blood glucose (mg/dl)	
	T0	T10
m, wt (5)	119 ± 15	97 ± 13
m, mt (5)	652 ± 110 [a]	674 ± 74 [a]
f, wt (5)	120 ± 5	106 ± 28
f, mt (5)	161 ± 30 [b]	130 ± 28

Table 4.7: Corresponding blood glucose levels to glucagon concentrations in Fig. 4.39

Male (m) mutant (mt) mice demonstrate 5.4-fold (T0) and 6.9-fold (T10) higher blood glucose levels than male wild-type (wt) mice. In female (f) wild-type and mutant mice these differences aren't as distinct (f, mt vs. f, wt: 1.3-fold (T0) and 1.2-fold (T10) increased).

Data are means ± SD; a, b: a) m, wt vs. m, mt; b) f, wt vs. f, mt; p<0.05;
(n): number of animals investigated
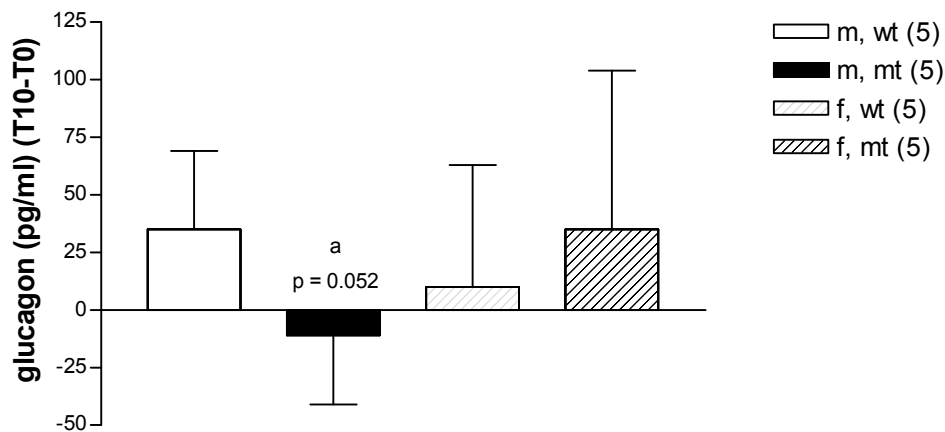
**Figure 4.40: Changes in serum glucagon levels 10 minutes after intraperitoneal insulin application**

Female (f) wild-type (wt), female mutant (mt) and male (m) wild-type mice show an increase in glucagon secretion after insulin injection, whereas glucagon levels in male mutants decrease. Data are means ± SEM; a: m, wt vs. m, mt; $p<0.05$; (n): number of animals investigated

4.3.4.2 Fasting serum glucagon and glucagon concentration 10 minutes after oral glucose application

Fasting glucagon concentrations of male and female mutant mice at the age of 230 days didn't differ from those of sex- and age-matched littermate controls. Female mutants exhibited significantly higher glucagon levels than female wild-type mice 10 minutes after glucose administration (Figure 4.41).

Glucagon concentrations of male and female wild-type mice decreased after glucose challenge (m, wt: -26 ± 40 pg/dl ; f, wt: -21 ± 34 pg/dl). In mutant mice of both genders, glucagon concentrations increased (m, mt: 25 ± 30 pg/dl; f, mt: 11 ± 20 pg/dl) in spite of rising blood glucose levels (Figure 4.42, Table 4.8).

(A)   fasting (T0)   **(B)   10 minutes after glucose application (T10)**
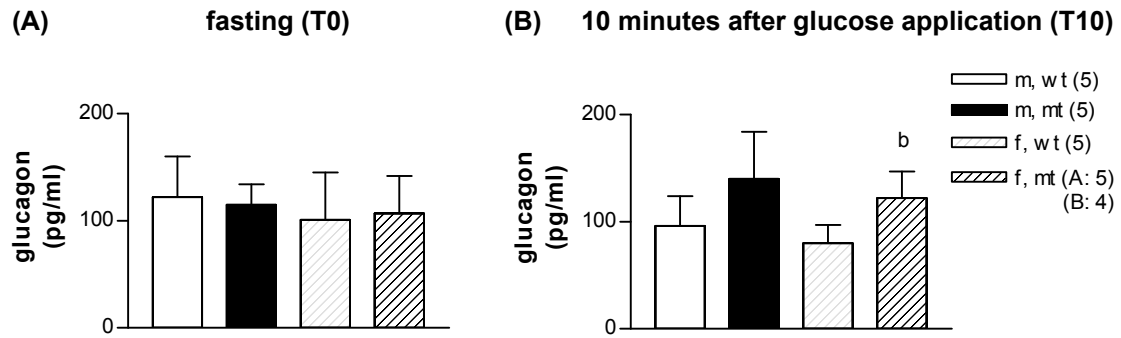
Figure 4.41 (A)/(B): Serum glucagon concentrations, fasting (T0; (A)) and 10 minutes after oral glucose administration (T10; (B)) at 230 days of age

Fasting glucagon concentrations are similar in male (m) mutant (mt) and wild-type (wt) mice as well as in female (f) mutant and wild-type mice. Ten minutes after glucose application, the glucagon levels of male and female mutants are higher than those of sex- and age-matched wild-type mice.

Data are means ± SEM; b: f, wt vs. f, mt; $p<0.05$; (n): number of animals investigated
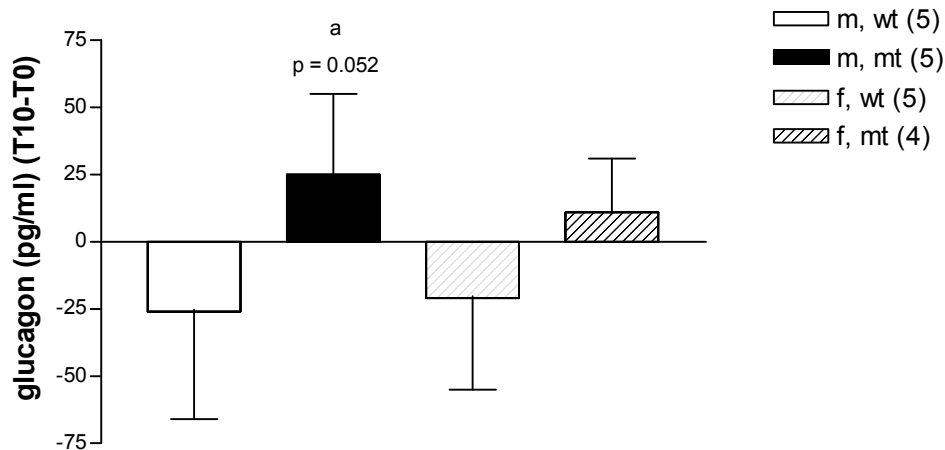
Figure 4.42: Changes in serum glucagon levels 10 minutes after oral glucose application

Glucagon concentrations of male (m) and female (f) mutant (mt) mice rise in spite of increasing blood glucose values 10 minutes after glucose administration. In wild-type (wt) mice of both sexes, glucagon levels decrease after glucose challenge.

Data are means ± SEM; a: m, wt vs. m, mt; (n): number of animals investigated

	blood glucose (mg/dl)	
group (n)	T0	T10
m, wt (5)	120 ± 16	296 ± 38
m, mt (5)	339 ± 173 [a]	635 ± 238 [a]
f, wt (5)	103 ± 9	304 ± 46
f, mt (5/4)	166 ± 15 [b]	477 ± 76 [b]

Table 4.8: Corresponding blood glucose concentrations to glucagon levels in Fig. 4.41

Male (m) mutant (mt) mice show 2.8-fold (T0) and 2.1-fold (T10) elevated blood glucose concentrations compared to male wild-type (wt) mice. In female (f) mutants blood glucose levels are 1.6-fold (T0 and T10) higher than in sex-matched wild-type mice.

Data are means ± SD; a, b: a) m, wt vs. m, mt; b) f, wt vs. f, mt; $p < 0.05$;

(n): number of animals investigated

5 Discussion

Male Munich $Ins2^{C95S}$ mutant mice exhibit a progressive diabetic phenotype with severe reduction of pancreatic β-cell mass (Herbach et al. 2007).

The present study was performed to analyse the mechanisms of β-cell loss in male Munich $Ins2^{C95S}$ mutant mice. Since homozygous male and female mutants died at a mean age of 46 and 52 days, respectively, and female heterozygous mutant mice demonstrated a mild diabetic phenotype (Herbach et al. 2007), male heterozygous mutants were used in this study. In order to investigate the influence of hyperglycaemia on β-cell loss in the pancreas of mutant mice, one group of mutants was treated with subcutaneous insulin-pellets to normalise blood glucose concentration. Placebo-treated wild-type and mutant mice served as controls.

5.1 Treated male Munich $Ins2^{C95S}$ mutant and wild-type mice

5.1.1 Glucose homeostasis

At weaning, mutant mice exhibited slightly higher randomly fed blood glucose concentrations compared to wild-type mice, but soon became hyperglycaemic, reaching blood glucose levels over 200 mg/dl at the age of 32 days. In heterozygous Akita mice, which also exhibit a mutation in the $Ins2$ gene, blood glucose concentrations were similar compared to wild-type mice up to 21 days of age. Like male Munich $Ins2^{C95S}$ mutant mice, male Akita mice became hyperglycaemic soon after weaning, showing randomly fed blood glucose levels of over 250 mg/dl at the age of 28 days (Yoshioka et al. 1997). In contrast, $Ins2$ knockout mice stay normoglycaemic, most likely due to compensation by increased $Ins1$ expression (Leroux et al. 2001). Since Munich $Ins2^{C95S}$ mutant mice become diabetic despite possessing one intact $Ins2$ allele and 2 intact $Ins1$ alleles, the mutant $Ins2$ seems to exert dominant negative effects on β-cell function and viability (Herbach et al. 2007). A similar dominant negative effect of one mutated $Ins2$ allele was found in Akita mice (Wang et al. 1999; Izumi et al. 2003).

In general, insulin treatment normalised blood glucose levels of mutant mice. To avoid hypoglycaemia due to additive effects of the old and the new insulin-pellet, it was accepted that insulin-treated mutants demonstrated higher blood

glucose levels compared to wild-type mice shortly before the next pellet injection. In placebo-treated mutants, blood glucose levels rose continuously. The progressive diabetic phenotype of placebo-treated mutants can be explained by impaired insulin secretion, development of insulin resistance and increasing loss of total β-cell volume (Herbach et al. 2007; this study). In type 1 diabetes, autoimmune destruction of β-cells results in gradual loss of functional β-cell mass, leading to hyperglycaemia (Al-Mutairi et al. 2007). Type 2 diabetes normally becomes overt when insulin secretion is insufficient to compensate for the elevated insulin demand, resulting from reduced insulin action (Ahren 2005).

In oral glucose tolerance tests, insulin-treated mutants showed similar or even lower areas under the blood glucose curve ($AUC_{blood\ glucose}$) compared to wild-type mice, which can be explained by the insulin released from the pellets. Placebo-treated mutant mice demonstrated a significantly elevated $AUC_{blood\ glucose}$ compared to wild-type mice, irrespective of age at sampling, confirming the diabetic phenotype described above and in an earlier study (Herbach et al. 2007).

In insulin-treated mutants, the decrease of blood glucose concentrations after glucose application was delayed compared to wild-type mice. Blood glucose concentrations of placebo-treated mutant mice declined even later than those of insulin-treated mutants. The delayed decline of blood glucose levels after glucose challenge in insulin- and placebo-treated mutant mice was most likely due to disturbed insulin secretion 10 minutes after glucose application (Herbach et al. 2007; this study). The earlier blood glucose decrease in insulin- versus placebo-treated mutants probably resulted from the insulin delivered by the pellets. In older mice, the higher insulin sensitivity in insulin- compared to placebo-treated mutant mice (see below) could have further contributed to the earlier decline of the blood glucose curves.

These findings demonstrate that glucose tolerance in insulin-treated mutants is almost normalised, whereas placebo-treated mutant mice exhibit an impaired glucose tolerance.

Since C-peptide is secreted concomitant and in equimolar amounts with insulin (Caumo and Luzi 2004; Luzi et al. 2007), C-peptide levels were

measured, in order to examine the endogenous randomly fed and glucose-stimulated insulin secretion (GSIS).

Randomly fed, C-peptide concentrations of insulin-treated mutants were largely reduced compared to those of both, wild-type and placebo-treated mutant mice. Likewise, intensive insulin treatment led to the decrease of fasting C-peptide levels in type 2 diabetics (Kärvestedt et al. 2002). In another study, insulin application in combination with oral anti-diabetic agents also resulted in reduced fasting C-peptide levels compared to treatment with oral anti-diabetic agents alone (Yki-Järvinen et al. 2000).

The effect of insulin on β-cells concerning insulin secretion is unclear. Earlier studies postulated a negative feedback of insulin on insulin secretion (Argoud et al. 1987; Ammon et al. 1991), whereas more recent studies demonstrated that insulin stimulates its own secretion by binding to the insulin receptor of β-cells (Aspinwall et al. 1999; Melloul et al. 2002; Borelli et al. 2004). However, other studies indicated that insulin has neither stimulatory nor inhibitory effects on insulin secretion (Wicksteed et al. 2003; Persaud et al. 2008). When insulin is secreted by β-cells, the insulin concentration within the islet capillaries is much higher compared to the insulin concentration in the whole circulation, since islet blood flow is less than 1% of total portal venous blood (Bonner-Weir 1991; Meier et al. 2006). Therefore, if insulin has auto- and paracrine effects on β-cells, these effects would be lower in insulin-treated mutants compared to wild-type mice and placebo-treated mutants, due to lower endogenous insulin secretion and consequently lower insulin levels in the intra-islet capillaries of insulin-treated mutants. The reduced potential positive feedback of insulin on insulin secretion could therefore contribute to the reduced C-peptide levels of randomly fed insulin-treated mutants compared to wild-type mice and placebo-treated mutants.

However, since glucose is the main stimulus for insulin secretion (Melloul et al. 2002; Kaiser et al. 2003; Li et al. 2006), reduced auto- or paracrine effects of insulin in insulin-treated mutants might probably be less important.

Placebo-treated mutants exhibited an approximately 50% reduction of randomly fed C-peptide concentrations compared to wild-type mice. In patients with *INS* mutations, exhibiting permanent neonatal diabetes mellitus, C-peptide levels were also very low or not detectable (Støy et al. 2007). The

randomly fed insulin levels in Akita mice were also largely reduced compared to those of wild-type mice (Yoshioka et al. 1997). The reduced C-peptide secretion of randomly fed placebo-treated Munich $Ins2^{C95S}$ mutant mice might be due to dominant negative effects of mutant proinsulin on secretory pathways (Izumi et al. 2003) and/or due to severely decreased pancreatic C-peptide content (described below).

The structure and secretion of different mutant proinsulins were analysed, including those with a disrupted A6-A11 intrachain disulfide bond ($C^{A6}Y$), similar to the mutation of Munich $Ins2^{C95S}$ mutant mice ($C^{A6}S$), and with a disrupted A7-B7 interchain disulfide bond ($C^{A7}Y$) as in the Akita mouse. In HEK293 cells expressing one of these mutant proinsulins ($C^{A6}Y$ or $C^{A7}Y$), the fraction of non-native proinsulin was increased compared to HEK293 cells expressing wild-type proinsulin, indicating defects in proinsulin folding. Furthermore, the secretion of mutant proinsulin was severely disturbed in these cells, and non-secreted proinsulin was probably intracellularly degraded (Colombo et al. 2008). *In vitro* studies demonstrated that the disruption of the A6-A11 intrachain disulfide bond has less influence on insulin conformation and stability than the disruption of the A7-B7 or A20-B19 interchain disulfide bond (Dai and Tang 1996; Chang et al. 2003). Further, it was shown that mutant proinsulin bearing the Akita mutation ($C^{A7}Y$) could virtually not be secreted from 293T cells, whereas $C^{A11}S$ mutant proinsulin was at least partially secreted (Liu et al. 2005). It was also demonstrated that the Akita mutation leads to a disturbed secretion of proinsulin in transfected CHO cells. The mutant proinsulin was described to form complexes with BiP and to be eventually degraded (Wang et al. 1999). The secretion of mutant insulin 2 of Akita mice was also impaired in transfected insulinoma cells (Nozaki et al. 2004). Furthermore, it was stated that the early secretory pathway in β-cells of Akita mice is nonspecifically impaired due to intracellular accumulation of misfolded proinsulin, leading to disturbed secretion of both, wild-type and mutant insulin (Izumi et al. 2003). However, determination of serum C-peptide II levels could show that mutant insulin 2 is effectively secreted in 21-day-old male heterozygous Munich $Ins2^{C95S}$ mutant mice. Further, fasting serum insulin levels and serum insulin after 2h refeeding did not differ comparing untreated mutants and wild-type mice of both genders (Herbach et al. 2007). This could lead to the assumption that there is no general defect in

insulin secretion in mutant mice. Alternatively, the clearance of mutant insulin 2 may be reduced due to decreased receptor binding to the insulin receptor, leading to reduced uptake and degradation, for example in hepatocytes or myocytes. Liver-specific insulin receptor knockout mice showed severe hyperinsulinaemia due to increased insulin secretion, but also due to reduced receptor-mediated insulin uptake and degradation in the liver (Michael et al. 2000). Point mutations in the *INS* gene in humans were described to result in reduced insulin receptor binding affinity and therefore decreased degradation, even leading to hyperinsulinaemia and an increased insulin to C-peptide ratio (Haneda et al. 1983; Nanjo et al. 1986; Nanjo et al. 1987; Steiner et al. 1990). Further, the disruption of the A6-A11 intrachain disulfide bond resulted in a largely reduced receptor binding activity of insulin *in vitro* (Dai and Tang 1996; Chang et al. 2003).

In conclusion, insulin treatment seems to lead to reduced randomly fed endogenous insulin secretion and therefore decreased serum C-peptide concentrations versus placebo-treated mutant mice. In male placebo-treated mutants the decreased insulin secretion probably results from partial misfolding of the mutant (pro-)insulin, thereby disturbing secretory pathways.

Ten minutes after oral glucose challenge, the insulin secretion of insulin- and placebo-treated mutant mice didn't increase, irrespective of age at sampling, whereas C-peptide levels of wild-type mice rose 1.5- to 3.6-fold. These results demonstrate that mutant mice suffer from a disturbed glucose-stimulated insulin secretion (GSIS). It has been described that GSIS is often impaired in type 1 and type 2 diabetics (Weir et al. 2001; Steele et al. 2004; Kahn et al. 2009), and *in vivo* and *in vitro* studies demonstrated that chronically high glucose concentrations cause an impaired GSIS (Zhang et al. 2005; Tsuboi et al. 2006), which could explain the disturbed GSIS of placebo-treated mutants. Since not only hyperglycaemic placebo-treated mutants, but also normoglycaemic insulin-treated mutant mice and female heterozygous mutants with a mild diabetic phenotype (Herbach et al. 2007) showed severely impaired GSIS, high blood glucose levels cannot be the main reason for the disturbed GSIS. Further, insulin-treated mutants demonstrated a higher pancreatic C-peptide content than placebo-treated mutants (see below), and

female mutant mice showed a higher pancreatic insulin content than male mutants (Herbach et al. 2007), which argues against depletion of insulin stores as a cause of disturbed GSIS. As described above, partial misfolding of mutant proinsulin may lead to disturbed insulin secretion (Izumi et al. 2003; Liu et al. 2005; Colombo et al. 2008). Further, isolated islets of 4-week-old male Akita mice demonstrated a disturbed GSIS compared to islets of sex-matched wild-type mice (Yoshioka et al. 1997).

Physiologically, glucose uptake causes an increase of the ATP/ADP ratio, leading to the closure of specific K_{ATP} channels, resulting in membrane depolarisation and opening of voltage-dependent calcium channels, and therefore in increasing intracellular Ca^{2+} concentrations. Finally mature insulin granules fuse with the plasma membrane, and insulin and C-peptide are secreted (Kaiser et al. 2003). Reduced increase of the ATP/ADP ratio due to energy consumption by chaperones upon ER stress or elevated intracellular Ca^{2+} levels due to Ca^{2+} release from the ER upon ER stress may be involved in the disturbed GSIS (Xu et al. 2005; Szegezdi et al. 2006; Scheuner and Kaufman 2008). It was stated that chronically elevated cytoplasmic Ca^{2+} concentrations might inhibit glucose-stimulated insulin secretion (Björklund et al. 2000; Grill and Björklund 2001). Therefore, mutant insulin may lead to ER stress and thereby disturbed GSIS in both Munich $Ins2^{C95S}$ and Akita mutant mice.

Taken together, since insulin- and placebo-treated mutants and untreated mutants of both genders demonstrated a severely disturbed glucose-stimulated insulin secretion, it is likely that misfolded (pro-)insulin 2 and ER stress lead to impaired GSIS. The exact mechanism of the disturbed GSIS remains to be investigated.

The C-peptide content in the pancreas of 100-day-old insulin-treated mutants was about 1/3 that of wild-type mice but over 4-fold higher compared to placebo-treated mutants, which demonstrated less than 1/10 of pancreatic C-peptide content versus wild-type mice. Morphological investigations of the pancreas demonstrated that the reduced pancreatic C-peptide content in 3-month-old untreated male mutant mice results from a decreased density of secretory granules within the β-cells and not from a reduction in β-cell mass

(Herbach et al. personal communication). These findings lead to the assumption that insulin production is largely decreased in Munich $Ins2^{C95S}$ mutant mice, and that normalisation of blood glucose levels improves C-peptide/insulin production. However, the reduced insulin secretion in insulin-treated mutants (see above), could also lead to less depletion of insulin stores and therefore to increased pancreatic C-peptide levels versus placebo-treated mutants. The findings of reduced pancreatic C-peptide content in placebo-treated mutants and of reduced pancreatic insulin content in untreated male and female mutant mice (Herbach et al. 2007) indicate disturbed insulin production and/or increased intracellular degradation. In the Akita mouse, the insulin and C-peptide content in the islets was also largely reduced (Wang et al. 1999; Zuber et al. 2004). Insulin production was shown to be unchanged in Akita islets, whereas intracellular degradation of mutant proinsulin was found to be increased (Izumi et al. 2003; Allen et al. 2004).

Randomly fed serum glucagon levels were similar in normoglycaemic insulin-treated mutant and wild-type mice, whereas in placebo-treated mutants, glucagon concentrations were elevated, despite higher blood glucose levels. Glucagon is produced and secreted by pancreatic α-cells. Physiologically, high blood glucose concentrations inhibit glucagon secretion via direct effects on α-cells and most likely also in an indirect manner, for example via increasing insulin secretion (Dunning et al. 2005; Franklin et al. 2005; Jacobson et al. 2009; Quoix et al. 2009). However, in diabetic patients glucose sensing of α-cells is disturbed, leading to elevated glucagon secretion, which further contributes to hyperglycaemia (Quesada et al. 2008; Jacobson et al. 2009). Therefore, increased randomly fed glucagon levels in placebo-treated mutants can be explained by defective glucose sensing of α-cells due to chronic hyperglycaemia. Insulin treatment of mutant mice normalised blood glucose concentrations, leading to physiological randomly fed serum glucagon levels.

Intraperitoneal insulin tolerance tests (ipITT) and a placebo-ipITT were performed to analyse insulin sensitivity. The percentaged decrease of blood glucose concentrations from basal value after intraperitoneal insulin or NaCl

0.9% injection was measured at distinct time points, and the corresponding area under the curve was calculated ($AUC_{blood\ glucose}$).

In the ipITT the $AUC_{blood\ glucose}$ of insulin-treated mutant mice was similar or even significantly lower compared to wild-type mice, which can be explained by the additional insulin, released from the pellets of insulin-treated mutants. At the age of 50 days, placebo-treated mutants showed a similar $AUC_{blood\ glucose}$ in the ipITT as wild-type mice, whereas the $AUC_{blood\ glucose}$ of 100- and 150-day-old placebo-treated mutant mice was significantly higher compared to wild-type mice, indicating reduced insulin sensitivity.

In order to examine the influence of the insulin delivered from the pellets on the ipITT of insulin-treated mutants, a placebo-ipITT with 150-day-old mice was performed. In contrast to wild-type and placebo-treated mutant mice, blood glucose concentrations of insulin-treated mutants decreased continuously during the placebo-ipITT, due to the insulin released from the pellets. However, blood glucose levels during the placebo-ipITT did not decline as much as during the ipITT, suggesting preserved sensitivity to intraperitoneally injected insulin in insulin-treated mutants.

A comparison of the $AUC_{blood\ glucose}$ of the ipITT and placebo-ipITT confirmed this assumption and showed that insulin administration significantly lowers the $AUC_{blood\ glucose}$ of both, insulin-treated mutant and wild-type mice as compared to 0.9% NaCl injection, indicating physiological insulin sensitivity. Since the relative differences between $AUC_{blood\ glucose}$ of the placebo-ipITT and the ipITT were similar in insulin-treated mutant and wild-type mice, insulin-therapy completely preserved insulin sensitivity in mutant mice.

In placebo-treated mutants, the $AUC_{blood\ glucose}$ during the ipITT was equal to that during the placebo-ipITT, demonstrating insulin resistance. Additionally performed ipITTs with untreated heterozygous mutant mice at different ages confirmed these results (see 5.3).

Since normoglycaemic insulin-treated mutants and female mutant mice with slightly elevated blood glucose concentrations showed similar insulin sensitivity compared to sex-matched wild-type mice, the development of insulin resistance in placebo-treated mutants is likely to be the consequence of chronic hyperglycaemia. Long-term high blood glucose concentrations lead to oxidative stress (Robertson 2004), which reduces insulin sensitivity, for example, in myocytes and adipocytes (Maddux et al. 2001; Houstis et al.

2006). The Akita mouse was also shown to exhibit severe peripheral and hepatic insulin resistance, and peripheral insulin resistance could be ameliorated by lowering blood glucose concentrations, using phloridzin (Hong et al. 2007). Ninety per cent pancreactomised (Px) male Sprague-Dawley rats developed diabetes mellitus including disturbed insulin sensitivity compared to shamPx rats (Park et al. 2007). In humans, insulin resistance is often associated with obesity and contributes to the development of diabetes type 2 (Ahren 2005). However, type 1 diabetics also develop insulin resistance, especially when blood glucose concentrations are poorly controlled (Greenbaum 2002; Heptulla et al. 2003). These studies and the findings in Munich $Ins2^{C95S}$ mutant mice underline the assumption that hyperglycaemia leads to insulin resistance. Developing insulin resistance contributes to the progressive diabetic phenotype of placebo-treated mutants.

5.1.2 Lipid peroxidation

Thiobarbituric acid reactive substances (TBARS) reveal the degree of lipid peroxidation and are often used as marker for oxidative stress in diabetic animal models and humans (Maritim et al. 2003; Ramakrishna and Jailkhani 2007). Serum TBARS levels were significantly higher in placebo-treated mutants, but were unchanged in insulin-treated mutants as compared to wild-type mice at 100 and 140 days of age. Further, blood glucose levels of the investigated groups correlated with lipid peroxidation in the serum. Therefore hyperglycaemia seems to have caused oxidative stress in placebo-treated mutants, whereas insulin-treatment prevented lipid peroxidation and probably oxidative stress in mutant mice. Elevated levels of TBARS can also be found in the serum of type 1 and type 2 diabetics (Kalaivanam et al. 2006; Ramakrishna and Jailkhani 2007; Song et al. 2007) and, for example, in the serum of STZ-induced diabetic Wistar rats (Ozansoy et al. 2001) and diabetic Zucker diabetic fatty (ZDF) rats (Coppey et al. 2002).

5.1.3 Islet isolation and ER stress

Isolation of islets, especially of placebo-treated mutants but also of insulin-treated mutant mice was very difficult. Due to the low insulin content in the islets, the colour of islets appeared different than that of wild-type mice. Further, islets of mutant mice were very fragile which led to deformation and

fragmentation of islets, resulting in irregularly shaped islet clusters that were hardly distinguishable from exocrine pancreas clusters. Therefore, the purity of islet isolates of mutant mice, particularly of placebo-treated mutants, was lower than that of wild-type mice. Similar difficulties were faced during islet isolation of Akita mice, leading to a considerable contamination of islet samples with non-endocrine tissue (around 30%) (Izumi et al. 2003). The accumulation of misfolded proinsulin in Akita islets was thought to non-specifically affect secretory pathways and might interfere with the transport of other cargo, including membrane proteins (Izumi et al. 2003). For example, the reduced transport of collagens, especially collagen type IV α1 and α2, which are components of the peri-insular capsule (Irving-Rodgers et al. 2008), may reduce islet resistance to collagenase digestion. Thus, the reduced integrity of isolated islets of Munich $Ins2^{C95S}$ mutants after collagenase digestion might be due to an altered collagen composition of the peri-insular capsule, resulting from a non-specific block in protein transport. Furthermore, hyperglycaemia leads to the generation of free radicals, which can directly interact with proteins and other macromolecules (Maritim et al. 2003; Robertson 2004). Determining the carbonyl content of proteins, it was demonstrated that hyperglycaemia-induced oxidative stress leads to oxidation of proteins in the serum of type 1 diabetics (Ramakrishna and Jailkhani 2007) and in the pancreata of hyperglycaemic Cohen diabetic rats (Ryu et al. 2008). Therefore, reactive oxygen species might interact with proteins within the peri-insular capsule of hyperglycaemic mice, reducing the stability of these islets. This assumption is in coincidence with the higher integrity of isolated islets of normoglycaemic insulin-treated mutant mice compared to hyperglycaemic placebo-treated mutants.

Isolated islets of 100-day-old insulin-treated mutants showed an increased abundance of CHOP and PeIF2α compared to wild-type mice. Placebo-treated mutants demonstrated similar amounts of BiP and PeIF2α, and a slightly higher abundance of CHOP compared to wild-type mice. However, the reduced sample purity (up to 40% contamination with exocrine pancreas tissue) results in decreased islet-protein content in samples of mutant mice, especially of placebo-treated mutants. Therefore, the abundance of ER stress

associated proteins in β-cells is likely to be underestimated, and Western blot analyses have to be interpreted carefully.

CHOP is involved in ER stress-induced apoptosis (Oyadomari and Mori 2003; Scheuner and Kaufman 2008), and *Chop* disruption in heterozygous Akita mice reduced β-cell apoptosis compared to Akita mice with intact *Chop* genes (Oyadomari et al. 2002b). *Chop* null mutation in Lepr[db/db] mice resulted in largely increased β-cell mass and reduced β-cell apoptosis compared to diabetic Lepr[db/db] mice with intact *Chop* (Song et al. 2008).

Therefore it is likely that CHOP-induced apoptosis also occurs in Munich *Ins2*[C95S] mutants.

ER stress leads to the phosphorylation of eucaryotic initiation factor 2α, which results in reduced translation of many mRNAs, thereby reducing protein biosynthesis (Harding et al. 1999; Oyadomari et al. 2002a). In islets of diabetic *db/db* mice for example, expression of various genes of the unfolded protein response (UPR) was increased including that of PeIF2α compared to non-diabetic controls (Laybutt et al. 2007). However, in CHO cells expressing proinsulin with the Akita mutation, neither proinsulin nor overall protein synthesis rates were decreased compared to CHO cells expressing wild-type proinsulin. Further, in isolated islets of 16-week-old male Akita mice, the overall protein synthesis was similar compared to wild-type islets. The authors concluded that mutant proinsulin does not profoundly reduce protein synthesis in Akita mice (Izumi et al. 2003). However, the finding of increased PeIF2α in islets of insulin-treated mutants argues for translational attenuation in Munich *Ins2*[C95S] mutant mice.

Misfolded proinsulin 2 accumulates in the β-cells of Akita mice and leads to the induction of several ER stress markers like BiP, HRD1, spliced XBP-1 and ATF6 in islets of Akita mice or in cell lines expressing the mutant insulin (Wang et al. 1999; Allen et al. 2004; Nozaki et al. 2004; Zuber et al. 2004). The ER stress markers BiP, CHOP and spliced XBP-1 were also increased in isolated islets of transgenic mice overexpressing human islet amyloid polypeptide, which aggregates in the β-cell, leading to increased β-cell apoptosis (Huang et al. 2007).

These findings indicate that misfolded (pro-)insulin induces ER stress in β-cells of insulin- and placebo-treated mutants, probably resulting in β-cell apoptosis and possibly in reduced insulin mRNA translation.

5.1.4 Qualitative-histological and quantitative-stereological analysis of the endocrine pancreas

Qualitative-histological analyses were performed, using sections immunostained for insulin or simultaneously stained for glucagon, somatostatin and pancreatic polypeptide (non-β-cells). Mutant mice exhibited fewer large islet profiles than wild-type mice. Immunostaining for non-β-cells, demonstrated an altered islet composition in mutant mice, especially in placebo-treated mutants. Normally islets are composed of a core of mainly β-cells, surrounded by a small rim of non-β-cells. In mutant mice, the proportion of non-β-cells was increased and non-β-cells were found distributed all over the islet profile. Further, immunostaining for insulin revealed a weak staining of β-cells of mutant mice, whereas insulin-treated mutants exhibited a stronger staining for insulin than placebo-treated mutants.

Quantitative-stereological investigations were performed using state-of-the-art unbiased model-independent stereological methods (Gundersen et al. 1988; Wanke et al. 1994).

Due to perfusion fixation, capillaries didn't collapse and accounted for about 25% of the total islet volume. The volume density of capillaries within the islets of insulin-treated mutants was similar to that of wild-type mice, whereas placebo-treated mutants demonstrated a slightly lower volume density of capillaries within the islets compared to wild-type mice and insulin-treated mutants. Chronically high blood glucose concentrations lead to structural changes in vessels, like increased basement membrane width, due to enhanced matrix deposition, and therefore to less elasticity of blood vessels, which could explain the lower $Vv_{(capillaries/islets)}$ of hyperglycaemic mutants (Di Mario and Pugliese 2001). Usually pancreata are not fixed via vascular perfusion, and therefore, the capillaries are collapsed. In order to generate data that can be compared to results of studies with non-perfused pancreata, the volume densities of β-cells and non-β-cells were referred to the endocrine compartment of the islet and not to the whole islet profile in this study.

The volume density of β-cells in the endocrine compartment of the pancreas was only slightly decreased in insulin-treated mutants compared to wild-type mice, representing almost 75% of all endocrine cells, whereas in placebo-treated mutants, the volume density of β-cells was reduced to less than 50% of the endocrine compartment, resulting in a large increase of the volume density of non-β-cells. It was shown previously, that most of the non-β-cells represent α-cells (Herbach et al. 2007). Other diabetic animal models also show a disturbed islet composition, irrespective of the causative genetic manipulation (e.g. GIPR[dn] transgenic mice (Herbach et al. 2005), GLP-1R knockout mice (Ling et al. 2001), MafA knockout mice (Zhang et al. 2005), PERK knockout mice (Harding et al. 2001) and dominant negative HNF-1α transgenic mice (Hagenfeldt-Johansson et al. 2001)). In addition, morphometric analyses of type 2 diabetic humans revealed an increased α-cell fraction in the islets (Yoon et al. 2003).

In islets of Akita mice, the proportion of insulin positive cells was also reduced compared to wild-type mice (Yoshioka et al. 1997). However, the insulin antibody used in other studies only detects wild-type, but not mutant insulin of Akita mice (Wang et al. 1999; Izumi et al. 2003), which leads to the assumption that the insulin antibody used in the study of Yoshioka et al. (1997) probably does not react with mutant insulin 2. Therefore, and due to severe degranulation of β-cells (Wang et al. 1999; Izumi et al. 2003), insulin staining might be insufficient to identify largely degranulated β-cells, leading to an underestimation of the proportion of β-cells in the islets of Akita mice. It was described that around 20% and 25% of the islet area of 4-week-old male Akita mice exhibited immunoreactivity for insulin and glucagon, respectively (Yoshioka et al. 1997). Since δ- and PP-cells account for a minor proportion in pancreatic islets (together less than ~10% (Brissova et al. 2005; Cabrera et al. 2006; Herbach et al. 2007)), it seems likely that many of the endocrine cells without detectable immunoreactivity for insulin were β-cells (almost 50%). The immunoreactivity for insulin was also severely reduced in β-cells of placebo-treated Munich *Ins2*[C95S] mutant mice. In order to avoid an underestimation of the volume density of β-cells, this parameter was determined in sections immunostained for non-β-cells in this study.

The total volume of non-β-cells of insulin-treated mutants, was similar to that of wild-type mice. In placebo-treated mutants, the total volume of non-β-cells was largely increased versus wild-type and insulin-treated mutant mice. Chronic hyperglycaemia of placebo-treated mutants may therefore lead to increased differentiation and development of non-β-cells, especially α-cells. Long-term hyperglycaemia reduces PDX-1 mRNA concentrations and PDX-1 DNA binding activity in pancreatic β-cells, which is essential for β-cell development and maintenance (Tanaka et al. 1999; Holland et al. 2002; Melloul et al. 2002; Miyazaki et al. 2004; Robertson and Harmon 2006; Andrali et al. 2008). It was demonstrated that inhibition of *Pdx-1* expression in adult transgenic mice using the tet regulatory system, which allows tissue-specific and doxycycline-inducible control of *Pdx-1* expression, results in increased volume density of glucagon positive cells in the islets. Further, the glucagon expressing cells were distributed homogeneously throughout the islets, similar as in placebo-treated mutants of the present study (Lottmann et al. 2001). Ahlgren et al. (1998) suggested that PDX-1 would suppress glucagon expression in β-cells and is necessary to maintain the β-cell phenotype. Physiologically, the proportion of insulin- to glucagon-expressing cells in pancreatic islets is 5:1, and these endocrine cells express either insulin or glucagon. Tissue specific reduction of *Pdx-1* expression, using the Cre-loxP technology, led to a 1:1 ratio of glucagon- to insulin-positive cells, and 22% of the endocrine cells co-expressed glucagon and insulin (Ahlgren et al. 1998). These findings were confirmed by a more recent study, which used the tet regulatory system to inhibit *Pdx-1* expression in rat insulinoma cells. Impairment of *Pdx-1* expression in INSrβ cells, which normally express insulin and show only an undetectable background of glucagon mRNA, severely increased glucagon mRNA levels and largely reduced *Ins* transcription. These results demonstrate that suppression of *Pdx-1* expression leads to the differentiation of an insulin-predominant β-cell lineage to a glucagon-predominant α-cell phenotype (Wang et al. 2001).

The findings of the different studies lead to the assumption that chronic hyperglycaemia in placebo-treated mutant mice suppresses the development of β-cells and might increase the differentiation of glucagon expressing α-cells from common progenitor cells and possibly from existing β-cells via trans-differentiation, which contributes to the altered ratio of β- to α-cells within the

endocrine compartment of the islets and results in the higher total volume of glucagon positive cells in the islets of placebo-treated mutants.

The total volume of β-cells in insulin-treated mutants was about half that of wild-type mice and approximately twice that of placebo-treated mutants. It was demonstrated that long-term exposure to high glucose concentrations leads to β-cell apoptosis in isolated human islets (Federici et al. 2001; Maedler et al. 2008), and studies in autopsies showed that type 2 diabetics exhibit a reduced volume density of β-cells in the pancreas and a decreased total β-cell mass compared to non-diabetic controls (Sakuraba et al. 2002; Butler et al. 2003; Cnop et al. 2005). Quantitative-stereological investigations of the pancreata of 3-month-old (Herbach et al. personal communication) and 6-month-old mice (Herbach et al. 2007, this study) demonstrated a severe reduction of total β-cell volume in male heterozygous mutant mice with age, which suggests that duration and increase of hyperglycaemia lead to β-cell loss. Since in insulin-treated mutants the total β-cell volume was higher compared to placebo-treated mutants, but lower versus wild-type mice, chronically elevated blood glucose levels seem to be only one reason for the reduced β-cell mass in placebo-treated mutants. Long-term ER stress is probably another essential factor, leading to reduced total β-cell volume in insulin- and placebo-treated mutant mice, via programmed cell death. As described above, the transcription factor CHOP, which is associated with ER stress-induced apoptosis (Oyadomari et al. 2002b; Oyadomari and Mori 2003), was elevated in isolated islets of 100-day-old insulin- and placebo-treated mutant mice. In the Akita mouse it was shown that CHOP is involved in β-cell apoptosis of heterozygous Akita mice (Oyadomari et al. 2002b).

Additionally to ER stress, reduced endogenous insulin secretion in insulin-treated mutants might possibly contribute to the reduced total β-cell volume in the islets compared to wild-type mice. Insulin-treated mutants demonstrated reduced randomly fed and glucose-stimulated insulin secretion, probably leading to decreased auto- and paracrine effects of insulin on β-cells, as described above. Different studies demonstrated that insulin has anti-apoptotic and proliferative effects on MIN6 β-cells (Muller et al. 2006; Beith et al. 2008). Furthermore, knockout of the insulin receptor of pancreatic β-cells in mice (βIRKO mice), using the Cre-loxP system, resulted in the development of

disturbed glucose tolerance, and some βIRKO mice became diabetic. Since not only diabetic but also non-diabetic βIRKO mice exhibited reduced β-cell mass at the age of 26 - 30 weeks, insulin-mediated signalling pathways seem to be essential to maintain pancreatic β-cell mass (Otani 2004).

The total volume of β-cells within the pancreas of adult mice depends on the balance between β-cell apoptosis and regeneration of β-cells either by replication of β-cells within an existing islet or by differentiation of new β-cells from progenitor cells within pancreatic ducts (Butler et al. 2003; Bonner-Weir et al. 2008; Xia et al. 2009). It was stated that progenitor cells in the epithelium of pancreatic ducts can differentiate into insulin-producing β-cells and bud from the duct to form new islets, not only in neonatal, but also in adult mice (Bonner-Weir et al. 2008; Inada et al. 2008).

The volume density and the total volume of isolated β-cells in the pancreas of insulin-treated mutant mice, were lower compared to wild-type mice and higher versus placebo-treated mutants, which leads to the assumption that reduced islet neogenesis might be one reason for the lower total islet and β-cell volumes of mutant mice.

As described above, in placebo-treated mutants reduced *Pdx-1* expression due to chronic and severe hyperglycaemia might be involved in the reduced differentiation of progenitor cells to β-cells, and therefore in the reduced total volume of isolated β-cells in the pancreas. In contrast to chronically elevated blood glucose levels, induction of severe hyperglycaemia for 48 hours via glucose infusion resulted in increased islet neogenesis in Wistar rats (Paris et al. 2003). Further, mild glucose infusion of male Sprague-Dawley rats for 96 hours led to slightly elevated blood glucose levels and increased islet neogenesis versus rats infused with saline (Jetton et al. 2008). These findings lead to the assumption that positive or negative effects of glucose concerning islet neogenesis are dependent on the duration and severity of hyperglycaemia. Physiological short-term increase of blood glucose concentrations, for example after meal intake, is essential for DNA binding of the transcription factors PDX-1, MafA and NeuroD1 in β-cells (Andrali et al. 2008), whereas long-term hyperglycaemia reduces PDX-1 DNA binding (Melloul 2004). Since PDX-1 plays an important role for the differentiation of progenitor cells to β-cells (Bonner-Weir et al. 2008), it seems likely that short-

term elevation of blood glucose levels results in increased islet neogenesis, whereas long-term hyperglycaemia has contrary effects. In the prediabetic state and at the beginning of hyperglycaemia in humans, compensatory mechanisms result in increased β-cell mass, whereas long-term elevated blood glucose concentrations lead to reduced β-cell mass in diabetics (Weir et al. 2001; Butler et al. 2003; Cnop et al. 2005). These findings confirm that short-term elevated blood glucose levels increase β-cell mass and possibly islet neogenesis, whereas long-term hyperglycaemia has contrary effects.

In insulin-treated mutants improved glucose control may therefore be responsible for the significantly higher total volume of isolated β-cells as compared to placebo-treated mutants. However, the total volume of isolated β-cells in insulin-treated mutants was reduced compared to wild-type mice. It was stated that increased insulin demand, for example due to reduced insulin action in obese humans and animal models, during pregnancy, and in the prediabetic period, results in compensatory increase of β-cell mass, via neogenesis, replication or hypertrophy (Weir et al. 2001; Yoon et al. 2003; Ahren 2005; Bouwens and Rooman 2005). In type 2 diabetics, in which the area density of islet β-cells in the pancreas was still unchanged, the area density of ductular β-cells in the pancreas was increased, indicating elevated islet neogenesis (Clark et al. 2001). This possibly suggests that the opposite, namely reduced insulin demand due to insulin treatment might contribute to lower islet neogenesis compared to wild-type mice.

The replication rate of β-cells in placebo-treated mutants was higher compared to insulin-treated mutants and wild-type mice. The influence of glucose and insulin on β-cell replication is discussed controversially (Bouwens and Rooman 2005). In *in vitro* studies, it was demonstrated that exogenous insulin has proliferative effects on mouse β-cells (Beith et al. 2008) and insulin-secreting MIN6 cells (Muller et al. 2006). In contrast, insulin infusion for 48 hours resulted in over 60-fold increased plasma insulin levels and drastically reduced β-cell proliferation in Wistar rats (Paris et al. 2003).

As described above, in the prediabetic period and at the beginning of hyperglycaemia compensatory mechanisms can lead to elevation of β-cell mass. However, mild glucose infusion of rats resulted in increased β-cell mass, whereas β-cell proliferation was unchanged for the first 36 hours and

afterwards was even lower compared to saline infused rats (Jetton et al. 2008). Glucose infusion of Wistar rats for 48 hours led to largely increased blood glucose concentrations and reduced β-cell replication (Paris et al. 2003). Further, β-cell replication was demonstrated to be reduced after prolonged exposure of isolated islets to high glucose concentrations (Maedler et al. 2001; Maedler et al. 2002).

Therefore, it seems surprising that β-cell replication was increased in placebo-treated mutants compared to wild-type mice, especially since the total β-cell volume of placebo-treated mutants was largely decreased compared to wild-type mice and insulin-treated mutants.

However, since only about 0.1% of the β-cells were BrdU-positive and the replication rate was analysed at a single time point in the present study, it is difficult to accurately quantify replication rates (Donath and Halban 2004).

The numerical fraction of TUNEL-positive β-cells was similar in the examined groups. However, the number of apoptotic β-cells was very low and showed substantial variation between the investigated mice. In the Akita mouse, whole islets were examined for apoptotic cells, using serial sections, and the number of TUNEL-positive β-cells was very low at the age of 4, 8 and 13 weeks (Izumi et al. 2003). The low number of TUNEL-positive cells results from the short duration of apoptotic events, and rapid clearance by macrophages, which makes it difficult to quantify programmed cell death (Weir et al. 2001; Izumi et al. 2003). Furthermore, the determination of apoptotic β-cells at a single time point can be an inaccurate representation of the real rate of programmed cell death in the analysed tissues (Donath and Halban 2004; Huerta et al. 2007). Thus, despite similar number of TUNEL-positive β-cells in the islets of insulin- and placebo-treated male Munich *Ins2*[C95S] mutants and wild-type mice, apoptosis may still account for the reduced total β-cell volume in mutant mice.

At 90 days of age, the total β-cell volume was still similar in mutants versus wild-type mice (Herbach et al. unpublished data), therefore, β-cell loss occurs between 90 and 180 days of age in male Munich *Ins2*[C95S] mutants (Herbach et al. 2007). Thus, the determination of apoptotic cells at 160 days of age may be too late, since the total β-cell volume is already reduced up to ~70% compared to wild-type mice.

In conclusion, in placebo-treated mutants chronic hyperglycaemia and ER stress lead to the reduced total β-cell volume, most likely due to increased β-cell apoptosis, decreased β-cell differentiation and reduced islet neogenesis. Insulin treatment prevented hyperglycaemia-induced β-cell apoptosis and partially preserved β-cell regeneration in mutant mice. Since glucose levels are generally normalised in insulin-treated mutants, ER stress seems to be a main reason for the reduced total β-cell volume in the pancreas of insulin-treated mutants compared to wild-type mice.

5.1.5 Electron microscopic findings in β-cells

Electron microscopy revealed that the different staining intensities of β-cells in the islets of the investigated groups, which were observed in sections immunostained for insulin, resulted from different densities of secretory granules within the β-cells.

In placebo-treated mutants most of the β-cells were almost completely degranulated, whereas in β-cells of insulin-treated mutants the density of secretory granules was in general higher compared to placebo-treated mutants, but lower than in wild-type β-cells. The reduced density of secretory granules is in coincidence with the reduced pancreatic C-peptide content of mutant mice (see 5.1.1).

The density of secretory granules within the β-cells depends on the rate of *Ins* transcription, insulin mRNA translation, (pro-)insulin processing and intracellular degradation of (pro-)insulin. Furthermore the relation between insulin production and insulin secretion must be considered. Since insulin-treated mutants demonstrated significantly lower randomly fed and glucose-stimulated C-peptide levels compared to placebo-treated mutants, lower insulin secretion seems to largely contribute to the higher density of secretory granules in insulin-treated mutants versus placebo-treated mutants.

It is unknown if insulin-treated mutants exhibit a lower, equal or higher insulin biosynthesis compared to placebo-treated mutant mice. A reduced insulin production in insulin-treated mutants would lead to decreased protein folding load and to decreased biosynthesis of mutant (pro-)insulin 2, and therefore to reduced ER stress versus placebo-treated mutants. However, determination of ER stress markers in isolated islets (see 5.1.3) and electron microscopic

findings (see below) indicate that β-cells of insulin-treated mutants suffer from as much ER stress as those of placebo-treated mutant mice.

In placebo-treated mutants, chronically high blood glucose concentrations and therefore oxidative stress may result in reduced *Ins* expression due to decreased insulin promoter binding activity of PDX-1 and other transcription factors, like MafA (Melloul et al. 2002; Melloul 2004; Andrali et al. 2008). Long-term incubation of HIT-T15 cells in 11.1 mM glucose resulted in reduced PDX-1 and MafA DNA binding activity and in reduced insulin mRNA content as well as decreased insulin concentrations, which was partially prevented by co-incubation with antioxidants (Tanaka et al. 1999). Exposure of isolated rat islets to H_2O_2 for 48 hours led also to decreased PDX-1 binding activity and reduced insulin mRNA levels (Kaneto et al. 2002). In isolated islets of 8- to 12-week-old Akita mice, total insulin mRNA levels were approximately 85 - 90% that of wild-type mice, and mutant insulin was transcribed in similar degree as wild-type insulin (Wang et al. 1999).

It was demonstrated that insulin stimulates its own expression via insulin receptor signalling (Leibiger et al. 1998; Melloul et al. 2002). *In vitro* studies with isolated pancreatic islets showed that exogenous insulin leads to increased proinsulin synthesis. Stimulation of insulin secretion via KCl also resulted in elevated proinsulin biosynthesis, and inhibition of insulin secretion via nifedipine reduced glucose-stimulated proinsulin biosynthesis. It was suggested that both, glucose and endogenous insulin secretion exert stimulatory effects on insulin biosynthesis, in an additive manner (Leibiger et al. 2000). Therefore, it seems possible that reduced endogenous insulin secretion in insulin-treated mutants contributes to decreased insulin biosynthesis. However, decreased insulin secretion in insulin-treated mutants has probably more effects on the density of secretory granules than a reduced insulin biosynthesis.

In addition to the influence of glucose on *Ins* transcription, ER stress in islets of insulin- and placebo-treated mutants possibly leads to reduced insulin mRNA translation. It is known that ER stress can reduce mRNA translation via phosphorylation of eIF2α (Rajan et al. 2007), and in isolated islets of insulin-treated mutants PeIF2α abundance was slightly increased compared to wild-type mice. As described above, it was stated that mutant proinsulin 2 does not

seem to severely reduce protein synthesis in islets of Akita mice or CHO cells (Izumi et al. 2003), but PeIF2α was not analysed.

In Akita mice it was demonstrated that misfolded and accumulated proinsulin was partially degraded via ERADI (Allen et al. 2004). Therefore it seems possible that, at least in part, misfolded (pro-)insulin might be also degraded in β-cells of insulin- and placebo-treated mutants, contributing to the reduced density of secretory granules.

In some β-cells of placebo- and insulin-treated mutant mice, the ER seemed to be dilated and filled with electron dense material, as described in Akita mice (Wang et al. 1999; Zuber et al. 2004). The denotation of structures between the perinuclear ER and the Golgi apparatus varies substantially, including rough ER, transitional ER and pre-Golgi intermediates (Ghadially 1988; Fan et al. 2003; Zuber et al. 2004; Riggs et al. 2005). The dilated structures in the Akita mouse were denoted transitional ER (Wang et al. 1999), ER-like structures (Izumi et al. 2003), and dilated rough ER and pre-Golgi intermediates (Zuber et al. 2004). The dilated structures of placebo- and insulin-treated Munich *Ins2*^C95S mutant mice mostly represent dilated rough ER that is found throughout the cytoplasm and, to a lower degree, pre-Golgi intermediates, that are located in close association to the Golgi complex. The electron-dense material in the lumen may represent the accumulation of secretory proteins. In Akita mice it was shown by immunogold labelling that this electron dense material is composed of proinsulin (Zuber et al. 2004), and it is likely that proinsulin accumulation also occurs in ER-like structures of Munich *Ins2*^C95S mutant mice. Dilated rough ER is thought to be an indicator of impairment of secretory pathways in the Akita mouse (Izumi et al. 2003) and ER distension was stated to be a characteristic of ER dysfunction (Scheuner and Kaufman 2008). Further, expansion of the ER was denominated as a characteristic of ER stress (Cnop et al. 2008; Malhotra et al. 2008). Dilated ER was also seen in other mouse models, exhibiting elevated ER stress markers, a disturbed ER stress response and/or intracellular accumulation of proteins, e.g. PERK knockout mice (Harding et al. 2001), βWfs knockout mice (Riggs et al. 2005), C57BL/6 mice overexpressing coagulation factor VIII, (Malhotra et al. 2008), Hsp47 knockout mice (Marutani et al. 2004).

In conclusion, the decreased density of secretory granules in β-cells of placebo-treated mutants compared to wild-type mice probably results from reduced *Ins* expression due to chronic hyperglycaemia and from the misfolded proinsulin 2, which probably accumulates in the ER and causes ER stress. In insulin-treated mutants, misfolded proinsulin 2 and ER stress may be mainly responsible for the lower density of secretory granules versus wild-type mice, and lower insulin secretion mainly accounts for higher granule density than in placebo-treated mutants.

Electron microscopy demonstrated that in some β-cells of placebo-treated mutants the mitochondria appeared swollen, versus wild-type and insulin-treated mutant mice. Oxidative stress can increase mitochondrial membrane permeability and alter the potential of the inner mitochondrial membrane (Kanwar et al. 2007). It was stated that altered membrane permeability leads to mitochondrial swelling and to cytochrome *c* release, thereby activating apoptotic mitochondrial pathways (Jiang et al. 2001; Zhang et al. 2008). Mitochondrial swelling was associated with oxidative stress e.g. in the retina (Kanwar et al. 2007) and the heart of of diabetic mice (Shen et al. 2004). ER stress can also alter the mitochondrial membrane permeability, lead to cytochrome *c* release and to apoptosis (Jimbo et al. 2003; Zhang et al. 2008). Swollen mitochondria were found in β-cells of different diabetic rodent models with β-cell loss, like the Akita mouse (Izumi et al. 2003), STZ-induced diabetic Wistar rats (Zhou et al. 2009) and diabetic Goto Kakizaki rats (Mizukami et al. 2008).

The lack of enlarged mitochondria in β-cells of insulin-treated mutants argues for chronic hyperglycaemia as main reason for mitochondrial swelling. Swollen mitochondria may be an early sign for apoptosis of the affected β-cells in placebo-treated mutants.

Glycogen deposits, which appear as small rosettes of dark granules (Bendayan et al. 2007), were only found in β-cells of placebo-treated mutant mice. Glycogen accumulation in β-cells was also found in other diabetic animals, e.g. Psammomys obesus (Bendayan et al. 1995), dogs (Hoenig 2002), or in glucose infused cats (Zini et al. 2009), and is associated with hyperglycaemia.

5.1.6 Body and organ weights

Body weights of 160-day-old randomly fed placebo-treated mutants were significantly lower compared to wild-type mice. Due to increased food intake, the gastrointestinal contents were heavier in diabetic placebo-treated mutant mice compared to wild-type mice and insulin-treated mutants. Experiments with mice lacking insulin receptors in the brain (Brüning et al. 2000) or in the hypothalamus (Obici et al. 2002) showed that missing insulin signalling in the brain, especially in the hypothalamus can lead to hyperphagia, a symptom sometimes observed in diabetics (ADA 2006). The increased food intake in placebo-treated mutant mice is assumed to be also the reason for the elevated weight of the emptied GIT of placebo-treated mutants compared to wild-type mice and insulin-treated mutants. It was described that enteral nutrients lead to adaption of the intestine, especially in the mucosal layer (Tappenden 2006). Diabetic polyphagic Wistar rats, for example, exhibited elevated weight of the intestine despite lower body weight compared to non-diabetic Wistar rats, which was mainly due to increased mucosa thickness of the intestine (Zhao et al. 2003).

When the GIT content was subtracted from the body weight, insulin-treated mutant mice were as heavy as wild-type mice and significantly heavier compared to placebo-treated mutants. Furthermore, insulin-treated mutants featured more fatty tissue compared to placebo-treated mutants, but less than wild-type mice.

These findings mirror the anabolic effects of insulin. Insulin promotes glucose uptake, increases lipogenesis and reduces lipolysis in adipocytes (Blüher et al. 2002; Nishino et al. 2007). In muscle cells, insulin mediates uptake of glucose and amino acids, increases glycogen synthesis, reduces proteolysis and increases protein synthesis (Kim et al. 2000; Fujita et al. 2006). Therefore, insulin treatment of mutant mice resulted in more fatty tissue and probably muscle mass, and consequently in higher body weight compared to placebo-treated mutants. The reason for the reduced fatty tissue of insulin-treated mutants compared to wild-type mice is unclear, since insulin normally leads to increased lipogenesis (Blüher et al. 2002; Nishino et al. 2007) and insulin treatment in humans is often associated with weight gain (Hollander et al. 2007; Raslova et al. 2007).

Testes weights of insulin-treated mutants and wild-type mice were similar, but higher as compared to placebo-treated mutants, which can be explained by insulin effects on the reproductive system. Male NIRKO mice, which demonstrate a knockout of the insulin receptor in the brain, featured reduced epididymal sperm content and decreased amounts of Leydig cells, which was associated with reduced plasma levels of luteinising hormone (LH) (Brüning et al. 2000). Hypogonadism, which is predominantly defined by reduced levels of testosterone, is also often observed in older men with type 2 diabetes (Corona et al. 2005; Kapoor et al. 2007).

Liver weights of insulin-treated mutants and wild-type mice were similar, whereas placebo-treated mutant mice featured elevated liver weights. In patients with type 1 or type 2 diabetes, increased contents of triglycerides (liver steatosis) and glycogen deposits in hepatocytes (hepatic glycogenosis) can lead to hepatomegaly. Since hepatic glycogenosis is often seen in type 1 diabetics with poorly controlled hyperglycaemia (Tomihira et al. 2004; Sayuk et al. 2007; Martocchia et al. 2008) and liver steatosis is absent in many lean type 1 diabetics (Torbenson et al. 2006), high blood glucose levels seem to be the main reason for hepatocellular glycogen deposits. Liver steatosis and hypertriglyceridaemia are frequently observed in obese type 2 diabetics (Toledo et al. 2006), and can be found in overweight patients with type 1 diabetes (Sayuk et al. 2007). These findings indicate that liver steatosis is mainly associated with obesity and dyslipidaemia, and hepatic glycogenosis results predominantly from hyperglycaemia. Since glycogen deposits were found in the β-cells of placebo-treated mutants and these mice are non-obese, it is likely that hepatic glycogenosis is the main reason for hepatomegaly in placebo-treated mutants. Glycogen and fat staining of liver tissue would be necessary to confirm this assumption and to show if liver steatosis is present in placebo-treated mutants.

Kidney weights of placebo-treated mutants were elevated compared to insulin-treated mutants and wild-type mice. Renal hypertrophy is an early pathological manifestation of diabetic kidney disease, and chronic hyperglycaemia plays a major role in the development of diabetic nephropathy (Mahimainathan et al. 2006; Forbes et al. 2007). Therefore it is possible that chronically elevated blood glucose concentrations lead to renal hypertrophy of placebo-treated mutants. Further analyses are necessary to investigate other possible

diabetes-associated kidney lesions, like glomerular hypertrophy and glomerulosclerosis, in placebo-treated mutants.

In summary, the clinical investigations showed that insulin treatment of mutant mice in general normalised blood glucose concentrations, and improved oral glucose tolerance compared to placebo-treated mutants. Further, insulin treatment preserved insulin sensitivity, but did not ameliorate the disturbed glucose-stimulated insulin secretion. Insulin therapy of mutants led to increased pancreatic C-peptide content versus placebo-treated mutants and prevented changes in body and organ weights, which were detected in placebo-treated mutant mice.

5.2 C-peptide II concentration in serum and pancreas of untreated male and female Munich $Ins2^{C95S}$ mutant and wild-type mice

Twenty-one-day-old homozygous mutant mice of both genders demonstrated severe randomly fed hyperglycaemia, whereas blood glucose concentrations of male and female heterozygous mutant mice were only slightly elevated compared to wild-type mice. The elevated blood glucose levels in mutant mice might be due to reduced insulin secretion and/or due to reduced receptor binding and biological activity of mutant insulin, as discussed above (5.1.1).

The secretion of mutant insulin 2 was analysed by determining C-peptide II concentrations in the serum of 21-day-old male and female homozygous Munich $Ins2^{C95S}$ mutant mice. Randomly fed C-peptide II concentrations in the serum of heterozygous mutants of both genders were higher compared to those of sex-matched homozygous mutants and lower compared to those of wild-type mice. The reduced serum C-peptide II concentrations in mutant mice may be due to disturbed secretory pathways in β-cells of Munich $Ins2^{C95S}$ mutant mice (see 5.1.1) and/or due to the significantly reduced pancreatic C-peptide II content.

The C-peptide II content in the pancreas of male and female heterozygous mutant mice was significantly reduced compared to sex-matched wild-type mice, but significantly higher than that of homozygous mutants. Similar observations were made in 14-day-old Akita mice (Kayo and Koizumi 1998).

Since 3-month-old heterozygous mutants exhibited a reduced density of secretory granules within the β-cells compared to wild-type mice, but an unchanged total volume of β-cells in the pancreas (Herbach et al. personal communication), it is likely that the reduced pancreatic C-peptide II content in 21-day-old heterozygous mutants also results from a decreased density of insulin secretory granules, but not from a reduced total β-cell volume. In 14-day-old homozygous Akita mice the total islet volume and the density of β-cells within the islets were largely reduced compared to heterozygous Akita and wild-type mice, leading to a reduced total β-cell volume (Kayo and Koizumi 1998). Therefore, the severely decreased C-peptide II content in the pancreas of homozygous Munich *Ins2*[C95S] mutant mice might be due to a decreased density of secretory granules within the β-cells and due to a reduced total volume of β-cells.

The more severe diabetic phenotype in homozygous Munich *Ins2*[C95S] mutant mice versus heterozygous mutants, with largely reduced pancreatic and serum C-peptide II content, severe hyperglycaemia and reduced lifespan (Herbach et al. 2007; this study) mirror the dosage effect of mutant insulin, which is also found in Akita mice (Kayo and Koizumi 1998).

Male and female homozygous mutants, as well as heterozygous mutant mice of both genders, demonstrated similar serum and pancreatic C-peptide II levels and similar blood glucose concentrations. These findings suggest that before sexual maturity, female mutants are as prone to become diabetic as male mutants, in contrast to adult animals. In several diabetic rodent models adult male mutants show a more severe diabetic phenotype than females, which seems to be associated with antidiabetic and antioxidative effects of estrogen (Louet et al. 2004; Le May et al. 2006). However, since sexual maturity in female mice does not occur before 28 days of age (Belle 2004) and the ovary is the major site for estrogen production (Lundholm et al. 2008), 21-day-old females might have estrogen levels comparable to those of male mutants. Therefore, 21-day-old female mutants probably don't demonstrate higher antioxidative defence mechanisms than male mutants, leading to the similar diabetic phenotype. In 14-day-old heterozygous and homozygous Akita mice pancreatic insulin content and morphological findings did not demonstrate gender differences, either (Kayo and Koizumi 1998), but female

heterozygous adult Akita mice exhibited a milder diabetic phenotype compared to male heterozygous Akita mice (Yoshioka et al. 1997).

In conclusion, the secretion of mutant insulin 2 is possible, thereby confirming previous *in vitro* observations (Liu et al. 2005). The homozygous mutation of *Ins2* results in a more severe diabetic phenotype compared to the heterozygous genotype, with earlier onset of diabetes and lower pancreatic and serum C-peptide II concentrations. Male and female mutants are affected in a similar manner, probably due to missing antidiabetic and antioxidative effects of estrogen in premature females.

5.3 Additional investigations of untreated male and female Munich *Ins2*[C95S] mutant and wild-type mice

In contrast to female heterozygous mutants, which demonstrated similar randomly fed body weights and only slightly elevated blood glucose concentrations compared to female wild-type mice, male heterozygous mutants developed reduced randomly fed body weights versus sex-matched wild-type mice and showed a progressive diabetic phenotype. These findings confirm the observations described in an earlier study (Herbach et al. 2007).

The mild diabetic phenotype of female heterozygous mutant mice is probably due to antioxidative and antidiabetic effects of female sexual hormones, especially estrogen. Several tissues of female rats demonstrated higher antioxidant capacity compared to those of male rats (Katalinic et al. 2005). It was shown that induction of oxidative stress via streptozotocin injection caused loss of β-cells and reduced pancreatic insulin content in male wild-type mice, and estradiol deficient ArKO^{-/-} mice of both genders, but not in female wild-type mice. Treatment with estradiol at physiological doses prevented β-cell loss in male wild-type and estradiol deficient ArKO^{-/-} mice (Le May et al. 2006). Further, in the Akita mouse, heterozygous male mutants exhibit a more severe diabetic phenotype than heterozygous female mutants (Yoshioka et al. 1997), and this phenomenon was also described in other mouse models (Louet et al. 2004). The findings of the different studies confirm the assumption that antioxidative and antidiabetic effects of estrogen are the main reasons for the mild form of diabetes in female Munich *Ins2*[C95S] mutant mice.

Intraperitoneal insulin tolerance tests at different ages showed that only male heterozygous mutants develop insulin resistance, thereby confirming the results of the homeostasis model assessment of insulin resistance index (HOMA IR (%)) (Herbach et al. 2007). The HOMA indices were developed to assess β-cell function in human beings (Wallace et al. 2004; Lee et al. 2008). However, a linear correlation between insulin sensitivity, determined during hyperinsulinaemic euglycaemic clamp studies in insulin resistant mice, and the surrogate index HOMA IR was proven (Lee et al. 2008) and is also confirmed in this study. As described above (5.1.1), heterozygous male mutants developed insulin resistance due to chronically elevated blood glucose concentrations. The preserved insulin sensitivity of female mutant mice might be due to the mild hyperglycaemia compared to male mutants, and probably due to antioxidative effects of estrogen. It was demonstrated that estrogen exerts antioxidative effects *in vivo* by upregulating the expression of mitochondrial superoxide dismutase and glutathione peroxidase via binding to the estrogen receptor and activation of the MAPK pathway (Viña et al. 2005). Oxidative stress leads to insulin resistance, for example in myocytes and adipocytes, probably via phosphorylation of IRS on threonine or serine residues (Maddux et al. 2001; Evans et al. 2002; Houstis et al. 2006). Therefore, estrogen might contribute to the preserved insulin sensitivity in female mutants via its antioxidative effects. Estradiol treatment of ovariectomised STZ-induced diabetic rats, for example, improved insulin sensitivity compared to non-treated ovariectomised diabetic rats (Ordónez et al. 2007). The preserved insulin sensitivity in female Munich $Ins2^{C95S}$ mutant mice contributes to the mild and stable diabetic phenotype, compared to male mutants.

Serum glucagon concentrations were determined randomly fed and after insulin injection at the age of 200 days, as well as fasted and after glucose challenge at the age of 230 days.

Male heterozygous mutants demonstrated elevated randomly fed serum glucagon levels compared to sex-matched wild-type mice, whereas randomly fed glucagon levels of female heterozygous mutant and female wild-type mice were similar. Under physiological conditions, high blood glucose levels suppress glucagon secretion from α-cells (Quoix et al. 2009). However, α-cells

of both, type 1 and type 2 diabetics have a defective glucose sensing, leading to increased glucagon secretion despite elevated blood glucose levels (Dunning et al. 2005; Jacobson et al. 2009). The mechanisms contributing to the α-cell pathology are still largely unknown (Quesada et al. 2008). A disturbed glucose sensing in α-cells of male mutants explains the elevated glucagon levels compared to sex-matched wild-type mice, despite drastically increased blood glucose levels. Female mutants exhibited a mild diabetic phenotype which can explain unaltered α-cell sensing and glucagon secretion. The same is true for insulin-treated male heterozygous mutant mice (see 5.1.1).

Ten minutes after insulin injection, serum glucagon levels of male mutants decreased, whereas those of wild-type mice and female mutants increased. In wild-type mice and female mutants, which demonstrated unchanged insulin sensitivity, insulin injection resulted in decreasing blood glucose levels, in contrast to insulin resistant male mutants. Decreasing blood glucose concentrations physiologically stimulate glucagon secretion in α-cells (Dunning and Gerich 2007), whereas in type 1 diabetics and patients with advanced type 2 diabetes, this counter-regulation of α-cells is impaired (Cryer and Cryer 2002). Therefore, decreasing blood glucose levels of wild-type mice and mild diabetic female mutants resulted in increasing glucagon secretion, whereas glucagon concentrations of male mutants didn't increase.

Fasted glucagon concentrations in mutant mice of both genders were similar to those of sex-matched wild-type mice. Diabetic patients regularly demonstrate elevated randomly fed serum glucagon levels and increased glucagon secretion after glucose challenge compared to healthy subjects (Dunning and Gerich 2007; Quesada et al. 2008). However, fasted glucagon concentrations may be similar or elevated versus non-diabetics (Gastaldelli et al. 2000; Bock et al. 2006; Abdul-Ghani and DeFronzo 2007). In the study of Abdul-Ghani and DeFronzo (2007), for example, the suppression of glucagon secretion in the oral glucose tolerance test was severely reduced in diabetics compared to non-diabetics, whereas the fasting glucagon levels were not significantly different.

Ten minutes after glucose challenge, glucagon concentrations of wild-type mice decreased, whereas those of male and female mutant mice increased.

The decreasing glucagon secretion in wild-type mice is in coincidence with the inhibition of glucagon secretion by increasing blood glucose levels (Dunning et al. 2005; Quoix et al. 2009). Type 2 diabetics with severe hyperglycaemia also demonstrated a paradoxical stimulation of glucagon secretion in the OGTT (Ohneda et al. 1978; Dunning et al. 2005), which explains the increased glucagon secretion in male Munich $Ins2^{C95S}$ mutants.

It was demonstrated that glucagon secretion is not only regulated by glucose, but also by paracrine factors like insulin. Physiologically increased blood glucose concentrations directly inhibit glucagon secretion of α-cells (Quoix et al. 2009), and stimulate insulin secretion (Andrali et al. 2008). Products of insulin secretion, like insulin and zinc, also inhibit glucagon secretion from α-cells in a paracrine manner (Dunning and Gerich 2007; Gromada et al. 2007; Quesada et al. 2008). Treatment of isolated islets and isolated α-cells with insulin or zinc, reduced glucagon secretion independent of glucose (Franklin et al. 2005). Therefore, the defective glucose-stimulated insulin secretion 10 minutes after glucose challenge in female and male mutants (Herbach et al. 2007), might contribute to the missing inhibition of glucagon secretion in mutant mice despite increasing blood glucose levels. This could explain the increasing glucagon secretion after glucose challenge in female mutants, despite unchanged randomly fed glucagon concentrations.

In conclusion, wild-type mice of both genders demonstrated physiological glucose sensing and glucagon secretion of α-cells, whereas severe hyperglycaemia in male mutants resulted in defective glucose sensing of α-cells, leading to randomly fed hyperglucagonaemia and increasing glucagon secretion after glucose challenge. Although female mutants featured unchanged randomly fed glucagon concentrations, glucagon secretion increased after glucose application, probably due to disturbed insulin secretion.

5.4 Summary

The present study demonstrated that hyperglycaemia-induced oxidative stress and ER stress are main reasons for the reduced total β-cell volume in male Munich $Ins2^{C95S}$ mutant mice. Furthermore, glycaemic control via insulin

treatment preserved insulin sensitivity and partially prevented β-cell loss. Therefore insulin resistance is most likely a mere consequence of hyperglycaemia, whereas β-cell loss is caused by both hyperglycaemia and ER stress in Munich $Ins2^{C95S}$ mutant mice.

Both, development of insulin resistance and β-cell loss are involved in the development of type 2 diabetes in humans, and contribute to the progressive diabetic phenotype in Munich $Ins2^{C95S}$ mutant mice.

Recently *INS* mutations in humans were described to cause permanent neonatal diabetes mellitus. Therefore, Munich $Ins2^{C95S}$ mutant mice provide an essential tool to further investigate the involvement of *INS* mutations in the development of diabetes mellitus, and to establish new treatment protocols.

6 Perspective

The involvement of oxidative stress in the loss of functional β-cell mass and in the development of insulin resistance in heterozygous male Munich $Ins2^{C95S}$ mutant mice may be further analysed, via treatment of heterozygous male mutants with antioxidants, like N-acetyl cysteine, lipoic acid and/or vitamins E and C.

In order to get more insights into the role of ER stress in the pathogenesis of diabetes mellitus and in the reduced total β-cell volume in male Munich $Ins2^{C95S}$ mutant mice, treatment of male heterozygous mutants with chemical chaperones, like 4-phenyl butyric acid or tauroursodeoxycholic acid, which increase ER folding capacity, would be useful.

In contrast to male Munich $Ins2^{C95S}$ mutant mice, female heterozygous mutants show a mild diabetic phenotype and preserved β-cell mass (Herbach et al. 2007). Therefore, investigations with ovariectomised mutants would be a helpful approach to investigate the antidiabetic and antioxidative effects of female sexual hormones, especially estrogen.

7 Summary

Mechanisms of β-cell loss in male Munich *Ins2*[C95S] mutant mice

Loss of functional β-cell mass is one major factor contributing to the development of diabetes mellitus in humans. Recently, mutations in the insulin gene were described in patients exhibiting early onset diabetes with severe hyperglycaemia. Munich *Ins2*[C95S] mutant mice exhibit a point mutation in the insulin 2 gene, leading to diabetes mellitus and a profound loss of β-cells in male mutants. Aim of the present study was to investigate the mechanisms resulting in the reduced total β-cell volume of heterozygous male Munich *Ins2*[C95S] mutant mice. In order to analyse the involvement of chronic hyperglycaemia and oxidative stress in the pathogenesis of β-cell loss, blood glucose concentrations of one group of male mutants were normalised via subcutaneous insulin-pellets. Placebo-treated mutants and wild-type mice served as controls. Several clinical parameters were examined, including randomly fed blood glucose concentration, oral glucose tolerance, insulin sensitivity, as well as serum and pancreatic C-peptide levels. Furthermore, oxidative stress was analysed in the serum, and ER stress markers were investigated in isolated pancreatic islets. Qualitative-histological and quantitative-stereological analyses of the pancreas were performed, and β-cell apoptosis as well as β-cell replication were determined. Additionally, secretion of mutant insulin 2 was investigated in untreated homozygous and heterozygous mutants of both genders, and compared to sex-matched wild-type mice.

Insulin treatment generally normalised blood glucose concentrations of mutant mice, whereas placebo-treated mutants exhibited a progressive and severe diabetic phenotype. Insulin-treated mutant mice demonstrated improved oral glucose tolerance, preserved insulin sensitivity and increased pancreatic C-peptide content compared to placebo-treated mutant mice, whereas insulin treatment did not ameliorate the disturbed glucose-stimulated insulin secretion in mutant mice. Normalising blood glucose concentrations of insulin-treated mutants inhibited oxidative stress, and resulted in higher total islet and β-cell volume as well as higher volume density of β-cells in the endocrine compartment of the islets as compared to placebo-treated mutants.

Furthermore, the total volume of isolated β-cells, which indicate islet neogenesis, was increased in insulin-treated mutants compared to placebo-treated mutant mice. However, insulin-treated mutants demonstrated a lower volume density of β-cells in the endocrine compartment of the islets, as well as lower total islet, β-cell, and isolated β-cell volumes than wild-type mice, showing that insulin treatment reduced, but did not completely prevent β-cell loss in mutant mice. Ultrastructural changes in the β-cells of mutant mice were less distinct in insulin-treated mutants than in placebo-treated mutants. In both, insulin- and placebo-treated mutant mice, the abundance of the ER stress marker CHOP was increased compared to wild-type mice. Furthermore, electron dense material accumulated in the dilated endoplasmic reticulum of mutant mice, suggesting ER stress.

In conclusion, insulin treatment prevented hyperglycaemia-induced loss of functional β-cell mass in male Munich $Ins2^{C95S}$ mutant mice, but did not completely preserve total β-cell volume, suggesting that β-cell loss is in part caused by ER stress.

8 Zusammenfassung

Mechanismen des β-Zell-Verlustes bei männlichen Munich *Ins2*^{C95S} Mausmutanten

Der Verlust funktioneller β-Zell-Masse ist einer der Hauptfaktoren, die zur Entstehung von Diabetes mellitus beim Menschen beitragen. Vor kurzem wurden Mutationen im Insulin-Gen von Patienten beschrieben, die einen früh einsetzenden Diabetes mellitus mit starker Hyperglykämie zeigten. Munich *Ins2*^{C95S} Mausmutanten weisen eine Punktmutation im Insulin 2 Gen auf, die zu Diabetes mellitus und bei männlichen Mutanten zu schwerwiegendem Verlust von β-Zellen führt. Ziel dieser Studie war es, die Mechanismen zu untersuchen, die zum verminderten Gesamt-β-Zell-Volumen von heterozygoten männlichen Munich *Ins2*^{C95S} Mausmutanten führen. Um die Beteiligung von chronischer Hyperglykämie und oxidativem Stress an der Pathogenese des β-Zell-Verlustes zu analysieren, wurde bei einem Teil der männlichen Mutanten der Blutzuckerspiegel mittels subkutaner Insulin-Pellets normalisiert. Placebo-behandelte Mausmutanten und Wild-Typ-Mäuse dienten als Kontrolle.

Verschiedene klinische Parameter wurden untersucht, einschließlich der freigefütterten Blutglukosekonzentration, der oralen Glukosetoleranz, der Insulinsensitivität, sowie der C-Peptidkonzentrationen im Serum und im Pankreas. Des Weiteren wurden das Serum bezüglich oxidativem Stress untersucht und ER-Stress Marker in isolierten pankreatischen Inseln analysiert. Qualitativ-histologische und quantitativ-stereologische Untersuchungen der Bauchspeicheldrüse wurden durchgeführt und β-Zell-Apoptose sowie β-Zell-Replikation bestimmt. Zusätzlich wurde die Sekretion des mutierten Insulin 2 an unbehandelten homozygoten und heterozygoten Mutanten beiderlei Geschlechtes untersucht und mit gleichgeschlechtlichen Wild-Typ-Mäusen verglichen.

Die Insulinbehandlung hat die Blutglukosekonzentrationen von Mausmutanten im Allgemeinen normalisiert, wohingegen Placebo-behandelte Mutanten einen progressiven und scherwiegenden diabetischen Phänotyp aufwiesen. Insulin-behandelte Mausmutanten zeigten eine verbesserte orale Glukosetoleranz, eine erhaltene Insulinsensitivität und einen höheren C-Peptidgehalt im

Pankreas als Placebo-behandelte Mausmutanten, wohingegen die Insulinbehandlung die Glukose-stimulierte Insulinsekretion in Munich $Ins2^{C95S}$ Mausmutanten nicht verbessert hat. Die Normalisierung der Blutglukosekonzentrationen von Insulin-behandelten Mausmutanten verhinderte die Entstehung von oxidativem Stress und führte zu einem höheren Gesamt-Insel- und Gesamt-β-Zell-Volumen sowie zu einer höheren Volumendichte von β-Zellen im endokrinen Teil der Inseln verglichen mit Placebo-behandelten Mausmutanten. Darüber hinaus war das Gesamtvolumen an isolierten β-Zellen, welche auf Inselneogenese hinweisen, in Insulin-behandelten Mutanten höher im Vergleich zu Placebo-behandelten Mausmutanten. Allerdings wiesen Insulin-behandelte Mutanten eine geringere Volumendichte an β-Zellen im endokrinen Teil der Inseln sowie geringere Gesamtvolumina an Inseln, β-Zellen und isolierten β-Zellen als Wild-Typ-Mäuse auf. Dies zeigt, dass die Insulinbehandlung den β-Zell-Verlust in Mausmutanten reduzierte, aber nicht vollständig verhinderte. Ultrastrukturelle Veränderungen in den β-Zellen von Mausmutanten waren in Insulin-behandelten Mutanten weniger deutlich ausgeprägt als in Placebo-behandelten Mutanten. Sowohl in Insulin- als auch in Placebo-behandelten Mausmutanten war die Abundanz des ER-Stress Markers CHOP im Vergleich zu Wild-Typ-Mäusen erhöht. Des Weiteren akkumulierte elektronendichtes Material im dilatierten Endoplasmatischen Retikulum von Mausmutanten, was auf ER-Stress hindeutet.

Schlussfolgerung: Die Insulinbehandlung verhinderte den Hyperglykämie-induzierten Verlust der funktionellen β-Zell-Masse in männlichen Munich $Ins2^{C95S}$ Mausmutanten, konnte aber den β-Zell-Verlust nicht vollständig aufhalten. Dies deutet darauf hin, dass der β-Zell-Verlust zum Teil durch ER-Stress verursacht wurde.

9 References

Abdul-Ghani, M. and DeFronzo, R. A. (2007). "Fasting hyperglycemia impairs glucose- but not insulin-mediated suppression of glucagon secretion". *J Clin Endocrinol Metab* 92 (5): 1778-1784.

American Diabetes Association (ADA) (2006). "Diagnosis and classification of diabetes mellitus". *Diabetes Care* 29 (suppl 1): s43-s48.

Aguilar-Bryan, L. and Bryan, J. (2008). "Neonatal diabetes mellitus". *Endocr Rev* 29 (3): 265-291.

Aguirre, V., Uchida, T., Yenush, L., Davis, R. and White, M. (2000). "The c-Jun NH_2-terminal kinase promotes insulin resistance during association with insulin receptor substrate-1 and phosphorylation of Ser307". *J Biol Chem* 275 (12): 9047-9054.

Ahlgren, U., Jonsson, J., Jonsson, L., Simu, K. and Edlund, H. (1998). "β-cell-specific inactivation of the mouse *Ipf1/Pdx1* gene results in loss of the β-cell phenotype and maturity onset diabetes". *Genes Dev* 12 (12): 1763-1768.

Ahmed, N. (2005). "Advanced glycation endproducts - role in pathology of diabetic complications". *Diabetes Res Clin Pract* 67 (1): 3-21.

Ahren, B. (2005). "Type 2 diabetes, insulin secretion and β-cell mass." *Curr Mol Med* 5 (3): 275-286.

Aigner, B., Rathkolb, B., Herbach, N., de Angelis, M. H., Wanke, R. and Wolf, E. (2008). "Diabetes models by screen for hyperglycemia in phenotype-driven ENU mouse mutagenesis projects". *Am J Physiol Endocrinol Metab* 294 (2): E232-240.

Allen, J. R., Nguyen, L. X., Sargent, K. E. G., Lipson, K. L., Hackett, A. and Urano, F. (2004). "High ER stress in β-cells stimulates intracellular degradation of misfolded insulin". *Biochem Biophys Res Commun* 324 (1): 166-170.

Al-Mutairi, H. F., Mohsen, A. M. and Al-Mazidi, Z. M. (2007). "Genetics of type 1 diabetes mellitus". *Kuwait Med J* 39 (2): 107-115.

Ametov, A. S., Barinov, A., Dyck, P. J., Hermann, R., Kozlova, N., Litchy, W. J., Low, P. A., Nehrdich, D., Novosadova, M., O'Brien, P. C., Reljanovic, M., Samigullin, R., Schütte, K., Strokov, I., Tritschler, H. J., Wessel, K., Yakhno, N. and Ziegler, D. (2003). "The sensory symptoms of diabetic polyneuropathy are improved with α-lipoic acid". *Diabetes Care* 26 (3): 770-776.

Ammon, H., Reiber, C. and Verspohl, E. (1991). "Indirect evidence for short-loop negative feedback of insulin secretion in the rat". *J Endocrinol* 128 (1): 27-34.

Andrali, S. S., Sampley, M. L., Vanderford, N. L. and Özcan, S. (2008). "Glucose regulation of insulin gene expression in pancreatic β-cells." *Biochem J* 415 (1): 1-10.

Argoud, G., Schade, D. and Eaton, R. (1987). "Insulin suppresses its own secretion in vivo". *Diabetes* 36 (8): 959-962.

Arolas, J. L., Aviles, F. X., Chang, J.-Y. and Ventura, S. (2006). "Folding of small disulfide-rich proteins: clarifying the puzzle". *Trends Biochem Sci* 31 (5): 292-301.

Aspinwall, C., Lakey, J. and Kennedy, R. (1999). "Insulin-stimulated insulin secretion in single pancreatic beta cells". *J Biol Chem* 274 (10): 6360-6365.

Augustin, M., Sedlmeier, R., Peters, T., Huffstadt, U., Kochmann, E., Simon, D., Schöniger, M., Garke-Mayerthaler, S., Laufs, J. and Mayhaus, M. (2005). "Efficient and fast targeted production of murine models based on ENU mutagenesis". *Mamm Genome* 16 (6): 405-413.

Baldwin, A. (2001). "Series introduction: the transcription factor NF-κB and human disease". *J Clin Invest* 107 (1): 3-6.

Beckman, J. A., Goldfine, A. B., Gordon, M. B., Garrett, L. A., Keaney, J. F., Jr. and Creager, M. A. (2003). "Oral antioxidant therapy improves endothelial function in type 1 but not type 2 diabetes mellitus". *Am J Physiol Heart Circ Physiol* 285 (6): H2392-2398.

Begum, N. and Ragolia, L. (2000). "High glucose and insulin inhibit VSMC MKP-1 expression by blocking iNOS via p38 MAPK activation". *Am J Physiol Cell Physiol* 278 (1): C81-91.

Beith, J. L., Alejandro, E. U. and Johnson, J. D. (2008). "Insulin stimulates primary β-cell proliferation via Raf-1 kinase". *Endocrinology* 149 (5): 2251-2260.

Belle, M. A. (2004). "Zuchtdaten zu Körpergewicht, Fruchtbarkeit und Aufzuchtleistung der Schleißheimer Mäusestämme zwischen 1990 und 2001". Ludwig-Maximilians-Universität München.

Bendayan, M., Londono, I., Gingras, D., Ruderman, N. and Prentki, M. (2007). "Association of AMP kinase β_2 subunit with glycogen particles as revealed by immunoelectron microscopy". *FASEB J* 21 (6): lb322.

Bendayan, M., Malide, D., Ziv, E., Levy, E., Ben-Sasson, R., Kalman, R., Bar-On, H., Chretien, M. and Seidah, N. (1995). "Immunocytochemical investigation of insulin secretion by pancreatic beta-cells in control and diabetic Psammomys obesus". *J Histochem Cytochem* 43 (8): 771-784.

Berg, J., Tymoczko, J. and Stryer, L. (2003). "Biochemie". Spektrum Akademischer Verlag, Heidelberg, Berlin.

Berndt, C., Lillig, C. H. and Holmgren, A. (2008). "Thioredoxins and glutaredoxins as facilitators of protein folding". *Biochim Biophys Acta* 1783 (4): 641-650.

Bertolotti, A., Zhang, Y., Hendershot, L. M., Harding, H. P. and Ron, D. (2000). "Dynamic interaction of BiP and ER stress transducers in the unfolded-protein response". *Nat Cell Biol* 2 (6): 326-332.

Betteridge, D. J. (2000). "What is oxidative stress?" *Metabolism* 49 (2, suppl 1): 3-8.

Biddinger, S. B. and Kahn, C. R. (2006). "From mice to men: Insights into the insulin resistance syndromes". *Annu Rev Physiol* 68 (1): 123-158.

Bierhaus, A., Schiekofer, S., Schwaninger, M., Andrassy, M., Humpert, P. M., Chen, J., Hong, M., Luther, T., Henle, T., Klöting, I., Morcos, M., Hofmann, M., Tritschler, H., Weigle, B., Kasper, M., Smith, M., Perry, G., Schmidt, A.-M., Stern, D. M., Häring, H.-U., Schleicher, E. and Nawroth, P. P. (2001). "Diabetes-associated sustained activation of the transcription factor nuclear factor-κB". *Diabetes* 50 (12): 2792-2808.

Björklund, A., Lansner, A. and Grill, V. (2000). "Glucose-induced $[Ca^{2+}]_i$ abnormalities in human pancreatic islets: important role of overstimulation". *Diabetes* 49 (11): 1840-1848.

Blüher, M., Michael, M., Peroni, O., Ueki, K., Carter, N., Kahn, B. and Kahn, C. (2002). "Adipose tissue selective insulin receptor knockout protects against obesity and obesity-related glucose intolerance". *Dev Cell* 3 (1): 25-38.

Bock, G., Dalla Man, C., Campioni, M., Chittilapilly, E., Basu, R., Toffolo, G., Cobelli, C. and Rizza, R. (2006). "Pathogenesis of pre-diabetes". *Diabetes* 55 (12): 3536-3549.

Bogoyevitch, M. A. and Kobe, B. (2006). "Uses for JNK: the many and varied substrates of the c-Jun N-terminal kinases". *Microbiol Mol Biol Rev* 70 (4): 1061-1095.

Bonnard, C., Durand, A., Peyrol, S., Chanseaume, E., Chauvin, M., Morio, B., Vidal, H. and Rieusset, J. (2008). "Mitochondrial dysfunction results from oxidative stress in the skeletal muscle of diet-induced insulin-resistant mice". *J Clin Invest* 118 (2): 789-800.

Bonner-Weir, S. (1991). "Anatomy of the islet of Langerhans". Lippincott Williams & Wilkins.

Bonner-Weir, S., Inada, A., Yatoh, S., Li, W., Aye, T., Toschi, E. and Sharma, A. (2008). "Transdifferentiation of pancreatic ductal cells to endocrine β-cells". *Biochem Soc Trans* 36 353-356.

Borelli, M., Francini, F. and Gagliardino, J. (2004). "Autocrine regulation of glucose metabolism in pancreatic islets". *Am J Physiol Endocrinol Metab* 286 (1): 111-115.

Bouwens, L. and Rooman, I. (2005). "Regulation of pancreatic beta-cell mass". *Physiol Rev* 85 (4): 1255-1270.

Brissova, M., Fowler, M. J., Nicholson, W. E., Chu, A., Hirshberg, B., Harlan, D. M. and Powers, A. C. (2005). "Assessment of human pancreatic islet architecture and composition by laser scanning confocal microscopy". *J Histochem Cytochem* 53 (9): 1087-1097.

Brownlee, M. (2005). "The pathobiology of diabetic complications". *Diabetes* 54 (6): 1615-1625.

Brüning, J. C., Gautam, D., Burks, D. J., Gillette, J., Schubert, M., Orban, P. C., Klein, R., Krone, W., Müller-Wieland, D. and Kahn, C. R. (2000). "Role of brain insulin receptor in control of body weight and reproduction". *Science* 289 (5487): 2122-2125.

Butler, A. E., Janson, J., Bonner-Weir, S., Ritzel, R., Rizza, R. A. and Butler, P. C. (2003). "β-cell deficit and increased β-cell apoptosis in humans with type 2 diabetes". *Diabetes* 52 (1): 102-110.

Caballero, F., Gerez, E., Batlle, A. and Vazquez, E. (2000). "Preventive aspirin treatment of streptozotocin induced diabetes: blockage of oxidative status and revertion of heme enzymes inhibition". *Chem Biol Interact* 126 (3): 215-225.

Cabrera, O., Berman, D. M., Kenyon, N. S., Ricordi, C., Berggren, P.-O. and Caicedo, A. (2006). "The unique cytoarchitecture of human pancreatic islets has implications for islet cell function". *PNAS* 103 (7): 2334-2339.

Cai, H. and Harrison, D. G. (2000). "Endothelial dysfunction in cardiovascular diseases: The role of oxidant stress". *Circ Res* 87 (10): 840-844.

Calfon, M., Zeng, H., Urano, F., Till, J. H., Hubbard, S. R., Harding, H. P., Clark, S. G. and Ron, D. (2002). "IRE1 couples endoplasmic reticulum load to secretory capacity by processing the *XBP-1* mRNA". *Nature* 415 (6867): 92-96.

Cardozo, A., Ortis, F., Storling, J., Feng, Y., Rasschaert, J., Tonnesen, M., Van Eylen, F., Mandrup-Poulsen, T., Herchuelz, A. and Eizirik, D. (2005). "Cytokines downregulate the sarcoendoplasmic reticulum pump Ca^{2+} ATPase 2b and deplete endoplasmic reticulum Ca^{2+}, leading to induction of endoplasmic reticulum stress in pancreatic β -cells". *Diabetes* 54 (2): 452-461.

Caumo, A. and Luzi, L. (2004). "First-phase insulin secretion: does it exist in real life? Considerations on shape and function". *Am J Physiol Endocrinol Metab* 287 (3): E371-385.

Chan, K., Han, X.-D. and Kan, Y. W. (2001). "An important function of Nrf2 in combating oxidative stress: Detoxification of acetaminophen". *PNAS* 98 (8): 4611-4616.

Chan, K. and Kan, Y. (1999). "Nrf2 is essential for protection against acute pulmonary injury in mice". *PNAS* 96 (22): 12731-12736.

Chan, S., Seino, S., Gruppuso, P., Schwartz, R. and Steiner, D. (1987). "A mutation in the B chain coding region is associated with impaired proinsulin conversion in a family with hyperproinsulinemia". *PNAS* 84 (8): 2194-2197.

Chang, S., Choi, K., Jang, S. and Shin, H. (2003). "Role of disulfide bonds in the structure and activity of human insulin". *Mol Cells* 16 (3): 323-330.

Chanwitheesuk, A., Teerawutgulrag, A. and Rakariyatham, N. (2005). "Screening of antioxidant activity and antioxidant compounds of some edible plants of Thailand". *Food Chem* 92 (3): 491-497.

Chong, Z. Z., Li, F. and Maiese, K. (2005). "Oxidative stress in the brain: Novel cellular targets that govern survival during neurodegenerative disease". *Prog Neurobiol* 75 (3): 207-246.

Chung, S. S. M., Ho, E. C. M., Lam, K. S. L. and Chung, S. K. (2003). "Contribution of polyol pathway to diabetes-induced oxidative stress". *J Am Soc Nephrol* 14 (Suppl): S233-236.

Clark, A., Jones, L., de Koning, E., Hansen, B. and Matthews, D. (2001). "Decreased insulin secretion in type 2 diabetes: a problem of cellular mass or function?" *Diabetes* 50 (Suppl 1): 169-171.

Clee, S. and Attie, A. (2007). "The genetic landscape of type 2 diabetes in mice". *Endocr Rev* 28 (1): 48-83.

Cnop, M., Igoillo-Esteve, M., Cunha, D. A., Ladrière, L. and Eizirik, D. L. (2008). "An update on lipotoxic endoplasmic reticulum stress in pancreatic β-cells". *Biochem Soc Trans* 36 (5): 909-915.

Cnop, M., Welsh, N., Jonas, J.-C., Jörns, A., Lenzen, S. and Eizirik, D. L. (2005). "Mechanisms of pancreatic β-cell death in type 1 and type 2 diabetes". *Diabetes* 54 (suppl 2): S97-S107.

Collinet, M., Berthelon, M., Bénit, P., Laborde, K., Desbuquois, B., Munnich, A. and Robert, J. (1998). "Familial hyperproinsulinaemia due to a mutation substituting histidine for arginine at position 65 in proinsulin: identification of the mutation by restriction enzyme mapping". *Eur J Pediatr* 157 (6): 456-460.

Colombo, C., Porzio, O., Liu, M., Massa, O., Vasta, M., Salardi, S., Beccaria, L., Monciotti, C., Toni, S., Pedersen, O., Hansen, T., Federici, L., Pesavento, R., Cadario, F., Federici, G., Ghirri, P., Arvan, P., Iafusco, D. and Barbetti, F. (2008). "Seven mutations in the human insulin gene linked to permanent neonatal/infancy-onset diabetes mellitus". *J Clin Invest* 118 (6): 2148-2156.

Concepcion, D., Seburn, K., Wen, G., Frankel, W. and Hamilton, B. (2004). "Mutation rate and predicted phenotypic target sizes in ethylnitrosourea-treated mice". *Genetics* 168 (2): 953-959.

Coppey, L. J., Gellett, J. S., Davidson, E. P., Dunlap, J. A. and Yorek, M. A. (2002). "Changes in endoneurial blood flow, motor nerve conduction velocity and vascular relaxation of epineurial arterioles of the sciatic nerve in ZDF-obese diabetic rats". *Diabetes Metab Rev* 18 (1): 49-56.

Corona, G., Mannucci, E., Petrone, L., Ricca, V., Balercia, G., Mansani, R., Chiarini, V., Giommi, R., Forti, G. and Maggi, M. (2005). "Association of hypogonadism and type II diabetes in men attending an outpatient erectile dysfunction clinic". *Int J Impot Res* 18 (2): 190-197.

Costa, A., Bescos, M., Velho, G., Chevre, J., Vidal, J., Sesmilo, G., Bellanne-Chantelot, C., Froguel, P., Casamitjana, R., Rivera-Fillat, F., Gomis, R. and Conget, I. (2000). "Genetic and clinical characterisation of maturity-onset diabetes of the young in Spanish families". *Eur J Endocrinol* 142 (4): 380-386.

Cryer and Cryer, P. (2002). "Hypoglycaemia: The limiting factor in the glycaemic management of type I and type II diabetes*". *Diabetologia* 45 (7): 937-948.

Cullinan, S. B., Zhang, D., Hannink, M., Arvisais, E., Kaufman, R. J. and Diehl, J. A. (2003). "Nrf2 is a direct PERK substrate and effector of PERK-dependent cell survival". *Mol Cell Biol* 23 (20): 7198-7209.

Dai, Y. and Tang, J. (1996). "Characteristic, activity and conformational studies of [A6-Ser, A11-Ser]-insulin". *Biochim Biophys Acta* 1296 (1): 63-68.

Degterev, A., Boyce, M. and Yuan, J. (2003). "A decade of caspases". *Oncogene* 22 (53): 8543-8567.

Desco, M.-C., Asensi, M., Márquez, R., Martínez-Valls, J., Vento, M., Pallardó, F. V., Sastre, J. and Viña, J. (2002). "Xanthine oxidase is involved in free radical production in type 1 diabetes". *Diabetes* 51 (4): 1118-1124.

Devaraj, S., Glaser, N., Griffen, S., Wang-Polagruto, J., Miguelino, E. and Jialal, I. (2006). "Increased monocytic activity and biomarkers of inflammation in patients with type 1 diabetes". *Diabetes* 55 (3): 774-779.

Di Mario, U. and Pugliese, G. (2001). "15th Golgi lecture: from hyperglycaemia to the dysregulation of vascular remodelling in diabetes". *Diabetologia* 44 (6): 674-692.

Donath, M. and Halban, P. (2004). "Decreased beta-cell mass in diabetes: significance, mechanisms and therapeutic implications". *Diabetologia* 47 (3): 581-589.

Du, X., Edelstein, D., Rossetti, L., Fantus, I., Goldberg, H., Ziyadeh, F., Wu, J. and Brownlee, M. (2000). "Hyperglycemia-induced mitochondrial superoxide overproduction activates the hexosamine pathway and induces plasminogen activator inhibitor-1 expression by increasing Sp1 glycosylation". *PNAS* 97 (22): 12222-12226.

Dunlop, M. E. and Muggli, E. E. (2000). "Small heat shock protein alteration provides a mechanism to reduce mesangial cell contractility in diabetes and oxidative stress". *Kidney Int* 57 (2): 464-475.

Dunning, B., Foley, J. and Ahrén, B. (2005). "Alpha cell function in health and disease: influence of glucagon-like peptide-1". *Diabetologia* 48 (9): 1700-1713.

Dunning, B. E. and Gerich, J. E. (2007). "The role of α-cell dysregulation in fasting and postprandial hyperglycemia in type 2 diabetes and therapeutic implications". *Endocr Rev* 28 (3): 253-283.

Duvillie, B., Cordonnier, N., Deltour, L., Dandoy-Dron, F., Itier, J., Monthioux, E., Jami, J., Joshi, R. and Bucchini, D. (1997). "Phenotypic alterations in insulin-deficient mutant mice". *PNAS* 94 (10): 5137-5140.

Duvillie, B., Currie, C., Chrones, T., Bucchini, D., Jami, J., Joshi, R. L. and Hill, D. J. (2002). "Increased islet cell proliferation, decreased apoptosis, and greater vascularization leading to β-cell hyperplasia in mutant mice lacking insulin". *Endocrinology* 143 (4): 1530-1537.

Edghill, E., Flanagan, S., Patch, A., Boustred, C., Parrish, A., Shields, B., Shepherd, M., Hussain, K., Kapoor, R. and Malecki, M. (2008). "Insulin mutation screening in 1,044 patients with diabetes". *Diabetes* 57 (4): 1034-1042.

Ellgaard, L. and Helenius, A. (2001). "ER quality control: towards an understanding at the molecular level". *Curr Opin Cell Biol* 13 (4): 431-437.

Elmalí, E., Altan, N. and Bukan, N. (2004). "Effect of the sulphonylurea glibenclamide on liver and kidney antioxidant enzymes in streptozocin-induced diabetic rats". *Drugs R D* 5 (4): 203-208.

Elouil, H., Bensellam, M., Guiot, Y., Vander Mierde, D., Pascal, S., Schuit, F. and Jonas, J. (2007). "Acute nutrient regulation of the unfolded protein response and integrated stress response in cultured rat pancreatic islets". *Diabetologia* 50 (7): 1442-1452.

Elouil, H., Cardozo, A., Eizirik, D., Henquin, J. and Jonas, J. (2005). "High glucose and hydrogen peroxide increase c-Myc and haeme-oxygenase 1 mRNA levels in rat pancreatic islets without activating NFκB". *Diabetologia* 48 (3): 496-505.

Evans, J., Goldfine, I., Maddux, B. and Grodsky, G. (2002). "Oxidative stress and stress-activated signaling pathways: a unifying hypothesis of type 2 diabetes". *Endocr Rev* 23 (5): 599-622.

Evans, J. L. and Goldfine, I. D. (2000). "α-lipoic acid: A multifunctional antioxidant that improves insulin sensitivity in patients with type 2 diabetes". *Diabetes Technol Ther* 2 (3): 401-413.

Fan, J.-Y., Roth, J. and Zuber, C. (2003). "Ultrastructural analysis of transitional endoplasmic reticulum and pre-Golgi intermediates: a highway for cars and trucks". *Histochem Cell Biol* 120 (6): 455-463.

Federici, M., Hribal, M., Perego, L., Ranalli, M., Caradonna, Z., Perego, C., Usellini, L., Nano, R., Bonini, P., Bertuzzi, F., Marlier, L. N. J. L., Davalli, A. M., Carandente, O., Pontiroli, A. E., Melino, G., Marchetti, P., Lauro, R., Sesti, G. and Folli, F. (2001). "High glucose causes apoptosis in cultured human pancreatic islets of Langerhans". *Diabetes* 50 (6): 1290-1301.

Fiordaliso, F., Bianchi, R., Staszewsky, L., Cuccovillo, I., Doni, M., Laragione, T., Salio, M., Savino, C., Melucci, S., Santangelo, F., Scanziani, E., Masson, S., Ghezzi, P. and Latini, R. (2004). "Antioxidant treatment attenuates hyperglycemia-induced cardiomyocyte death in rats". *J Mol Cell Cardiol* 37 (5): 959-968.

Fonseca, S., Fukuma, M., Lipson, K., Nguyen, L., Allen, J., Oka, Y. and Urano, F. (2005). "WFS1 is a novel component of the unfolded protein response and maintains homeostasis of the endoplasmic reticulum in pancreatic β-cells". *J Biol Chem* 280 (47): 39609-39615.

Forbes, J., Fukami, K. and Cooper, M. (2007). "Diabetic nephropathy: Where hemodynamics meets metabolism". *Exp Clin Endocrinol Diabetes* 115 (2): 69-84.

Franklin, I., Gromada, J., Gjinovci, A., Theander, S. and Wollheim, C. B. (2005). "β-cell secretory products activate α-cell ATP-dependent potassium channels to inhibit glucagon release". *Diabetes* 54 (6): 1808-1815.

Fujita, E., Kouroku, Y., Isoai, A., Kumagai, H., Misutani, A., Matsuda, C., Hayashi, Y. K. and Momoi, T. (2007). "Two endoplasmic reticulum-associated degradation (ERAD) systems for the novel variant of the mutant dysferlin: ubiquitin/proteasome ERAD(I) and autophagy/lysosome ERAD(II)". *Hum Mol Genet* 16 (6): 618-629.

Fujita, S., Rasmussen, B. B., Cadenas, J. G., Grady, J. J. and Volpi, E. (2006). "Effect of insulin on human skeletal muscle protein synthesis is modulated by insulin-induced changes in muscle blood flow and amino acid availability". *Am J Physiol Endocrinol Metab* 291 (4): E745-754.

Gabius, H.-J. (Ed.) (2009). "The sugar code: Fundamentals of glycosciences". Wiley-Blackwell.

Gæde, P., Poulsen, H. E., Parving, H.-H. and Pedersen, O. (2001). "Double-blind, randomised study of the effect of combined treatment with vitamin C and E on albuminuria in type 2 diabetic patients". *Diabetic Med* 18 (9): 756-760.

Gastaldelli, A., Baldi, S., Pettiti, M., Toschi, E., Camastra, S., Natali, A., Landau, B. and Ferrannini, E. (2000). "Influence of obesity and type 2 diabetes on gluconeogenesis and glucose output in humans: a quantitative study". *Diabetes* 49 (8): 1367-1373.

Ghadially, F. (1988). "Ultrastructural pathology of the cell and matrix Vol. 1". Butterworths, London.

Greenbaum, C. J. (2002). "Insulin resistance in type 1 diabetes". *Diabetes Metab Rev* 18 (3): 192-200.

Grill, V. and Björklund, A. (2001). "Overstimulation and β-cell function". *Diabetes* 50 (suppl 1): S122-S124.

Gromada, J., Franklin, I. and Wollheim, C. B. (2007). "α-cells of the endocrine pancreas: 35 years of research but the enigma remains". *Endocr Rev* 28 (1): 84-116.

Gumieniczek, A., Hopkala, H., Rolinski, J. and Bojarska-Junak, A. (2005). "Antioxidative and anti-inflammatory effects of repaglinide in plasma of diabetic animals". *Pharmacol Res* 52 (2): 162-166.

Gundersen, H., Bendtsen, T., Korbo, L., Marcussen, N., Moller, A., Nielsen, K., Nyengaard, J., Pakkenberg, B., Sorensen, F. and Vesterby, A. (1988). "Some new, simple and efficient stereological methods and their use in pathological research and diagnosis". *APMIS* 96 (5): 379-394.

Hagenfeldt-Johansson, K. A., Herrera, P. L., Wang, H., Gjinovci, A., Ishihara, H. and Wollheim, C. B. (2001). "β-cell-targeted expression of a dominant-negative hepatocyte nuclear factor-1α induces a maturity-onset diabetes of the young (MODY)3-like phenotype in transgenic mice". *Endocrinology* 142 (12): 5311-5320.

Haneda, M., Chan, S. J., Kwok, S. C., Rubenstein, A. H. and Steiner, D. F. (1983). "Studies on mutant human insulin genes: identification and sequence analysis of a gene encoding [SerB24]insulin". *PNAS* 80 (20): 6366-6370.

Harding, H., Novoa, I., Zhang, Y., Zeng, H., Wek, R., Schapira, M. and Ron, D. (2000). "Regulated translation initiation controls stress-induced gene expression in mammalian cells". *Mol Cell* 6 (5): 1099-1108.

Harding, H. P., Zeng, H., Zhang, Y., Jungries, R., Chung, P., Plesken, H., Sabatini, D. D. and Ron, D. (2001). "Diabetes mellitus and exocrine pancreatic dysfunction in *Perk-/-* mice reveals a role for translational control in secretory cell survival". *Mol Cell* 7 (6): 1153-1163.

Harding, H. P., Zhang, Y. and Ron, D. (1999). "Protein translation and folding are coupled by an endoplasmic-reticulum-resident kinase". *Nature* 397 (6716): 271-274.

Harding, H. P., Zhang, Y., Zeng, H., Novoa, I., Lu, P. D., Calfon, M., Sadri, N., Yun, C., Popko, B., Paules, R., Stojdl, D. F., Bell, J. C., Hettmann, T., Leiden, J. M. and Ron, D. (2003). "An integrated stress response regulates amino acid metabolism and resistance to oxidative stress". *Mol Cell* 11 (3): 619-633.

Hattersley, A. (2005). "Molecular genetics goes to the diabetes clinic." *Clin Med* 5 (5): 476-481.

Hattersley, A. and Pearson, E. (2006). "Minireview: pharmacogenetics and beyond: the interaction of therapeutic response, β-cell physiology, and genetics in diabetes". *Endocrinology* 147 (6): 2657-2663.

HelmholtzCenter Munich, Institute of experimental genetics (2009). "The ENU screen". Retrieved 16.08. 2009 from http://www.helmholtz-muenchen.de/en/ieg/group-functional-genetics/enu-screen/index.html.

Heptulla, R. A., Stewart, A., Enocksson, S., Rife, F., Ma, T. Y.-Z., Sherwin, R. S., Tamborlane, W. V. and Caprio, S. (2003). "In situ evidence that peripheral insulin resistance in adolescents with poorly controlled type 1 diabetes is associated with impaired suppression of lipolysis: A microdialysis study". *Pediatr Res* 53 (5): 830-835.

Herbach, N., Goeke, B., Schneider, M., Hermanns, W., Wolf, E. and Wanke, R. (2005). "Overexpression of a dominant negative GIP receptor in transgenic mice results in disturbed postnatal pancreatic islet and beta-cell development". *Regul Pept* 125 (1-3): 103-117.

Herbach, N., Rathkolb, B., Kemter, E., Pichl, L., Klaften, M., de Angelis, M., Halban, P., Wolf, E., Aigner, B. and Wanke, R. (2007). "Dominant-negative effects of a novel mutated *Ins2* allele causes early-onset diabetes and severe β-cell loss in Munich *Ins2*[C95S] mutant mice". *Diabetes* 56 (5): 1268-1276.

Hodgson, J., Watts, G., Playford, D., Burke, V. and Croft, K. (2002). "Coenzyme Q10 improves blood pressure and glycaemic control: A controlled trial in subjects with type 2 diabetes." *Eur J Clin Nutr* 56 (11): 1137-1142.

Hoenig, M. (2002). "Comparative aspects of diabetes mellitus in dogs and cats". *Mol Cell Endocrinol* 197 (1-2): 221-229.

Holland, A. M., Hale, M. A., Kagami, H., Hammer, R. E. and MacDonald, R. J. (2002). "Experimental control of pancreatic development and maintenance". *PNAS* 99 (19): 12236-12241.

Hollander, P., Krasner, A., Klioze, S., Schwartz, P. and Duggan, W. (2007). "Body weight changes associated with insulin therapy". *Diabetes Care* 30 (10): 2508-2510.

Hollien, J. and Weissman, J. (2006). "Decay of endoplasmic reticulum-localized mRNAs during the unfolded protein response". *Science* 313 (5783): 104-107.

Hong, E.-G., Jung, D. Y., Ko, H. J., Zhang, Z., Ma, Z., Jun, J. Y., Kim, J. H., Sumner, A. D., Vary, T. C., Gardner, T. W., Bronson, S. K. and Kim, J. K. (2007). "Nonobese, insulin-deficient Ins2[Akita] mice develop type 2 diabetes phenotypes including insulin resistance and cardiac remodeling". *Am J Physiol Endocrinol Metab* 293 (6): E1687-1696.

Houstis, N., Rosen, E. D. and Lander, E. S. (2006). "Reactive oxygen species have a causal role in multiple forms of insulin resistance". *Nature* 440 (7086): 944-948.

Hu, P., Han, Z., Couvillon, A. D., Kaufman, R. J. and Exton, J. H. (2006). "Autocrine tumor necrosis factor alpha links endoplasmic reticulum stress to the membrane death receptor pathway through IRE1α-mediated NF-κB activation and down-regulation of TRAF2 expression". *Mol Cell Biol* 26 (8): 3071-3084.

Hua, Q.-x., Liu, M., Hu, S.-Q., Jia, W., Arvan, P. and Weiss, M. A. (2006). "A conserved histidine in insulin is required for the foldability of human proinsulin". *J Biol Chem* 281 (34): 24889-24899.

Huang, C.-j., Haataja, L., Gurlo, T., Butler, A. E., Wu, X., Soeller, W. C. and Butler, P. C. (2007). "Induction of endoplasmic reticulum stress-induced β-cell apoptosis and accumulation of polyubiquitinated proteins by human islet amyloid polypeptide". *Am J Physiol Endocrinol Metab* 293 (6): E1656-1662.

Huerta, S., Goulet, E., Huerta-Yepez, S. and Livingston, E. (2007). "Screening and detection of apoptosis". *J Surg Res* 139 (1): 143-156.

International Diabetes Federation (IDF) (2009a). "Diabetes Atlas - Amputation". Retrieved 16.08. 2009 from http://www.eatlas.idf.org/index552f.html.

International Diabetes Federation (IDF) (2009b). "Diabetes Atlas - Cardiovascular disease". Retrieved 16.08. 2009 from http://www.eatlas.idf.org/indexd602.html.

International Diabetes Federation (IDF) (2009c). "Diabetes Atlas - Diabetic complications". Retrieved 16.08. 2009 from http://www.eatlas.idf.org/index711b.html.

International Diabetes Federation (IDF) (2009d). "Diabetes Atlas - Economic impacts". Retrieved 16.08. 2009 from http://www.eatlas.idf.org/indexd894.html.

International Diabetes Federation (IDF) (2009e). "Diabetes Atlas - Major diabetic complications". Retrieved 16.08. 2009 from http://www.eatlas.idf.org/indexef09.html.

International Diabetes Federation (IDF) (2009f). "Diabetes Atlas - Nephropathy". Retrieved 16.08. 2009 from http://www.eatlas.idf.org/index691e.html.

International Diabetes Federation (IDF) (2009g). "Diabetes Atlas - Neuropathy". Retrieved 16.08. 2009 from http://www.eatlas.idf.org/index8788.html.

International Diabetes Federation (IDF) (2009h). "Diabetes Atlas - Prevalence and projections". Retrieved 16.08. 2009 from http://www.eatlas.idf.org/index2983.html.
International Diabetes Federation (IDF) (2009i). "Diabetes Atlas - Results". Retrieved 16.08. 2009 from http://www.eatlas.idf.org/index74cc.html.

International Diabetes Federation (IDF) (2009j). "Diabetes Atlas - Retinopathy". Retrieved 16.08. 2009 from http://www.eatlas.idf.org/index0923.html.

International Diabetes Federation (IDF) (2009k). "Diabetes Atlas - Type 1 diabetes incidence". Retrieved 16.08. 2009 from http://www.eatlas.idf.org/index5c31.html.

International Diabetes Federation (IDF) (2009l). "Diabetes Atlas - Type 2 diabetes". Retrieved 16.08. 2009 from http://www.eatlas.idf.org/index755a.html.

International Diabetes Federation (IDF) (2009m). "Diabetes Atlas - Type 2 diabetes in the young". Retrieved 16.08. 2009 from http://www.eatlas.idf.org/index2608.html.

International Diabetes Federation (IDF) (2009n). "Diabetes Atlas - What do medical expenditures for diabetes buy". Retrieved 16.08. 2009 from http://www.eatlas.idf.org/index5bc6.html.

International Diabetes Federation (IDF) (2009o). "Diabetes Prevalence". Retrieved 16.08. 2009 from http://www.idf.org/diabetes-prevalence.

Inada, A., Nienaber, C., Katsuta, H., Fujitani, Y., Levine, J., Morita, R., Sharma, A. and Bonner-Weir, S. (2008). "Carbonic anhydrase II-positive pancreatic cells are progenitors for both endocrine and exocrine pancreas after birth". *PNAS* 105 (50): 19915-19919.

Irving-Rodgers, H., Ziolkowski, A., Parish, C., Sado, Y., Ninomiya, Y., Simeonovic, C. and Rodgers, R. (2008). "Molecular composition of the peri-islet basement membrane in NOD mice: a barrier against destructive insulitis". *Diabetologia* 51 (9): 1680-1688.

Izumi, T., Yokota-Hashimoto, H., Zhao, S., Wang, J., Halban, P. A. and Takeuchi, T. (2003). "Dominant negative pathogenesis by mutant proinsulin in the Akita diabetic mouse". *Diabetes* 52 (2): 409-416.

Jacobson, D. A., Wicksteed, B. L. and Philipson, L. H. (2009). "The α-cell conundrum: ATP-sensitive K^+ channels and glucose sensing". *Diabetes* 58 (2): 304-306.

Jang, Y. Y., Song, J. H., Shin, Y. K., Han, E. S. and Lee, C. S. (2000). "Protective effect of boldine on oxidative mitochondrial damage in streptozotocin-induced diabetic rats". *Pharmacol Res* 42 (4): 361-371.

Jetton, T. L., Everill, B., Lausier, J., Roskens, V., Habibovic, A., LaRock, K., Gokin, A., Peshavaria, M. and Leahy, J. L. (2008). "Enhanced β-cell mass without increased proliferation following chronic mild glucose infusion". *Am J Physiol Endocrinol Metab* 294 (4): E679-687.

Jiang, D., Sullivan, P. G., Sensi, S. L., Steward, O. and Weiss, J. H. (2001). "Zn^{2+} induces permeability transition pore opening and release of pro-apoptotic peptides from neuronal mitochondria". *J Biol Chem* 276 (50): 47524-47529.

Jimbo, A., Fujita, E., Kouroku, Y., Ohnishi, J., Inohara, N., Kuida, K., Sakamaki, K., Yonehara, S. and Momoi, T. (2003). "ER stress induces caspase-8 activation, stimulating cytochrome *c* release and caspase-9 activation". *Exp Cell Res* 283 (2): 156-166.

Johansen, J., Harris, A., Rychly, D. and Ergul, A. (2005). "Oxidative stress and the use of antioxidants in diabetes: Linking basic science to clinical practice". *Cardiovasc Diabetol* 4 (1): 5.

Jonas, J.-C., Sharma, A., Hasenkamp, W., Ilkova, H., Patane, G., Laybutt, R., Bonner-Weir, S. and Weir, G. C. (1999). "Chronic hyperglycemia triggers loss of pancreatic β cell differentiation in an animal model of diabetes". *J Biol Chem* 274 (20): 14112-14121.

Kahn, S., Zraika, S., Utzschneider, K. and Hull, R. (2009). "The beta cell lesion in type 2 diabetes: there has to be a primary functional abnormality". *Diabetologia* 52 (6): 1003-1012.

Kaiser, N., Leibowitz, G. and Nesher, R. (2003). "Glucotoxicity and beta-cell failure in type 2 diabetes mellitus." *J Pediatr Endocrinol Metab* 16 (1): 5-22.

Kalaivanam, K. N., Dharmalingam, M. and Marcus, S. R. (2006). "Lipid peroxidation in type 2 diabetes mellitus". *Int J Diab Dev Ctries* 26 (1): 30-32.

Kaneto, H., Kajimoto, Y., Miyagawa, J., Matsuoka, T., Fujitani, Y., Umayahara, Y., Hanafusa, T., Matsuzawa, Y., Yamasaki, Y. and Hori, M. (1999). "Beneficial effects of antioxidants in diabetes: possible protection of pancreatic beta-cells against glucose toxicity". *Diabetes* 48 (12): 2398-2406.

Kaneto, H., Nakatani, Y., Kawamori, D., Miyatsuka, T. and Matsuoka, T. (2004). "Involvement of oxidative stress and the JNK pathway in glucose toxicity". *Rev Diabet Stud* 1 (4): 165-174.

Kaneto, H., Xu, G., Fujii, N., Kim, S., Bonner-Weir, S. and Weir, G. (2002). "Involvement of c-Jun N-terminal kinase in oxidative stress-mediated suppression of insulin gene expression". *J Biol Chem* 277 (33): 30010-30018.

Kanwar, M., Chan, P.-S., Kern, T. S. and Kowluru, R. A. (2007). "Oxidative damage in the retinal mitochondria of diabetic mice: Possible protection by superoxide dismutase". *Invest Ophthalmol Vis Sci* 48 (8): 3805-3811.

Kapoor, D., Aldred, H., Clark, S., Channer, K. S. and Jones, T. H. (2007). "Clinical and biochemical assessment of hypogonadism in men with type 2 diabetes". *Diabetes Care* 30 (4): 911-917.

Kärvestedt, L., Andersson, G., Efendic, S. and Grill, V. (2002). "A rapid increase in β-cell function by multiple insulin injections in type 2 diabetic patients is not further enhanced by prolonging treatment." *J Intern Med* 251 (4): 307-316.

Katalinic, V., Modun, D., Music, I. and Boban, M. (2005). "Gender differences in antioxidant capacity of rat tissues determined by 2,2'-azinobis (3-ethylbenzothiazoline 6-sulfonate; ABTS) and ferric reducing antioxidant power (FRAP) assays". *Comp Biochem Physiol, C* 140 (1): 47-52.

Kayo, T. and Koizumi, A. (1998). "Mapping of murine diabetogenic gene *Mody* on chromosome 7 at D7Mit258 and its involvement in pancreatic islet and β cell development during the perinatal period". *J Clin Invest* 101 (10): 2112-2118.

Keays, D., Clark, T. and Flint, J. (2006). "Estimating the number of coding mutations in genotypic-and phenotypic-driven *N*-ethyl-*N*-nitrosourea (ENU) screens". *Mamm Genome* 17 (3): 230-238.

Kedziora-Kornatowska, K., Szram, S., Kornatowski, T., Szadujkis-Szadurski, L., Kedziora, J. and Bartosz, G. (2003). "Effect of vitamin E and vitamin C supplementation on antioxidative state and renal glomerular basement membrane thickness in diabetic kidney". *Nephron Exp Nephrol* 95 (4): 134-143.

Kedziora-Kornatowska, K. Z., Luciak, M. and Paszkowski, J. (2000). "Lipid peroxidation and activities of antioxidant enzymes in the diabetic kidney: Effect of treatment with angiotensin convertase inhibitors". *IUBMB Life* 49 (4): 303-307.

Kharroubi, I., Ladriere, L., Cardozo, A. K., Dogusan, Z., Cnop, M. and Eizirik, D. L. (2004). "Free fatty acids and cytokines induce pancreatic β-cell apoptosis by different mechanisms: Role of nuclear factor-κB and endoplasmic reticulum stress". *Endocrinology* 145 (11): 5087-5096.

Kim, J., Michael, M., Previs, S., Peroni, O., Mauvais-Jarvis, F., Neschen, S., Kahn, B., Kahn, C. and Shulman, G. (2000). "Redistribution of substrates to adipose tissue promotes obesity in mice with selective insulin resistance in muscle". *J Clin Invest* 105 (12): 1791-1797.

Kim, W.-H., Lee, J. W., Suh, Y. H., Hong, S. H., Choi, J. S., Lim, J. H., Song, J. H., Gao, B. and Jung, M. H. (2005). "Exposure to chronic high glucose induces β-cell apoptosis through decreased interaction of glucokinase with mitochondria". *Diabetes* 54 (9): 2602-2611.

Kincaid, M. M. and Cooper, A. A. (2007a). "ERADicate ER stress or die trying". *Antioxid Redox Signal* 9 (12): 2373-2387.

Kincaid, M. M. and Cooper, A. A. (2007b). "Misfolded proteins traffic from the endoplasmic reticulum (ER) due to ER export signals". *Mol Biol Cell* 18 (2): 455-463.

Knowler, W., Barrett-Connor, E., Fowler, S., Hamman, R., Lachin, J., Walker, E. and Nathan, D. (2002). "Reduction in the incidence of type 2 diabetes with lifestyle intervention or metformin". *N Engl J Med* 346 (6): 393-403.

Kocak, G., Aktan, F., Canbolat, O., Ozo ul, C., Elbe , S., Yildizoglu-Ari, N. and Karasu, C. (2000). "Alpha-lipoic acid treatment ameliorates metabolic parameters, blood pressure, vascular reactivity and morphology of vessels already damaged by streptozotocin-diabetes." *Diabetes Nutr Metab* 13 (6): 308-318.

Kojima, E., Takeuchi, A., Haneda, M., Yagi, F., Hasegawa, T., Yamaki, K.-i., Takeda, K., Akira, S., Shimokata, K. and Isobe, K.-i. (2003). "The function of GADD34 is a recovery from a shutoff of protein synthesis induced by ER stress: elucidation by GADD34-deficient mice". *FASEB J* 17 (11): 1573-1575.

Kondo, T., Khattabi, I. E., Nishimura, W., Laybutt, D. R., Geraldes, P., Shah, S., King, G., Bonner-Weir, S., Weir, G. and Sharma, A. (2009). "p38 MAPK is a major regulator of MafA protein stability under oxidative stress". *Mol Endocrinol* 23 (8): 1281-1290.

Korshunov, S. S., Skulachev, V. P. and Starkov, A. A. (1997). "High protonic potential actuates a mechanism of production of reactive oxygen species in mitochondria". *FEBS Lett* 416 (1): 15-18.

Koya, D. and King, G. (1998). "Protein kinase C activation and the development of diabetic complications". *Diabetes* 47 (6): 859-866.

Kukreja, A. and Maclaren, N. (1999). "Autoimmunity and diabetes". *J Clin Endocrinol Metab* 84 (12): 4371-4378.

Kwok, S. C., Steiner, D. F., Rubenstein, A. H. and Tager, H. S. (1983). "Identification of a point mutation in the human insulin gene giving rise to a structurally abnormal insulin (insulin Chicago)." *Diabetes* 32 (9): 872-875.

Lakhani, S., Masud, A., Kuida, K., Porter, G., Booth, C., Mehal, W., Inayat, I. and Flavell, R. (2006). "Caspases 3 and 7: key mediators of mitochondrial events of apoptosis". *Science* 311 (5762): 847-851.

Laybutt, D., Preston, A., Åkerfeldt, M., Kench, J., Busch, A., Biankin, A. and Biden, T. (2007). "Endoplasmic reticulum stress contributes to beta cell apoptosis in type 2 diabetes". *Diabetologia* 50 (4): 752-763.

Le May, C., Chu, K., Hu, M., Ortega, C., Simpson, E., Korach, K., Tsai, M. and Mauvais-Jarvis, F. (2006). "Estrogens protect pancreatic β-cells from apoptosis and prevent insulin-deficient diabetes mellitus in mice". *PNAS* 103 (24): 9232-9237.

Lee, A., Iwakoshi, N. and Glimcher, L. (2003). "XBP-1 regulates a subset of endoplasmic reticulum resident chaperone genes in the unfolded protein response". *Mol Cell Biol* 23 (21): 7448-7459.

Lee, M., Miller, E., Goldberg, J., Orci, L. and Schekman, R. (2004). "Bi-directional protein transport between the ER and Golgi". *Annu Rev Cell Dev Biol* 20 (1): 87-123.

Lee, S., Muniyappa, R., Yan, X., Chen, H., Yue, L. Q., Hong, E.-G., Kim, J. K. and Quon, M. J. (2008). "Comparison between surrogate indexes of insulin sensitivity and resistance and hyperinsulinemic euglycemic clamp estimates in mice". *Am J Physiol Endocrinol Metab* 294 (2): E261-270.

Lehmann, R. and Spinas, G. A. (2005). "Diagnostik und Pathogenese des Diabetes mellitus Typ 2". *Schweizerisches Medizin-Forum* 39 968-975.

Leibiger, B., Wahlander, K., Berggren, P.-O. and Leibiger, I. B. (2000). "Glucose-stimulated insulin biosynthesis depends on insulin-stimulated insulin gene transcription". *J Biol Chem* 275 (39): 30153-30156.

Leibiger, I. B., Leibiger, B., Moede, T. and Berggren, P.-O. (1998). "Exocytosis of insulin promotes insulin gene transcription via the insulin receptor/PI-3 kinase/p70 s6 kinase and CaM kinase pathways". *Mol Cell* 1 (6): 933-938.

Lenzen, S., Drinkgern, J. and Tiedge, M. (1996). "Low antioxidant enzyme gene expression in pancreatic islets compared with various other mouse tissues". *Free Radic Biol Med* 20 (3): 463-466.

Leroux, L., Desbois, P., Lamotte, L., Duvillié, B., Cordonnier, N., Jackerott, M., Jami, J., Bucchini, D. and Joshi, R. (2001). "Compensatory responses in mice carrying a null mutation for *Ins1* or *Ins2*". *Diabetes* 50 (suppl 1): S150-S153.

Leroux, L., Durel, B., Autier, V., Deltour, L., Bucchini, D., Jami, J. and Joshi, R. (2003). "*Ins1* gene up-regulated in a β-cell line derived from *Ins2* knockout mice". *Exp Diabesity Res* 4 (1): 7-12.

Li, J., Kuang, Y. and Mason, C. (2006). "Modeling the glucose–insulin regulatory system and ultradian insulin secretory oscillations with two explicit time delays". *J Theor Biol* 242 (3): 722-735.

Ling, Z., Wu, D., Zambre, Y., Flamez, D., Drucker, D. J., Pipeleers, D. G. and Schuit, F. C. (2001). "Glucagon-like peptide 1 receptor signaling influences topography of islet cells in mice". *Virchows Arch* 438 (4): 382-387.

Liu, C. Y. and Kaufman, R. J. (2003). "The unfolded protein response". *J Cell Sci* 116 (10): 1861-1862.

Liu, C. Y., Schroder, M. and Kaufman, R. J. (2000). "Ligand-independent dimerization activates the stress response kinases IRE1 and PERK in the lumen of the endoplasmic reticulum". *J Biol Chem* 275 (32): 24881-24885.

Liu, M., Li, Y., Cavener, D. and Arvan, P. (2005). "Proinsulin disulfide maturation and misfolding in the endoplasmic reticulum". *J Biol Chem* 280 (14): 13209-13212.

Lorenzo, C., Okoloise, M., Williams, K., Stern, M. P. and Haffner, S. M. (2003). "The metabolic syndrome as predictor of type 2 diabetes". *Diabetes Care* 26 (11): 3153-3159.

Lottmann, H., Vanselow, J., Hessabi, B. and Walther, R. (2001). "The Tet-On system in transgenic mice: Inhibition of the mouse *pdx-1* gene activity by antisense RNA expression in pancreatic β-cells". *J Mol Med* 79 (5): 321-328.

Louet, J.-F., LeMay, C. and Mauvais-Jarvis, F. (2004). "Antidiabetic actions of estrogen: Insight from human and genetic mouse models". *Curr Atheroscler Rep* 6 (3): 180-185.

Lu, S. C. (2009). "Regulation of glutathione synthesis". *Mol Aspects Med* 30 (1-2): 42-59.

Luirink, J. and Sinning, I. (2004). "SRP-mediated protein targeting: structure and function revisited". *Biochim Biophys Acta* 1694 (1-3): 17-35.

Luzi, L., Zerbini, G. and Caumo, A. (2007). "C-peptide: a redundant relative of insulin?" *Diabetologia* 50 (3): 500-502.

Ma, Y., Brewer, J. W., Alan Diehl, J. and Hendershot, L. M. (2002). "Two distinct stress signaling pathways converge upon the CHOP promoter during the mammalian unfolded protein response". *J Mol Biol* 318 (5): 1351-1365.

Ma, Y. and Hendershot, L. M. (2002). "The mammalian endoplasmic reticulum as a sensor for cellular stress". *Cell Stress Chaperones* 7 (2): 222-229.

Maddux, B. A., See, W., Lawrence, J. C., Goldfine, A. L., Goldfine, I. D. and Evans, J. L. (2001). "Protection against oxidative stress-induced insulin resistance in rat L6 muscle cells by micromolar concentrations of α-lipoic acid". *Diabetes* 50 (2): 404-410.

Maedler, K., Fontana, A., Ris, F., Sergeev, P., Toso, C., Oberholzer, J., Lehmann, R., Bachmann, F., Tasinato, A., Spinas, G. A., Halban, P. A. and Donath, M. Y. (2002). "FLIP switches Fas-mediated glucose signaling in human pancreatic β cells from apoptosis to cell replication". *PNAS* 99 (12): 8236-8241.

Maedler, K., Schulthess, F. T., Bielman, C., Berney, T., Bonny, C., Prentki, M., Donath, M. Y. and Roduit, R. (2008). "Glucose and leptin induce apoptosis in human β-cells and impair glucose-stimulated insulin secretion through activation of c-Jun N-terminal kinases". *FASEB J* 22 (6): 1905-1913.

Maedler, K., Spinas, G. A., Lehmann, R., Sergeev, P., Weber, M., Fontana, A., Kaiser, N. and Donath, M. Y. (2001). "Glucose induces β-cell apoptosis via upregulation of the Fas receptor in human islets". *Diabetes* 50 (8): 1683-1690.

Mahimainathan, L., Das, F., Venkatesan, B. and Choudhury, G. G. (2006). "Mesangial cell hypertrophy by high glucose is mediated by downregulation of the tumor suppressor PTEN". *Diabetes* 55 (7): 2115-2125.

Malhotra, J. D., Miao, H., Zhang, K., Wolfson, A., Pennathur, S., Pipe, S. W. and Kaufman, R. J. (2008). "Antioxidants reduce endoplasmic reticulum stress and improve protein secretion". *PNAS* 105 (47): 18525-18530.

Marciniak, S. J., Yun, C. Y., Oyadomari, S., Novoa, I., Zhang, Y., Jungreis, R., Nagata, K., Harding, H. P. and Ron, D. (2004). "CHOP induces death by promoting protein synthesis and oxidation in the stressed endoplasmic reticulum". *Genes Dev* 18 (24): 3066-3077.

Maritim, A., Sanders, R. and Watkins III, J. (2003). "Diabetes, oxidative stress, and antioxidants: a review". *J Biochem Mol Toxicol* 17 (1): 24-38.

Martocchia, A., Risicato, M., Mattioli, C., Antonelli, M., Ruco, L. and Falaschi, P. (2008). "Association of diffuse liver glycogenosis and mild focal macrovesicular steatosis in a patient with poorly controlled type 1 diabetes". *Intern Emerg Med* 3 (3): 273-274.

Marutani, T., Yamamoto, A., Nagai, N., Kubota, H. and Nagata, K. (2004). "Accumulation of type IV collagen in dilated ER leads to apoptosis in *Hsp47*-knockout mouse embryos via induction of CHOP". *J Cell Sci* 117 (24): 5913-5922.

McCullough, K. D., Martindale, J. L., Klotz, L.-O., Aw, T.-Y. and Holbrook, N. J. (2001). "Gadd153 sensitizes cells to endoplasmic reticulum stress by down-regulating Bcl2 and perturbing the cellular redox state". *Mol Cell Biol* 21 (4): 1249-1259.

McKinnon, C. M. and Docherty, K. (2001). "Pancreatic duodenal homeobox-1, PDX-1, a major regulator of beta cell identity and function". *Diabetologia* 44 (10): 1203-1214.

Meier, J., Kjems, L., Veldhuis, J., Lefèbvre, P. and Butler, P. (2006). "Postprandial suppression of glucagon secretion depends on intact pulsatile insulin secretion". *Diabetes* 55 (4): 1051-1056.

Melloul, D. (2004). "Transcription factors in islet development and physiology: Role of PDX-1 in beta-cell function". *Ann NY Acad Sci* 1014 28-37.

Melloul, D., Marshak, S. and Cerasi, E. (2002). "Regulation of insulin gene transcription". *Diabetologia* 45 (3): 309-326.

Michael, M. D., Kulkarni, R. N., Postic, C., Previs, S. F., Shulman, G. I., Magnuson, M. A. and Kahn, C. R. (2000). "Loss of insulin signaling in hepatocytes leads to severe insulin resistance and progressive hepatic dysfunction". *Mol Cell* 6 (1): 87-97.

Miyazaki, S., Yamato, E. and Miyazaki, J.-i. (2004). "Regulated expression of pdx-1 promotes in vitro differentiation of insulin-producing cells from embryonic stem cells". *Diabetes* 53 (4): 1030-1037.

Mizukami, H., Wada, R., Koyama, M., Takeo, T., Suga, S., Wakui, M. and Yagihashi, S. (2008). "Augmented β cell loss and mitochondrial abnormalities in sucrose-fed GK rats". *Virchows Arch* 452 (4): 383-392.

Molven, A., Ringdal, M., Nordbø, A., Ræder, H., Støy, J., Lipkind, G., Steiner, D., Philipson, L., Bergmann, I. and Aarskog, D. (2008). "Mutations in the insulin gene can cause MODY and autoantibody-negative type 1 diabetes". *Diabetes* 57 (4): 1131-1135.

Morishima, N., Nakanishi, K., Takenouchi, H., Shibata, T. and Yasuhiko, Y. (2002). "An endoplasmic reticulum stress-specific caspase cascade in apoptosis". *J Biol Chem* 277 (37): 34287-34294.

Movassagh, M. and Foo, R. (2008). "Simplified apoptotic cascades". *Heart Fail Rev* 13 (2): 111-119.

Muller, D., Jones, P. M. and Persaud, S. J. (2006). "Autocrine anti-apoptotic and proliferative effects of insulin in pancreatic β-cells". *FEBS Lett* 580 (30): 6977-6980.

Nakagawa, S. H., Hua, Q.-x., Hu, S.-Q., Jia, W., Wang, S., Katsoyannis, P. G. and Weiss, M. A. (2006). "Chiral mutagenesis of insulin". *J Biol Chem* 281 (31): 22386-22396.

Nanjo, K., Miyano, M., Kondo, M., Sanke, T., Nishimura, S., Miyamura, K., Inouye, K., Given, B., Chan, S. and Polonsky, K. (1987). "Insulin Wakayama: familial mutant insulin syndrome in Japan". *Diabetologia* 30 (2): 87-92.

Nanjo, K., Sanke, T., Miyano, M., Okai, K., Sowa, R., Kondo, M., Nishimura, S., Iwo, K., Miyamura, K. and Given, B. (1986). "Diabetes due to secretion of a structurally abnormal insulin (insulin Wakayama)" *J Clin Invest* 77 (2): 514-519.

National Institutes of Health (NIH) (2004). "Image processing and analysis in Java". Retrieved 16.08. 2009 from http://rsb.info.nih.gov/ij/.

Nishikawa, T., Edelstein, D., Du, X. L., Yamagishi, S.-i., Matsumura, T., Kaneda, Y., Yorek, M. A., Beebe, D., Oates, P. J., Hammes, H.-P., Giardino, I. and Brownlee, M. (2000). "Normalizing mitochondrial superoxide production blocks three pathways of hyperglycaemic damage". *Nature* 404 (6779): 787-790.

Nishino, N., Tamori, Y. and Kasuga, M. (2007). "Insulin efficiently stores triglycerides in adipocytes by inhibiting lipolysis and repressing PGC-1α induction." *Kobe J Med Sci* 53 (3): 99-106.

Nishitoh, H., Matsuzawa, A., Tobiume, K., Saegusa, K., Takeda, K., Inoue, K., Hori, S., Kakizuka, A. and Ichijo, H. (2002). "ASK1 is essential for endoplasmic reticulum stress-induced neuronal cell death triggered by expanded polyglutamine repeats". *Genes Dev* 16 (11): 1345-1355.

Njolstad, P., Sovik, O., Cuesta-Munoz, A., Bjorkhaug, L., Massa, O., Barbetti, F., Undlien, D., Shiota, C., Magnuson, M. and Molven, A. (2001). "Neonatal diabetes mellitus due to complete glucokinase deficiency". *N Engl J Med* 344 (21): 1588-1592.

Nozaki, J. i., Kubota, H., Yoshida, H., Naitoh, M., Goji, J., Yoshinaga, T., Mori, K., Koizumi, A. and Nagata, K. (2004). "The endoplasmic reticulum stress response is stimulated through the continuous activation of transcription factors ATF6 and XBP1 in *Ins2*^+/Akita pancreatic β cells". *Genes Cells* 9 (3): 261-270.

Obici, S., Feng, Z., Karkanias, G., Baskin, D. and Rossetti, L. (2002). "Decreasing hypothalamic insulin receptors causes hyperphagia and insulin resistance in rats". *Nature Neurosci* 5 (6): 566-572.

Ohneda, A., Wantanabe, K., Horigome, K., Sakai, T., Kai, Y. and Oikawa, S.-I. (1978). "Abnormal response of pancreatic glucagon to glycemic changes in diabetes mellitus". *J Clin Endocrinol Metab* 46 (3): 504-510.

Ohoka, N., Yoshii, S., Hattori, T., Onozaki, K. and Hayashi, H. (2005). "*TRB 3*, a novel ER stress-inducible gene, is induced via ATF 4–CHOP pathway and is involved in cell death". *EMBO J* 24 (6): 1243-1255.

Ohshiro, Y., Ma, R. C., Yasuda, Y., Hiraoka-Yamamoto, J., Clermont, A. C., Isshiki, K., Yagi, K., Arikawa, E., Kern, T. S. and King, G. L. (2006). "Reduction of diabetes-induced oxidative stress, fibrotic cytokine expression, and renal dysfunction in protein kinase Cβ-null mice". *Diabetes* 55 (11): 3112-3120.

Okada, T., Yoshida, H., Akazawa, R., Negishi, M. and Mori, K. (2002). "Distinct roles of activating transcription factor 6 (ATF6) and double-stranded RNA-activated protein kinase-like endoplasmic reticulum kinase (PERK) in transcription during the mammalian unfolded protein response". *Biochem J* 366 (2): 585-594.

Oohashi, H., Ohgawara, H., Nanjo, K., Tasaka, Y., Cao, Q. P., Chan, S. J., Rubenstein, A. H., Steiner, D. F. and Omori, Y. (1993). "Familial hyperproinsulinemia associated with NIDDM. A case study." *Diabetes Care* 16 (10): 1340-1346.

Ordónez, P., Moreno, M., Alonso, A., Fernández, R., Díaz, F. and González, C. (2007). "Insulin sensitivity in streptozotocin-induced diabetic rats treated with different doses of 17β-oestradiol or progesterone". *Exp Physiol* 92 (1): 241-249.

Ouslimani, N., Peynet, J., Bonnefont-Rousselot, D., Thérond, P., Legrand, A. and Beaudeux, J.-L. (2005). "Metformin decreases intracellular production of reactive oxygen species in aortic endothelial cells". *Metabolism* 54 (6): 829-834.

Oyadomari, S., Araki, E. and Mori, M. (2002a). "Endoplasmic reticulum stress-mediated apoptosis in pancreatic β-cells". *Apoptosis* 7 (4): 335-345.

Oyadomari, S., Koizumi, A., Takeda, K., Gotoh, T., Akira, S., Araki, E. and Mori, M. (2002b). "Targeted disruption of the *Chop* gene delays endoplasmic reticulum stress-mediated diabetes". *J Clin Invest* 109 (4): 525-532.

Oyadomari, S. and Mori, M. (2003). "Roles of CHOP/GADD153 in endoplasmic reticulum stress". *Cell Death Differ* 11 (4): 381-389.

Ozansoy, G., Akin, B., Aktan, F. and Karasu, C. (2001). "Short-term gemfibrozil treatment reverses lipid profile and peroxidation but does not alter blood glucose and tissue antioxidant enzymes in chronically diabetic rats". *Mol Cell Biochem* 216 (1): 59-63.

Ozawa, K., Miyazaki, M., Matsuhisa, M., Takano, K., Nakatani, Y., Hatazaki, M., Tamatani, T., Yamagata, K., Miyagawa, J.-i., Kitao, Y., Hori, O., Yamasaki, Y. and Ogawa, S. (2005). "The endoplasmic reticulum chaperone improves insulin resistance in type 2 diabetes". *Diabetes* 54 (3): 657-663.

Özcan, U., Yilmaz, E., Ozcan, L., Furuhashi, M., Vaillancourt, E., Smith, R. O., Gorgun, C. Z. and Hotamisligil, G. S. (2006). "Chemical chaperones reduce ER stress and restore glucose homeostasis in a mouse model of type 2 diabetes". *Science* 313 (5790): 1137-1140.

Palmeira, C., Rolo, A., Berthiaume, J., Bjork, J. and Wallace, K. (2007). "Hyperglycemia decreases mitochondrial function: The regulatory role of mitochondrial biogenesis". *Toxicol Appl Pharmacol* 225 (2): 214-220.

Paris, M., Bernard-Kargar, C., Berthault, M.-F., Bouwens, L. and Ktorza, A. (2003). "Specific and combined effects of insulin and glucose on functional pancreatic β-cell mass *in vivo* in adult rats". *Endocrinology* 144 (6): 2717-2727.

Park, S., Jang, J. S. and Hong, S. M. (2007). "Long-term consumption of caffeine improves glucose homeostasis by enhancing insulinotropic action through islet insulin/insulin-like growth factor 1 signaling in diabetic rats". *Metabolism* 56 (5): 599-607.

Paz, K., Hemi, R., LeRoith, D., Karasik, A., Elhanany, E., Kanety, H. and Zick, Y. (1997). "A molecular basis for insulin resistance". *J Biol Chem* 272 (47): 29911-29918.

Persaud, S. J., Muller, D. and Jones, P. M. (2008). "Insulin signalling in islets". *Biochem Soc Trans* 36 (3): 290-293.

Pfeiffer, S., Lass, A., Schmidt, K. and Mayer, B. (2001). "Protein tyrosine nitration in cytokine-activated murine macrophages". *J Biol Chem* 276 (36): 34051-34058.

Pirot, P. (2007). "Identification and characterization of the endoplasmic reticulum (ER)-stress pathways in pancreatic beta-cells." Université Libre de Bruxelles

Pociot, F. and McDermott, M. (2002). "Genetics of type 1 diabetes mellitus". *Genes Immun* 3 (5): 235-249.

Polak, M. and Cavé, H. (2007). "Neonatal diabetes mellitus: a disease linked to multiple mechanisms". *Orphanet J Rare Dis* 2 (1): 12.

Polak, M., Dechaume, A., Cavé, H., Nimri, R., Crosnier, H., Sulmont, V., de Kerdanet, M., Scharfmann, R., Lebenthal, Y. and Froguel, P. (2008). "Heterozygous missense mutations in the insulin gene are linked to permanent diabetes appearing in the neonatal period or in early infancy". *Diabetes* 57 (4): 1115-1119.

Porte, D., Sherwin, R., Baron, A., Ellenberg, M. and Rifkin, H. (2002). "Ellenberg & Rifkin's diabetes mellitus". McGraw-Hill Professional.

Puthalakath, H., O'Reilly, L. A., Gunn, P., Lee, L., Kelly, P. N., Huntington, N. D., Hughes, P. D., Michalak, E. M., McKimm-Breschkin, J., Motoyama, N., Gotoh, T., Akira, S., Bouillet, P. and Strasser, A. (2007). "ER stress triggers apoptosis by activating BH3-only protein Bim". *Cell* 129 (7): 1337-1349.

Quesada, I., Tuduri, E., Ripoll, C. and Nadal, A. (2008). "Physiology of the pancreatic α-cell and glucagon secretion: Role in glucose homeostasis and diabetes". *J Endocrinol* 199 (1): 5-19.

Quoix, N., Cheng-Xue, R., Mattart, L., Zeinoun, Z., Guiot, Y., Beauvois, M. C., Henquin, J.-C. and Gilon, P. (2009). "Glucose and pharmacological modulators of ATP-sensitive K^+ channels control $[Ca^{2+}]_c$ by different mechanisms in isolated mouse α-cells". *Diabetes* 58 (2): 412-421.

Rahimi, R., Nikfar, S., Larijani, B. and Abdollahi, M. (2005). "A review on the role of antioxidants in the management of diabetes and its complications". *Biomed Pharmacother* 59 (7): 365-373.

Rajan, S., Srinivasan, V., Balasubramanyam, M. and Tatu, U. (2007). "Endoplasmic reticulum (ER) stress & diabetes". *Indian J Med Res* 125 (3): 411-424.

Ramakrishna, V. and Jailkhani, R. (2007). "Evaluation of oxidative stress in insulin dependent diabetes mellitus (IDDM) patients". *Diagn Pathol* 2 (1): 22.

Raslova, K., Tamer, S., Clauson, P. and Karl, D. (2007). "Insulin detemir results in less weight gain than NPH insulin when used in basal-bolus therapy for type 2 diabetes mellitus, and this advantage increases with baseline body mass index". *Clin Drug Invest* 27 (4): 279-285.

Resnick, H., Valsania, P., Halter, J. and Lin, X. (2000). "Relation of weight gain and weight loss on subsequent diabetes risk in overweight adults". *J Epidemiol Community Health* 54 (8): 596-602.

Riggs, A., Bernal-Mizrachi, E., Ohsugi, M., Wasson, J., Fatrai, S., Welling, C., Murray, J., Schmidt, R., Herrera, P. and Permutt, M. (2005). "Mice conditionally lacking the Wolfram gene in pancreatic islet beta cells exhibit diabetes as a result of enhanced endoplasmic reticulum stress and apoptosis". *Diabetologia* 48 (11): 2313-2321.

Robertson, R. (2004). "Chronic oxidative stress as a central mechanism for glucose toxicity in pancreatic islet beta cells in diabetes". *J Biol Chem* 279 (41): 42351-42354.

Robertson, R. and Harmon, J. (2006). "Diabetes, glucose toxicity, and oxidative stress: A case of double jeopardy for the pancreatic islet β cell". *Free Radic Biol Med* 41 (2): 177-184.

Robertson, R. P. (2006). "Oxidative stress and impaired insulin secretion in type 2 diabetes". *Curr Opin Pharmacol* 6 (6): 615-619.

Roglic, G., Unwin, N., Bennett, P., Mathers, C., Tuomilehto, J., Nag, S., Connolly, V. and King, H. (2005). "The burden of mortality attributable to diabetes". *Diabetes Care* 28 (9): 2130-2135.

Römisch, K., Collie, N., Soto, N., Logue, J., Lindsay, M., Scheper, W. and Cheng, C.-H. C. (2003). "Protein translocation across the endoplasmic reticulum membrane in cold-adapted organisms". *J Cell Sci* 116 (14): 2875-2883.

Roux, P. P. and Blenis, J. (2004). "ERK and p38 MAPK-activated protein kinases: A family of protein kinases with diverse biological functions". *Microbiol Mol Biol Rev* 68 (2): 320-344.

Russell, W., Kelly, E., Hunsicker, P., Bangham, J., Maddux, S. and Phipps, E. (1979). "Specific-locus test shows ethylnitrosourea to be the most potent mutagen in the mouse". *PNAS* 76 (11): 5818-5819.

Rutkowski, D. T., Arnold, S. M., Miller, C. N., Wu, J., Li, J., Gunnison, K. M., Mori, K., Sadighi Akha, A. A., Raden, D. and Kaufman, R. J. (2006). "Adaptation to ER stress is mediated by differential stabilities of pro-survival and pro-apoptotic mRNAs and proteins". *PLoS Biol* 4 (11): e374.

Rutkowski, D. T. and Kaufman, R. J. (2004). "A trip to the ER: coping with stress". *Trends Cell Biol* 14 (1): 20-28.

Ryu, S., Ornoy, A., Samuni, A., Zangen, S. and Kohen, R. (2008). "Oxidative stress in Cohen diabetic rat model by high-sucrose, low-copper diet: inducing pancreatic damage and diabetes". *Metabolism* 57 (9): 1253-1261.

Sakuraba, H., Mizukami, H., Yagihashi, N., Wada, R., Hanyu, C. and Yagihashi, S. (2002). "Reduced beta-cell mass and expression of oxidative stress-related DNA damage in the islet of japanese type II diabetic patients". *Diabetologia* 45 (1): 85-96.

Sayuk, G., Elwing, J. and Lisker-Melman, M. (2007). "Hepatic glycogenosis: an underrecognized source of abnormal liver function tests?" *Dig Dis Sci* 52 (4): 936-938.

Scheuner, D. and Kaufman, R. (2008). "The unfolded protein response: a pathway that links insulin demand with β-cell failure and diabetes". *Endocr Rev* 29 (3): 317-333.

Scheuner, D., Song, B., McEwen, E., Liu, C., Laybutt, R., Gillespie, P., Saunders, T., Bonner-Weir, S. and Kaufman, R. J. (2001). "Translational control is required for the unfolded protein response and in vivo glucose homeostasis". *Mol Cell* 7 (6): 1165-1176.

Schmidt, A. M. and Stern, D. M. (2000). "RAGE: A new target for the prevention and treatment of the vascular and inflammatory complications of diabetes". *Trends Endocrinol Metabol* 11 (9): 368-375.

Scorrano, L. and Korsmeyer, S. J. (2003). "Mechanisms of cytochrome *c* release by proapoptotic BCL-2 family members". *Biochem Biophys Res Commun* 304 (3): 437-444.

Senee, V., Vattem, K. M., Delepine, M., Rainbow, L. A., Haton, C., Lecoq, A., Shaw, N. J., Robert, J.-J., Rooman, R., Diatloff-Zito, C., Michaud, J. L., Bin-Abbas, B., Taha, D., Zabel, B., Franceschini, P., Topaloglu, A. K., Lathrop, G. M., Barrett, T. G., Nicolino, M., Wek, R. C. and Julier, C. (2004). "Wolcott-Rallison syndrome". *Diabetes* 53 (7): 1876-1883.

Shah, S., Iqbal, M., Karam, J., Salifu, M. and McFarlane, S. (2007). "Oxidative stress, glucose metabolism, and the prevention of type 2 diabetes: pathophysiological insights". *Antioxid Redox Signal* 9 (7): 911-929.

Shen, J., Chen, X., Hendershot, L. and Prywes, R. (2002). "ER stress regulation of ATF6 localization by dissociation of BiP/GRP78 binding and unmasking of Golgi localization signals". *Dev Cell* 3 (1): 99-111.

Shen, X., Zheng, S., Thongboonkerd, V., Xu, M., Pierce, W. M., Jr., Klein, J. B. and Epstein, P. N. (2004). "Cardiac mitochondrial damage and biogenesis in a chronic model of type 1 diabetes". *Am J Physiol Endocrinol Metab* 287 (5): E896-905.

Sigfrid, L., Cunningham, J., Beeharry, N., Håkan Borg, L., Rosales Hernandez, A., Carlsson, C., Bone, A. and Green, I. (2004). "Antioxidant enzyme activity and mRNA expression in the islets of Langerhans from the BB/S rat model of type 1 diabetes and an insulin-producing cell line". *J Mol Med* 82 (5): 325-335.

Song, B., Scheuner, D., Ron, D., Pennathur, S. and Kaufman, R. J. (2008). "Chop deletion reduces oxidative stress, improves beta cell function, and promotes cell survival in multiple mouse models of diabetes". *J Clin Invest* 118 (10): 3378-89.

Song, F., Jia, W., Yao, Y., Hu, Y., Lei, L., Lin, J., Sun, X. and Liu, L. (2007). "Oxidative stress, antioxidant status and DNA damage in patients with impaired glucose regulation and newly diagnosed Type 2 diabetes". *Clin Sci* 112 (12): 599-606.

Spinas, G. and Lehmann, R. (2001). "Der Diabetes mellitus: Diagnose, Klassifikation, und Pathogenese". *Schweizerisches Medizin-Forum* 20 519-525.

Srinivasan, K. and Ramarao, P. (2007). "Animal model in type 2 diabetes research: An overview". *Indian J Med Res* 125 (3): 451-472.

Stanford, W., Cohn, J. and Cordes, S. (2001). "Gene-trap mutagenesis: past, present and beyond". *Nature Rev Genet* 2 (10): 756-768.

Stanik, J., Gasperikova, D., Paskova, M., Barak, L., Javorkova, J., Jancova, E., Ciljakova, M., Hlava, P., Michalek, J. and Flanagan, S. (2007). "Prevalence of permanent neonatal diabetes in Slovakia and successful replacement of insulin with sulfonylurea therapy in KCNJ11 and ABCC8 mutation carriers". *J Clin Endocrinol Metab* 92 (4): 1276-1282.

Steele, C., Hagopian, W., Gitelman, S., Masharani, U., Cavaghan, M., Rother, K., Donaldson, D., Harlan, D., Bluestone, J. and Herold, K. (2004). "Insulin secretion in type 1 diabetes". *Diabetes* 53 (2): 426-433.

Steiner, D. F., Tager, H. S., Chan, S. J., Nanjo, K., Sanke, T. and Rubenstein, A. H. (1990). "Lessons learned from molecular biology of insulin-gene mutations." *Diabetes Care* 13 (6): 600-609.

Støy, J., Edghill, E., Flanagan, S., Ye, H., Paz, V., Pluzhnikov, A., Below, J., Hayes, M., Cox, N. and Lipkind, G. (2007). "Insulin gene mutations as a cause of permanent neonatal diabetes". *PNAS* 104 (38): 15040-15044.

Szegezdi, E., Logue, S., Gorman, A. and Samali, A. (2006). "Mediators of endoplasmic reticulum stress-induced apoptosis". *EMBO Rep* 7 (9): 880-885.

Tager, H., Given, B., Baldwin, D., Mako, M., Markese, J., Rubenstein, A., Olefsky, J., Kobayashi, M., Kolterman, O. and Poucher, R. (1979). "A structurally abnormal insulin causing human diabetes". *Nature* 281 (5727): 122-125.

Tan, Y., Dourdin, N., Wu, C., De Veyra, T., Elce, J. S. and Greer, P. A. (2006). "Ubiquitous calpains promote caspase-12 and JNK activation during endoplasmic reticulum stress-induced apoptosis". *J Biol Chem* 281 (23): 16016-16024.

Tanaka, Y., Gleason, C. E., Tran, P. O. T., Harmon, J. S. and Robertson, R. P. (1999). "Prevention of glucose toxicity in HIT-T15 cells and Zucker diabetic fatty rats by antioxidants". *PNAS* 96 (19): 10857-10862.

Tappenden, K. A. (2006). "Mechanisms of enteral nutrient-enhanced intestinal adaptation". *Gastroenterology* 130 (2, suppl 1): S93-S99.

Thameem, F., Farook, V. S., Bogardus, C. and Prochazka, M. (2006). "Association of amino acid variants in the activating transcription factor 6 gene (*ATF6*) on 1q21-q23 with type 2 diabetes in Pima Indians". *Diabetes* 55 (3): 839-842.

The expert committee on the diagnosis and classification of diabetes mellitus (2002). "Report of the expert committee on the diagnosis of diabetes mellitus". *Diabetes Care* 25 (suppl 1): S5-S20

The expert committee on the diagnosis and classification of diabetes mellitus (2003). "Follow-up report on the diagnosis of diabetes mellitus". *Diabetes Care* 26 (11): 3160-3167

Tiedge, M., Lortz, S., Drinkgern, J. and Lenzen, S. (1997). "Relation between antioxidant enzyme gene expression and antioxidative defence status of insulin-producing cells." *Diabetes* 46 (11): 1733-1742.

Toledo, F. G. S., Sniderman, A. D. and Kelley, D. E. (2006). "Influence of hepatic steatosis (fatty liver) on severity and composition of dyslipidemia in type 2 diabetes". *Diabetes Care* 29 (8): 1845-1850.

Tomihira, M., Kawasaki, E., Nakajima, H., Imamura, Y., Sato, Y., Sata, M., Kage, M., Sugie, H. and Nunoi, K. (2004). "Intermittent and recurrent hepatomegaly due to glycogen storage in a patient with type 1 diabetes: Genetic analysis of the liver glycogen phosphorylase gene (*PYGL*)". *Diabetes Res Clin Pract* 65 (2): 175-182.

Torbenson, M., Chen, Y.-Y., Brunt, E., Cummings, O. W., Gottfried, M., Jakate, S., Liu, Y.-C., Yeh, M. M. and Ferrell, L. (2006). "Glycogenic hepatopathy: An underrecognized hepatic complication of diabetes mellitus". *Am J Surg Pathol* 30 (4): 508-513.

Tsuboi, T., Ravier, M. A., Parton, L. E. and Rutter, G. A. (2006). "Sustained exposure to high glucose concentrations modifies glucose signaling and the mechanics of secretory vesicle fusion in primary rat pancreatic β-cells". *Diabetes* 55 (4): 1057-1065.

Tu, B. and Weissman, J. (2002). "The FAD- and O_2-dependent reaction cycle of Ero1-mediated oxidative protein folding in the endoplasmic reticulum". *Mol Cell* 10 (5): 983-994.

Tu, B. P. and Weissman, J. S. (2004). "Oxidative protein folding in eukaryotes: mechanisms and consequences". *J Cell Biol* 164 (3): 341-346.

Ueda, K., Kawano, J., Takeda, K., Yujiri, T., Tanabe, K., Anno, T., Akiyama, M., Nozaki, J., Yoshinaga, T., Koizumi, A., Shinoda, K., Oka, Y. and Tanizawa, Y. (2005). "Endoplasmic reticulum stress induces *Wfs1* gene expression in pancreatic β-cells via transcriptional activation". *Eur J Endocrinol* 153 (1): 167-176.

Umpierrez, G., Murphy, M. and Kitabchi, A. (2002). "Diabetic ketoacidosis and hyperglycemic hyperosmolar syndrome". *Diabetes Spectrum* 15 (1): 28-36.

Urano, F., Wang, X., Bertolotti, A., Zhang, Y., Chung, P., Harding, H. P. and Ron, D. (2000). "Coupling of stress in the ER to activation of JNK protein kinases by transmembrane protein kinase IRE1". *Science* 287 (5453): 664-666.

Valko, M., Leibfritz, D., Moncol, J., Cronin, M. T. D., Mazur, M. and Telser, J. (2007). "Free radicals and antioxidants in normal physiological functions and human disease". *Int J Biochem Cell Biol* 39 (1): 44-84.

Vattem, K. and Wek, R. (2004). "Reinitiation involving upstream ORFs regulates *ATF4* mRNA translation in mammalian cells". *PNAS* 101 (31): 11269-11274.

Vaxillaire, M. and Froguel, P. (2006). "Genetic basis of maturity-onset diabetes of the young". *Endocrinol Metab Clin North Am* 35 (2): 371-384.

Viña, J., Borrás, C., Gambini, J., Sastre, J. and Pallardó, F. V. (2005). "Why females live longer than males? Importance of the upregulation of longevity-associated genes by oestrogenic compounds". *FEBS Lett* 579 (12): 2541-2545.

Wallace, T. M., Levy, J. C. and Matthews, D. R. (2004). "Use and abuse of HOMA modeling". *Diabetes Care* 27 (6): 1487-1495.

Walsh, G. and Jefferis, R. (2006). "Post-translational modifications in the context of therapeutic proteins". *Nature Biotechnol* 24 (10): 1241-1252.

Walter, P. and Johnson, A. (1994). "Signal sequence recognition and protein targeting to the endoplasmic reticulum membrane". *Annu Rev Cell Biol* 10 (1): 87-119.

Wang, H., Maechler, P., Ritz-Laser, B., Hagenfeldt, K. A., Ishihara, H., Philippe, J. and Wollheim, C. B. (2001). "Pdx1 level defines pancreatic gene expression pattern and cell lineage differentiation". *J Biol Chem* 276 (27): 25279-25286.

Wang, J., Takeuchi, T., Tanaka, S., Kubo, S., Kayo, T., Lu, D., Takata, K., Koizumi, A. and Izumi, T. (1999). "A mutation in the insulin 2 gene induces diabetes with severe pancreatic β-cell dysfunction in the *Mody* mouse". *J Clin Invest* 103 (1): 27-37.

Wanke, R., Weis, S., Kluge, D., Kahnt, E., Schenck, E., Brem, G. and Hermanns, W. (1994). "Morphometric evaluation of the pancreas of growth hormone-transgenic mice". *Acta Stereologica* 13 3-3.

Weir, G., Laybutt, D., Kaneto, H., Bonner-Weir, S. and Sharma, A. (2001). "Beta-cell adaptation and decompensation during the progression of diabetes". *Diabetes* 50 (suppl 1): S154-S159.

World Health Organization (2009). "Chronic disease information sheet Diabetes". Retrieved 16.08. 2009 from http://www.who.int/dietphysicalactivity/publications/facts/diabetes/en/index.html.

Wicksteed, B., Alarcon, C., Briaud, I., Lingohr, M. K. and Rhodes, C. J. (2003). "Glucose-induced translational control of proinsulin biosynthesis is proportional to preproinsulin mRNA levels in islet β-cells but not regulated via a positive feedback of secreted insulin". *J Biol Chem* 278 (43): 42080-42090.

Wild, S., Roglic, G., Green, A., Sicree, R. and King, H. (2004). "Global prevalence of diabetes estimates for the year 2000 and projections for 2030". *Diabetes care* 27 (5): 1047-1053.

Xia, B., Zhan, X., Yi, R. and Yang, B. (2009). "Can pancreatic duct-derived progenitors be a source of islet regeneration?" *Biochem Biophys Res Commun* 283 (4): 383-385.

Xu, C., Bailly-Maitre, B. and Reed, J. (2005). "Endoplasmic reticulum stress: cell life and death decisions". *J Clin Invest* 115 (10): 2656-2664.

Yamamoto, K., Sato, T., Matsui, T., Sato, M., Okada, T., Yoshida, H., Harada, A. and Mori, K. (2007). "Transcriptional induction of mammalian ER quality control proteins is mediated by single or combined action of ATF6α and XBP1". *Dev Cell* 13 (3): 365-376.

Yamamoto, K., Yoshida, H., Kokame, K., Kaufman, R. J. and Mori, K. (2004). "Differential contributions of ATF6 and XBP1 to the activation of endoplasmic reticulum stress-responsive *cis*-acting elements ERSE, UPRE and ERSE-II". *J Biochem* 136 (3): 343-350.

Yano, H., Kitano, N., Morimoto, M., Polonsky, K., Imura, H. and Seino, Y. (1992). "A novel point mutation in the human insulin gene giving rise to hyperproinsulinemia (proinsulin Kyoto)." *J Clin Invest* 89 (6): 1902-1907.

Yki-Järvinen, H., Dressler, A. and Ziemen, M. (2000). "Less nocturnal hypoglycemia and better post-dinner glucose control with bedtime insulin glargine compared with bedtime NPH insulin during insulin combination therapy in type 2 diabetes." *Diabetes Care* 23 (8): 1130-1136.

Yoon, K. H., Ko, S. H., Cho, J. H., Lee, J. M., Ahn, Y. B., Song, K. H., Yoo, S. J., Kang, M. I., Cha, B. Y., Lee, K. W., Son, H. Y., Kang, S. K., Kim, H. S., Lee, I. K. and Bonner-Weir, S. (2003). "Selective β-cell loss and α-cell expansion in patients with type 2 diabetes mellitus in Korea". *J Clin Endocrinol Metab* 88 (5): 2300-2308.

Yoshinaga, T., Nakatome, K., Nozaki, J.-i., Naitoh, M., Hoseki, J., Kubota, H., Nagata, K. and Koizumi, A. (2005). "Proinsulin lacking the A7-B7 disulfide bond, Ins2[Akita], tends to aggregate due to the exposed hydrophobic surface". *Biol Chem* 386 (11): 1077-1085.

Yoshioka, M., Kayo, T., Ikeda, T. and Koizumi, A. (1997). "A novel locus, *Mody4*, distal to D7Mit189 on chromosome 7 determines early-onset NIDDM in nonobese C57BL/6 (Akita) mutant mice." *Diabetes* 46 (5): 887-894.

Zhang, C., Moriguchi, T., Kajihara, M., Esaki, R., Harada, A., Shimohata, H., Oishi, H., Hamada, M., Morito, N., Hasegawa, K., Kudo, T., Engel, J. D., Yamamoto, M. and Takahashi, S. (2005). "MafA is a key regulator of glucose-stimulated insulin secretion". *Mol Cell Biol* 25 (12): 4969-4976.

Zhang, D., Lu, C., Whiteman, M., Chance, B. and Armstrong, J. S. (2008). "The mitochondrial permeability transition regulates cytochrome *c* release for apoptosis during endoplasmic reticulum stress by remodeling the cristae junction". *J Biol Chem* 283 (6): 3476-3486.

Zhao, J., Yang, J. and Gregersen, H. (2003). "Biomechanical and morphometric intestinal remodelling during experimental diabetes in rats". *Diabetologia* 46 (12): 1688-1697.

Zhou, J., Zhou, S., Tang, J., Zhang, K., Guang, L., Huang, Y., Xu, Y., Ying, Y., Zhang, L. and Li, D. (2009). "Protective effect of berberine on beta cells in streptozotocin- and high-carbohydrate/high-fat diet-induced diabetic rats". *Eur J Pharmacol* 606 (1-3): 262-268.

Ziegler, D., Hanefeld, M., Ruhnau, K. J., Hasche, H., Lobisch, M., Schütte, K., Kerum, G. and Malessa, R. (1999). "Treatment of symptomatic diabetic polyneuropathy with the antioxidant alpha-lipoic acid: A 7-month multicenter randomized controlled trial (ALADIN III Study)" *Diabetes Care* 22 (8): 1296-1301.

Ziegler, D., Hanefeld, M., Ruhnau, K. J., Meißner, H. P., Lobisch, M., Schütte, K. and Gries, F. A. (1995). "Treatment of symptomatic diabetic peripheral neuropathy with the anti-oxidant α-lipoic acid". *Diabetologia* 38 (12): 1425-1433.

Zini, E., Osto, M., Franchini, M., Guscetti, F., Donath, M., Perren, A., Heller, R., Linscheid, P., Bouwman, M. and Ackermann, M. (2009). "Hyperglycaemia but not hyperlipidaemia causes beta cell dysfunction and beta cell loss in the domestic cat". *Diabetologia* 52 (2): 336-346.

Zuber, C., Fan, J.-Y., Guhl, B. and Roth, J. (2004). "Misfolded proinsulin accumulates in expanded pre-Golgi intermediates and endoplasmic reticulum subdomains in pancreatic beta cells of Akita mice". Retrieved 15.07.2009 from http://www.fasebj.org/cgi/reprint/03-1210fjev1.pdf

10 Appendix

10.1 List of abbreviations

ATF	activating transcription factor
BiP	binding Ig protein
C/EBP	CCAAT/enhancer binding protein
CAT	catalase
CHO	Chinese hamster ovarian
CHOP	C/EBP homologous protein
CoQ$_{10}$	coenzyme Q$_{10}$
eIF2	eucaryotic initiation factor 2
ENU	*N*-ethyl-*N*-nitrosourea
ER	endoplasmic reticulum
ERAD	ER-associated degradation
ERO1	ER oxidoreductase 1
ERSE	ER stress response element
FFA	free fatty acid
GADD	growth arrest and DNA damage
GR	glutathione reductase
GRP	glucose regulated protein
Grx	glutaredoxin
GSH	reduced glutathione
GSH-Px	glutathione peroxidase
GSSG	oxidised glutathione
IFNγ	interferon-γ
IL	interleukine
IPF	insulin promoter factor
ipITT	intraperitoneal insulin tolerance test
IR	insulin receptor
IRE1	inositol requiring 1
IRS	insulin receptor substrate
JNK	C-Jun NH$_2$ terminal kinase
LA	α-lipoic acid
MAPK	mitogen-activated protein kinase

MEF	mouse embryo fibroblast
MnSOD	manganese superoxide dismutase
MODY	maturity-onset diabetes of the young
NAC	*N*-acetyl cysteine
NDM	neonatal diabetes mellitus
NF-κB	nuclear factor-κB
Nrf	nuclear respiratory factor
OGTT	oral glucose tolerance test
PDI	protein disulfide isomerase
PeIF2α	phosphorylated eIF2
PERK	double-stranded RNA-activated protein kinase like endoplasmic reticulum kinase
PKC	protein kinase C
PNDM	permanent neonatal diabetes mellitus
ROS	reactive oxygen species
SOD	superoxide dismutase
STZ	streptozotocin
TBARS	thiobarbituric acid reactive substances
UPR	unfolded protein response
UPRE	unfolded protein response element
XBP-1	X-box binding protein-1

10.2 Assay procedures

10.2.1 Radioimmunoassay (RIA)

10.2.1.1 C-peptide

C-peptide concentrations in the serum and pancreas were determined by a Rat C-Peptide RIA Kit (Linco Research, USA). The assay was performed using half amount of sample and assay reagents as denoted in the instruction sheet. Pancreas homogenate was diluted 1:1,000 (wild-type mice), 1:400 (insulin-treated mutant mice) and 1:100 (placebo-treated mutant mice) in PBS.

On the first day, 150 µl of assay buffer were filled into the non-specific binding tubes (tube 3, 4) and 100 µl into the reference tubes (tube 5, 6). The remaining tubes (tube 7 onwards) were loaded with 50 µl assay buffer. Fifty µl of standards and quality controls were pipetted in duplicate into tube 7-24. The same amount of sample was added to the rest of the tubes. After adding 50 µl of rat C-peptide antibody into tube 5 onwards, the tubes were vortexed, covered with parafilm and incubated overnight (4°C, 22 hours).

The next day 50 µl of ^{125}I-rat C-peptide tracer were added to all tubes. Subsequently, the tubes were vortexed, covered with parafilm and incubated overnight (4°C, 22 hours).

Half a ml of cold precipitating reagent (4°C) was pipetted into all tubes, except total count tubes (tube 1, 2) on the third day. After vortexing, covering and incubating (20 minutes, 4°C) the tubes, they were centrifuged (Megafuge 1.0 R, HERAEUS Sepatech, Germany; 20 minutes, 3,000 x g, 4°C). The supernatant was decanted from tube 3 onwards by inverting them and draining them for 60 seconds. Serum C-peptide concentrations were determined by a gamma counter (LB 2111, BERTHOLD TECHNOLOGIES, Germany) within 1 minute. Calculation was run by the program Berthold-MULTI-WELL (BERTHOLD TECHNOLOGIES, Germany).

Materials:

Materials were components of the assay kit.

Assay buffer:
        Phosphosaline 0.05 M, pH 7.4
        EDTA 0.025 M
        Sodium azide 0.08%
        RIA grade BSA 1%

Guinea pig anti-rat C-peptide antibody:
        diluted in assay buffer

^{125}I-rat C-peptide tracer:
        HPLC purified, lyophilised

Hydrate with label hydrating buffer 30 minutes before use while mixing gently once in a while.

Label hydrating buffer:
        Assay buffer containing normal guinea pig serum as carrier

Rat C-peptide standards:
        purified recombinant rat C-peptide diluted in assay buffer
        25, 50, 100, 200, 400, 800 and 1,600 pM

Quality controls 1 and 2:
        purified recombinant rat C-peptide diluted in assay buffer

Precipitating reagent:
        Goat anti-guinea pig IgG
        PEG 3%
        Triton X-100 0.05%
        Phosphosaline 0.05 M
        EDTA 0.025 M
        Sodium azide 0.08%

10.2.1.2 Glucagon

Serum glucagon levels were analysed by a Glucagon RIA KIT (Linco Research, USA), using half the reaction batch volumes.

The procedure of this RIA is similar to the one of the Rat C-Peptide RIA Kit (Linco Research, USA; 10.2.1.1 C-peptide). Compared to the C-Peptide RIA the Glucagon RIA comprises two standards less. It utilises Glucagon Antibody and ^{125}I-Glucagon tracer to analyse serum glucagon concentration.

Materials:

Materials were components of the assay kit.

Assay buffer:
  Glycine 0.2 M, pH 8.8
  EDTA 0.03 M
  Sodium azide 0.08%
  RIA grade BSA 1%

Guinea pig anti-glucagon antibody:
  diluted in assay buffer

^{125}I-glucagon tracer:
  HPLC purified, lyophilised
  hydrate with label hydrating buffer 30 minutes before use while mixing
  gently once in a while

Label hydrating buffer:
  Assay buffer containing glycine as carrier

Glucagon standards:
  Glucagon diluted in assay buffer
  20, 50, 100, 200 and 400 pg/ml

Quality controls 1 and 2:
  purified recombinant glucagon diluted in assay buffer

Precipitating reagent:
  Goat anti-guinea pig IgG
  PEG 3%
  Triton X-100 0.05%
  Phosphosaline 0.05 M
  EDTA 0.025 M
  Sodium azide 0.08%

10.2.2 C-peptide II ELISA

A Mouse C-Peptide II ELISA (KAMIYA, USA) was used to determine the C-peptid II concentrations in serum and pancreas. Pancreas homogenates were diluted 1:20 (wild-type mice) and 1:10 (heterozygous and homozygous mutants) with distilled water.

The C-peptide II calibrator solutions were prepared by diluting the 100 ng/ml calibrator solution 1 to 3 with buffer solution. The serial dilution was repeated 5

times attaining the following standards: 100, 33.33, 11.11, 3.704, 1.235, 0.412 and 0 ng/ml. Twenty-five µl of the particular standard or sample were filled into the wells of a goat anti-rabbit IgG antibody-coated plate. Afterwards, 100 µl of labelled antigen and 50 µl of C-peptide II antibody were added. The plate was covered with a plate seal and incubated for 17 hours at 4°C.

The next day, the plate was placed on a plate rotator for 1 hour at room temperature. After removing the seal and washing the wells 3 times with wash solution (320 µl per well), 100 µl of SA-HRP solution were pipetted into each well. The plate was covered with a plate seal and incubated on a plate rotator (1 hour, room temperature). After washing 5 times with wash solution, 100 µl of substrate solution were added, the plate was covered with a seal and incubated for 30 minutes at room temperature. Finally, 100 µl of stop solution were filled into the wells to stop the colour reaction. The optical absorbance was determined at 492 nm, using the microplate reader SUNRISE (Tecan, Germany). C-peptide II concentrations were calculated via the computer program Magellan 2 (Tecan, Germany).

Materials:

Materials were components of the assay kit.

Antibody-coated plate:
      96 well microtiter plate, ready to use

C-peptide II calibrator (lyophilised):
      add 1 ml buffer solution to the vial and vortex to obtain 100 ng/ml
      calibrator solution

Labelled antigen (lyophilised):
      Biotinylated mouse C-peptide II
      add 12 ml Buffer Solution to the vial, vortex

Buffer solution:
      Phosphate buffer, ready to use

C-peptide II antibody:
      Rabbit anti-mouse C-peptide II, ready to use

SA-HRP solution:
      HRP (horse radish peroxidase) labelled streptavidin, ready to use

OPD tablet:
   o-Phenylenediamine dihydrochloride

Substrate buffer:
   Hydrogen peroxide 0.015%

Substrate solution:
   dissolve one OPD tablet in 12 ml substrate buffer
   (immediately before use)

Stop solution:
   H_2SO_4 1 M, ready to use

Wash solution concentrate:
   Concentrated saline
   add 50 ml wash solution concentrate to 1,000 ml distilled water

Plate seal: 3 sheets

10.2.3 Thiobarbituric Acid Reactive Substances (TBARS)

Lipid peroxidation in the serum was analysed using a TBARS Assay Kit[®] (Cayman, USA). Serum was diluted 1:1 with HPLC grade water.

The 8 Malondialdehyde (MDA) standards (0-50 pM) were obtained pipetting the adequate amount of MDA and HPLC grade water into glass tubes. One hundred µl of standard or sample were filled into labelled 12 ml polypropylene screw-cap centrifuge tubes. Subsequently, 100 µl of the SDS solution were pipetted into each tube, tubes were vortexed, and 4 ml of colour reagent were added. After boiling in a water bath (GFL, Germany; 1 hour), the tubes were incubated for 10 minutes on ice in order to stop the reaction. The tubes were centrifuged (4K15C centrifuge, Sigma, Germany; 10 minutes, 1,600 x g, 4°C), and 150 µl supernatant were pipetted into a 96 well plate. Standards were pipetted in duplicate. The absorbance was read by a microplate reader (SUNRISE, Tecan, Germany) at 532 nm. Concentrations of TBARS expressed as MDA equivalents were calculated, using the program Magellan 2 (Tecan, Germany).

Materials:

Materials were components of the assay kit, except for HPLC grade water

Colour reagent: for each standard or sample:

Acetic acid:	2 ml
Thiobarbituric acid powder:	21.2 mg
Sodium hydroxide:	2 ml

Acetic acid:

Acetic Acid, stock solution:	40 ml
HPLC grade water:	160 ml

Sodium hydroxide :

Sodium hydroxide, stock solution (x10):	20 ml
HPLC grade water:	180 ml

Thiobarbituric acid powder (2 g)

SDS solution, ready to use

Malondialdehyde standard (500 µM):
    Standard solutions (0.000, 0.625, 1.25, 2.5, 5, 10, 25, 50 pM) were
    prepared according to the manufacturer's manual

Acknowledgements